UNDERSTANDING THE METABOLISM OF DRUG LIKE MOLECULES BY HEME & NON-HEME MODELLED ENZYMES USING QUANTUM MECHANICAL TOOLS

THESIS

SUBMITTED FOR THE AWARD OF THE DEGREE

Of

Doctor of Philosophy

In

Applied Physics

Submitted By

Nidhi Awasthi

Enrollment No.: 664/15

Under the Supervision of

Prof. Devesh Kumar

DEPARTMENT OF APPLIED PHYSICS

SCHOOL FOR PHYSICAL SCIENCES

BABASAHEB BHIMRAO AMBEDKAR UNIVERSITY

(A CENTRAL UNIVERSITY)

LUCKNOW (U.P.), INDIA – 226025

2021

THIS THESIS

IS

DEDICATED

TO

MY FAMILY

DECLARATION

I declare that the thesis entitled **"Understanding the metabolism of drug like Molecules by Heme & Non-Heme Modelled Enzymes Using Quantum Mechanical Tools"** has been prepared by me under the supervision of **Prof. Devesh Kumar**, Department of Applied Physics, School for Physical Sciences, Babasaheb Bhimrao Ambedkar University, Lucknow. No part of this thesis has formed the basis for the award of any degree, diploma or fellowship previously. Further, I declare that the material embodied in the present work is based on original research work and the indebtedness to others has been duly acknowledged at relevant places. This is also declared that the thesis is essentially free from all kinds of plagiarism.

Date: 8/10/2021
Place: Lucknow

Nidhi Awasthi

(Nidhi Awasthi)
Enrollment no. 664/15
Ph.D Scholar
Department of Applied Physics
School for Physical Sciences
Babasaheb Bhimrao Ambedkar University
Vidya Vihar, Rae Bareli Road
Lucknow, (U.P.), India-226025

CERTIFICATE

This is to certify that the thesis titled **"Understanding the metabolism of drug like Molecules by Heme & Non-Heme Modelled Enzymes Using Quantum Mechanical Tools"** submitted by **Ms. Nidhi Awasthi** is an original research work and has not been previously submitted in part or full for the award of any other degree or diploma to this or any other university.

The thesis submitted to Babasaheb Bhimrao Ambedkar University, Lucknow satisfies all the requirements as stipulated in the *Doctor of Philosophy (Ph.D.) regulations -1999 as amended in 2008/2010/2013* and it is fit for submission and evaluation for the award of the degree of Doctor of Philosophy of the University.

Date: 08 | 10 | 2021

Supervisor

Head of the Department

ACKNOWLEDGEMENT

Foremost, I am highly grateful to God for his blessings that continue to flow into my life, and because of You, I made this through against all odds. I am very much indebted to my supervisor **Prof. Devesh Kumar,** Department of Applied Physics, Babasaheb Bhimrao Ambedkar University, Lucknow,for his generoussupport, encouragement, guidance and providing me inspiring research atmosphere during the period of my research work. I am thankful to him for introducing the subject to me as well as keeping me on the right track throughout my research activities. I would like to extend my thanks for his patience with which he dealt me, his critical remarks, valuable suggestions and his attachment on personal level have proven guiding lamp on the road to success.

I would like to express my sincere thanks to **Prof. Bal Chandra Yadav,** Head of Department, for providing me all the necessary facilities available in the Department during my research work.

I am also grateful to my faculty members **Dr. Ramesh Chandra, Dr. Anil Kumar Yadav, Dr. Khem Bahadur Thapa and Dr. Devendra Singh** for their blessings, constant encouragement and cooperation during this work.

I deeply acknowledge the help of office staff of the department who was always ready to support me at everystage of my research work.

A special thanks to **Prof. C. V. Sastri** for providing me the computational facilities during my research.

Further, I would like to thank the facilities of Central Library and the Computer Center of Babasaheb Bhimrao Ambedkar University, Lucknow which were useful at every stage of the research work.

I am also thankful to my colleagues **Ms. Anamika Shukla, Ms. Bhavna Pal, Ms. Varsha Gautam, Mr. Mritunjai Mishra, Mr. Sachin Kumar Yadav, Mr. Ajeet Singh, Mr. Pratham Singh, Mr. Siddhant Agnihotri, Mr. Sumit Tiwari, Mr. Manish Kumar** and **Mr. Manish Kumar Maurya** for their consistent support in every situation. I specially thank to my friend **Mr. Anuj Bhadauriya** from IIT Bombay for his precious support during my research. I am also grateful to my senior **Dr. Amarjeet Yadav, Dr. Jeevitesh Kumar Rajput, Dr. Narinder Kumar, Dr. Anwesh Pandey, Dr. Asheesh Kumar, Dr. Deep Kumar, Dr. Jitendra Kumar, Dr. Krishanpal, Dr. Ashish Kumar** and **Dr. Shivani Chaudhary** for being with me as well as for helping and supporting me in every manner. I am especially thankful to my super senior **Dr. Ruchi Mishra** and **Dr. Rajkamal Shastri** for their unconditional support in every situation. I am heartily thankful to my senior **Dr. Pawan Singh** for their unconditional support and valuable suggestions.

The last I would like to thanks from the depth of my heart to my senior **Ms. Rolly Yadav** for her continuous support in every state of my research. Without her support, my research work could not be possible. So, again I am very thankful to her.

I gratefully acknowledge the financial support from the University Grant Commission (UGC Non-NET), Government of India, New Delhi.

Finally, I have no words to express my feelings of gratitude towards my family members, specially my parents **Mr. Manoj Awasthi,** and **Mrs. Kiran Awasthi,** My younger brother **Mr. Vivek Awasthi,** my Grandfather **Mr. Rajaram Shukla,** my

brother **Mr. Abhishek Dixit** and his wife **Mrs. Seema Dixit** for their unconditional love and support in all state of research. Without their blessings, inspiration and encouragement, this work could have never been accomplished in the present form.

Last but not least, I would like to thank one and all, who directly or indirectly help me during my studies leading to this thesis.

Nidhi Awasthi

Nidhi Awasthi

(Ph.D. Scholar)

LIST OF PUBLICATION

Part of thesis published and communicated in the refereed journals

1. **Nidhi Awasthi**, RollyYadav, Anamika Shukla, Devesh Kumar, "Interplay between two degenerate spin state determines the hydroxylation of 4-nitrophenol catalyzed via Cytochrome P450", ***Inorganic Chemistry Communications***, 132, 108857, (2021).

2. Janardan Prasad Pandey, Arvind Kumar Dwivedi, Rajesh Kumar Singh, Alok Shukla,Anamika Shukla, **Nidhi Awasthi**, "Study of Physical Properties of Several Cyp450 Inhibiting Drugs, Using DFT Methodology", ***Journal of Scientific Computing***, 9, 33-38, (2020).

3. **Nidhi Awasthi**, Abhishek Tiwari, "Computational study of electrical properties of various anti fungal drugs that metabolised via Cytochrome P450",***Journal of Information and Computational Science***, 11, 22-26, (2021).

4. **Nidhi Awasthi**, Rolly Yadav, Anamika Shukla, Devesh Kumar, "Optimization of Azole- Antifungal Drugs: An Attempt for Search of Better Drug for Treatment of TB with CYP450 from Mycobacterium Tuberculosis", ***International Journal of. Engineering. Science. Advanced Research***, 6, 53-55, (2020).

5. **Nidhi Awasthi**, Rolly Yadav, Anamika Shukla, Devesh Kumar, "Metabolism of 8-aminoquinoline (8AQ) Primaquine via aromatic hydroxylation step mediated by Cytochrome P450 enzyme using Density Functional Theory", ***Journal of Organometallic Chemistry (Comunicated)***.

6. A. K. Dwivedi, **Nidhi Awasthi**, Rolly Yadav, Shivani Chaudhary, Anamika Shukla,Narinder Kumar*, "Spectroscopic Analysis of Porphyrin (C20H12N4) ring studiedby DFT Methodology", ***Journal of Information and Computational Science***, 9, 89-99, (2019).

7. Arvind Kumar, Rajesh Kumar Singh, Janardan Prasad Pandey, Alok Shukla, **Nidhi Awasthi**, Rolly Yadav, "A Theoretical Perspective of controversy in rebound mechanism of hydroxylatiom by Cytochrome P450: A Microreview", ***Journal of Scientific Computing***, 9, 17-32, (2020).

Work not included in the thesis:

1. Rolly Yadav, **Nidhi Awasthi**, Anamika Shukla, Devesh Kumar, "Modeling the hydroxylation of estragole via human liver cytochrome P450", ***Journal of Molecular Modeling,*** 27, 199, (2021).

2. Rolly Yadav, Anwesh Pandey, **Nidhi Awasthi**, Anamika Shukla," Molecular Docking Studies of Enzyme Binding Drugs on Family of Cytochrome P450 Enzymes",***Advanced Science,Engineering and Medicine***, 11, 1–5, (2019).

3. A.K. Dwivedi, Ruchi Mishra, Asheesh Kumar, Rolly Yadav, **Nidhi Awasthi**, Anamika Shukla, "Computational Molecular Characterization of important flavonoids: An insilicostudy", ***Compliance Engineering Journal***, 10, 123-132, (2019).

4. Rajesh Kumar Singh, Arvind Kumar Dwivedi, Janardan Prasad Pandey, Rolly Yadav, **Nidhi Awasthi**, Anamika Shukla, "A Review on the Interaction of various types of Flavonoids with DNA",***Journal of Scientific Computing***, 9, 39-51, (2020).

5. Alok Shukla, A.K. Dwivedi, **Nidhi Awasthi**, Rolly Yadav, "Interaction of Carbazoles and their analogs with human Cytochrome",***Compliance Engineering Journal***, 11, 187-194, (2020).

6. Alok Shukla, Arvind Kumar Dwivedi, **Nidhi Awasthi**, Anamika Shukla, "Molecular Docking studies of Azole Derivatives with DNA", ***Compliance Engineering Journal***, 11, 195-202, (2020).

CONFERENCE AND SEMINARS

1. Attended National Conferences **"Science and Tech. for sustainable future"** held on 10-11 January 2018, in BBAU Lucknow U.P.

2. Attended **"National Science Day"**, held on 27-28 February 2018, in BBAU Lucknow, U.P.

3. Poster presentation in "**International Conference on Chemical Sciences: National and Global Prospective"** held on 29-31 October 2018, in Lucknow Christian College, Lucknow, U.P.

4. Poster presentation in "**National Symposium on Advanced Materials Science"** held on 7-8 December 2018, in Deen Dayal Upadhyaya Gorakhpur University, Lucknow, U.P.

5. Poster present in **"International conference on Advanced Chemical and Structural Biology (ICACSB-2019)"**, held on 19-21 February 2019, in Prist Manamai Campus near Mahabalipuram, Chennai.

6. Poster presentation in **"International Conference on Ultrasonics and Materials Science for Advanced Technology"**, held on 16-18 November 2019, in V.B.S.P.U. Jaunpur, U.P.

7. Attended **"107th Indian Science Congress, University of Agricultural Sciences"** held on 3-7 January 2020, GKVK, Banglore.

8. Poster presentation in **"National conference on material and devices (NCMD-2020)"**, held on 18-19 December 2020, in Teerthankar Mahaveer University, Moradabad, U.P.

9. Attended **"International Workshop on Tools and Techniques to Perform Molecular Modeling and Computer Aided Drug Design (MMTT-2021)"**, held on 11-17 January 2021, in National Institute of Pharmaceutical Education and Research (NIPER), Guwahati.

10. Attended **"National Webinar on Recent Development in Magneto-Mechano-Electric (MME) generator and future prospects"**, held on 1st Febuary 2021, in Govt. college Sailana, M.P.

11. Attended **"Virtual Symposium on Biophysics (Biophysika-5)"**, held on 23 February 2021, in Jamia Millia Islamia, New Delhi.

12. Paper presentation in **"International conference on Recent Advances in science"**, held on 30 April - 1 May 2021, in Invertis University, Barreilly, U.P.

13. Attended Special public lecture in **"Certainity of Supermassive Black Hole"** by "Professor Andrea Ghez, Nobel Laureate Physics 2020.

ABSTRACT

Nature utilizes a range of metalloenzymes for biosynthesis, biodegradation and metabolism processes. In metalloenzymes, like most heme and nonheme iron dioxygenases and monoxygenases, the active species is a high valent iron(IV)-oxospecies, which in the cytochromes P450 is called Compound I. In nature, these enzymes catalyze oxygen atom transfer reactions in the liver as a means to detoxify compounds, including aliphatic and aromatic hydroxylation, epoxidation and hetero atom oxidation. As these enzymes often perform these reactions regio and stereo specifically, the reactions are of big interest to the biotechnological and pharmaceutical industries. Since Compound I is short lived, controversies have arisen whether or not it actually is the active oxidant and several alternative oxidants have been proposed in the process such asits iron(III)-hydroperoxo and iron(III)-superoxo intermediates in the catalytic cycle. Experimental studies in this field, however, are difficult due to the short lifetime of thesecatalytic intermediates, and therefore, we have performed a series of high-level computational studies. Thus, advances in computational chemistry over the past few decades as well as improved computational resources enables the use of quantum chemical methods to systems of 100 – 200 atoms these days with good accuracy and assuch enzymatic modelling has been performed with the aim to guide and assist experimental efforts in the field. In our group, we have applied a combination of Density Functional Theory studies on model complexes and combined Quantum Mechanics/Molecular Mechanics on enzymatic systems with the aims to elucidate the catalytic mechanism of enzymes and find the fundamental properties of the active oxidant. Over the years, we modelled the reactivity of heme enzymes, such as the cytochromes P450 as well as heme peroxidases and catalases, but

also nonheme iron enzymes including taurine/α-ketoglutarate dioxygenase, prolyl-4-hydroxylase and cysteine dioxygenase. The computational studies give additional insight into the electronic properties of oxidants and their reactivity patterns that is difficult to obtainfrom the experimental data; often the work is in close collaboration with experimental work. Our calculations have established catalytic mechanisms for aliphatic and aromatic hydroxylation reactions by iron(IV)-oxoheme cation radical oxidants, which identified the rate determining step in the mechanism and the electronic features of oxidant, substrate and enzyme environment that drive the reaction. The aliphatic hydroxylation and epoxidation reactions are stepwise via radical intermediates, whereas the aromatic hydroxylation and sulphoxidation reactions areelectrophilic with the formation of an O–C/O–S chemical bond. We established the factors that determine the rate constants of substrate activation by Compound I and showed that the rate determining step in aliphatic hydroxylation has a barrier proportionalto the strength of the C–H bond of the substrate that is broken as well as to the strength ofthe O–H bond that is formed and set up a mathematical model which enables one topredict rate constants from empirical values. Therefore, have provided a deep understanding on chemical catalysis by high valentmetal-oxo oxidants and have set the scene for future studies in the field.

PREFACE

The thesis entitled **"Understanding the metabolism of drug like Molecules by Heme & Non-Heme Modelled Enzymes Using Quantum Mechanical Tools"** encapsulate the results of theoretical investigations carried out in the Department of Applied Physics, Babasaheb Bhimrao Ambedkar University, Lucknow, in between 2017-2021 under the supervision of **Prof. Devesh Kumar,** Professor in Applied Physics, Babasaheb Bhimrao Ambedkar University, Lucknow. Iron containing metalloenzymes are found throughout the natural world and are vital catalysts in many crucial metabolic and biosynthetic biological pathways (Solomon,Brunold et al. 2000, De Visser, Kumar et al. 2011). Iron containing enzymes are classified into two main groups: heme enzymes and non-heme enzymes (Montellano 1992, Müllerand Bröring 2008). The bulk of the work discussed here concerns mononuclear iron systems, however, in nature both multi iron systems (Siegbahn, Crabtree et al. 1998) anda variety of different transition metal cofactors are used (Rehder 2008, Conte and Floris2010). Computational modelling helps in studying the properties of short lived intermediates and transition state complexes. Therefore computational methods are vital tools in the investigation of reaction pathways. This thesis will focus on the reaction mechanics of enzymes that incorporate transition metals into their active sites. Specific attention will be paid to the ability of many of these biocatalysts to use transition metalcofactors in the activation of molecular oxygen. There will also be a focus on howsynthetic substituted catalysts may be used to imitate their reaction mechanisms. The thesis is divided in six chapters.

Chapter 1 reviews the theoretical work done so far on heme and non heme type enzyme and also discuss the suitability of various computational quantum mechanical methods available in terms of accuracy etc.

Chapter 2 gives the development and mathematical details of quantum mechanical methods.

Chapter 3 deals with the results obtained from the calculation for aromatic hydroxylation mechanism of Primaquine (an anti-malarial Drug) of modelled Cytochrome P450.

Chapter 4 focused on the results obtained from the study of the aromatic hydroxylation mechanism of 4-nitrophenol via Cytochrome P450 enzyme. A comparison of reactivity mechanism based on quantum mechanical methods obtain energy profile was also made in this chapter.

Chapter 5 provides computational study of electrical properties of various drugs that metabolized via Cytochrome P450, which can be helpful for further metabolic studies of various drugs.

Chapter 6. gives the general conclusions and future prospects drawn from the present thesis. Hopefully, a better understanding of this important group of naturally occurring and synthetic catalysts will enable more efficient and effective work of computational chemistry to be performed, well into the future.

LIST OF ABBREVIATIONS AND SYMBOLS

1.	B1	Basis set 1 - LACVP or LANL2DZ basis set
2.	B2	Basis set 2 - LACVP** basis set which adds polarisation functions to first row atoms and hydrogen
3.	BS	Basis Set
4.	BA	Benzyl Alcohol
5.	CID	Collision Induced Dissociation
6.	CHD	Cyclohexadiene
7.	CT	Charge-Transfer
8.	CI	Configuration-Interaction
9.	Cpd0	Compound 0, Iron-Hydroperoxo Intermediate
10.	CpdI	Compound I, Iron-oxo Ferryl Species
11.	CpdII	Compound II, One-Electron reduced form of CpdI
12.	CPO	Chloroperoxidase
13.	CDO	Cysteine Dioxygenase
14.	CYP	Cytochrome P450
15.	D	Doubly-reduced pentacoordinated complex of P450
16.	DNA	Deoxyribonucleic acid
17.	DHA	Dihydroanthracene
18.	DMS	Dimethylsulfide

19.	DFT	Density Functional Theory
20.	EA	Electron Affinity
21.	EE	Electrostatic Embedding
22.	ECP	Effective Core Potential
23.	EPR	Electron Paramagnetic Resonance
24.	FT-ICR	Fourier Transform-Ion Cyclotron Resonance
25.	GTO	Gaussian type orbital
26.	HAT	Hydrogen Atom Abstraction
27.	HAT	Hartree-Fock
28.	HOMO	Highest Occupied Molecular Orbital
29.	HTP	Heme-Thiolate Proteins
30.	IE	Ionization Energy
31.	KIE	Kinetic Isotope Effect
32.	LCAO	Linear Combination of Atomic Orbital
33.	LUMO	Lowest Unoccupied Molecular Orbital
34.	MM	Molecular Mechanics
35.	MD	Molecular Dynamics
36.	MS	Mass Spectrometry
37.	MNHID	Mononuclear Nonheme Iron Dioxygenases
38.	OAT	Oxygen Atom Transfer
39.	PDB	Protein Data Bank

40.	PES	Potential Energy Surface
41.	P450	Cytochrome P450 enzyme
43.	P450cam	Cytochrome P450 from Pseudomonas putida, hydroxylase of Camphor
46.	QM	Quantum Mechanics
47.	RHF	Restricted Hartree-Fock
49.	SCF	Self Consistent Field
50.	STO	Slater Type Orbital
51.	Tp	Trispyrazolylborato
52.	TS	Transition State
53.	UHF	Unrestricted Hartree-Fock
54.	ZPE	Zero Point Energy
55.	TSR	Two State Reactivity
56.	MSR	Multi State Reactivity
57.	SSR	Single State Reactivity

LIST OF AMINO ACID ABBREVIATIONS

S. No.	Amino Acid	Three letter code
1.	Alanine	Ala
2.	Arginine	Arg
3.	Asparagine	Asn
4.	Aspartic acid	Asp
5.	Cysteine	Cys
6.	Glutamine	Gln
7.	Glutamic acid	Glu
8.	Glycine	Gly
9.	Histidine	His
10.	Isoleucine	Ile
11.	Leucine	Leu
12.	Lysine	Lys
13.	Methionine	Met
14.	Phenylalanine	Phe
15.	Proline	Pro
16.	Serine	Ser
17.	Valine	Val
18.	Threonine	Thr
19.	Tryptophan	Trp
20.	Tyrosine	Tyr

LIST OF TABLES

Table No.	Table caption	Page No.
Table 3.1:	Spin densities and charges of Cpd1 & 2PQ position of substrate (Primaquine) using BS1 basis set.	81
Table 3.2:	Spin densities and charges of Cpd1 & 4PQ position of substrate (Primaquine) using BS1 basis set.	88
Table 4.1:	Spin densities and charges of Cpd1 & substrate (4-nitrophenol) using DFT at the B3LYP/6-31G level of theory.	109
Table 5.1:	Optimization energy and HOMO-LUMO bandgap of Diacetylmorphine, Losartan, Primaquine, Verapamil drugs**.**	125
Table 5.2:	Optimization energy and HOMO-LUMO bandgap of Azoles.	126
Table 5.3:	Optimization energy and HOMO-LUMO bandgap of anti-fungal drugs.	127

LIST OF FIGURES

Figure No.	Figure caption	Page No.
Figure 1.1:	Active site of Cytochrome P450 as taken from PDB file 1W0E.	4
Figure 1.2:	Active site of HEME enzyme as taken from the PDB file 5B4Z.	6
Figure 1.3:	Active site of Tetrahydrobiopterin-dependent hydroxylases as taken from the PDB file1MMT.	7
Figure 1.4:	Active site of Alpha-Ketoacid dependent oxygenases (alpha KAOs) as taken from the PDB file5YBN.	8
Figure 1.5:	Active site of Methane monooxygenase (MMO) as taken from the PDB file 1MTY).	9
Figure 1.6:	Active site Ribonucleotide Reductaseas taken from the PDB file 2XO4.	10
Figure 1.7:	Catalytic Cycle of Cytochrome P450.	12
Figure 1.8:	Catalytic cycle of Cytochrome P450.	14
Figure 1.9:	Reaction profile of C-H hydroxylation by Cpd I, calculated by density functional theory, show high-spin (HS) state and low-spin (LS) state components.	15
Figure 1.10:	The two-oxidant hypothesis using Cpd I &Cpd 0.	16
Figure 1.11:	Key orbitals of Cpd 1 of Cytochrome P450.	18
Figure 1.12:	KIE_s in Norbornane of HS and LS C-H bond activations.	21
Figure 1.13:	Optimized geometry of porphyrin ring.	23
Figure 2.1:	Potential energy surfaces for a single-step reaction (a)	62

and three-step reaction (b).

Figure 3.1: Aromatic hydroxylation of Primaquine at ortho (2PQ) and para (4PQ) position by Cytochrome P450. 73

Figure 3.2: Potential energy surface of hydroxylation of Primaquine (2PQ) by Cytochrome P450 with energies in kcal/mol. Bond length, bond angle and imaginary frequencies (in cm^{-1}) of quartet as well as doublet (in bracket) spin state is shown. All energies are calculated at B3LYP/BS1//B3LYP/BS2 level of theory. 76

Figure 3.3: Key orbitals of Cpd I in order of their energy. 78

Figure 3.4: Optimized geometries of Reactant complex (RC), Transition state (TS), Intermediate complex (IM), and Product complex (PC) with differences in the bond lengths for respective atoms for LS of 2PQ. 79

Figure 3.5: Optimized geometries of Reactant complex (RC), Transition state (TS), Intermediate complex (IM), and Product complex (PC) of quartet spin state (HS) of 2PQ. 80

Figure 3.6: Optimized geometries of Reactant complex (RC), Transition state (TS), Intermediate complex (IM), and Product complex (PC) for doublet state (LS) of 4PQ. 84

Figure 3.7: Potential energy surface of hydroxylation of Primaquine (4PQ) by Cytochrome P450 4 with energies in kcal/mol. Bond length, bond angle and imaginary frequencies (in cm^{-1}) of quartet (in green color) as well as doublet (in bracket in red color) spin state is shown. 85

All energies are calculated at B3LYP/BS1//B3LYP/BS2 level of theory.

Figure 3.8: Optimized geometries of Reactant complex (RC), Transition state (TS), Intermediate complex (IM), and Product complex (PC) for quartet state (HS) of 4PQ. 86

Figure 3.9: Scan results of 2PQ at low spin surface. 87

Figure 3.10: Scan results of 4PQ at low spin surface. 87

Figure 4.1: Aromatic hydroxylation of 4-nitrophenol via CytochromeP450. 101

Figure 4.2: Key orbital of Cpd I in order of their energy. 103

Figure 4.3: Potential energy surface of hydroxylation of 4-nitrophenol by Cytochrome P450 with energies in kcal/mol, Bond length (in Å), bond angle (in °), and imaginary frequencies (in cm^{-1}) of the quartet (in green color) as well as a doublet (in blue color) spin state is shown. All energies are calculated at the B3LYP/BS1 level of theory. 105

Figure 4.4: Optimized geometries of Reactant complex (RC), Transition state (TS), Intermediate complex (IM), and Product complex (PC) with differences in the bond lengths for respective atoms for HS of 4-nitrophenol. 107

Figure 4.5: Optimized geometries of Reactant complex (RC), Transition state (TS), Intermediate complex (IM), and Product complex (PC) with differences in the bond lengths for respective atoms for LS of 4-nitrophenol. 108

Figure 4.6:	Optimized geometries of Reactant complex (RC) of 4-nitrophenol in original Gaussian view image. Arrow denote the number of the corresponding atom.	109
Figure 4.7:	Scan results at low spin surface.	111
Figure 5.1:	Optimizedmolecularstructuresof(a)Diacetylmorphine,(b)Losartan,(c)Primaquine, (d)Verapamil.	121
Figure 5.2:	Geometrical structure of (a) Azaconazole, (b) Bifonazole, (c) Clotrimazole, (d) Furafylline, (e) Miconazole.	123
Figure 5.3:	Optimized structures of (a) Econazole, (b) Ketoconazole, (c) Terconazole.	128

TABLE OF CONTENTS

Chapter	Contents	Page No.
Chapter1:	**Introduction**	**1**
	1.1 Introduction	1
	1.2 Cytochrome P450	4
	1.3 Heme Enzyme	5
	1.4 Non-Heme Enzyme	7
	1.4.1 Mononuclear Non-Heme Iron Enzyme	7
	1.4.1.1 Tetrahydrobiopterin-dependent hydroxylases (PDHs)	7
	1.4.1.2 Alpha-Ketoacid dependent oxygenases (alpha KAOs)	8
	1.4.2 Dinuclear Non-heme iron enzyme	9
	1.4.2.1. Methane monooxygenase (MMO)	9
	1.4.2.2 Ribonucleotide Reductase	10
	1.5 Heme Iron Vs Non-Heme Iron	10
	1.6 Catalytic Cycle	11
	1.7 Rebound Controversy	13
	1.8 Origin of TSR/MSR of Cpd I	17
	1.9 Product Isotope Effect in TSR	18

1.10 Porphyrin 21

References 24

Chapter 2 Computational Methodology 46

2.1 Quantum Mechanical Calculations 46

2.2 Hartree Fock Method 48

2.3 Electron Correlation 50

2.4 Density Functional Theory 51

2.5 Hybrid Function 54

2.6 Basis Sets 55

2.7 Solvent effects 58

2.8 Application of Ab-initio and DFT Methods 59

2.8.1 Molecular Geometry 59

2.8.2 Vibrational Frequencies 60

2.8.3 Chemical Reaction 61

References 64

Chapter 3 Metabolism of 8-aminoquinoline (8AQ) Primaquine via aromatic hydroxylation step mediated by Cytochrome P450 enzyme using Density Functional Theory 70

3.1 Introduction 70

3.2 Methodology 74

3.3 Results and Discussion 75

3.3.1 Hydroxylation of Primaquine at ortho position (2PQ) 75

3.3.2 Hydroxylation of Primaquine at para position (4PQ) 83

3.4 Conclusion 90

References 92

Chapter 4 Interplay between two degenerate spin state determines the hydroxylation of 4-nitrophenol catalyzed via Cytochrome P450 99

4.1 Introduction 99

4.2 Methodological Overview 101

4.3 Key Orbital of Cpd1 with substrate 102

4.4 Results and discussion 103

4.5 Conclusion 112

References 114

Chapter 5 Computational Study of Electrical Properties of Various Drugs that Metabolized via Cytochrome P450 119

5.1 Introduction 119

5.2 Computational Details 124

5.3 Results and discussion 125

5.4 Conclusion 129

References 131

Chapter 6 Conclusion and Future Scope 136

Chapter-I

Introduction

Chapter-1

Introduction

1.1 Introduction

Enzymes are proteins that typically increase the rate of biochemical reactions which continuously occur in human cells [1]. These are very important for functions of the body, such as digestion, respiration, muscle nervous system, and metabolism [2]. Many enzymes are used for breaking large compounds into small parts, so that it is more easily absorbed by the body [3]. Some enzymes bind the two different molecules and form a new molecule with different properties. Each enzyme increases only the rate of a specific reaction, so these are selective catalysts [4]. Enzymes are the catalysts of life. All enzymes are originated from living organisms. The general way of searching enzymes is growing the organism and isolating it from animal organs, parts of plants, inside microorganisms [5].

First, enzymes were found from animal and plant parts. These enzymes are protease papain from papaya fruit or rennet from calve's stomach. Nowadays, enzymes originated from microorganisms. It has been studied vigorously. It is the most technical enzyme. The microorganism is omnipresent. They are found in freezing Antarctica water, in hot water, in acidic spring water on the volcanoes and in alkaline lakes [6]. Protein enzymes are made of one or more amino acid chains. This chain is usually called polypeptide chains [7]. These chains determine the characteristic of the

protein's structure. If the temperature or pH of enzymes is changed, the protein may change its denature and enzymatic ability. An enzyme interacts with a specific type of substance or a group of substances usually called substrate, for catalyzing the chemical reactions [8]. For initiating the reaction, an energy barrier should be overcome, which is present in most of the reactions [9].

These barriers protect the unrespectable degradations of complex molecules [10]. So, it is useful for the preservation of life. During the metabolic process, these energy barriers are surmounted and break down of the complex molecules is initiated [11]. For completing the reaction some additional heat is needed called as "activation energy". But high activation energy increases the required temperature that would kill the cell [12].

Here, enzyme plays an important role in lowering the activation energy [13]. They react with some specific substrate and form an intermediate complex, a "transition state", that requires less energy for further proceeding the reaction [14]. This intermediate complex is rapidly broken down and forms a product. The unchanged enzyme is then ready to react with other substrates. The region, which binds to the substrate, is called the active site [15]. It forms one type of cavity, where the substrate binds. It permits only some particular substrate; hence, it is also used for determining the specificity of enzymes [16].

Metalloenzymes are enzyme-containing metal ions, which are directly bound with the protein or non-protein compounds known as prosthetic groups. About one-third of all enzymes are metalloenzyme [17]. These metallic ions are positively charged; hence they are ready for sharing the electron pair to other groups or atoms to form a tight bond. These ions behave like hydrogen ions [18]. By donating the electron to the metal ion, many atoms or groups of atoms form a bond with these ions, usually

known as ligand [19]. These ligands are positively charged. The coordination numbers of metal ion show the number of ligands which are connected to the metal ion. These are viewed by the concentric sphere [19]. The atoms which are connected by atoms are shown by an inner sphere and the atoms which are connected by the inner sphere are known as the second sphere [20]. The number of the atoms in these spheres is given by the size of metal ions as well as the size of ligands [21]. There are two models developed to study the mechanism of the catalytic cycle of a metalloenzyme. In one model only a small number of atoms is treated as quantum mechanically. Firstly this quantum mechanical model was used in 1997, with Density Functional Theory (DFT) methods to study the internal mechanism of methane monooxygenase (MMO) [22].

It used only a small number of atoms, normally 100 - 200 atoms at a time. In another method, the whole enzyme is treated quantum mechanically [23]. The active site of the enzyme is described quantum mechanically and the rest of the enzyme is described molecular mechanically. This model is known as the Quantum Mechanical/Molecular Mechanical (QM/MM) model [24]. In 2000, firstly the mechanism of galactose oxidase was understanding by the QM/MM model [25]. Nowadays, the results from the theoretical models have more importance for determining and explaining the mechanism of chemical reactions in the presence of metalloenzyme, than the traditional spectroscopic techniques [26].

Spectroscopic techniques apply to the actual system, so these techniques have many advantages. But, their interpretations of the results are extremely difficult, which makes it less preferable than QM/MM models [27] [28].

1.2 Cytochrome P450

Cytochrome P450 enzymes are the superfamily of enzymes containing heme cofactor present in all kingdoms of life, like in animals, plants, fungi, protists, bacteria, and also in viruses [29]. They have not been found in Escherichia coli [30]. More than 50,000 enzymes are found [31]. In Cytochrome P450, the term P450 has derived from the spectrometric peak at wavelength 450 nm of the absorption maximum of the enzyme when it is in a reduced state and complexed with carbon monoxide [32]. These enzymes are responsible for many chemical reactions like detoxification, synthesis etc [33]. Many of the Cytochrome enzymes are required a protein to transfer one or more electrons to reduce the iron. The P450 enzyme metabolized various compounds [34] using high-valent iron (IV) oxo species complex, generally known as Cpd1 [35]. This complex is formed during the catalytic cycle of Cytochrome P450 [36]. Initially, in the catalytic cycle, P450 is resting and a water molecule is ligated with it [37]. Whenever substrate enters, it tightly binds with Porphyrin [38] by expelling the water molecule [39].

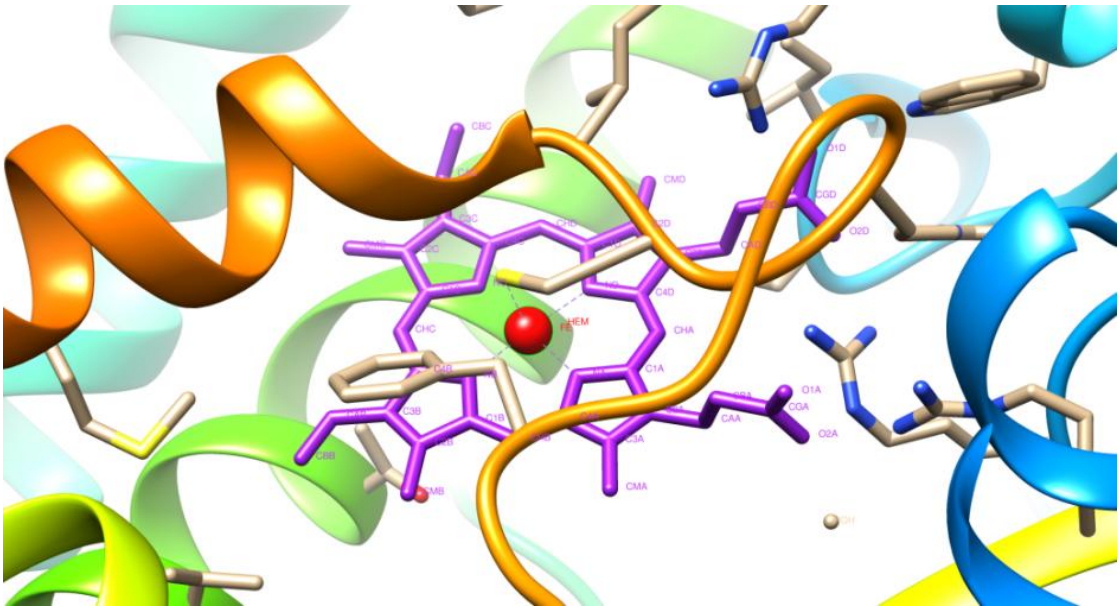

Figure 1.1: Active site of Cytochrome P450 as taken from PDB file 1W0E.

After the oxidation steps, ferric peroxide species is formed, known as compound 0 (Cpd 0), and then Cpd 0 converts into iron (IV)-oxo Porphyrin cation radical oxidants, known as compound I (Cpd I) through a protonation step [40]. It is the primary oxidant that is involved in the oxidation reaction of all members of P450 [41]. It has two degenerate spin state one is a quartet and the other is doublet [42]. These energy states are known as low spin energy states and high spin energy states [43]. A low spin energy state has no energy barrier [44] for completing the reaction while the high spin energy state has an energy barrier to cross for completing the reaction [45]. Active site of P450 is shown in Figure 1.1 as taken from the PDB file 1W0E.

1.3 Heme Enzyme

Heme enzyme is one of the most useful enzyme in biochemical reactions, especially in catalytic reactions [46]. It contains heme cofactor [12]. The main function of the heme enzyme is- to transfer the electron, to store and transfer the oxygen molecules [47]. In the structure of the heme enzyme [48][49], an iron ion is present at the center of the Porphyrin ring, and this iron is ready to react with specific substrates [9]. Cytochrome P450 is a superfamily of many enzymes containing heme cofactor [50]. In Cytochrome P450, the heme group is the active site of the enzyme [51]. Like Cytochrome P450, heme-copper oxidase is also a superfamily of another enzyme [52]. It also contains the heme factor and useful in the catalysis of various biochemical reactions [53]. These are membrane enzymes which catalyze the oxidation, aggregate the formation of many proteins and degradation of proteins in small peptides [48]. The formation of cytotoxic lipid peroxide is also catalyzed by the heme enzyme [54]. It is used in removal of toxicity of the liver, kidney, cardiac tissue, and central nervous system [55]. All over, the heme enzyme is a very useful enzyme in detoxification of internal organs [56] as well as in catalysis in many biochemical reactions [57].

Heme enzyme is a protein, formed by the combination of prosthetic group and found almost in all biological systems [58]. The structural and functional studies of the heme enzyme are done in a good deal [12]. These studies are comparatively easy due to the detectable spectroscopic properties of the prosthetic group that helpful in studies of many intermediate states of enzymes by various spectral methods [59].

These studies give better information that how the chemistry of the heme group is controlled by proteins [60]. Hence, it may be understood that the heme enzyme provided a rich system for detailed studies [61].

The study of heme enzyme by model mechanism is quite demanding [62]. This modeling is done by computer using various quantum mechanical methods [63]. It included almost 40 atoms [64]. In the study of Cytochrome P450 studies [65], the heme model without chain is used [66]. But, in many chemical reactions, the redox properties are usually affected by side-chain reactions [67][68]. So, a side chain model might be included for a proper and detailed study of biochemical reactions [69]. Active site of HEME enzyme is shown in Figure 1.2 as taken from the PDB file 5B4Z.

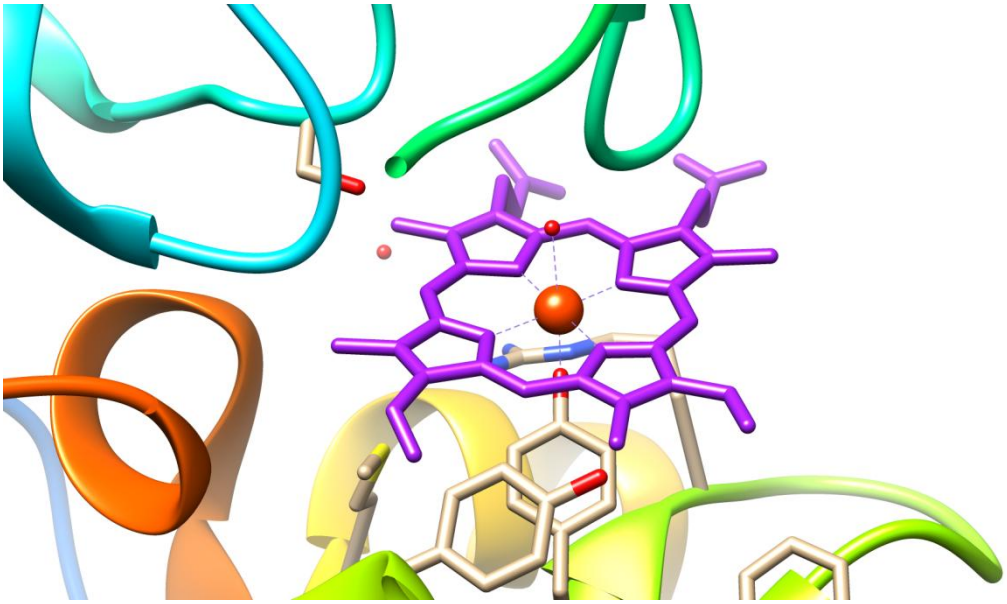

Figure 1.2: Active site of HEME enzyme as taken from the PDB file 5B4Z.

1.4 Non-Heme Enzyme

This enzyme is the same as the heme enzyme, but it does not contain the Porphyrin prosthetic group [70]. These enzymes also participate in biochemical processes [71] [72]. Non-heme enzymes are divided into two main categories:

1. Mononuclear Non-Heme enzyme iron enzyme
2. Dinuclear Non-Heme enzyme iron enzyme

1.4.1 Mononuclear non-heme iron enzyme

1.4.1.1 Tetrahydrobiopterin-dependent hydroxylases (PDHs)

Tetrahydrobiopterin-dependent hydroxylases (PDHs) are the largest family of enzymes which include the aromatic amino acid hydroxylase, such as phenylalanine hydroxylase (PAH) [73], tryptophan hydroxylase (TrpH) and tyrosine hydroxylase (TyrH), etc.

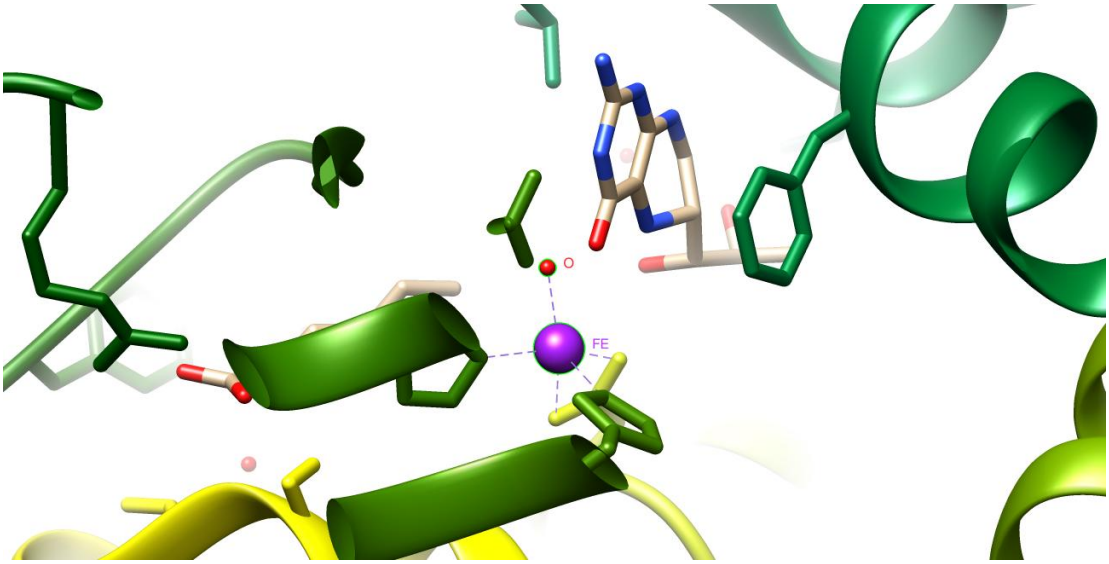

Figure 1.3: Active site of Tetrahydrobiopterin-dependent hydroxylases as taken from the PDB file 1MMT.

All of these enzymes catalyze the amino acid and biopterin cofactor. Active site of Tetrahydrobiopterin-dependent hydroxylases is shown in Figure 1.3 as taken from the PDB file 1MMT**.**

1.4.1.2 Alpha-Ketoacid dependent oxygenases (alpha KAOs)

These enzymes formed a large group of enzymes that is responsible for the catalysis of oxidative transformation like in aliphatic as well as aromatic hydroxylation,

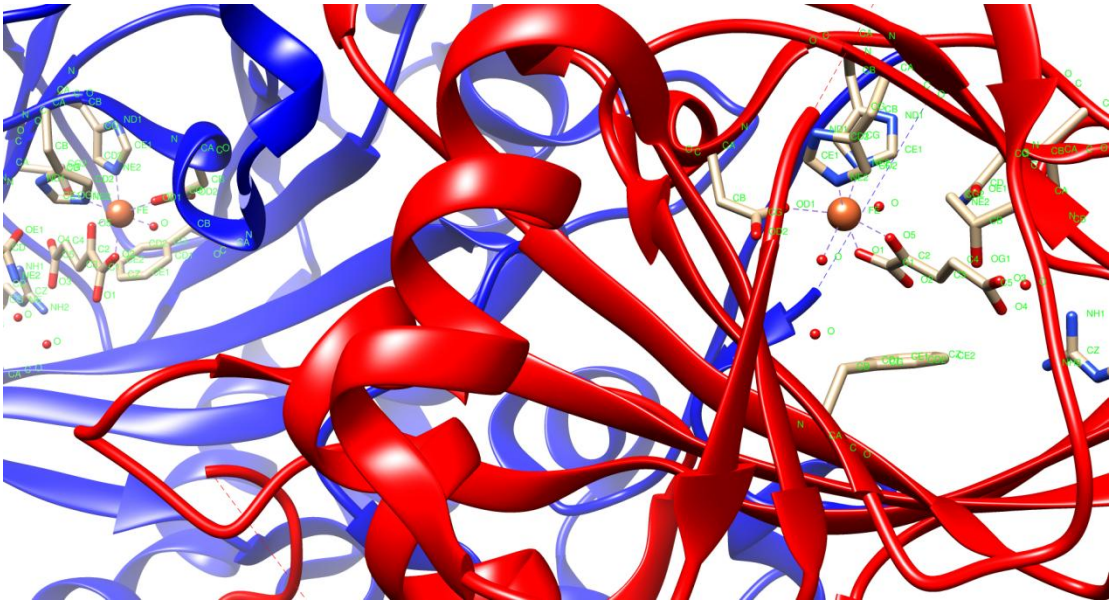

Figure 1.4: Active site of Alpha-Ketoacid dependent oxygenases (alpha KAOs) as taken from the PDB file 5YBN.

halogenations, epimerization, desaturation, ring expansion, and ring closure, etc [74]. These reactions are parts of many biochemical processes like regulation of gene expression [75]. DNA or RNA repair [76], cellular oxygen sensing [77], synthesis of antibiotics etc [78]. Active site of Alpha-Ketoacid dependent oxygenases (alpha KAOs) is shown in Figure 1.4 as taken from the PDB file5YBN.

1.4.2 Dinuclear Non-Heme Iron Enzyme

1.4.2.1 Methane monooxygenase (MMO)

The methane monooxygenase usually form methanol by oxidizing the methane gas. It contains an iron dimer complex linked by oxygen ligands [79]. It has four glutamates and two histidines [80].

One of the oxo groups activates methane by a hydrogen atom abstraction, and TS forms Fe_2 (III), Fe_2(IV) with a methyl radical [13], [44], [71], [81]. Active site of Methane monooxygenase (MMO) is shown in Figure 1.5 as taken from the PDB file 1MTY. Methane monooxygenases are often found in methanotrophic bacteria [82]. It is a class of bacteria that exist at the interface of various aerobic (oxygen-containing) as well as anaerobic (oxygen-devoid) environments [83]. One of the widely studied bacteria of this type is Methylococcus capsulatus [84].

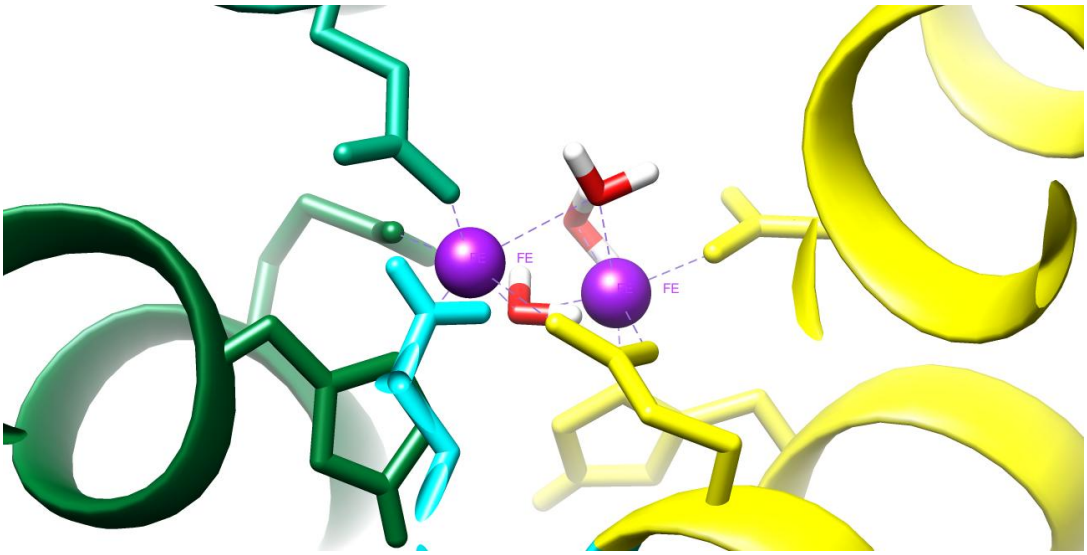

Figure 1.5: Active site of Methane monooxygenase (MMO) as taken from the PDB file 1MTY.

1.4.2.2 Ribonucleotide Reductase

It is also one type of dinuclear non-heme enzyme which catalyzes by replacing the hydrogen with hydroxide on the ribonucleotide to form deoxyribonucleotides,

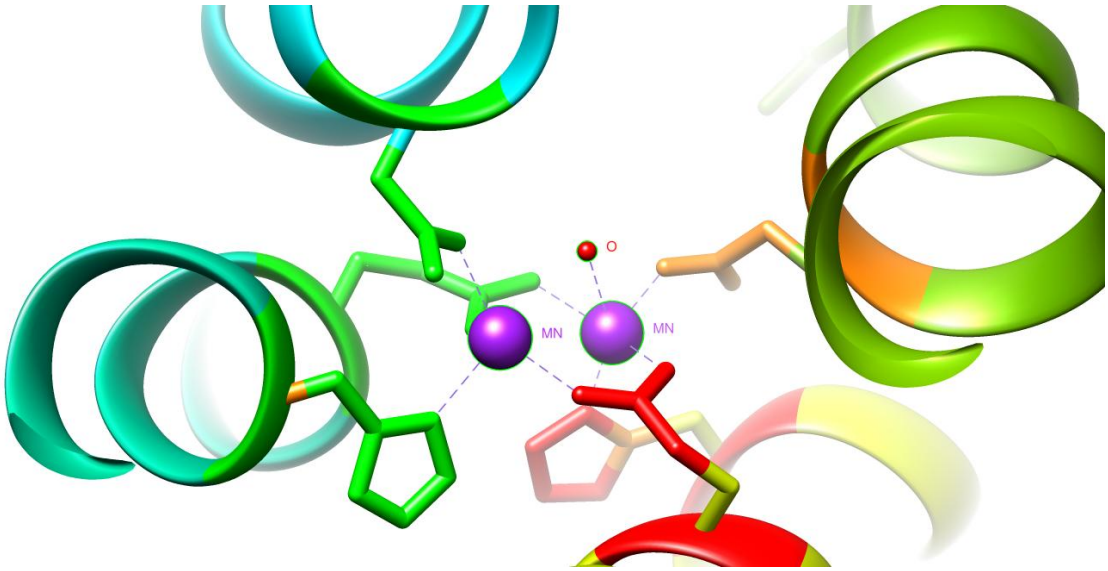

Figure 1.6: Active site Ribonucleotide Reductase as taken from the PDB file 2XO4.

which is the building block of the DNA. DFT studies [85] of these enzymes explain the whole mechanism very carefully. RNA has two subunits in which the second subunit is very stable Tyr radical [86]. These iron dimer complexes are the same as MMO [75] complexes, but the only difference that the glutamate ligand is replaced by a spartate. Active site Ribonucleotide Reductase is shown in Figure 1.6 as taken from the PDB file 2XO4.

1.5 Heme Iron Vs Non-Heme Iron

- The main difference of heme and non-heme enzyme is that, in heme enzyme Porphyrin ring is formed, while in non-heme enzyme it does not form [87].
- Heme iron is easily absorbed by the body, so that it is a big source of dietary iron for people both with or without hemochromatosis, while non-heme iron

does not absorb easily, that's why it is not a big source of iron. But, yes, it is different for people with homochromatosis [88].

In the human diet, heme iron is found in animal proteins, like meat, seafood, fish, etc., while non-heme iron is found in plant food like vegetables, grains, beans, nuts, fruits, seeds, but of course, it is also found in animals product like eggs, dairy product/milk etc [89] and also in animal meat. This means animal meat is the combination of both heme and non-heme iron.

1.6 Catalytic Cycle

It is one of the main reaction which operates the all biochemical reaction processes. The catalytic cycle of Cytochrome P450 is like an automatic nano-machine that once it operates [90], continuously run. This cyclic reaction is completing in seven steps, as shown in Figure 1.7 [43]. The cyclic reaction starts with the resting state (1), in which a distal water molecule is bound to the six ligated positions of the low spin state of hexa-coordinated ferric ion [91].

The entry of the substrate, like alkane AlkH, displace the water molecule, the Penta-coordinated ferric-Porphyrin (2) [92], remains this ferric complex has a slightly better electron accepter tendency than the resting state, therefore it takes one electron from the reductase protein and triggers from low spin state to high spin state and form five coordinated high spin state of ferrous complex (3), this ferrous complex further binds with O_2 and formed ferrous dioxygen complex (4), it has a good electron accepter tendency, which accepts one electron from reductase protein, resulting in ferric-peroxo anion species (5), this is rate determining step in catalytic cycle [93].

Due to good Lewis base, it is quickly protonated and forms a ferric hydroperoxide complex (6), which is called Cpd 0. It is also a good Lewis base, which abstracts a

proton to form Cpd 1 (7) and also produces water. Cpd 1 transfers an oxygen atom to the substrate by converting alkane into alcohol and this alcohol species contains a pocket in which water molecule binds, and hence restoring the resting state. Yet, this catalytic cycle, if once started it occurs continuously. That's why it is also known as an automatic nanomachine [52]. This is shown in the Figure 1.7.

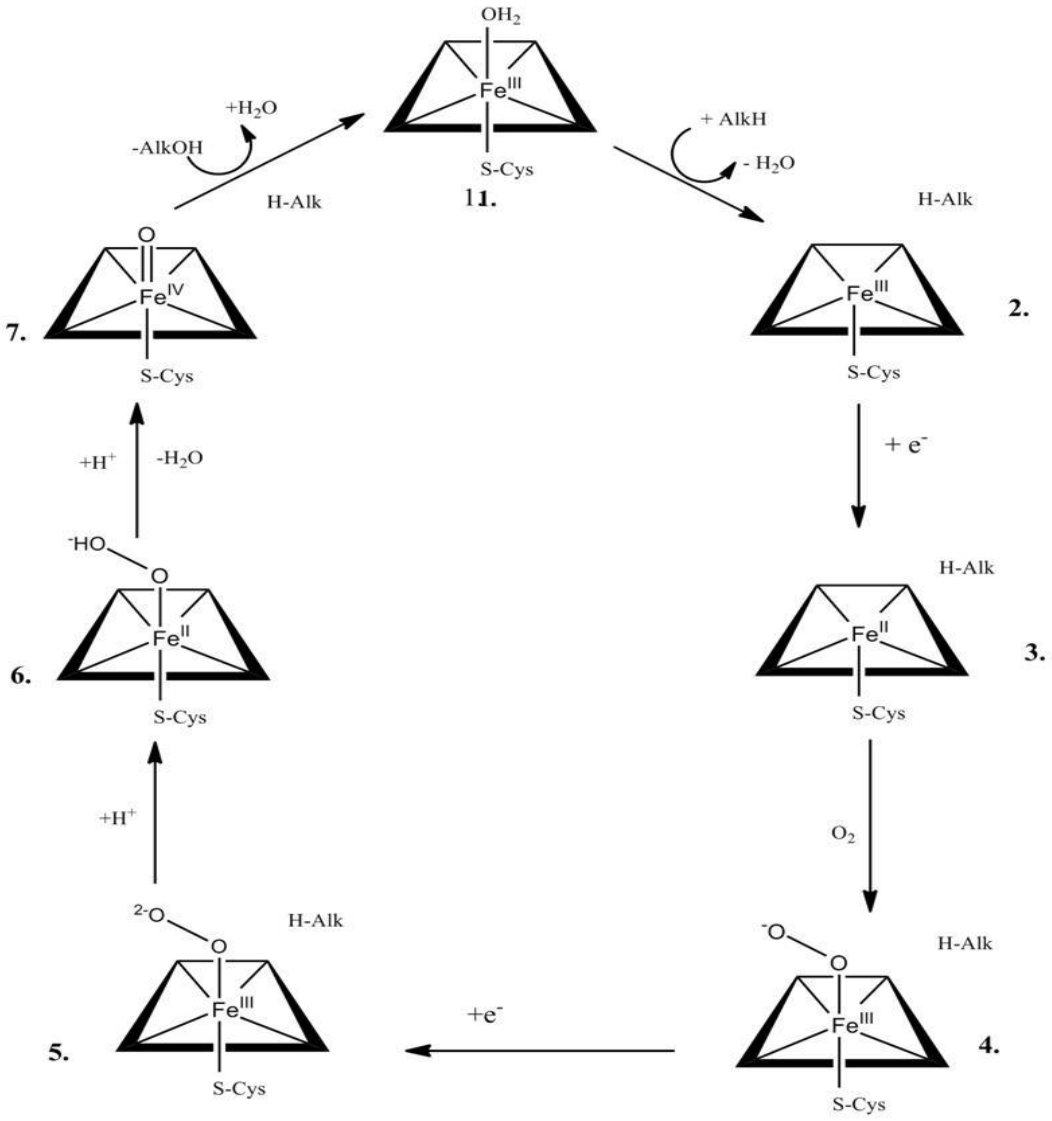

Figure 1.7: Catalytic Cycle of Cytochrome P450.

The efficiency of catalytic cycle is sufficiently good, but there is some factor which affects it. The first one is the donor ability of the thiolate ligand. It is usually referred to as the "Push Effect" [94]. The second one is protonation as shown in step (6), which

converts Cpd 0into cpd1. It prevents the further generation of hydrogen peroxide and other oxygen species. And the last one is excess of a water molecule into the alcohol species pocket [95].

This makes the binding between the enzyme and substrate comparatively weak. Water molecule is important for the protonation [96], but too much water molecules lead to the uncoupling of enzyme and substrate [79].

So, it is important to find the modified enzyme which gives better stability and activity to the catalytic cycle [98]. After much theoretical work, it is found that the interaction of the amidic group of the $Gln_{360,}$ $Gly_{359,}$ Leu_{358} with the sulfur of ligated cysteine and also the interaction of Gln_{360} with the carbonyl group [99] gave stable and comparatively good enzyme reactivity [100].

1.7 Rebound Controversy

P450 used in metabolism of various molecules and chemicals within cells. So this enzyme plays an important role in the synthesis of many molecules, such as steroid hormones, cholesterol and various other fatty acids [101]. P450 enzymes also metabolize external substances, like medications, as well as internal substances, like toxins. Approximately 60 P450 enzymes are found in human body [102]. Cytochrome P450 catalyzes various substances via aromatic as well as aliphatic hydroxylation [60], N-dealkylation, N-demethylation, etc., C-H hydroxylation via P450 is one of the most important reactions in the catalytic cycle of Cytochrome P450. Iron-containing Porphyrin complexes convert into the high valent iron-oxo species usually known as Cpd I shown in Figure 1.8. Then rebound step of the alkyl radical forms ferric alcohol complex. Focusing on the controversy which is closely related to the rebound mechanism in C-H hydroxylation reaction [103], this rebound mechanism was first

introduced by Grooves and McClusky in 1976 [104]. According to him, in alkane hydroxylation, the rebound mechanism is proceeded through P450 enzyme. It is followed by mainly two steps, in the first step Cpd1 forms Cpd 0via abstracting the hydrogen atom from the alkenes, as a result, one alkyl radical is formed. In the second step of the rebound mechanism, alkyl free radical is partitioned into two various processes which are often competing with each other. It can either rebound to form an unrearranged (U) alcohol complex, contain the original stereochemical information which is possessed by the alkane, or it can first undergo skeletal rearrangement then rebound and form the rearranged (R) alcohol complex as shown in Figure 1.9 [105]. The ratio of the energy of these two alcohol complexes give the lifetime of alkyl free radicals [106].

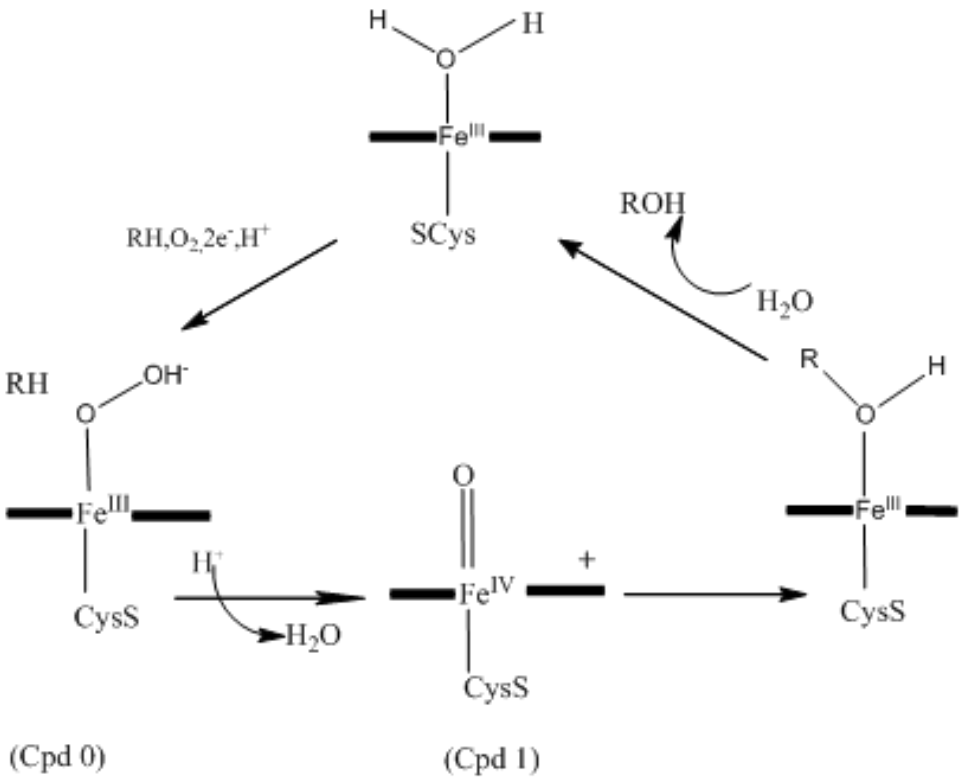

Figure 1.8: Catalytic cycle of Cytochrome P450.

It was firstly calculated by Ortiz de Montellano and Stearns [6, 42], using bicyclo pentane [107], approximately 50 ns. The real intermediate radical species has too short

lifetime These unrealistic lifetimes of free radicals with rearranged alcohol complex products have led Newcomb and co-workers [108] to suggest that radical intermediates are not present during the reaction, and C-H hydroxylation proceeds by two competing mechanisms from two oxidant species of the enzyme, Cpd I and ferric peroxide species, Cpd 0 (Figure 1.8) [109]. In the Figure 1.10 it is shown that in one mechanism a concerted (O) insertion from Cpd I into the C-H bond is formed, while in second hydroxo ion (OH^-) insertion from Cpd 0 into the C-H bond is formed [110].

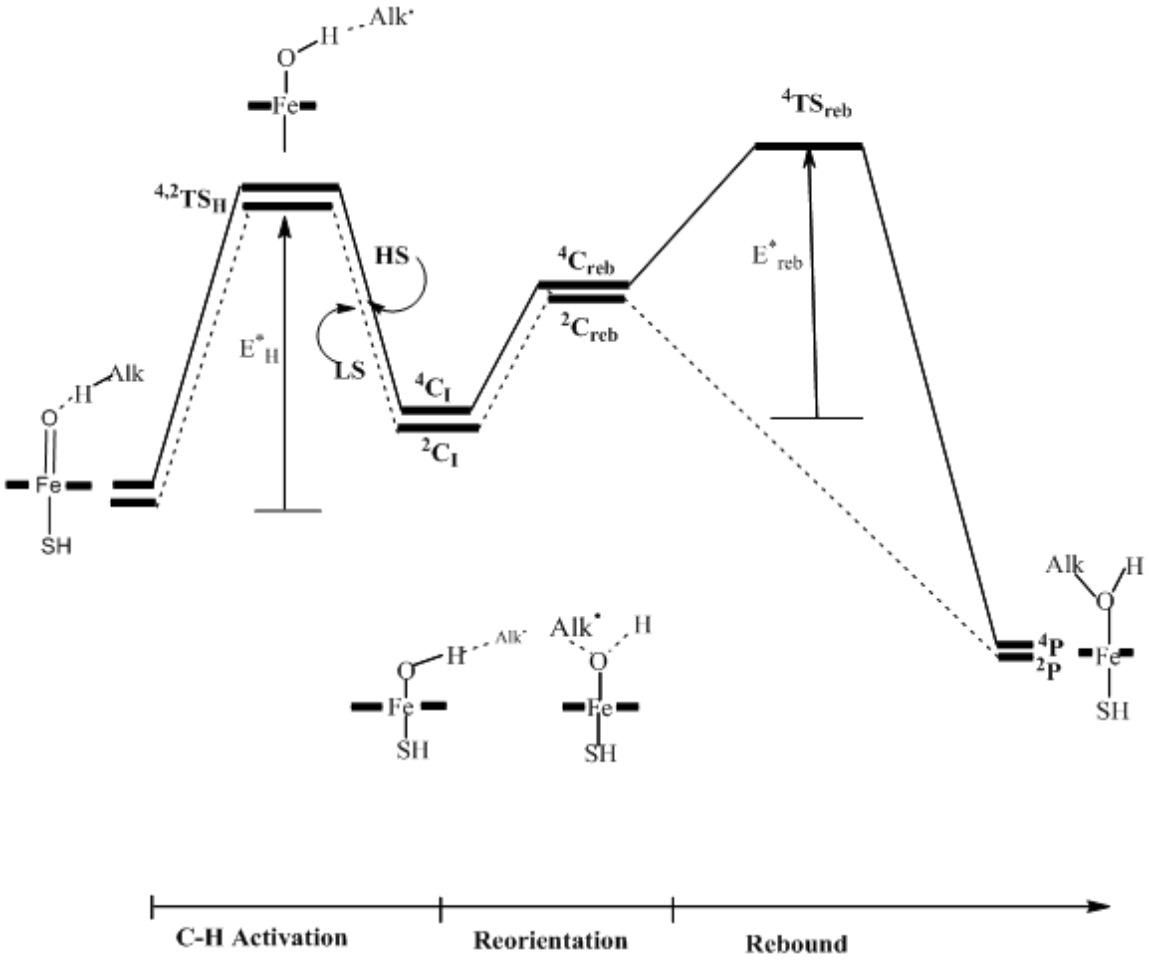

Figure 1.9: Reaction profile of C-H hydroxylation by Cpd I, calculated by density functional theory, show high-spin (HS) state and low-spin (LS) state components.

Finally, an alcohol complex product is formed [111]. From the Ortiz de Montellano and Stearns calculation, it is given that oxidant of cpd1 is two-stage process, called as "Two-State Reactivity" (TSR). DFT calculations [112] have also offered a simple resolution for controversy, through the study of C-H hydroxylation [113].

In terms of a two-state reactivity (TSR) of Cpd I; named as, "one oxidation with two different pathways". It has been further demonstrated [114], that Cpd I is highly versatile and can lead to multi-state reactivity, (MSR) [115]. There are at least seven different low-lying spin states that are possible in the product distribution. These TSR and MSR scenarios are responsible for the different paths of single oxidant species, Cpd I. Many theory have already offered a resolution for this controvers [116]. So then, few more theories are performed by the Jerusalem group [117] and by Yoshizawa et al. [117].

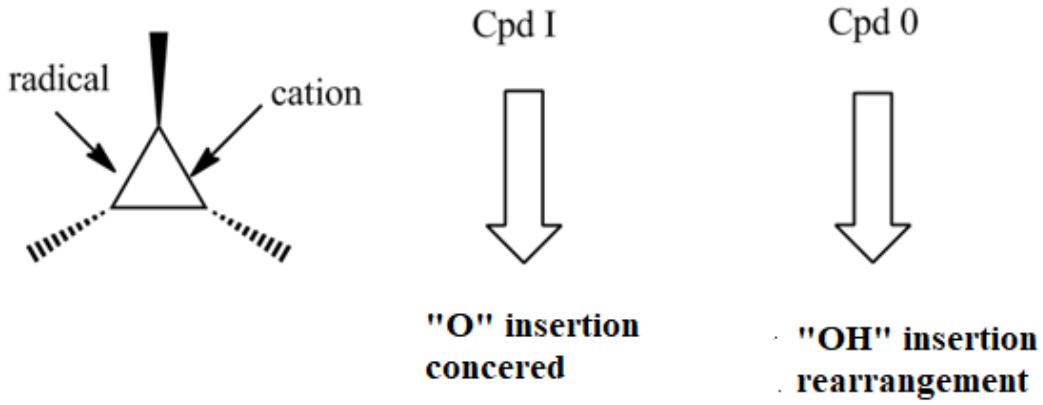

Figure 1.10: The two-oxidant using Cpd I and Cpd 0**.**

Also Gualar et al. [8], by using molecular dynamics simulations, described the rebound step in the methyl monooxygenase (MMO) enzyme [118], and compare to the rebound in P450 enzyme. These studies cover wide range of results which explained the rebound mechanism in alkane hydroxylation, that is appears as the origin of the current controversy [119].

1.8 Origin of TSR/MSR of Cpd I

Why the oxidation reaction of Cpd I shows two-state or multistate reactivity? Here are some answers to this question which explains the origin of the TSR and MSR. Cpd1 has d-orbitals with five subshells, $\boldsymbol{\delta_{x^2-y^2}}$, $\boldsymbol{\pi^*_{xz}}$, $\boldsymbol{\pi^*_{yz}}$, $\boldsymbol{\sigma^*_{z^2}}$, and $\boldsymbol{\sigma^*_{xy}}$, and a ligand with mixed orbital a_{2u} as shown in Figure 1.11. These orbitals are the key orbitals of Cpd I, here only δ orbital is pure nonbonding orbital, while the remaining have antibonding interaction with various ligands [120]. There are three odd electrons in π^* and a_{2u} orbital. These orbitals are virtually disjoint, so there is very weak interaction between these electrons [121].

As a result, the ferromagnetic state with all spins up and antiferromagnetic state, with opposite spin states are formed. DFT and QM/MM calculations give proximity to these two states [122]. Recently Quantum mechanical/ Molecular Mechanical (QM/MM) calculations of Cpd I of P450cam [123] which explained that antiferromagnetic state is ground state, while at 10-21 cm^{-1} above the ground state ferromagnetic state lies, by offering the electronic structure [124].

So it is concluded that Cpd I has a degenerate ground state, one is low spin (LS) state and another is high spin (HS) state [125]. So the arisen controversy of two-state reactivity is resolved by giving the above theory [126]. Ligands of P450 have all high lying orbitals, close to d-orbital [112]. During the reaction, substrate is formed at high lying orbital [127]. As a result, the number of closely lying singly occupied orbital is large and continually increases as the reaction progresses [128]. It gives the rise to a dense manifold of states [129].There is different factor for exchanging the interaction between the electrons in d orbital, that favors the high-spin state [130].

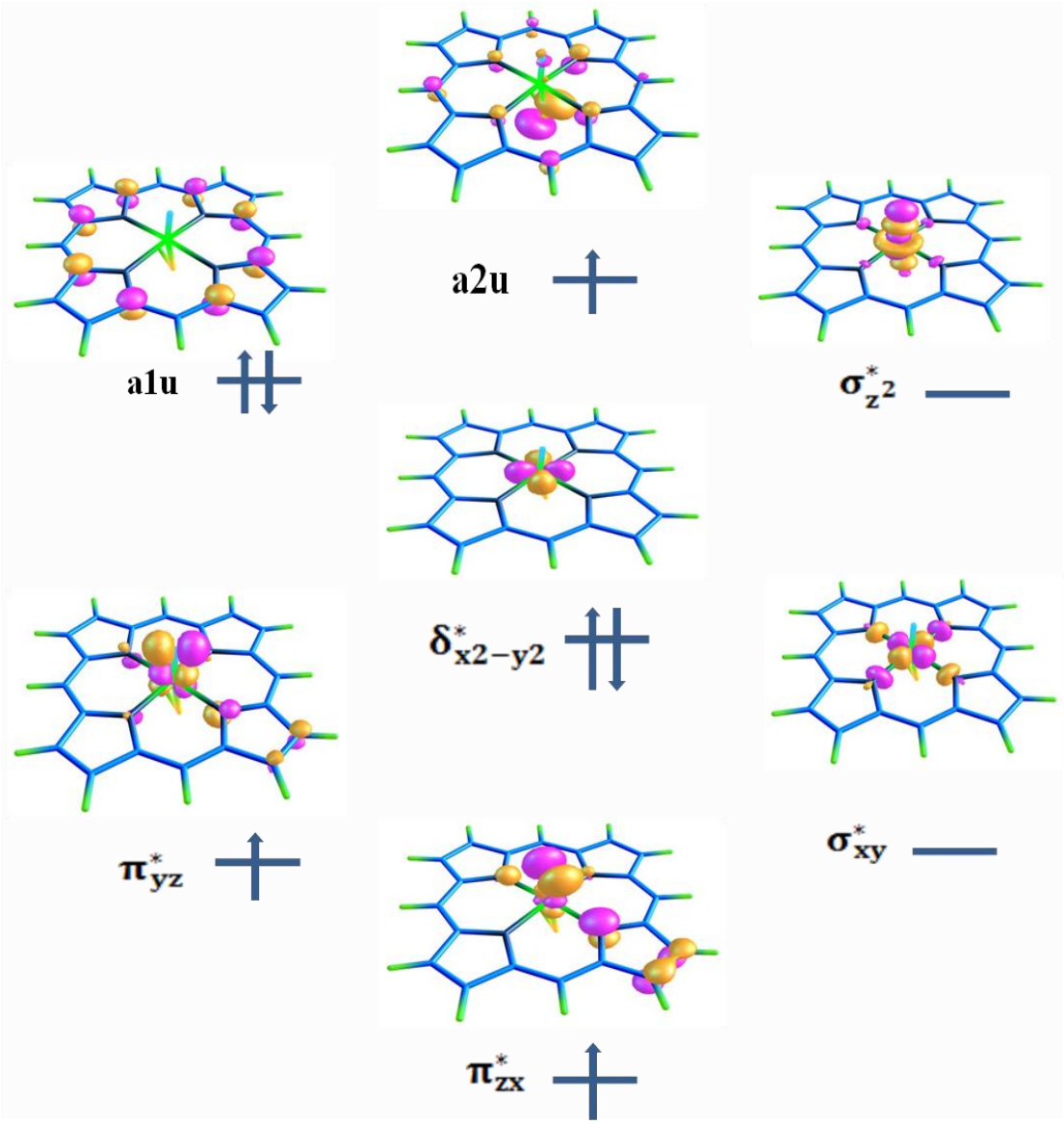

Figure 1.11: Key orbitals of Cpd 1 of Cytochrome P450.

Generally, these states remain close to the reaction pathway [131]. When the orbitals of a molecule undergoing oxidation [132], become accessible, the number of states increases and the TSR/MSR scenario is obtained as shown in Figure 1.9 [133]. Hence the controversy of TSR/MSR is resolved by giving the above explanation [134].

1.9 Product Isotope Effect in TSR

Two state reactivity (TSR) models have been given many predictions [135]. It specially concerns with the product isotope effect [136]. A product isotope effect,

namely PIE in the hydroxylation [115], when the hydrogen atom transferred from the alkane to iron-oxo species, is basically replaced by the deuterium atom, then the product ratio [U/R] shows an isotopic effect [137], it is observed that the Unarranged (U) and Rearranged (R) product could not be generated from a single pathway. The product must be mediated by two different pathways or from two different sources. So, two-state reactivity (TSR) [115] scenarios predict that there should be a Product Isotope Effect (PIE) on the [U/R] quantity [122].

The TSR model concerns the different sensitivity of the high spin as well as low spins state products to C-H and C-D substitution in bond during hydroxylation [138]. Since high spin and low spin hydrogen-abstraction transitions ($^{4,2}TS_H$) are quite different, thus their corresponding kinetic isotope effects (KIE) will also be different, as $KIE_{LS} \neq KIE_{HS}$.

This will be offered an intrinsic product isotope effect, (PIE_{int}) [102] on the rearranged (R) and unarranged (U) products, defined by Eq. 1.1

$$PIE_{int} = PIE_{TSR} = \frac{[U_H/U_D]}{[R_H/R_D]_{int}} = \frac{KIE_{LS}}{KIE_{HS}} \qquad 1.1$$

In the above equations, U arises from the low spin mechanism, while R arises from the high spin path. The deviation of PIE_{int} from unity will depend on the structures of $^{2}TS_H$ versus $^{4}TS_H$ [102]. Recently many calculations show that PIE_{int} for probe substrate is >1, in the same direction as the observed quantity derived from intrinsic isotope effect values [139].

After few years, Jones and co-workers [140] wrote an expression for observed product isotope effect, $PIE_{obs,}$ based on Two State Reactivity is shown in Eq. 1.2:

$$PIE_{obs} = \frac{[U_H/U_D]}{[R_H/R_D]_{obs}} = \left(\frac{KIE_{LS}}{KIE_{HS}}\right)\left\{\frac{([ES_H/ES_D]_{LS})}{([ES_H/ES_D]_{HS})}\right\} = \boldsymbol{PIE_{int}}\left\{\frac{([\boldsymbol{ES_H}/\boldsymbol{ES_D}])_{\boldsymbol{LS}}}{([\boldsymbol{ES_H}]/[\boldsymbol{ES_D}])_{\boldsymbol{HS}}}\right\} \qquad \mathbf{1.2}$$

From the above expression it is observed that PIE_{obs} will depend on the intrinsic quantity, and on the relative concentrations, of low spin and high spin enzyme-substrate (ES) species of the Protio and Deuterio with ^{2,4}Cpd I species. So PIE_{obs} will also involve those effects which are concerned with the switching dynamics of enzymes–substrate (ES) of the Protio as well as Deuterio varieties and various reactivity sites.

These effects are not basically direct related to the Intrinsic Product Isotopic Effect (PIE_{int}). Nevertheless, elucidation of the present complex dynamics will be required often to understand the observed PIEs [50]. The TSR model has been given various predictions. It concerns with the product isotope effect. Two-state reactivity scenario predicts that there should be PIE on the [U/R] quantity [119].

In Figure 1.12, an example of the spin-dependent Kinetic Isotope Effect (KIE) is shown. During the bond activation of non borane by FeO^+ in gas phase, the KIE value for the $C\text{-}H_{endo}$ bond is much more smaller than the $C\text{-}H_{exo}$ bond [140]. These differences are basically explained by spin-dependent two-state reactivity, one is low spin state (LS) activating the $C\text{-}H_{endo}$ bond, while high spin state (HS) activating the C. Various studies of gas-phase reactivity of FeO^+ cation have been made with hydrogen, methane [116], benzene [141], and several other organic substrate [71]. Hallmark is formal hydrocarbons of C-H bond observed with FeO^+, because of its relevance to biocatalysts like Cytochrome P450 [142] as well as Methane monooxygenase, which bear high-valent iron-oxo units as a key part of active sites. After the density functional study of C-H bond activation of norbornane by FeO^+, its different KIE [143] values are observed as shown in Figure 1.12.

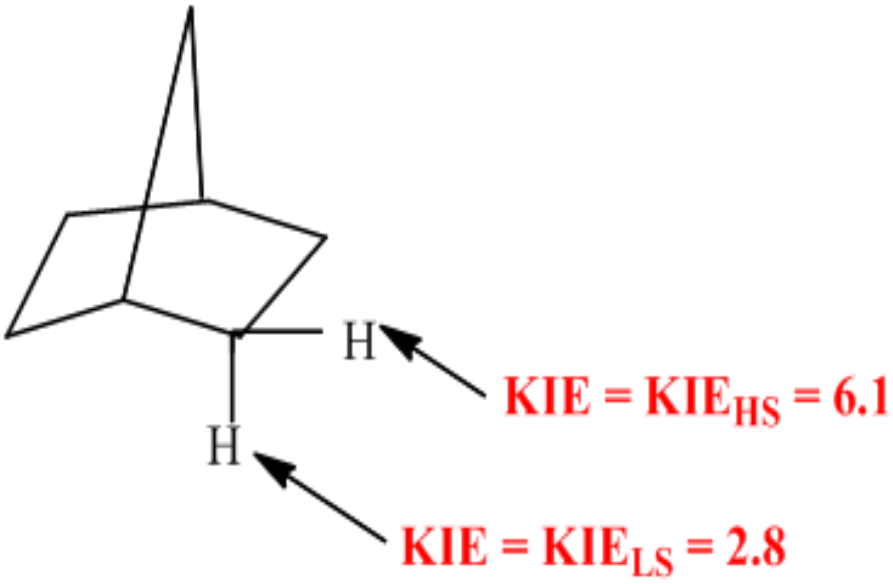

Figure 1.12: KIE_s in Norbornane of HS and LS C-H bond activations.

A different Kinetic Isotope Effect (KIE) value for the different C-H bonds of norbornane is originated by different spin state selectivity [144] of their corresponding reactions of bond activation [145].

1.10 Porphyrin

Porphyrin is a normal end product of hemoglobin metabolism and is the substance responsible for the reddish staining that is seen around the eyes of some breeds of dogs [81]. A Porphyrin is a group of macrocyclic aromatic compounds [146] made of four pyrrole rings which are internally connected by a methane bridge (=CH-) [147]. It is a square planar molecule and can extend its structure due to its aromatic character [148]. Pyrrole rings are attached in such a manner, that nitrogen atoms facing at the center [149] and form Porphyrin [150].

A metal ion is captured by the center of Porphyrin [151], which naturally forms a stable metallic complex [152]. Metal ions of these complexes, accept six coordinating ligands form an octahedral structure [153]. So, these complexes are widely used in

chemical reactions of a biological system [154]. Hence, the study of Porphyrin is essential for the investigations of drug metabolism through Cytochrome P450 enzymes [155].

Porphyrin contains a total of 26 π-electrons, in which 18 electrons are formed an aromatic compound [155]. It has a deep color due to strong absorption in the visible region of the electromagnetic spectrum [75]. Porphyrin name is derived from the Greek word [156], which means "purple" [157].

Heme, is a pigment in red blood cells, Protein hemoglobin are the best-known families of Porphyrin complexes [58]. Without a metal ion, Porphyrin reacts as a free base [122]. Porphyrin, in which iron metal [158] is attached at the center known as the "Heme" enzyme. It is responsible for many biochemical reactions [159]. Porphyrins are present in many living organisms [160].

They are found in animals as well as plants, and responsible for many chemical reactions [161]. Tetrapyrrolic Porphyrin is responsible in many fields due to optical and redox properties [162]. It is widely used in the biomedical field [163], as photosensitizers in photodynamic therapy [142].

Expanded Porphyrins [164] have many important properties, which are useful in area of non-linear optics [128] anion recognitions [165], anticancer drug development, cation coordination [166] and study of properties of the aromatic compound in many hetero-annulenes. Expanded Porphyrins have liquid crystalline behavior [167], were first reported more than three decades ago [167]. The derived results of liquid crystals from expanded Porphyrins are exceedingly rare [161] [135]. There are two main expanded Porphyrin mesophase and both are derived from oligopyrrolic macrocycles [168]. Tetraphenyl Porphyrins [169], an expanded Porphyrin having liquid crystal

behavior [170] at room temperature has been reported one decade ago [171]. The liquid crystal behavior [172] found with tetraphenyl as well as octa-substituted is columnar [14], this is due to, the planar discotic structure of the Porphyrin macrocycle [173]. Expanded Porphyrins have a "liquid crystal" property [174], [175]. Nowadays, it is the center point of research.

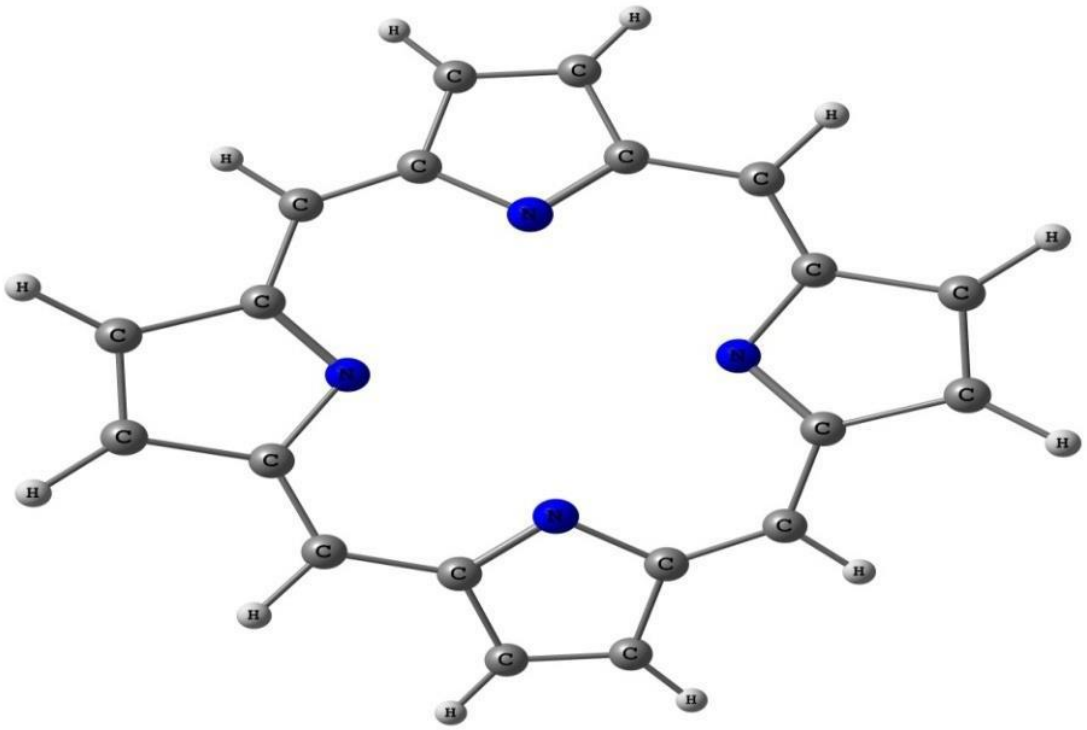

Figure 1.13: Optimized geometry of Porphyrin ring.

As discussed above, Porphyrins, serve wide range of purposes in animals, plants, and bacteria also because of their useful optical, redox, electronics, spectral and many other properties. So, this is also known as an evolutionarily conserved molecule. And they are continuously modified for use of multipurpose many fields. The optimized geometry of the Porphyrin ring is shown in Figure 1.13.

References

[1] N. J. Kershaw, M. E. C. Caines, M. C. Sleeman, C. J. Schofield, "The enzymology of clavam and carbapenem biosynthesis", *Chemical Communications*, 34, 4251–4263, **2005**.

[2] A. J. Lee, M. X. Cai, P. E. Thomas, A. H. Conney, B. T. Zhu, "Characterization of the oxidative metabolites of 17β-estradiol and estrone formed by 15 selectively expressed human cytochrome P450 isoforms", *Endocrinology*, 144, 3382–3398, **2003**.

[3] Z. Huang, F. P. Guengerich, L. S. Kaminsky, "16α-Hydroxylation of estrone by human cytochrome P4503A4/5", *Carcinogenesis*, 19, 867–872, **1998**.

[4] A. C. Rosenzweig, P. Nordlund, P. M. Takahara, C. A. Frederick, S. J. Lippard, "Geometry of the soluble methane monooxygenase catalytic diiron center in two oxidation states.", *Chem. Biol.*, 2, 409–18, **1995**.

[5] J. T. Groves, "Key elements of the chemistry of cytochrome P-450: The oxygen rebound mechanism", *J. Chem. Educ.*, 62, 924–927, **1985**.

[6] N. Suzuki, "Novel iron porphyrin-alkanethiolate complex with intramolecular NH···S hydrogen bond: Synthesis, spectroscopy, and reactivity ", *J. Am. Chem. Soc.*, 121, 11571–11572, **1999**.

[7] F. Esteves, P. Urban, J. Rueff, G. Truan, M. Kranendonk, "Interaction modes of microsomal cytochrome p450s with its reductase and the role of substrate binding", *Int. J. Mol. Sci.*, 21, **2020**.

[8] A. Altun, V. Guallar, R. A. Friesner, S. Shaik, W. Thiel, "The effect of heme environment on the hydrogen abstraction reaction of camphor in P450cam

catalysis: A QM/MM study", *J. Am. Chem. Soc.*, 128, 3924–3925, **2006**.

[9] R. Raag, "Crystal Structure of the Cytochrome P-450CAM Active Site Mutant Thr252Ala", *Biochemistry*, 30, 11420–11429, **1991**.

[10] S. Kumar, U. Bandyopadhyay, "Free heme toxicity and its detoxification systems in human.", *Toxicol. Lett.*, 157, 175–88, **2005**.

[11] M. Tuberculosis, "Optimization of Azole- Antifungal Drugs : An Attempt for Search of Better Drug for Treatment of TB with CYP450 from", *Intl. J. Engg. Sci. Adv. Research*, 6, 53–55, **2020.**

[12] S. Narimatsu, M. Tachibana, Y. Masubuchi, S. Imaoka, Y. Funae, T. Suzuki, "Cytochrome P450 Isozymes Involved in Aromatic Hydroxylation and Side-Chain N-Desisopropylation of Alprenolol in Rat Liver Microsomes.", *Biol. Pharm. Bull.*, 18, 1060–1065, **1995.**

[13] L. Ji, Abayomi S. Faponle, Matthew G. Quesne, Mala A. Sainna, Jing Zhang, Alicja Franke, "Drug metabolism by cytochrome P450 enzymes: What distinguishes the pathways leading to substrate hydroxylation over desaturation?", *Chem. - A Eur. J.*, 21, 9083–9092, **2015.**

[14] M. Arend, B. Westermann, N. Risch, "Modern Variants of the Mannich Reaction", *Angew. Chemie Int. Ed.*, 37, 1044–1070, **1998**.

[15] M. R. A. Blomberg, P. E. M. Siegbahn, G. T. Babcock, M. Wikström, "Modeling cytochrome oxidase: A quantum chemical study of the O-O bond cleavage mechanism", *J. Am. Chem. Soc.*, 122, 12848–12858, **2000**.

[16] C. M. Bathelt, L. Ridder, A. J. Mulholland, J. N. Harvey, "Aromatic Hydroxylation by Cytochrome P450: Model Calculations of Mechanism and Substituent Effects," *J. Am. Chem. Soc.*, 125, 15004–15005, **2003.**

[17] J. Holm ,Rainer Hillenbrand, Volker Steuber,Udo Bartsch,Marion Moos, Volker Steuber,Udo Bartsch,Marion Moos, "Structural features of a close homologue of L1 (CHL1) in the mouse: A new member of the L1 family of neural recognition molecules", *Eur. J. Neurosci.*, 8, 1613–1629, **1996**.

[18] Y. Wang Hui Chen, Masatomo Makino, Yoshitsugu Shiro, Shingo Nagano Shumpei Asamizu Hiroyasu Onaka Sason Shaik, "Theoretical and experimental studies of the conversion of chromopyrrolic acid to an antitumor derivative by cytochrome P450 StaP: The catalytic role of water molecules", *J. Am. Chem. Soc.*, 131, 6748–6762, **2009.**

[19] P. E. M. Siegbahn, R. H. Crabtree, "Mechanism of C-H activation by diiron methane monooxygenases: Quantum chemical studies", *J. Am. Chem. Soc.*, 119, 3103–3113, **1997**.

[20] J. Seo, J. Jang, S. Warnke, S. Gewinner, W. Schöllkopf, G. Von Helden, "Stacking Geometries of Early Protoporphyrin IX Aggregates Revealed by Gas-Phase Infrared Spectroscopy", *J. Am. Chem. Soc.*, 138, 16315–16321, **2016**.

[21] Toshihiro Okamoto, "Development of innovative organic semiconductors driven by state of art analytical instruments", *Rigaku Journal*, 4, **2019.**

[22] R. Verma, U. Schwaneberg, D. Roccatano, "Insight into the redox partner interaction mechanism in cytochrome P450BM-3 using molecular dynamics simulations", *Biopolymers*, 101, 197–209, **2014**.

[23] A. Warshel, M. Levitt, "Theoretical studies of enzymic reactions: Dielectric, electrostatic and steric stabilization of the carbonium ion in the reaction of lysozyme", *J. Mol. Biol.*, 103, 227–249, **1976.**

[24] S. Shaik, S. Cohen, Y. Wang, H. Chen, D. Kumar, W. Thiel, "*P450 enzymes:*

Their structure, reactivity, and selectivity - Modeled by QM/MM calculations", 110,15-35, **2010.**

[25] X. Chen, M. Chu, D. P. Giedroc, "Spectroscopic characterization of Co(II)-, Ni(II)-, and Cd(II)-substituted wild-type and non-native retroviral-type zinc finger peptides.", *J. Biol. Inorg. Chem.*, 5, 93–101, 2000, **2019.**

[26] J. L. Sessler, Nyancy, Halder, Krushna Chandra Sahoo, Kumar Gaurav, "Inverted sapphyrin: A new family of doubly N-confused expanded porphyrins", *J. Am. Chem. Soc.*, 128, 12640–12641, **2006**.

[27] R. L. Hill, M. Gouterman, A. Ulman, "Tetraphenylporphyrin Molecules Containing Heteroatoms Other Than Nitrogen. 7. Emission and Electronic Structure of Rings Containing Sulfur and Selenium", *Inorg. Chem.*, 21, 1450–1455, **1982.**

[28] J. C. Schöneboom, "The elusive oxidant species of cytochrome P450 enzymes: Characterization by combined quantum mechanical/molecular mechanical (QM/MM) calculations", *J. Am. Chem. Soc.*, 124, 8142–8151, **2002**.

[29] D. C. Lamb, Li Lei, G. Andrew, S. Warrilow, I. Galina Lepesheva, G. L. Jonathan Mullins, Michael R Waterman, Steven L Kelly, "The First Virally Encoded Cytochrome P450", *J. Virol.*, 83, 8266–8269, **2009**.

[30] Y. K. Booth, W. Kitching, J. J. De Voss, "Biosynthesis of insect spiroacetals", *Nat. Prod. Rep.*, 26, 490–525, **2009**.

[31] D. R. Nelson, "The cytochrome P450 homepage", *Hum. Genomics*, 4, 59–65, **2009**.

[32] I. Schlichting, Mathias A.S.Hass, Yuki Kikui, Wei-Min Liu, Betül Ölmez,

Simon P. Skinner, Anneloes Blok, "The catalytic pathway of cytochrome P450cam at atomic resolution", *Journal of Molecular Biology*, 287, 1615–1622, **2000**.

[33] J. Yoo, E. Jeoung, C. H. Lee, "Fluorophore-appended calix[4]pyrroles: Conformationally flexible fluorometric chemosensors", *Supramol. Chem.*, 21, 164–172, **2009.**

[34] J. L. Vennerstrom, "8-Aminoquinolines active against blood stage Plasmodium falciparum in vitro inhibit hematin polymerization", *Antimicrob. Agents Chemother.*, 43, 598–602, **1999**.

[35] X. Y. Wang, "Do two oxidants (ferric-peroxo and ferryl-oxo species) act in the biosynthesis of estrogens? A DFT calculation", *RSC Adv.*, 8, 15196–15201, **2018**.

[36] N. Vale, R. Moreira, P. Gomes, "Primaquine revisited six decades after its discovery", *Eur. J. Med. Chem.*, 44, 937–953, **2009.**

[37] S. Shaik, S. P. De Visser, "Computational approaches to cytochrome P450 function", *Cytochrome P450 Struct. Mech. Biochem, Third Ed.*, 67, 45–85, **2005**.

[38] D. R. Hill, J. K. Baird, M. E. Parise, L. S. Lewis, E. T. Ryan, A. J. Magill, "Primaquine: Report from CDC expert meeting on malaria chemoprophylaxis I", *Am. J. Trop. Med. Hyg.*, 75, 402–415, **2006**.

[39] C. Z. Ai, Y. Liu, D. C. Chen, Y. Saeed, Y. Z. Jiang, "Conformational turn triggers regio-selectivity in the bioactivation of thiophene-contained compounds mediated by cytochrome P450", *J. Biol. Inorg. Chem.*, 24, 1023–1033, **2019**.

[40] A. Altun, S. Shaik, W. Thiel, "What is the active species of cytochrome P450

during camphor hydroxylation? QM/MM studies of different electronic states of compound I and of reduced and oxidized iron-oxo intermediates", *J. Am. Chem. Soc.*, 129, 8978–8987, **2007**.

[41] B. S. Pybus, "CYP450 phenotyping and accurate mass identification of metabolites of the 8-aminoquinoline , anti-malarial drug primaquine", 1–9, **2012**.

[42] S. Shaik, W. Lai, H. Chen, Y. Wang, "The valence bond way: Reactivity patterns of cytochrome P450 enzymes and synthetic analogs", *Acc. Chem. Res.*, 43, 1154–1165, **2010**.

[43] P. K. Sharma, S. P. De Visser, F. Ogliaro, S. Shaik, "Is the ruthenium analogue of compound I of cytochrome P450 an efficient oxidant? A theoretical investigation of the methane hydroxylation reaction", *J. Am. Chem. Soc.*, 125, 2291–2300, **2003**.

[44] S. Shaik, H. Hirao, D. Kumar, "Reactivity patterns of cytochrome P450 enzymes: Multifunctionality of the active species, and the two states-two oxidants conundrum", *Nat. Prod. Rep.*, 24, 533–552, **2007**.

[45] F. Ogliaro, N. Harris, S. Cohen, M. Filatov, S. P. De Visser, S. Shaik, "A model 'rebound' mechanism of hydroxylation by cytochrome P450: Stepwise and effectively concerted pathways, and their reactivity patterns", *J. Am. Chem. Soc.*, 122, 8977–8989, **2000**.

[46] R. Ullrich, M. Hofrichter, "Enzymatic hydroxylation of aromatic compounds", *Cell. Mol. Life Sci.*, 64, 271–293, **2007**.

[47] J. F. Arambula, C. Preihs, D. Borthwick, D. Magda, J. L. Sessler, "Texaphyrins: Tumor Localizing Redox Active Expanded Porphyrins", *Anticancer. Agents*

Med. Chem., 11, 222–232, **2012**.

[48] A. Fallis, "*International Drug Price Indicator Guide"*, 53, **2013**.

[49] R. J. Klose, Kenichi Yamane, Yangjin Bae, Dianzheng Zhang, Hediye Erdjument-Bromage, Dianzheng Zhang, Hediye Erdjument-Bromage, "The transcriptional repressor JHDM3A demethylates trimethyl histone H3 lysine 9 and lysine 36", *Nature*, 442, 312, **2006**.

[50] S. Shaik, S. P. De Visser, D. Kumar, "One oxidant, many pathways: A theoretical perspective of monooxygenation mechanisms by cytochrome P450 enzymes", *J. Biol. Inorg. Chem.*, 9, 661–668, **2004**.

[51] S. Sason, K. Devesh, P. de V. Samuël, A. Ahmet, T. Walter, "*Theoretical Perspective on the Structure and Mechanism of Cytochrome P450 Enzymes"*, 46, 105, **2005**.

[52] K. D. Dubey, S. Shaik, "Cytochrome P450 - The Wonderful Nanomachine Revealed through Dynamic Simulations of the Catalytic Cycle", *Acc. Chem. Res.*, 52, 389–399, **2019**.

[53] J. S. Hanna, E. S. Kroll, V. Lundblad, F. A. Spencer, "Saccharomyces cerevisiae CTF18 and CTF4 Are Required for Sister Chromatid Cohesion", *Mol. Cell. Biol.*, 21, 3144–3158, **2001**.

[54] M. Vidakovic, S. G. Sligar, H. Li, T. L. Poulos, "Understanding the role of the essential Asp251 in cytochrome P450cam using site-directed mutagenesis, crystallography, and kinetic solvent isotope effect", *Biochemistry*, 37, 9211–9219, **1998**.

[55] P. R. Ortiz De Montellano, J. J. De Voss, "Substrate oxidation by cytochrome P450 enzymes", in *Cytochrome P450: Structure, Mechanism, and*

Biochemistry: Third edition, Springer US, 183–245, **2005**.

[56] F. Moschona, I. Savvopoulou, M. Tsitopoulou, D. Tataraki, G. Rassias, "Epoxide syntheses and ring-opening reactions in drug development", *Catalysts*, 10, 1–65, **2020**.

[57] J. G. M. Bessems, N. P. E. Vermeulen, "Paracetamol (acetaminophen)-induced toxicity: Molecular and biochemical mechanisms, analogues and protective approaches", *Crit. Rev. Toxicol.*, 31, 55–138, **2001**.

[58] C. Preihs *et al.*, "Recent developments in texaphyrin chemistry and drug discovery", *Inorg. Chem.*, 52, 12184–12192, **2013**.

[59] W. M. Atkins, S. G. Sligar, "The roles of active site hydrogen bonding in cytochrome P-450(cam) as revealed by site-directed mutagenesis", *J. Biol. Chem.*, 263, 18842–18849, **1988**.

[60] S. P. De Visser, "Trends in substrate hydroxylation reactions by heme and nonheme iron(IV)-oxo oxidants give correlations between intrinsic properties of the oxidant with barrier height", *J. Am. Chem. Soc.*, 132, 1087–1097, **2010**.

[61] V. Y. Kuznetsov, T. L. Poulos, I. F. Sevrioukova, "Putidaredoxin-to-cytochrome P450cam electron transfer: Differences between the two reductive steps required for catalysis", *Biochemistry*, 45, 11934–11944, **2006**.

[62] D. Harris, G. Loew, "Mechanistic Origin of the Correlation between Spin State and Spectra of Model Cytochrome P450 Ferric Heme Proteins", *J. Am. Chem. Soc.*, 115, 5799–5802, **1993**.

[63] C. Com, "Chemical Structure Drawing Standard", *Chem. Eng. News*, 73, 16-34, **2010**.

[64] A. Sigel, H. Sigel, R. K. O. Sigel, "*The ubiquitous roles of cytochrome P450 proteins"*, John Wiley, 15, 35-67, **2007**.

[65] N. Awasthi, R. Yadav, A. Shukla, D. Kumar, "Interplay between two degenerate spin state determines the hydroxylation of 4-nitrophenol catalyzed via Cytochrome P450", *Inorg. Chem. Commun.*, 34, 108857, **2021**.

[66] R. Yadav, N. Awasthi, A. Shukla, D. Kumar, "Modeling the hydroxylation of estragole via human liver cytochrome P450", *Journal of Molecular Modelling*, 26, 64-83, **2021**.

[67] G. H. Loew, D. L. Harris, "Role of the Heme Active Site and Protein Environment in Structure, Spectra, and Function of the Cytochrome P450s", *Chemical Reviews*, 100, 407–419, **2000**.

[68] E. Flashman, C. J. Schofield, "The most versatile of all reactive intermediates?", *Nat. Chem. Biol.*, 3, 86–7, **2007**.

[69] S. Shaik, S. Cohen, Y. Wang, H. Chen, D. Kumar, W. Thiel, "P450 enzymes: their structure, reactivity, and selectivity-modeled by QM/MM calculations.", *Chem. Rev.*, 110, 949–1017, **2010**.

[70] H. Hirao, D. Kumar, L. Que, S. Shaik, "Two-state reactivity in alkane hydroxylation by non-heme iron-oxo comolexes", *J. Am. Chem. Soc.*, 128, 8590–8606, **2006.**

[71] P. E. M. Siegbahn, M. R. A. Blomberg, "Transition-Metal Systems in Biochemistry Studied by High-Accuracy Quantum Chemical Methods" *Chemical Reviews*, 100, American Chemical Society, 45, 421–437, **2000**.

[72] E. I. Solomon, A. Decker, N. Lehnert, "Non-heme iron enzymes: Contrasts to heme catalysis", *Proc. Natl. Acad. Sci. U. S. A.*, 100, 3589–3594, **2003.**

[73] P. C. A. Bruijnincx, G. van Koten, R. J. M. Klein Gebbink, "Mononuclear non-heme iron enzymes with the 2-His-1-carboxylate facial triad: Recent developments in enzymology and modeling studies", *Chem. Soc. Rev.*, 37, 2716–2744, **2008**.

[74] R. P. Hausinger, "FeII/alpha-ketoglutarate-dependent hydroxylases and related enzymes", *Crit. Rev. Biochem. Mol. Biol.*, 39, 21–68, **2004.**

[75] A. S. Ivanov, A. I. Boldyrev, "Deciphering aromaticity in porphyrinoids via adaptive natural density partitioning", *Org. Biomol. Chem.*, 12, 6145–6150, **2014**.

[76] P. Ø. Falnes, R. F. Johansen, E. Seeberg, "AlkB-mediated oxidative demethylation reverses DNA damage in Escherichia coli.", *Nature*, 419, 178–82, **2002**.

[77] Z. Wang, "Synthesis and biologic properties of hydrophilic sapphyrins, a new class of tumor-selective inhibitors of gene expression", *Mol. Cancer*, 6, 1–12, **2007**.

[78] K. S. Hewitson, "Hypoxia-inducible factor (HIF) asparagine hydroxylase is identical to factor inhibiting HIF (FIH) and is related to the cupin structural family", *J. Biol. Chem.*, 277, 26351–26355, **2002**.

[79] P. E. M. Siegbahn, R. H. Crabtree, "Mechanism of C-H activation by diiron methane monooxygenases: Quantum chemical studies", *J. Am. Chem. Soc.*, 119, 3103–3113, **1997**.

[80] R. Iwahori, A., Hirota, Y., Sampe, "NII-Electronic Library Service", *Chem. Pharm. Bull.*, 43, 2091, **1970**.

[81] F. Himo, P. E. M. Siegbahn, "Quantum Chemical Studies of Radical-Containing

Enzymes", 16, 34-63, **2003**.

[82] U. M. Zanger, M. Schwab, "Cytochrome P450 enzymes in drug metabolism: Regulation of gene expression, enzyme activities, and impact of genetic variation", *Pharmacol. Ther.*, 138, 103–141, **2013**.

[83] M. Sono, M. P. Roach, E. D. Coulter, J. H. Dawson, "Heme-containing oxygenases", *Chem. Rev.*, 96, 2841–2887, **1996**.

[84] S. G. Bell, R. J. Sowden, L. L. Wong, "Engineering the haem monooxygenase cytochrome P450cam for monoterpene oxidation", *Chem. Commun.*, 7, 635–636, **2001.**

[85] S. T. Mathews, R. Selvam, "Changes in glutathione metabolic enzymes in erythrocytes of Plasmodium vivax infected patients", *Clin. Chim. Acta*, 219, 159–165, **1993**.

[86] A. Ehrenberg, P. Reichard, "Electron Spin Resonance of the Iron-containing Protein B2 from Ribonucleotide Reductase", 12, 43-65, **1972**.

[87] N. Abbaspour, R. Hurrell, R. Kelishadi, "Review on iron and its importance for human health", 16, 3–11, **2014**.

[88] J. Hooda, A. Shah, L. Zhang, "Heme, an Essential Nutrient from Dietary Proteins, Critically Impacts Diverse Physiological and Pathological Processes", 21, 1080–1102, **2014**.

[89] M. Shionoya, H. Furuta, V. Lynch, A. Harriman, J. L. Sessler, "Diprotonated Sapphyrin: A Fluoride Selective Halide Anion Receptor", *J. Am. Chem. Soc.*, 114, 5714–5722, **1992**.

[90] M. Torrent, D. G. Musaev, H. Basch, K. Morokuma, "Computational studies of

reaction mechanisms of methane monooxygenase and ribonucleotide reductase", *J. Comput. Chem.*, 23, 59–76, **2002**.

[91] S. Yoshioka, S. Takahashi, K. Ishimori, I. Morishima, "Roles of the axial push effect in cytochrome P450cam studied with the site-directed mutagenesis at the heme proximal site", *J. Inorg. Biochem.*, 81, 141–151, **2000**.

[92] A. Ninfa, D. Ballou, M. Benore, "Approaches for Biochemistry and Biotechnology", 23, 164–179, **2010**.

[93] Ortiz de Montellano, R**.** Paul "Cytochrome P450: Structure, Mechanism, and Biochemistry", *Pharmacology & Toxicology*, 2019

[94] F. Ogliaro, S. P. de Visser, S. Cohen, P. K. Sharma, S. Shaik, "Searching for the second oxidant in the catalytic cycle of cytochrome P450: a theoretical investigation of the iron(III)-hydroperoxo species and its epoxidation pathways.", *J. Am. Chem. Soc.*, 124, 2806–17, **2002**.

[95] T. L. Poulos, B. C. Finzel, A. J. Howard, "High-resolution crystal structure of cytochrome P450cam", *J. Mol. Biol.*, 195, 687–700, **1987**.

[96] M. Vidakovic, S. G. Sligar, H. Li, T. L. Poulos, "Understanding the role of the essential Asp251 in cytochrome P450cam using site-directed mutagenesis, crystallography, and kinetic solvent isotope effect", *Biochemistry*, 37, 9211–9219, **1998**.

[97] R. Raag, "Crystal Structure of the Cytochrome P-450CAM Active Site Mutant Thr252Ala", *Biochemistry*, 30, 11420–11429, **1991**.

[98] S. Cohen, S. Kozuch, C. Hazan, S. Shaik, "Does substrate oxidation determine the regioselectivity of cyclohexene and propene oxidation by cytochrome P450?", *J. Am. Chem. Soc.*, 128, 11028–11029, **2006**.

[99] T. L. Poulos, "The role of the proximal ligand in heme enzymes", *J. Biol. Inorg. Chem.*, 1, 356–359, **1996.**

[100] S. P. De Visser, S. Shaik, "A proton-shuttle mechanism mediated by the porphyrin in benzene hydroxylation by cytochrome P450 enzymes", *J. Am. Chem. Soc.*, 125, 7413–7424, **2003** .

[101] K. D. Dubey, B. Wang, S. Shaik, "Molecular Dynamics and QM/MM Calculations Predict the Substrate-Induced Gating of Cytochrome P450 BM3 and the Regio- and Stereoselectivity of Fatty Acid Hydroxylation", *J. Am. Chem. Soc.*, 138, 837–845, **2016.**

[102] D. Kumar, P. De Visser, P. K. Sharma, S. Cohen, S. Shaik, "Kumar et al. - 2004 - Radical Clock Substrates, Their C−H Hydroxylation", 12, 1907–1920, **2004**.

[103] F. P. Guengerich, T. L. Macdonald, "Mechanisms of cytochrome P-450 catalysis", *FASEB Journal*, 4, 2453–2459, **1990.**

[104] J. T. Groves, G. A. McClusky, "Aliphatic Hydroxylation via Oxygen Rebound. Oxygen Transfer Catalyzed by Iron", *J. Am. Chem. Soc.*, 98, 859–861, **1976**.

[105] M. Newcomb, P. H. Toy, "Hypersensitive radical and the mechanisms of cytochrome P450-catalyzed hydroxylation reactions", *Acc. Chem. Res.*, 33, 449–455, **2000**.

[106] F. Carvalho, "Repeated administration of d-amphetamine results in a time-dependent and dose-independent sustained increase in urinary excretion of p-hydroxyamphetamine in mice", *J. Heal. Sci.*, 53, 371–377, **2007**.

[107] P. R. Ortiz De Montellano, R. A. Stearns, "Timing of the Radical Recombination Step in Cytochrome P-450 Catalysis with Ring-Strained Probes", *J. Am. Chem. Soc.*, 109, 3415–3420, **1987**.

[108] M.-H. Baik, M. Newcomb, R. A. Friesner, S. J. Lippard, "Mechanistic studies on the hydroxylation of methane by methane monooxygenase", *Chem. Rev.*, 103, 2385–419, **2003**.

[109] C. M. Brown, B. Reisfeld, A. N. Mayeno, "*Cytochromes P450: A structure-based summary of biotransformations using representative substrates"*, 40, 65-78, **2008**.

[110] J. Wen, D. Chennamadhavuni, S. R. Morel, M. K. Hadden, "Truncated Itraconazole Analogues Exhibiting Potent Anti-Hedgehog Activity and Improved Drug-like Properties", *ACS Med. Chem. Lett.*, 10, 1290–1295, **2019**.

[111] S. Agarwal, U. R. Gupta, C. S. Daniel, R. C. Gupta, N. Anand, S. S. Agarwal, "Susceptibility of glucose-6-phosphate dehydrogenase deficient red cells to primaquine, primaquine enantiomers, and its two putative metabolites. II. Effect on red blood cell membrane, lipid peroxidation, MC-540 staining, and scanning electron microscopic ", *Biochem. Pharmacol.*, 41, 17–21, **1991**.

[112] A. M. Khenkin, D. Kumar, S. Shaik, R. Neumann, "Characterization of manganese(V)-oxo polyoxometalate intermediates and their properties in oxygen-transfer reactions", *J. Am. Chem. Soc.*, 128, 15451–15460, **2006**.

[113] R. Rutter, L. P. Hager, H. Dhonau, M. Hendrich, P. Debrunner, M. Valentine, "Chloroperoxidase Compound I: Electron Paramagnetic Resonance and Mössbauer Studies", *Biochemistry,* 23, 6809–6816, **1984**.

[114] Y. Shiota, K. Yoshizawa, "Methane-to-methanol conversion by first-row transition-metal oxide ions: ScO+, TiO+, VO+, CrO+, MnO+, FeO+, CoO+, NiO+, and CuO+", *J. Am. Chem. Soc.*, 122, 12317–12326, **2000**.

[115] S. Shaik, D. Danovich, A. Fiedler, D. Schröder, H. Schwarz, "Two-State

Reactivity in Organometallic Gas-Phase Ion Chemistry", *Helv. Chim. Acta*, 78, 1393–1407, **1995**.

[116] D. Schröder, S. Shaik, H. Schwarz, "Two-state reactivity as a new concept in organometallic chemistry", *Acc. Chem. Res.*, 33, 139–145, **2000**.

[117] T. Kamachi, K. Yoshizawa, "P450ja0208862.pdf," 4652–4661, **2003**.

[118] K. Monostory, E. Hazai, L. Vereczkey, "Inhibition of cytochrome P450 enzymes participating in p-nitrophenol hydroxylation by drugs known as CYP2E1 inhibitors", *Chem. Biol. Interact.*, 147, 331–340, **2004**.

[119] S. Shaik, Devesh Kumar, Sam P. De Visser, "The 'Rebound Controversy': An Overview and Theoretical Modeling of the Rebound Step in C-H Hydroxylation by Cytochrome P450", *Eur. J. Inorg. Chem.*, 15, 207–226, **2004**.

[120] M. Albeck, S. Shaik, "Publications of Sason Shaik", *J. Phys. Chem. A*, 112, 2741–12753, **2008**.

[121] S. A. Hollingsworth, B. D. Nguyen, G. Chreifi, A. P. Arce, T. L. Poulos, "Insights into the Dynamics and Dissociation Mechanism of a Protein Redox Complex Using Molecular Dynamics", *J. Chem. Inf. Model.*, 57, 2344–2350, **2017**.

[122] S. Shaik, H. Hirao, D. Kumar, "Reactivity patterns of cytochrome P450 enzymes: Multifunctionality of the active species, and the two states-two oxidants conundrum", *Nat. Prod. Rep.*, 24, 533–552, **2007**.

[123] G. Camarda *et al.*, "Antimalarial activity of primaquine operates via a two-step biochemical relay", *Nat. Commun.*, 10, 75-98, **2019.**

[124] D. Danovich, S. Shaik, "Spin-orbit coupling in the oxidative activation of H-H

by FeO+. Selection rules and reactivity effects", *J. Am. Chem. Soc.*, 119, 1773–1786, **1997.**

[125] M. Aschi, M. Brönstrup, M. Diefenbach, J. N. Harvey, D. Schröder, H. Schwarz, "A gas phase model for the Pt+-catalyzed coupling of methane and ammonia", *Angew. Chemie - Int. Ed.*, 37, 829–832, **1998**.

[126] F. P. Guengerich, "Cytochrome P-450 3A4: Regulation and role in drug metabolism", *Annu. Rev. Pharmacol. Toxicol.*, 39, 1–17, **1999**.

[127] W. R. Wadt, P. J. Hay, "Ab initio effective core potentials for molecular calculations. Potentials for main group elements Na to Bi", *J. Chem. Phys.*, 82, 284–298, **1985**.

[128] Y. Xia, "A flexible bis(pyridylcarbamate) anion receptor: Binding of infinite double-stranded phosphate, [-sulfate-(H2O)2-]n, and hydrogen-bridged helical perchlorate chain", *CrystEngComm*, 11, 1849–1856, **2009**.

[129] L. Xu, G. M. Ferrence, T. D. Lash, "Vinylogous Expanded Porphyrin", *Society*, 2, 6–9, **2006**.

[130] E. A. Carter, W. A. Goddard, "Relationships between bond energies in coordinatively unsaturated and coordinatively saturated transition-metal complexes: A quantitative guide for single, double, and triple bonds", *J. Phys. Chem.*, 92, 5679–5683, **1988**.

[131] E. A. Carter, W. A. Goddard, "Early- versus late-transition-metal-oxo bonds: The electronic structure of VO+ and RuO+", *J. Phys. Chem.*, 92, 2109–2115, **1988**.

[132] R. Zhou, F. Josse, W. Göpel, Z. Z. Öztürk, Ö. Bekaroğlu, "Phthalocyanines as sensitive materials for chemical sensors", *Appl. Organomet. Chem.*, 10, 557–

577, **1996**.

[133] S. Shaik, H. Hirao, D. Kumar, "Reactivity of high-valent iron-oxo species in enzymes and synthetic reagents: A tale of many states", *Acc. Chem. Res.*, 40, 532–542, **2007**.

[134] D. R. Koop, "Oxidative and reductive metabolism by cytochrome P450 2E1", *FASEB J.*, 6, 724–730, **1992**.

[135] T. Cardinaels, J. Ramaekers, D. Guillon, B. Donnio, K. Binnemans, "A propeller-like uranyl metallomesogen", *J. Am. Chem. Soc.*, 127, 17602–17603, **2005**.

[136] K. Yoshizawa, Y. Kagawa, Y. Shiota, "Kinetic isotope effects in a C-H bond dissociation by the iron-oxo species of cytochrome P450", *J. Phys. Chem. B*, 104, 12365–12370, **2000**.

[137] S. Shaik, H. Hirao, D. Kumar, "Reactivity of High-Valent Iron – Oxo Species in Enzymes and Synthetic Reagents : A Tale of Many States TSR / MSR Scenarios in Bond Activation", *Acc. Chem. Res.*, 40, 532–542, **2007**.

[138] D. Riccardi, P. Schaefer, Q. Cui, "PK a calculations in solution and proteins with QM/MM free energy perturbation simulations: A quantitative test of QM/MM protocols", *J. Phys. Chem. B*, 109, 17715–17733, **2005**.

[139] M. Newcomb, D. Aebisher, R. Shen, R. E. P. Chandrasena, P. F. Hollenberg, M. J. Coon, "Kinetic isotope effects implicate two electrophilic oxidants in cytochrome P450-catalyzed hydroxylations", *J. Am. Chem. Soc.*, 125, 6064–6065, **2003**.

[140] N. Harris, S. Shaik, D. Schroder, H. H. Schwarz, "Single- and two-state reactivity in the gas-phase C-H bond activation of norbornane by 'bare' FeO+",

Helv. Chim. Acta, 82, 1784–1797, **1999**.

[141] M. R. Sievers, Y. M. Chen, P. B. Armentrout, "Metal oxide and carbide thermochemistry of Y+, Zr+, Nb+, and Mo+", *J. Chem. Phys.*, 105, 6322–6333, **1996**.

[142] A. Nowak-Król, D. Gryko, D. T. Gryko, "Meso-substituted liquid porphyrins", *Chem. - An Asian J.*, 5, 904–909, **2010**.

[143] J. Guo, A. Liu, H. Cao, Y. Luo, J. M. Pezzuto, R. B. Van Breemen, "Biotransformation of the chemopreventive agent 2',4',4-trihydroxychalcone (isoliquiritigenin) by UDP-glucuronosyltransferases", *Drug Metab. Dispos.*, 36, 2104–2112, **2008**.

[144] R. Z. Liao, P. E. M. Siegbahn, "Mechanism and selectivity of the dinuclear iron benzoyl-coenzyme A epoxidase BoxB", *Chem. Sci.*, 6, 2754–2764, **2015**.

[145] B. A. Gregg, "Entropy of charge separation in organic photovoltaic cells: The benefit of higher dimensionality", *J. Phys. Chem. Lett.*, 2, 3013–3015, **2011**.

[146] A. S. Ivanov, A. I. Boldyrev, "Deciphering aromaticity in porphyrinoids via adaptive natural density partitioning", *Org. Biomol. Chem.*, 12, 6145–6150, **2014.**

[147] L. Zhang, "thione , C 10 H 12 N 4 OS", *Journal of Molecular Structure*, 223, 289–290, **2008.**

[148] C. Section, "Comparative Photophysics of [26] - and [28] Hexaphyrins (1.1.1.1.1.1.): Large two photon absorption Cross Section of Aromatic [26] Hexaphyrins(1.1.1.1.1.1.) ", *Journal of American Journal Society*, 127 37, 12856–12861, **2005**.

[149] G. I. Vargas-Zúñiga, J. L. Sessler, "Pyrrole N–H anion complexes", *Coord. Chem. Rev.*, 345, 281–296, **2017**.

[150] M. Castella, F. López-Calahorra, D. Velasco, H. Finkelmann, "The first asymmetrically β-polysubstituted porphyrin-based hexagonal columnar liquid crystal", *Chem. Commun.*, 2, 2348–2349, **2002**.

[151] S. Hiroto, H. Shinokubo, A. Osuka, "Porphyrin synthesis in water provides new expanded porphyrins with direct bipyrrole linkages: Isolation and characterization of two heptaphyrins", *J. Am. Chem. Soc.*, 128, 6568–6569, **2006.**

[152] T. K. Chandrashekar, S. Venkatraman, "Core-modified expanded porphyrins: New generation organic materials", *Acc. Chem. Res.*, 36, 676–691, **2003**.

[153] J. I. T. Costa, A. S. F. Farinha, F. A. Almeida Paz, A. C. Tomé, "A convenient synthesis of pentaporphyrins and supramolecular complexes with a fulleropyrrolidine", *Molecules*, 24, 1–17, **2019**.

[154] A. Abebayehu, D. Park, S. Hwang, R. Dutta, C. H. Lee, "Synthesis and spectroscopic behaviour of metal complexes of meso-alkylidenyl carbaporphyrinoids and their expanded analogues", *Dalt. Trans.*, 45, 3093–3101, **2016.**

[155] P. S. S. Lacerda, "[1,2,3]Triazolo[4,5-b]porphyrins: New building blocks for porphyrinic materials", *Angew. Chemie - Int. Ed.*, 45, 5487–5491, **2006**.

[156] T. D. Lash, "Origin of aromatic character in porphyrinoid systems", *J. Porphyr. Phthalocyanines*, 15, 1093–1115, **2011**.

[157] M. S. Rodríguez-Morgade, T. Torres, "Preface from M. Salomé Rodríguez-Morgade and Tomás Torres", *J. Porphyr. Phthalocyanines*, 15, 2011-2102,

2011.

[158] J. L. Sessler, D. Seidel, "Synthetic Expanded Porphyrin Chemistry", *Angewandte Chemie - International Edition*, 42, 5134–5175, **2003**.

[159] G. P. Arsenault, E. Bullock, S. F. MacDonald, "Pyrromethanes and Porphyrins Therefrom", *J. Am. Chem. Soc.*, 82, 4384–4389, **1960**.

[160] K. M. Kadish, K. M. Smith, Â. S. Gabriel, R. Guilard, "The Porphyrin Handbook. Academic press, Boston", *Porphyr. Handbook. Acad. Press. Boston.*, 7, 1–423, **2000**.

[161] J. L. Sessler, D. Seidel, "Synthetic Expanded Porphyrin Chemistry", *Angew. Chemie - Int. Ed.*, 42, 5134–5175, **2003**.

[162] D. Xia, Pi Wang, Xiofan Ji, Niveem M. Khashab, Jonathan L. Sessler, Feihe Huang, "Functional Supramolecular Polymeric Networks: The Marriage of Covalent Polymers and Macrocycle-Based Host-Guest Interactions", *Chem. Rev.*, 23, 231-245, **2020**.

[163] C. M. Drain, A. Varotto, I. Radivojevic, "Cr8002483.Pdf," 1630–1658, **2009**.

[164] A. E. Ahsen, A. Segade, D. Velasco, Z. Z. Öztürk, "Liquid crystal porphyrins as chemically sensitive coating materials for chemical sensors", *J. Porphyr. Phthalocyanines*, 13, 1188–1195, **2009**.

[165] A. S. Ivanov, A. I. Boldyrev, "Deciphering aromaticity in porphyrinoids via adaptive natural density partitioning", *Org. Biomol. Chem.*, 12, 6145–6150, **2014**.

[166] S. B. Kahl, J. J. Schaeck, M.-S. Koo, "Improved Methods for the Synthesis of Porphyrin Alcohols and Aldehydes from Protoporphyrin IX Dimethyl Ester and

Their Further Modification", *J. Org. Chem.*, 62, 1875–1880, **1997**.

[167] V. J. Bauer Hadiqa Zafar, Harrison D. Root, Gregory D. Thiabaud, "Sapphyrins: Novel Aromatic Pentapyrrolic Macrocycles", *J. Am. Chem. Soc.*, 105, 6429–6436, **1983**.

[168] M. Asaka, H. Fujii, "Participation of Electron Transfer Process in Rate-Limiting Step of Aromatic Hydroxylation Reactions by Compound i Models of Heme Enzymes", *J. Am. Chem. Soc.*, 138, 8048–8051, **2016**.

[169] C. J. Judd, D. V. Kondratuk, H. L. Anderson, A. Saywell, "On-Surface Synthesis within a Porphyrin Nanoring Template", *Sci. Rep.*, 9, 1–8, **2019**.

[170] Y. Agam, R. Nandi, A. Kaushansky, U. Peskin, N. Amdursky, "The porphyrin ring rather than the metal ion dictates long-range electron transport across proteins suggesting coherence-assisted mechanism", *Proc. Natl. Acad. Sci. U. S. A.*, 117, 32260–32266, **2020**.

[171] S. Mori, A. Osuka, "Aromatic and antiaromatic gold(III) hexaphyrins with multiple gold-carbon bonds", *J. Am. Chem. Soc.*, 127, 8030–8031, **2005**.

[172] L. Cook, G. Brewer, W. Wong-Ng, "Structural aspects of porphyrins for functional materials applications", *Crystals*, 7, 112-130, **2017.**

[173] M. Imran, M. Ramzan, A. K. Qureshi, M. Azhar Khan, M. Tariq, "Emerging applications of porphyrins and metalloporphyrins in biomedicine and diagnostic magnetic resonance imaging", *Biosensors*, 8, 1–17, **2018**.

[174] A. Segade, M. Castella, F. López-Calahorra, D. Velasco, "Synthesis and characterization of unsymmetrically β-substituted porphyrin liquid crystals: Influence of the chemical structure on the mesophase ordering", *Chem. Mater.*, 17, 5366–5374, **2005**.

[175] A. S. Chandrasekhar, C. Frank, J. D. Litster, W. H. De Jeu, L. Lei, "Liquid crystals of disc-like molecules", *Philosophical Transactions of the Royal Society of Lindon, Series A, Mathematical and Physical Sciences*, 309, 93-103, **2014**.

Chapter-2

Computational Methodology

Chapter-2

Computational Methodology

2.1 Quantum Mechanical Calculations

A molecule is formed by atoms. Atoms are formed from electrons, protons & neutrons. Protons & neutrons are placed inside the nucleus and electrons move around the nucleus in different path in various energy levels also called the orbit or shell. This is the basic idea of the arrangement of subatomic particles inside an atom. This arrangement of subatomic particles inside the atom in a definite manner leads them to hold and exhibit unique physical and chemical properties, like stable geometry, charge distribution, dipole moment, vibrational frequency, lowest possible energy, etc. These unique sets of physical and chemical properties can be precisely calculated using quantum mechanical formulations for a given set of atoms or molecules [1].

According to Quantum Mechanics (QM), wave function (ψ) of any molecular system hold all information related to that molecular system and it is obtained by solving the Schrödinger wave equation:

$$H\Psi = E\Psi \tag{2.1}$$

This is well known time-independent Schrödinger wave equation, where H is the Hamiltonian Operator of the given molecular system and E is the energy eigenvalue of the corresponding Hamiltonian Operator H. Ψ is a well behaved mathematical function also known as the wave function, whose square represents the probability density [3].

The wave function of the molecule represents its nuclear as well as electronic motions together, by using Born Oppenheimer approximation, the electronic wave function is separated from the total wave function [4-6].

When the nuclei of two or more atoms are fixed at a particular distance, then their electronic wave function sufficiently provides all the physical and chemical properties of the molecule. But for a multi-electron system, the electronic part of the Hamiltonian operator of the Schrödinger equation is given by:

$$H_e = -\sum_P \frac{1}{2}\nabla_P^2 - \sum_A \sum_P Z_A r_{AP}^{-1} + \sum_{p<q} r_{pq}^{-1} \qquad (2.2)$$

In the above equation, the first term represents the kinetic energy; the second term is the potential energy, whereas the third term is potential energy, raised due to inter-electron interactions. Thus the modified Schrödinger wave equation for the 'n' electron system is given by [7]:

$$H_e(1,2,....,n)\Psi_e(1,2,....,n) = E_e\Psi_e(1,2,....,n) \qquad (2.3)$$

In the above equation, Ψ_e is an electronic part of the total wave function. The detailed treatment of quantum mechanical problems involving the electronic structure of the molecule is equivalent to the complete solution of the appropriate Schrödinger equation. Due to the inter-electronic repulsion term, the Schrödinger equation for a single atom is not separable; therefore we obtain the solution Ψ_0, by neglecting the inter-electronic repulsion term. The wave function Ψ_0 for the 'n' electrons is given by the product of 'n' single electronic wave functions. This product of the wave function is known as Hartree Product of the wave function [8], given as:

$$\Psi_0 = \Psi_1(r_1,\theta_1,\varphi_1)\Psi_2(r_2,\theta_2,\varphi_2).....\Psi_n(r_n,\theta_n,\varphi_n) \qquad (2.4)$$

The electrons are fermions and thus obey Fermi-Dirac statistics [9]. One electron wave functions are the molecular orbitals, which are the products of the spatial orbitals and the spin functions (α or β) [10].To satisfy Pauli's exclusion principle, the wave function must be anti-symmetric [11].The anti-symmetry wave functions may be derived from Slater Determinants [12]. The spin-orbital Slater determinant for 'n' electrons is given by:

$$\Psi = \frac{1}{\sqrt{N}} \begin{vmatrix} \varphi_1^{(1)}\alpha^{(1)} & \varphi_2^{(1)}\beta^{(1)} \ldots\ldots\ldots & \varphi_n^{(1)}\beta^{(1)} \\ \varphi_1^{(2)}\alpha^{(2)} & \varphi_2^{(2)}\beta^{(2)} \ldots\ldots\ldots & \varphi_n^{(2)}\beta^{(2)} \\ \varphi_1^{(n)}\alpha^{(n)} & \varphi_1^{(n)}\alpha^{(n)} \ldots\ldots\ldots & \phi_n^{(n)}\beta^{(2)} \end{vmatrix} \tag{2.5}$$

The solution of the above equation can be obtained by using perturbation over the solution Ψ_0 and a trial wave function is constructed with the help of this Slater determinant by applying the variational principle. The equation of energy of the system given below is written in the form of Dirac notation, the equation of the energy of the system is given by [13-15];

$$E_e = \frac{\left\langle \Psi'_i \mid H_e \mid \Psi'_i \right\rangle}{\left\langle \Psi'_i \middle| \Psi'_j \right\rangle} \tag{2.6}$$

2.2 Hartree Fock Method

The solution of the electronic Schrödinger wave equation of molecule, which is formed by Slater determinant, consists of the nuclear–nuclear interaction energy, which has a constant value for a given geometry, the nuclear-electron attraction, which is dependent on one electron coordinate and the electron-electron repulsion, which depends on two-electron coordinates [16,17]. The Hamiltonian is given as:

$$H_e = \sum_{p}^{N} h + \sum_{i=1}^{N}\sum_{j>i}^{N} g_{ij} + V_{nn} \tag{2.7}$$

where,

$$h_p = -\frac{1}{2}\nabla^2 - \sum_a \frac{Z_a}{|R_a - r_p|} \tag{2.8}$$

and

$$g_{ij} = \frac{1}{|r_i - r_j|} \tag{2.9}$$

where one-electron operator (h_i) describes the motion of an i[th] electron in the field of all nuclei, (g_{ij}) is two-electron operator giving the repulsion between two electrons while V_{nn} is the nuclear-nuclear interaction energy. The energy can be expressed as:

$$E = \sum_i^N \langle \varphi_i | h_i | \varphi_i \rangle + \frac{1}{2}\sum_{ij}^N \left(\langle \varphi_j | J_i | \varphi_j \rangle - \langle \varphi_j | K_i | \varphi_j \rangle \right) + V_{nn} \tag{2.10}$$

$$J_{12} = \langle \varphi_1^{(1)} \varphi_2^{(2)} | g_{12} | \varphi_1^{(1)} \varphi_2^{(2)} \rangle \tag{2.11}$$

Where, J operator represents the classical repulsion between the two charge distributions described by $\varphi_{12}(1)$ and $\varphi_{22}(2)$:

$$K_{12} = \langle \varphi_1^2 \varphi_2^{(2)} | g_{12} | \varphi_2^{(1)} \varphi_1^{(2)} \rangle \tag{2.12}$$

The K operator represents the exchange integral that has no classical analog [18]. To determine the set of Molecular Orbital (MO), which has minimum energy or is stationary in respect to change of orbital, variation is carried out in a manner that the MO's should remain orthogonal and normalized. This type of optimization is termed constrained optimization and this can be achieved by the Lagrange multipliers method [16,19]. The Lagrange function is stationary for the orbital variations:

$$L = E - \sum_{ij}^N \lambda_{ij} \left(\langle \varphi_i | \varphi_j \rangle - \delta_{ij} \right) \tag{2.13}$$

L is the Lagrange function. A variation of the Lagrange function is written as:

$$\delta L = \delta E - \sum_{ij}^{N} \left(\langle \delta\varphi_i \mid \varphi_i \rangle + \langle \varphi_i \mid \delta\varphi_i \rangle \right) = 0 \tag{2.14}$$

$$F_i = h_i + \sum_{j}^{N} \left(J_j - K_j \right) \tag{2.15}$$

Where, F_i is the Fock Operator; whereas operator J is the electron repulsion term, known as the Coulomb Operator while operator K is termed as the Exchange Operator. Hence, the Hartree Fock equation can be written as below [16, 20]:

$$F_i \phi_i = \varepsilon_i \phi_i \tag{2.16}$$

A set of functions that are the solutions of the above equation is called Self-Consistent Field Orbitals and is determined through an iterative method. The Hartree Fock method is known as the mean field approximation in which the average electron-electron repulsion is taken into account [21].

2.3 Electron Correlation

Electrons, which are present in the system, avoid confronting themselves due to repulsion between them. Such effect of electron repulsion is also called "electron correlation". Thus the motion of the electron is considered to be correlated and hence affected due to the motion of the other electrons present in the system. When the molecules are formed, there is a possibility for the existence of an angular electron correlation around the bond direction. Within the Hartree-Fock formalism, the anti-symmetric wave function is approximated by a single Slater determinant, which does not include this Coulomb correlation or electron correlation. Therefore the energy calculated with the Hartree-Fock method is different from the exact energy of the

system. This difference between these two energies is called the correlation energy and given as:

$$E_{corr} = E_{exact} - E_{HF} \tag{2.17}$$

There exist much significantly developed methods which accurately determined the contributions of correlations and thus leads to form a broader category of an approach called the "post-Hartree-Fock methods". Many post-Hartree-Fock calculations include configuration interaction (CI), Moller-Plesset perturbation theory (MPn), multi configurational self-consistent field (MCSCF),and coupled-cluster theory (CC) considers the electron correlation.

2.4 Density Functional Theory

Density functional theory (DFT), in contrast to wave function in Quantum Mechanics, describes the energy as a functional of the electron cloud density [ρ (Ψr)] [22]. Kohn et al. derived a set of single-electron equations that enables one to calculate the electron density and consequently the total energy of the system [22]. This methodology has been proven itself to be very successful in recent years as the calculations involving this method have shown themselves to be less computationally expensive, while the results obtained through it shows reasonable agreement with experiments for relatively large chemical systems [23]. Thus, similar to Hartree-Fock calculations, the total energy (E_{el}) of a DFT calculation is split into a kinetic energy term, a term representing the electron-nucleus attractions, a term for the Coulomb interactions between the electrons, and an exchange-correlation term (E_{xc}), respectively [23, 24]. The first three terms resemble the Hartree-Fock Hamiltonian shown in equation 2.7, 2.8 and 2.9 above as a function of the nuclear coordinates (R), and the coordinates of the electrons (r), and is shown below:

$$E_{el} = -\frac{1}{2}\sum_i \int \varphi_i(r_1)\nabla^2\varphi_i(r_1)dr_1 + \sum_A \int \frac{Z_A}{|R_A - r_1|}\rho(r_1)dr_1 + \frac{1}{2}\frac{\rho(r_1)\rho(r_2)}{|r_1 - r_2|}dr_1 dr_2 + E_{XC}$$

(2.18)

The exchange-correlation functional is generally unknown and therefore adequate approximate equations have been set up to estimate its contribution. Generally, Exchange-Correlation Functional (E_{xc}) splits into two function one is an exchange functional (E_X) and other is correlation functional (E_C). The exchange functional, essentially represents the interactions of two spins in different orbits, whereas the correlation functional represents the pairing energy of present electrons in same orbital [25,26].

The exchange energy is generally estimated from Slater exchange function given by:

$$E_X^{Slater} = -\frac{9}{4\alpha_{ex}}\left(\frac{3}{4\pi}\right)^{1/3}\sum_\gamma \int \left[\rho_1^\gamma(r_1)\right]^{4/3}dr_1 \qquad (2.19)$$

In the above equation, α_{ex} is an exchange scale factor, which has the value 2/3 for an electron gas system. The commonly used correlation energy functional (E_C^{VWN}) was named after Vosko, Wilk,and Nusair[25] and represents the correlation energy per electron in an electron gas system $\varepsilon_C\left[\rho_1^\alpha \rho_1^\beta\right]$ with spin densities ρ_1^α and ρ_1^β, and it is given as:

$$E_C^{VWN} = \int \rho_1(r_1)\varepsilon_c\left[\rho_1^\alpha(r_1), \rho_1^\beta(r_1)\right]dr_1 \qquad (2.20)$$

The combination of Slater exchange functional and Vosko-Wilk-Nusair correlation functional gives the Local Density Approximation (LDA). Both functionals are directly derived from the homogenous electron gas equations.However, to correct the non-local terms to other exchange and correlation functionals have now been

developed for better and accurate results. Two popular approaches are named Lee, Yang & Parr (LYP correlational functional) [26] and Perdew & Wang (PW91 correlational functional) [27]. But there are also many other available functionals, each with its unique qualities as well as drawbacks.

A much appreciated and groundbreaking breakthrough applications of density functional theory to computational chemistry, in general, appeared when Becke developed the hybrid density functional procedures [28]. Becke benchmarked the density functional theory basically against a test set of experimentally pre-known ionization energies, electron affinities, and proton affinities with close accuracies. He came with a three-parameter (hybrid) density functional method to estimate the contributions of the exchange and correlation functionals and optimized the values of these three fit parameters (A, B, and C) against the experimental data in the test set. There are several possibilities of combining various exchange as well as correlation functional, but throughout the years the most popular has been the B3LYP method, although it should be realized that it is not essentially the most accurate one [28]. It is necessary the hybrid density functional method B3LYP has the following form:

$$E_{XC}^{B3LYP} = AE_X^{Slater} + (1-A)E_X^{HF} + B\Delta E_X^{Becke} + E_C^{VWN} + C\Delta E_C^{LYP} \qquad (2.21)$$

The B3LYP method, in essence, is not an ab-initio method. Strictly, the term ab-initio referred as starting from scratch without prior knowledge of the experiment. The B3LYP method, as well as other hybrid and non-hybrid DFT methods, is extremely accurate and versatile for computational chemists. The accuracy of DFT and high-level ab-initio methods, like coupled-cluster methods, their speed in combination with the reasonable accuracy makes them very popular as well as useful methodology.

Becke already published in his original paper, calculated energies within 2 (kcal/mol) of the experiment, which is not far off from the ultimate accuracy result of computational chemistry of 1 (kcal/mol) (chemical accuracy) defined by Pople et. al. [7]. Recent comparative calculations on the complete test-set molecules using three different techniques, i.e. Hartree-Fock theory, MP2 theory and DFT methods (using B3LYP) showed that the B3LYP methodology gives a considerable improvement over Hartree-Fock as well as over MP2 calculations [29]. Therefore, DFT is a low-cost alternative to quantum mechanical procedures and as such highly suitable to perform calculations on biochemical systems [30,31].

2.5 Hybrid Function

Hybrid density functionals have allowed a significant improvement over General Gradient Approximation (GGA) for many molecular properties. A hybrid exchange-correlation energy functional [32-34] is defined as follows:

$$E_{XC} - \int_0^1 U_{XC}^{\lambda}\, d\lambda \qquad (2.22)$$

Where λ is called coupling strength or parameter such that when λ=0 $E_{XC} - E_X^{exact}$ and when λ=1, $E_{XC} - E_X^{GGA} + E_C^{GGA}$, and U_{XC}^{λ} is the potential energy exchange-correlation at coupling strength λ.

More specifically, we can write

$$E_{XC} - \frac{1}{2} E_{XC}^{\lambda=0} + \frac{1}{2} E_{XC}^{\lambda=1} \qquad (2.23)$$

As this functional (E_{XC}) contains half-half contributions from each of the exact exchange energy(without correlation) and GGA exchange-correlation energy, it is called hybrid density functional (H-GGA).

In 1993, Becke [33] developed a 3-parameter hybrid functional called the B3 hybrid functional as:

$$E_{XC}^{B3} - E_{XC}^{LSDA} + a\left(E_{XC}^{\lambda=0} - E_{XC}^{LSDA}\right) + bE_X^B + cE_C^{PW91} \qquad (2.24)$$

Where a, b and c are parameters that were fitted in such a way that the atomization and ionization energies, as well as the proton affinities included in the G2 data base and some total energies, were optimally reproduced. The fitted values of these parameters are a=0.20, b=0.72 and c=0.81. The most popular and extensively used hybrid functional is the B3LYP [33] which has the following form [32, 35]:

$$E_{XC}^{B3LYP} - (1-a)E_{XC}^{LSDA} + a\left(E_{XC}^{\lambda=0}\right) + bE_X^{B88} + cE_C^{LYP} + (1-c)E_C^{LSDA} \quad (2.25)$$

where a, b, and c have the same values as those given above.

Several other hybrid density functionals [9,24] including BH and HLYP, B3PW91, B3P86, B97-1, B98, MPW1K, mPW3LYP, O3LYP, and X3LYP have also been developed. Further, a different class of density functionals called hybrid-meta GGA (HM-GGA) functionals, based on a similar concept as the M-GGA functionals have also been developed [35]. These functionals use M-GGAs instead of the standard GGAs. Thus, these methods depend on the Hartree-Fock exchange, electron density and its gradient, and kinetic energy density. Examples of the HM- GGA functionals are B1B95 [36, 37] BB1K [36,37,38] MPW1B95 etc. [39,40]. These methods are more reliable for the determination of barrier heights and atomization energies.

2.6 Basis Sets

A basis set represents a group of mathematical functions which describe the shape of the orbitals of an atom. To solve the Schrödinger equation, one has to optimize the wave function with the help of perturbations from the Hamilton operator to find the

energy eigenvalues. There is no straightforward method to obtain the wave functions for molecules as well as that of atoms in which distinct levels of orbitals. To overcome this problem, the Linear Combination of Atomic Orbitals (LCAO) approach [41] is used to describe the molecular wave function through molecular orbitals. In this approach, occupied atomic orbitals (□) of all atoms in the molecule are taken to create a set of molecular orbitals (φ_i) through fractions (c_{ri}) of all atomic orbital components as shown in the equation below:

$$\varphi_i = \sum_r c_{ri}\chi_r \tag{2.26}$$

The number of active orbitals and virtual orbitals are taken into consideration decides the quality of molecular orbitals thus obtained. Hence, to achieve a good quality of molecular orbital wave function calculations, large number of such orbitals are required to be considered in the calculations so that the energy gets converge within the basis set limit.

There are two broad classes of basis sets, i.e., Slater Type Orbitals (STO's) [42,43] and Gaussian Type Orbitals (GTO's) [44]. A Slater Type Orbital for ans-type atomic orbital has the following form:

$$S(r) = N_s e^{-\zeta r^2} \tag{2.27}$$

where, r is the radial distance from the nucleus of an atom, N_s, is the normalization constant, and ζ is a constant known as the orbital exponent, which governs with the size of the orbital. Gaussian Type Orbitals are s-type atomic orbital with the same orbital exponent as STO. It has the following form:

$$g(r) = N_g e^{-\zeta r^2} \tag{2.28}$$

where N_g is the normalization constant.

The STO basis set has the advantage that they have a direct physical interpretation. The STOs have the shortcoming that most of the required integrals needed for the SCF procedure must be calculated numerically, hence it is computationally expensive, whereas wave functions with the GTO basis set are much easier to compute. The smallest basis set, which represents one basis function for each type of occupied orbital in the separated atoms, is called a minimal basis set [45]. The most commonly used minimal basis set is the STO-3G basis set. This notation indicates that the basis set approximates the shape of an STO orbital by using a single contraction of three GTO. One such contraction would then be used for each orbital, which is the definition of a minimal basis.

The Pople basis set [46,47] is the other family of basis sets. They are written by the notation 6-31G. This means that each core orbital is described by a single contraction of six GTO primitives. It describes each core orbital with two contractions, of which one with three primitives while another with one primitive describe each valence shell orbital. The Pople basis sets are a very popular choice for organic molecules. These basis sets can be modified by adding one or two asterisks (*), such as 6-31G* or 6-31G**. A single asterisk means a set of *d*-primitives has been added to atoms other than the hydrogen atom. Two asterisks mean that a set of *p*-primitives have been added to a hydrogen atom. These are called polarization functions because they give the wave function more flexibility to change shape. Similarly, one or two plus signs can also be added, such as 6-31+G* or 6-31++G*. A single plus sign indicates that diffuse functions have been added to atoms other than hydrogen. The second plus sign indicates that diffuse functions are being used for all atoms. Diffuse functions are used for anions, which have larger electron density distributions. They are also used for

describing interactions at long distances, such as Vander Waal's interactions. The effect of adding the diffuse functions is usually related to change the relative energies of various geometries associated with these systems. Basis sets with the diffuse functions are generally known as augmented basis sets [46,48].

Due to the variational principle, the electronic energy of a molecule approaches the exact value closely with an increase in the number of basis functions used in a calculation; it is usually useful to construct basis sets that have more basis function than the number of basis functions in minimal basis set. The Double Zeta (DZ) basis set uses two basis functions of each type of the minimal basis function for separated atoms. Since coefficients of hybrid density functional theory are benchmarked against experimental data using calculations through a double- quality basis set. This type of basis set is generally sufficient in Density Functional Theory (DFT) calculations for the geometry optimizations [49].

2.7 Solvent effects

Energies calculated by using computational Quantum methods refer to only gas-phase data. To make computational results at par with experimental results for comparison, the effect of solvent needs to be incorporated into the calculations. To add solvent molecules in the model system and re-optimize the resultant structure is the simplest way to achieve this effect. But these types of calculations will increase computational time and also it is not always practical. Because the solvent molecules can exist in several conformations [49]. Hence, instead of adding the solvent molecule, a more common approach is to add solvent corrections to the energetics using an implicit solvent model. This can either be done at a single point level, whereby the energy is recalculated with a solvent model of the gas phase optimized geometry, or by re-

optimizing the structure using a solvent model. The popular software packages, such as Gaussian and Jaguar, include solvent models like the Polarizable Continuum Model (PCM) [50]. In Polarizable Continuum Model calculations, the solvent is described as a perturbation of the molecule with a dielectric constant and the molecule is placed in a cavity that is surrounded by the dielectric continuum. The cavity is described as an area around the molecule that contains less than a pre-defined amount of electron density of the molecule and is often based on Vander Waals radii of atoms. The classical Poisson equations are then used to calculate the electronic potential arising from the molecule-solvent interactions using a defined dielectric constant.

2.8 Application of ab-initio and DFT Methods

DFT and ab-initio methods are applied for several molecular properties such as geometry, vibrational frequencies, barriers to internal rotation, energy differences between conformational isomers, charge distributions, dipole moments, molecular electrostatic potentials (MEP), electronic spectra, infrared and Raman spectra, NMR spectra, polarizabilities, salvation, intermolecular interactions and reactions [32,52,53]. Some of those that have been studied in this thesis are described here briefly.

2.8.1 Molecular Geometry

The equilibrium geometry of a molecule is a global total energy minimum on the potential energy surface obtained using the Born-Oppenheimer approximation. It can be obtained by minimizing the total energy with respect to the internal coordinates, i.e. bond lengths, bond angles,and dihedral angles. Minimization of total energy with respect to internal coordinates is called geometry optimization. Several algorithms are available to search the total energy minimum of a molecule. Vibrational frequency

analysis, as discussed below, has to be carried out to ensure that the total energy minimum has been located on the potential energy surface.

2.8.2 Vibrational Frequencies

Calculation of vibrational frequencies is important for ascertaining the nature of minima and maxima on the potential energy surface and to explain the vibrational spectra of molecules. For a molecule, the vibrational frequencies are calculated using the mass-weighted Hessian matrix.

A Hessian matrix is the matrix of second derivatives of the total energy with respect to geometrical parameters. The elements of the Hessian matrix are defined as:

$$H_{i,j} - \frac{\delta^2 E}{\delta X_i \, \delta X_j} \tag{2.29}$$

and are generated by the use of finite displacements, that is, for each atomic coordinate x_i, the coordinate is first incremented by a small amount, the gradients calculated, then the coordinate is decremented and the gradients re-calculated. The second derivative of this matrix is then obtained from the difference of the two derivatives and the step size:

$$H_{i,j} - \frac{\left(\frac{\partial E}{\partial X_i}\right)(+0.5\Delta X_j) - \left(\frac{\partial E}{\partial X_i}\right)(-0.5\Delta X_j)}{\Delta X_j} \tag{2.30}$$

This is done for all the 3N Cartesian coordinates where N is the number of atoms. The random errors that occur in the gradients can be reduced by re-defining the Hessian because it is symmetric, that is $H_{i,j} = H_{j,i}$, and is defined by

$$H_{i,j} - \frac{1}{2}\left(\frac{\left(\frac{\partial E}{\partial X_i}\right)(+0.5\Delta X_j) - \left(\frac{\partial E}{\partial X_i}\right)(-0.5\Delta X_j)}{\Delta X_j} + \frac{\left(\frac{\partial E}{\partial X_j}\right)(+0.5\Delta X_i) - \left(\frac{\partial E}{\partial X_j}\right)(-0.5\Delta X_i)}{\Delta X_i}\right) \tag{2.31}$$

Diagonalization of this matrix yields the force constants of the system.

To calculate vibrational frequencies, the Hessian matrix is the first mass-weighted. Thus,

$$H_{i,j}^{m} - \frac{H_{i,j}}{\sqrt{M_i}\sqrt{M_j}} \quad (2.32)$$

Diagonalization of this matrix yields eigenvalues, □ᵢ's. Then, in harmonic approximation, the vibrational frequencies ν_i can be calculated using the following relation:

$$v_i - \frac{1}{2}\sqrt{\varepsilon_i} \ \ (i = 1,2,3 \ldots \ldots 3N - 6) \quad (2.33)$$

2.8.3 Chemical Reaction

A chemical reaction can be studied using quantum chemical ab-initio and density functional theoretical (DFT) methods, employing the concept of transition state theory (TST) [40]. The theory assumes a special type of chemical equilibrium (quasi-equilibrium) between reactants and the transition state. TST assumes that even when the reactants and products are not in equilibrium with each other, the activated complexes are in quasi-equilibrium with the reactants. Transition state theory fails for some reactions at high temperatures. The theory assumes that the reaction system would pass over the lowest energy saddle point on the potential energy surface. Other forms of TST, such as microcanonical variational TST, canonical variational TST, and improved canonical variational TST, where the transition state is not necessarily located at the saddle point, are referred to as a generalized transition state theory. According to TST, a simple one-step chemical reaction starts from a reactant complex (RC) and proceeds through a transition state called (TS) from where the product complex (PC) is formed. On the PES, the energy difference between the total energies, of TS and RC is termed as the barrier energy

(ΔE^b), and the difference in total energies of the TS and PC is termed as released energy (ΔE^r) (Figure. 2.1(a)). The barrier energy of a reaction can be obtained using the concept of potential energy surface (PES).

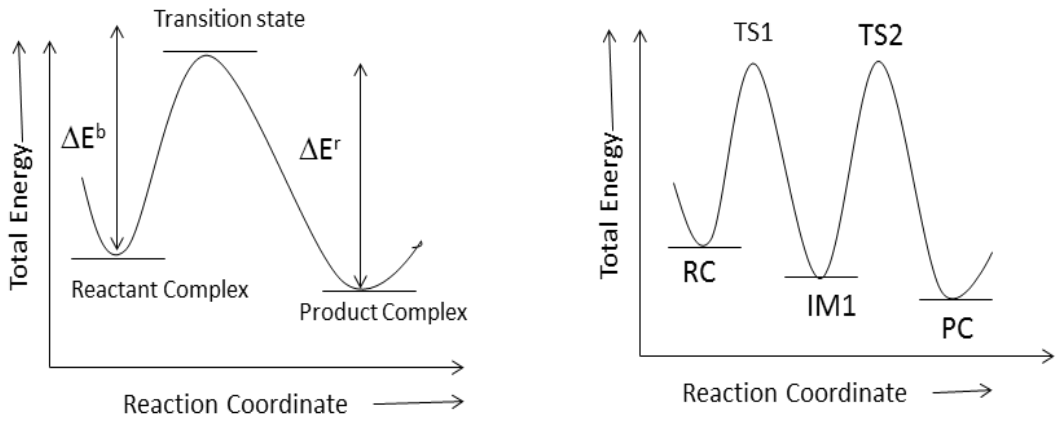

Figure. 2.1. Potential energy surfaces for (a) single-step reaction and (b) three-step reaction.

The PES is based on the fact that the total energy of a molecule or another type of atomic arrangement can be represented as a curve or multidimensional surface, with atomic positions as variables. On the PES, RC and PC are minima that are characterized by all real vibrational frequencies, while TS is a maximum that is characterized by an imaginary vibrational frequency. Corresponding to each TS, there are minima located on either side of it on the PES. In a complex multi-step reaction, there may be several TSs and minima other than the RC and PC, known as intermediate complexes (ICs) (Figure. 2.1(b)). The structural changes that occur between the reactant complex and the final product complex, through the transition states and intermediate complexes, constitute a reaction mechanism. To able to get energies that are appropriate for comparison with the experiment, one applies zero-point energy (ZPE) correction or appropriate thermal energy correction to the

calculated total energies. The calculation of barrier energies of a reaction is an important step for predicting its feasibility. By searching all the extrema on the PES of a reaction, one would get information about the structures of RC, ICs, PC, and TSs. In this way, one can easily get information about the favoured mechanism of a reaction.

References:

[1] L. I. Shiff, "Electron Spin and Proton Spin in the Hydrogen and Hydrogen-Like Atomic Systems", *Quantum Mechanics*, 5, **1968.**

[2] E. Schroedinger, "Bohr's Spectrum of Quantum States in the Atomic Hydrogen Deduced from the Uncertainty Principle for Energy and Time", *Ann. Physik*, 79, 361, **1926.**

[3] L. Pauling, E. B. Wilson, "The Genesis of the Quantum Theory of the Chemical Bond", *Introduction to Quantum Mechanics*, 3, 5, **1935.**

[4] M. Born, J. R. Oppenheimer, W. Kolos, L. Wolniewicz, "On the quantum theory of molecules", *Ann. Physik.*, 84, 457, **1927.**

[5] W. Kolos, L.Wolniewicz, "Accurate Adiabatic Treatment of the Ground State of the Hydrogen Molecule", *J. Chem. Phys.*, 41, 3663, **1964.**

[6] B. T. Sutsliffe, "Transannular interactions in S_8^{2+} and Se_8^{2+}: Reality or artifact?", *Adv. Quantum. Chem.*, 28, 65, **1997.**

[7] J. A. Pople, D. L. Beveridge, "Approximate Molecular Orbital Theory of Nuclear and Electron Magnetic Resonance Parameters", *Approximate Molecular Orbital Theory*, 8, 163-214, **1970**.

[8] D. R. Hartree, "The Wave Mechanics of an Atom with a Non-Coulomb Central Field. Part I. Theory and Methods", *Proc. Cambridge Phil. Soc.*, 24, 111, **1928.**

[9] G. Uhlenbeck, S. Goudsmit, "Electron Spin and Proton Spin in the Hydrogen and Hydrogen-Like Atomic Systems", *Nature wissenschaften*, 13, 953, **1925.**

[10] J. A. Pople, D. L. Beveridge, P. A. Dobosh, "Approximate Self-Consistent Molecular-Orbital Theory. V. Intermediate Neglect of Differential Overlap", *J. Chem. Phys.*, 47, 2026, **1967.**

[11] W. Pauli, "On the Connexion between the Completion of Electron Groups in an Atom with the Complex Structure of Spectra", *Z. Physik.*, 31, 765, **1925**.

[12] J. C. Slater, "Cohesion in Monovalent Metals", *Phys. Rev*., 35, 509, **1930.**

[13] P. A. M. Dirac, *The Principle of Quantum Mechanics*, Oxford University Press, London, **1958.**

[14] J. K. L. McDonald, "Successive Approximations by the Rayleigh-Ritz Variation Method", *Phys. Rev*., 43, 830, **1933.**

[15] R. H. Young, "Chapter II - Applications of the Variation Method," *Int. J. Quant. Chem*., 6, 596, **1972.**

[16] F. Jenson, *Introduction to Computational Chemistry,* 2nd edition, John Wiley & Sons Ltd., Chichester, Computational Chemistry & Molecular Modeling, 1-624, **2007**.

[17] I. N. Levine, "Chapter-11, The Hartree Fock Self- Consistent Method", *Computational Methods in Quantum Chemistry*, 2, 39-78, **2000.**

[18] I. N. Levine, "Chapter-8, Perturbation Theory", *Quantum Chemistry*, 8, 23, **2000**.

[19] J. A. Pople, D. L Beveridge, "Molecular Modelling Methods", *Z. Physik.*, 61, 126, **1930**.

[20] J. E. Lennard-Jones, "The molecular orbital theory of chemical valency", *Proc. Roy. Soc. (London),* A198, 14, **1949.**

[21] C. Edimiston, K. Ruedenberg, "Localization of open-shell molecular orbitals via least change from fragments to molecule", *Rev. Mol. Phys.*, 34, 457, 1963.

[22] S. Robin, Mc Dowell, "Vibrational—Rotational Angular-Momentum Coupling in Spherical-Top Molecules. II. General Zeta Sums", *J. Chem. Phys.*, 43, 597, **1965.**

[23] T. Ziegler, "Approximate density functional theory as a practical tool in molecular energetics and dynamics", *Chem. Rev.*, 91, 651, **1991.**

[24] W. Khon, L. Sham, "Self-Consistent Equations Including Exchange and Correlation Effects", *J. Phys. Rev.*, 140, 1133, **1965.**

[25] P. Hohenberg, W. Khon, "Inhomogeneous Electron Gas", *Phys. Rev.*,136, B 864, **1964.**

[26] S. H. Vosko, L. Wilk, M. Nusair, "Accurate spin-dependent electron liquid correlation energies for local spin density calculations: a critical analysis", *Can. J. Phys.*, 58, 1200, **1980**.

[27] C. Lee, W. Yang, R. G. Parr, "Development of the Colle-Salvetti correlation-energy formula into a functional of the electron density", *Phys. Rev.*, B37, 785, **1988**.

[28] J. P. Perdew, Y. Wang, "Accurate and simple analytic representation of the electron-gas correlation energy", *Phys. Rev.*, B45, 13244, **1992**.

[29] A. D. Becke, "Density-functional thermochemistry. III. The role of exact exchange", *J. Chem. Phys.*, 98, 5648, **1993.**

[30] R. G. Parr, W. Yang, "Density-functional thermochemistry. III. The role of exact exchange", *Density Functional Theory*, Oxford University Press, 98, 5648, **1989**.

[31] P. E. M. Siegbahn, "A Theoretical Study of the Mechanism for the Biogenesis of Cofactor Topaquinone in Copper Amine Oxidases", *Quaet. Rev. Biophys*., 36, 91, **2003**.

[32] E. Hückel, "Quantentheoretische Beiträge zum Benzolproblem", *Z. Physik.*, 70, 204, **1931.**

[33] W. Koch, M. C., Holthausen, "A chemist's guide to density functional theory", *Wiley-VCH Verlag GmbH* ,34, 1-313, **2001**.

[34] A. D. Becke, "A new mixing of Hartree–Fock and local density-functional theories", *J. Chem*. *Phys.*, 98, 1372, **1993.**

[35] A. D. Becke, "Density-functional thermochemistry. III. The role of exact exchange", *J. Chem*. *Phys.*, 98, 5648, **1993.**

[36] S. F. Sousa, P. A. Fernandes, M. J., Ramos, "General performance of density functional", *J. Phys. Chem*. *A*, 111, 10439, **2007.**

[37] A. D. Becke, "Density-functional exchange-energy approximation with correct asymptotic behavior", *Phys. Rev. A*, 38, 3098, **1988.**

[38] A. D. Becke, "Density-functional thermochemistry. IV. A new dynamical correlation functional and implications for exact-exchange mixing", *J. Chem*. *Phys.*, 104, 1040, **1996.**

[39] Y., Zhao, B. J. Lynch, D. G., Truhlar, "Development and assessment of a new hybrid density functional model for thermochemical kinetics", *J. Phys. Chem*. *A*, 108**,** 2715, **2004.**

[40] Y. Zhao, and D. G., Truhlar, "Hybrid meta density functional theory methods for thermochemistry, thermochemical kinetics, and noncovalent interactions:

The MPW1B95 and MPWB1K models and comparative assessments for hydrogen bonding and van der Waals interactions", *J. Phys. Chem. A,* 108, 6908, **2004.**

[41] K. J., Laidler, "Chemical Kinetics", *Pearson Education (Singapore),* 1-428, **2004.**

[42] D. Feller, E. R. Davidson, "Systematic sequences of well-balanced Gaussian basis sets", *Rev. Comp. Chem.,* 72, 1741, **1990.**

[43] T. Helgaker, P. R. Taylor, "Modern Electronic Structure Theory, Part II", *World Scientific*, 45, 727, **1995.**

[44] S. F. Boys, " Electronic wave functions - I. A general method of calculation for the stationary states of any molecular system", *Proc. Roy. Soc.,* (London), A 200, 542, **1950.**

[45] W. J. Hehre, R. F. Stewart, J. A. Pople, "Self-Consistent Molecular-Orbital Methods. I. Use of Gaussian Expansions of Slater-Type Atomic Orbitals", *J. Chem. Phys.,* 51, 2657, **1969.**

[46] J. S. Binkley, J. A. Pople, "Self-consistent molecular orbital methods. 21. Small split-valence basis sets for first-row elements", *J. Am. Chem. Soc*., 102, 939, **1980.**

[47] M. J. Frisch, J. A. Pople, Binkley, "Structure, stability, and fragmentation of small carbon clusters", *J. Chem. Phys.,* 80, 3265, **1984.**

[48] W. J. Hehre, R. Ditchfield, J. A. Pople, "Self-Consistent Molecular Orbital Methods. XIV. An Extended Gaussian-Type Basis for Molecular Orbital

Studies of Organic Molecules. Inclusion of Second Row Elements", *J. Chem. Phys.*, 56, 2257, **1972.**

[49] T. H. Dunning Jr. P. J. Hay, "Spin-Orbit Electronic Structure of the ScBr Molecule Modern", *Theoretical Chemistry*, 3, 1, **1977.**

[50] J. H. Jensen, "Molecular Modeling Basics", *Taylor and Francis*, 1, 189, **2010.**

[51] J. Tomasi, B. Mennucci and R. Cammi, *Chem. Rev.*, 105, 2999, **2005.**

[52] W. Koch, M. C., Holthausen, "A chemist's guide to density functional theory", *Wiley*, 1-293, **2001.**

[53] A. Szabo, and N. S., Ostlund, "Introduction of Advanced Electronic Structure Theory", *Modern quantum chemistry,*1-461 **1996.**

[54] F., Neese, "Prediction of molecular properties and molecular spectroscopy with densityfunctional theory : From fundamental theory to exchange-coupling", *Coord. Chem. Rev.*, 253, 527-553, **2008.**

Chapter-3

Metabolism of 8-aminoquinoline (8AQ) Primaquine via aromatic hydroxylation step mediated by Cytochrome P450 enzyme using Density Functional Theory

Chapter-3

Metabolism of 8-aminoquinoline (8AQ) Primaquine via aromatic hydroxylation step mediated by Cytochrome P450 enzyme using Density Functional Theory

3.1 Introduction

Cytochrome P450 is an important enzyme of nature, basically in biosystems. In humans, it is found in the liver [1]. But it is also highly expressed in areas of the central nervous system.These enzymes catalyze a variety of stereo-specific and regio-selective mono-oxygenation reaction processes. It is also used in detoxification processes and is a key drug-metabolizing enzyme involved in the metabolism of drugs [2]. It reacts as mono-oxygenases that transfer oxygen atom to the substrate. This oxygen can be transferred either by hydroxylation, epoxidation or sulfoxidation [3–6]. Due to its large versatility in the activation of the substrate, Cytochrome P450 is an essential enzyme, not only in biology but also, in biotechnological and pharmaceutical applications for investigations of drugs [7]. Moreover, its drug metabolism and involvement in brain chemistry make this enzyme a target for the drug industry and biomedical research [8–11].

Fundamentally, hydroxylation is of two types – one is (a) aliphatic, another is (b)

aromatic. Both hydroxylations are important and their reaction pattern is different. Present research is focused on the study of aromatic hydroxylation. In the modern synthesis chemistry, direct insertion of hydroxyl group into the aromatic compound is one of the most challenging fields, because of the strong bond of hydrogen and carbon (C-H) atom of the benzene ring. But, despite this ambivalence, Cytochrome P450 catalyzes aromatic compound in relatively easy way. Hydroxylations of aromatic rings are important chemical reactions and are catalyzed by several metalloenzymes [8,9]. In biosystems, there are various essential processes of chemical reactions which lead to aromatic hydroxylation with Cytochrome P450 and convert several non-degradable compounds into biodegradable compounds [10,11].

Aromatic hydroxylation step via P450s is responsible for the breakdown of xenobiotics into water-soluble enzymes [3]. P450 catalyses estrogen hormone into 16-hydroxy-estrogen via aromatic hydroxylation step, which basically triggers breast cancer [15–17]. Moreover, plant P450 enzyme catalyze the isoliquiritigenin into the product, which has antitumor, antioxidant and phytoestrogenic activity [18]. Aromatic hydroxylation via P450 is also the centre of research for drug metabolism including para-hydroxylation of Amphetamine and Tamoxifen [19–21] and several other substrates, like, β-blocker alprenolol [22] and the neurotoxin 1-methyl-4-phenyl-1,2,3,6-tetrahydropyridine which is a chemical inducer of Parkinson's disease [23].

So, in the field of bio-chemistry, aromatic hydroxylation via P450 is a crucial activity, but researchers are always fascinated by aromatic hydroxylation due to its unknown reaction mechanism with Cytochrome P450 [21-22]. The Cytochrome P450 metabolize various compounds using high-valent iron (iv) oxo species complex, generally known as Cpd1. This complex is formed during the catalytic cycle of Cytochrome P450 [26–29]. Initially, in catalytic cycle, Cytochrome P450 is at the

resting state and the water molecule is ligated. The entry of the substrate expels the water molecule and tightly binds with the enzyme. Further, the oxidation step forms ferric peroxide species known as compound 0 (Cpd 0), and then after the protonation step Cpd 0 converts into active species of enzyme, iron (IV)-oxo complex, known as compound I (Cpd I). It is the primary oxidant involved in the oxidation reaction of all super family of P450s and here truncated model of Cpd I is used to explore the overall reaction.

For large number of atoms a more suitable method is used generally known as QM/MM (Quantum Mechanical/ Molecular Mechanical) method. The utility of this method is revealed by the first QM/MM study [30] of the active species. It was done by increasing molecules in all the species in the catalytic cycle of P450cam, [31] the active species of human isoforms, [26-32] and some of organic molecules [33-34].

Moreover, the QM/MM approach is used for two- layer to three-layer of system, one can easily understand it by continuum solvation model which is used for third layer [35] or by ONIOM-type method in which system is divided in two layers two different layers one is inner QM layer and another is outer MM layer [36]. Such more involved QM/MM treatments have not yet been applied to P450 enzymes. Present study addresses the aromatic hydroxylation of 8-aminoquinoline (8AQ), an anti-malarial drug Primaquine via Cpd I of P450. Primaquine is metabolized by CYP 2D6 enzyme [37]. CYP 2D6 is a member of the P450 enzyme, so the active site is similar for both enzymes. That's why P450 enzyme is used here for hydroxylation.

The 8-aminoquinoline (8AQ) drug Primaquine (PQ) is a prime anti-malarial drug, used in the treatment of malaria due to plasmodium vivax and plasmodium ovale [38]. It is also used in the treatment of pneumocystis pneumonia together with clindamycin, as an alternate treatment. It is one of the safest and most effective drugs and is placed in

the list of essential drugs of World Health Organization (WHO) [39]. It was developed over 70 years ago. But, unfortunately, the reaction pathway was still blurred.

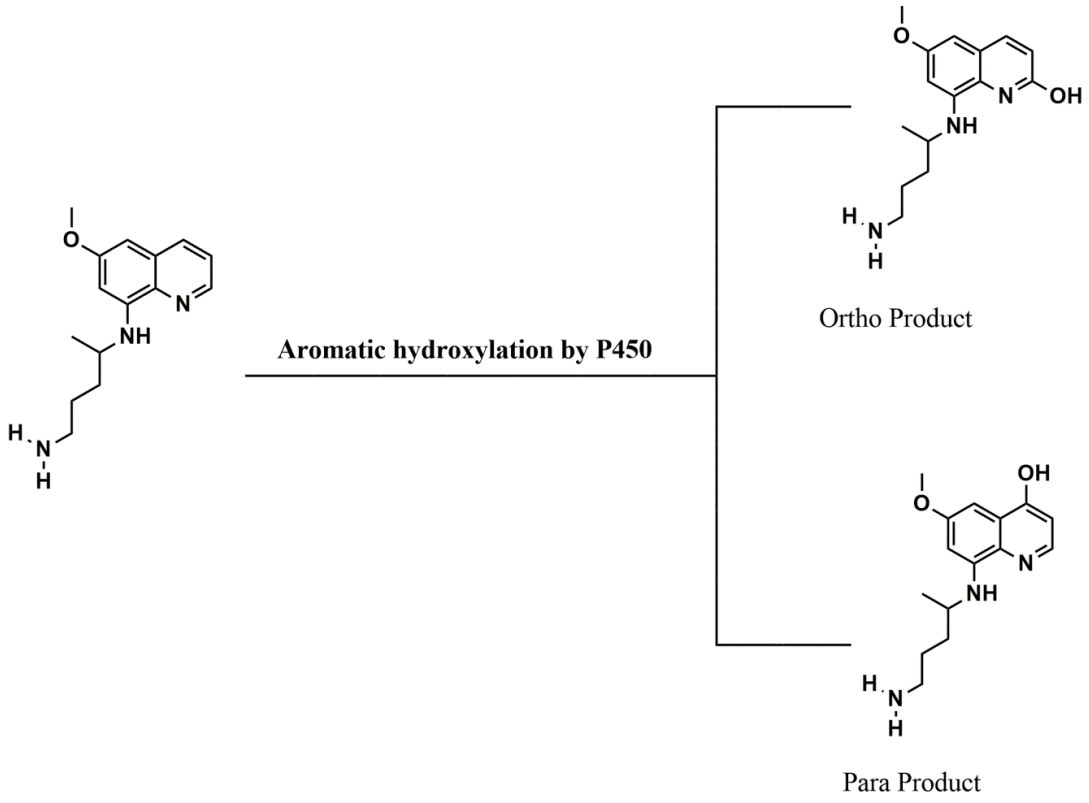

Figure 3.1: Aromatic hydroxylation of Primaquine at ortho (2PQ) and para (4PQ) position by Cytochrome P450.

The hydroxylated metabolite of Primaquine is also responsible for many essential sexual transmission stages of Plasmodium falciparum [40]. There are six metabolites of 8AQ identified [37]. These metabolites are formed by the hydroxylation step, at each position of the benzene ring. Current study is investigating the hydroxylation step at ortho (2PQ) as well as para (4PQ) position of the benzene ring of Primaquine. DFT method is the most accurate and reliable for studying the reactivity pattern of Cpd I and also of several other essential metalloenzyme with hybrid function B3LYP of DFT [41]. The C-H hydroxylation of the substrate with Cpd I is followed by two different spin surfaces, one is, high spin state (HS) and the other is, low spin state (LS). These

two different spin state energy barriers lead to two-state reactivity (TSR) pattern [25,26]. In the present work, we have studied aromatic hydroxylation at the ortho position (2PQ) as well as at the para position of Primaquine (4PQ) (Figure 1). The reaction patterns for reaction complex (RC), transition state (TS), intermediate state (IM) and product complex (PC) for both spin state, doublet (LS) as well as quartet (HS), are shown in energy profiles as will discuss later. All calculations are done for isolated reaction coordinate. Further, we cross checked the results calculating single point energy using basis set LACVP, solvent effect with benzene, and in presence of two ammonium molecule, and results are overlapping to each other, which showed the reliability of results.

3.2 Methodology

Present study comprises an investigation of reaction energy profile by Quantum Mechanical (QM) method. Density functional theory (DFT) was involved using Gaussian 09 software [43]. In this work, all calculations were performed for porphyrin cation radical iron (IV) oxo species i.e $Por^{+\cdot}Fe^{iv}=O$, which is commonly referred as (Cpd I), in two different spin states, doublet as well as quartet with Primaquine as a substrate. Optimization geometries of reactant, intermediate, product is performed and a genuine pathway for the reaction mechanism is found on potential energy surface (PES) with subsequent transition states. Initially, optimization of geometry was calculated by hybrid density functional B3LYP using LANL2DZ basis set on iron atom and 6-31G basis set on the rest of the atom (BS1) abbreviated as B3LYP/BS1 [44].

Analytic frequency calculations performed after optimization confirmed the local minima of reactant, intermediate, product by showing the real frequencies and first-

order saddle point i.e., transition state with single imaginary frequency. Moreover, results are crosschecked at B3LYP/BS2 theory by performing single-point calculations. This basis set involves triple zeta effective core potential on iron and 6-31+G* basis rest on remaining atoms. Further, we calculated single point energy using basis set LACVP, solvent effect with Benzene and in presence of ammonia and results are overlapping to each other, which showed the reliability of results. Barrier heights are calculated by isolated reactant geometries using 6-31G, 6-31+G*, LACVP, solvent effect with benzene and in presence of ammonia are shown in Figure 3.2 and Figure 3.7.

3.3 Results and Discussion

3.3.1 Hydroxylation of Primaquine at ortho position (2PQ)

The proposed work tried to explain aromatic hydroxylation of Primaquine at ortho position of the aromatic ring (C-2), to a complex intermediate (IM1) by attaching at the ortho position of carbon (C-2) with oxygen atom of Cpd I. In the next step, hydrogen atom (H-2) at ortho position gets attached with one of nitrogen atom of porphyrin ring forming a second intermediate state (IM2). Further, this hydrogen atom attaches to the abstracted oxygen atom of Cpd I, and form a product complex (PC). The electronic configuration of CpdI must be clearly identified, for better understanding of its reaction pathway $3d_z^2$ orbital of iron and $2p_z$ orbital of oxygen of Cpd I together formed $\sigma_{z^2}^*$ anti-bonding orbital, whereas interaction of $3d_{xy}$ orbital of iron and $2p_{xy}$ orbital of nitrogen atoms of porphyrin together form anti-bonding orbital σ_{xy}^* . These orbitals are found to be unfilled initially due to their high energy state and filled in later part of the reaction process. Further, $\delta_{x^2-y^2}$ Is orbital of lone pair electron the porphyrin ring. The low-lying bonding orbital π_{xz}/π_{yz} as well as

antibonding orbital π^*_{xz} / π^*_{yz} is formed by the interaction between $3d_{xz}$ /$3d_{yz}$ orbital of iron and $2p_x$ /$2p_y$ orbital of oxygen .These low-lying bonding π_{xz} /π_{yz} orbitals are always filled. Optimized orbitals are shown in Figure 3.3.

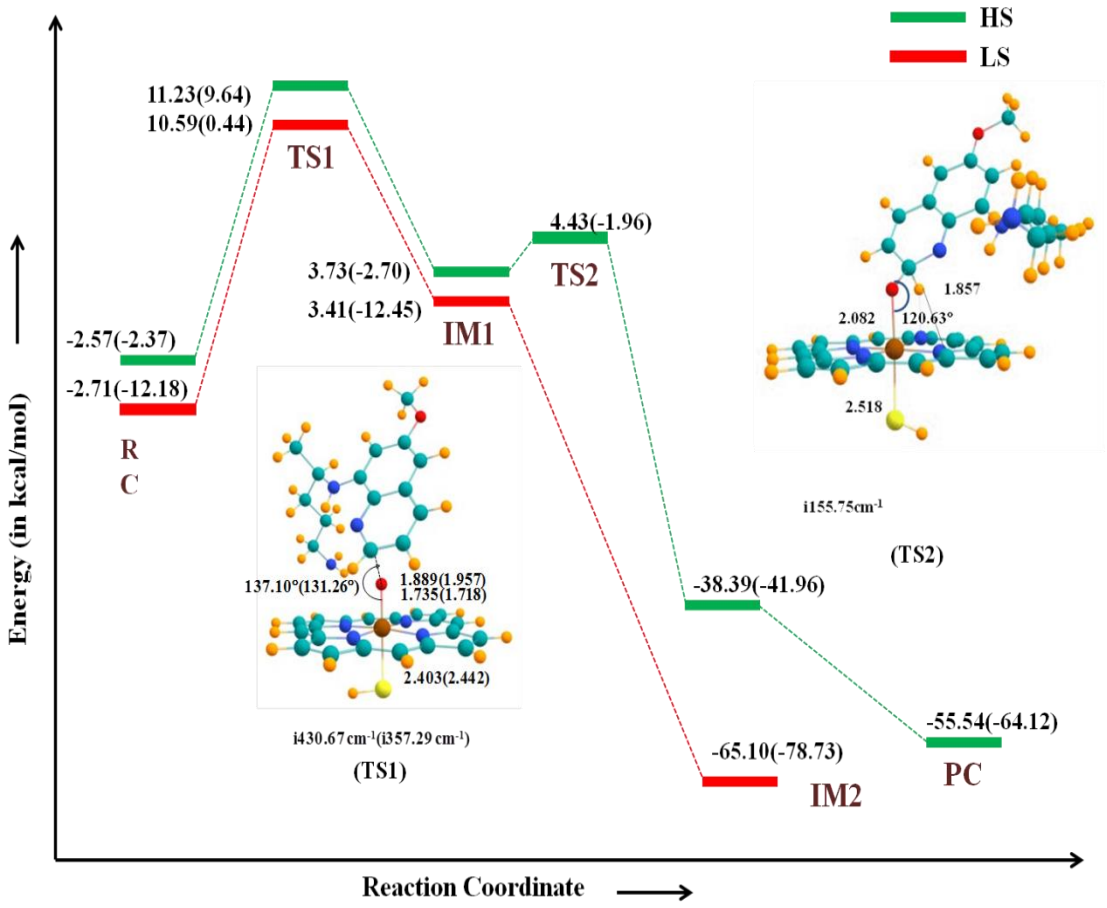

Figure 3.2: Potential energy surface of hydroxylation of Primaquine (2PQ) by Cytochrome P450 with energies in kcal/mol. Bond length, bond angle and imaginary frequencies (in cm^{-1}) of quartet as well as doublet (in bracket) spin state is shown. All energies are calculated at B3LYP/BS1//B3LYP/BS2 level of theory.

Other than these five metal orbitals, two highlying orbitals of heterocyclic ring (a_{1u} and a_{2u}) are also involved. But, in enzymatic systems a_{2u} orbital is slightly high in energy due to mixing from the sigma orbital of the axial ligand. So, two spin states

result with ferromagnetic and anti-ferromagnetic coupling between π_{xz}^{*1} π_{yz}^{*1} and a_{1u}^{2} respectively, whereas a_{1u} remains fully occupied.

DFT calculations revealed nearly ~ 1kcal/mol energy gap between quartet and doublet spin state as shown in Figure 3.3. Substrate (Primaquine) and Cpd I together form reactant complex (RC) when put at interacting distance with each other.

Nature of electron in substrate φ_c^1 (up and down) determines the spin state and also conserves the overall quartet and doublet spins (Figure 3.2). The electronic configuration of first transition state (TS1) is same as configuration of first intermediate (IM1). After this, in high spin (HS) state, first intermediate leads to second intermediate (IM2) by transfer of charge from ortho carbon (C-2) to one of the nitrogen atom of porphyrin ring (=N-H) following electronic configuration.

$\delta_{x^2-y^2}^{*2}$ π_{xz}^{*1} π_{yz}^{*1} $\sigma_{z^2}^{*1}$ σ_{xy}^{*0} a_{1u}^{2} a_{2u}^{2} φ_c^0, and the configuration of low spin state of second intermediate (IM2) state is δ_{x2-y2}^{*2} π_{xz}^{*1} π_{yz}^{*2} $\sigma_{z^2}^{*1}$ σ_{xy}^{*0} a_{1u}^{2} a_{2u}^{2} φ_c^0. Second transition state (TS2) of high spin state is observed as $\delta_{x^2-y^2}^{*2}$ π_{xz}^{*1} π_{yz}^{*1} $\sigma_{z^2}^{*1}$ σ_{xy}^{*0} a_{1u}^{2} a_{2u}^{2} φ_c^1. Further, product complex (PC) is formed by transfer of the hydrogen atom from nitrogen, and bind to the oxygen which has already been transferred at ortho position in second intermediate. The overall configuration of product is $\delta_{x^2-y^2}^{*2}$ π_{xz}^{*1} π_{yz}^{*1} $\sigma_{z^2}^{*1}$ σ_{xy}^{*0} a_{1u}^{2} a_{2u}^{2} φ_c^2, product formation is not observed in case of doublet spin state, due to formation of suicidal complex. The electronic configurations must change due to transfer of charge, so that occupancy of orbital a_{2u} ,π^*, σ^* and φ_c is also changed. As we discussed earlier, all three electrons of orbital π_{xz}^*, π_{yz}^* and a_{2u} combine ferromagnetically or anti-ferromagnetically to form quartet or doublet spin state respectively. These type of reaction mechanism lead to the two state reactivity (TSR) pattern [45–48]. These calculations are done by quantum mechanical (QM) method

using B3LYP basis set. There is a minor energy difference between doublet -2.71 kcal/mol and quartet spin state with energy -2.57 kcal/mol, of optimized reactant complex (RC) as shown in Figure 3.3.

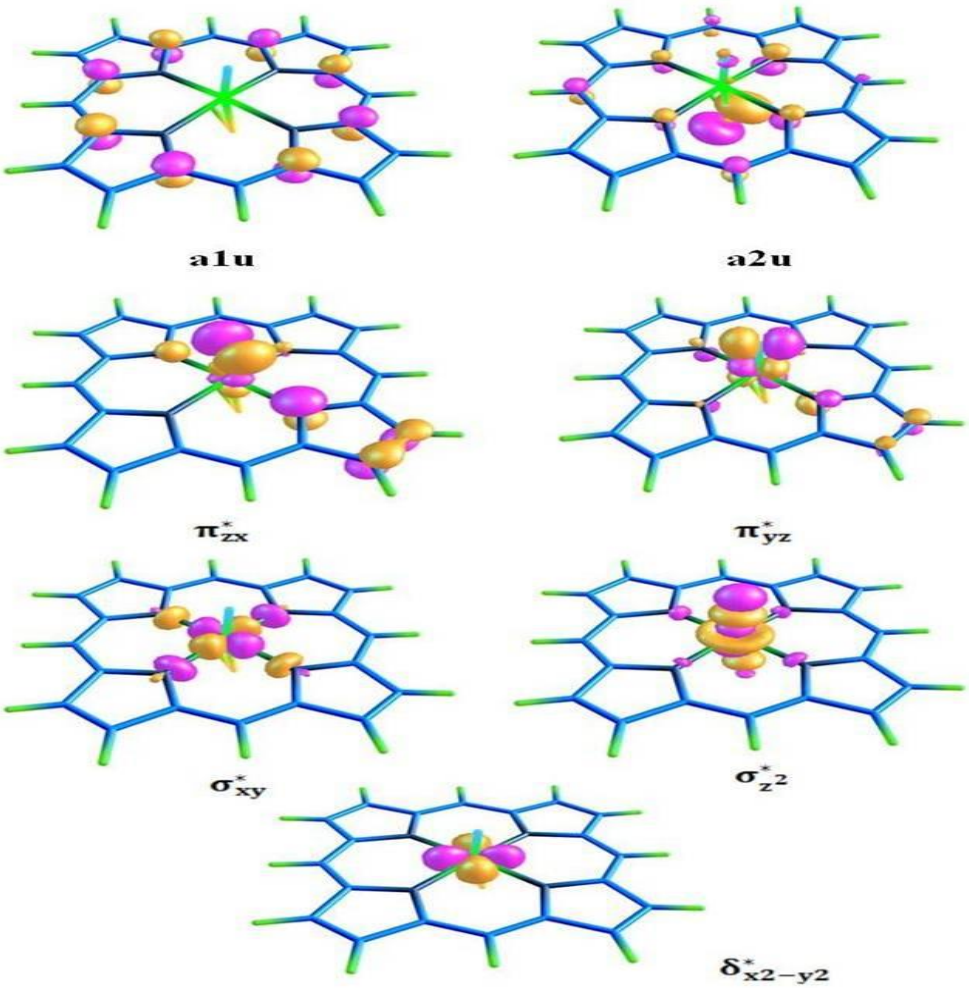

Figure 3.3: Key orbitals of Cpd I in order of their energy.

The energy gap between these two states is very close, i.e., these are degenerate energy state as we have discussed above. Optimized structure of reactant complex (RC), transition state (TS), intermediate state (IM), and product complex (PC) for doublet and quartet spin state is shown in Figure 3.4 and Figure 3.5 respectively. And their spin densities with mulliken charges are compiled in Table 1. The energy of first transition state (TS1) of doublet spin state is 10.59 kcal/mol, it forms more stable state than quartet spin state having energy 11.23 kcal/mol. The energy of first intermediate

(IM1) of doublet spin state is 3.41 kcal/mol, and it is comparable to quartet spin state 3.73 kcal/mol.

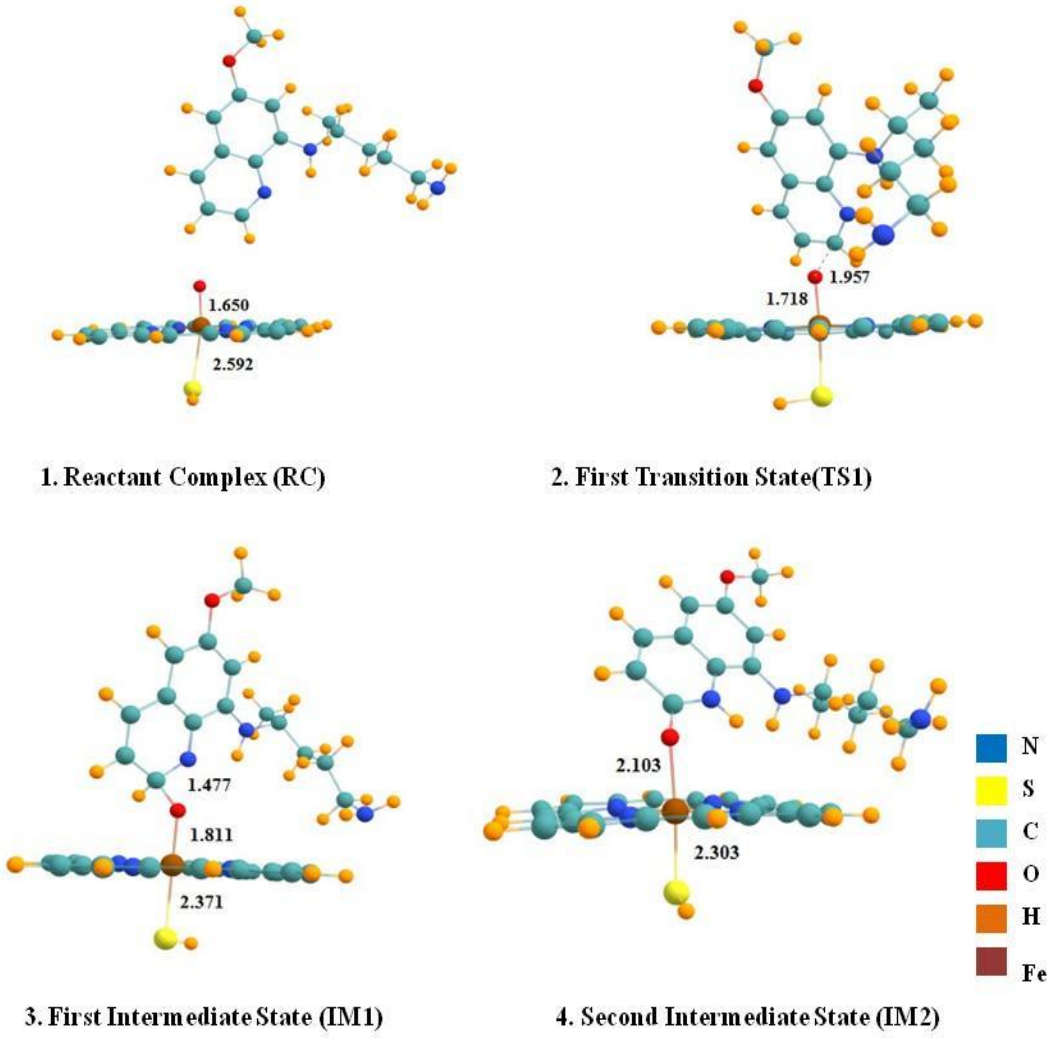

Figure 3.4: Optimized geometries of Reactant complex (RC), Transition state (TS), Intermediate complex (IM), and Product complex (PC) with differences in the bond lengths for respective atoms for LS of 2PQ.

Further, the energy of second transition state (TS2) of quartet spin state is 4.40 kcal/mol. These two degenerate states continuously maintain energy gap of (<1kcal/mol) between them. The energy of second intermediate (IM2) of doublet spin state is -65.10 kcal/mol, and the energy of quartet spin state is -38.39 kcal/mol,

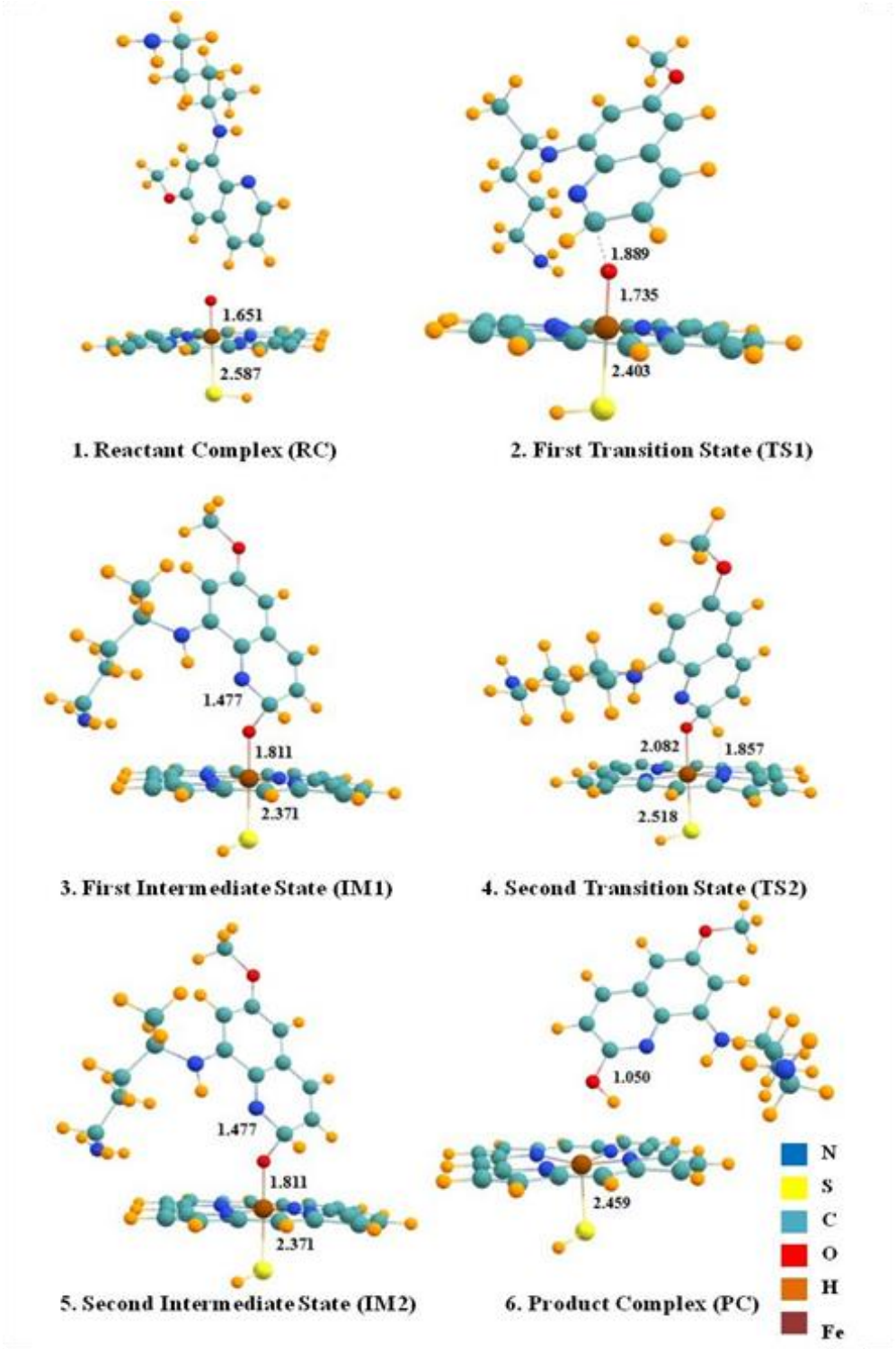

Figure 3.5: Optimized geometries of Reactant complex (RC), Transition state (TS), Intermediate complex (IM), and Product complex (PC) of quartet spin state (HS) of 2PQ.

this means it is more stable than quartet. LS surfaces offered formation of suicidal complexes, confirmed by reverse scan curves. At the end, it forms product complex

(PC) with energy -55.54 kcal/mol at high spin state. And the formed product is chemically named as 2-hydroxylated Primaquine (2-OH PQ).

With the frequency calculations, the reported imaginary frequencies of TS1 and TS2 of quartet spin state are 430.67i cm^{-1} and 155.75i cm^{-1} respectively. And imaginary frequency of TS1 of low spin state is 357.29i cm^{-1}. As shown in the energy profile Figure 3.2, intercrossing of the energy states indicates the spin cross over during the catalytic cycle [33-34].Moreover, the transfer of electron and spins of electron is also investigated by charges and spin densities (Mulliken and NBO atomic charges) using BS1 basis set and is reported in Table 3.1.

Table 3.1: Spin densities and charges of Cpd1 & 2PQ position of substrate (Primaquine) using BS1 basis set.

Reactant Complex										
Spin Density						**Charge**				
	Fe	**O**	**Por.**	**Sub.**	**SH**	**Fe**	**O**	**Por.**	**Sub.**	**SH**
M_4	1.07	0.94	0.43	-0.00	0.54	0.50	-0.34	0.10	0.00	-0.04
M_2	1.20	0.89	-0.50	-0.00	-0.58	0.51	-0.34	-0.11	0.00	-0.05
TS 1										
Spin Density						**Charge**				
	Fe	**O**	**Por.**	**Sub.**	**SH**	**Fe**	**O**	**Por.**	**Sub.**	**SH**

M_4	1.35	0.74	0.02	0.60	0.27	0.45	-0.41	-0.37	0.35	-0.02
M_2	1.59	0.33	-0.22	-0.49	0.21	0.45	-0.42	-0.34	0.37	-0.07
Intermediate 1										
Spin Density						**Charge**				
	Fe	**O**	**Por.**	**Sub.**	**SH**	**Fe**	**O**	**Por.**	**Sub.**	**SH**
M_4	1.89	0.35	-0.13	0.91	-0.03	0.49	-0.50	-0.35	0.35	0.01
M_2	1.77	0.28	-0.13	-0.85	-0.08	0.47	-0.50	-0.35	0.35	0.02
TS 2										
Spin Density						**Charge**				
	Fe	**O**	**Por.**	**Sub.**	**SH**	**Fe**	**O**	**Por.**	**Sub.**	**SH**
M_4	2.62	0.09	-0.10	0.22	0.26	0.53	-0.54	-0.44	0.15	-0.23
Intermediate 2										
Spin Density						**Charge**				
	Fe	**O**	**Por.**	**Sub.**	**SH**	**Fe**	**O**	**Por.**	**Sub.**	**SH**
M_4	2.83	0.09	0.04	-0.11	0.00	0.51	-0.62	0.02	-0.41	-0.12
M_2	1.10	0.00	-0.08	0.00	-0.28	0.35	-0.51	-0.56	0.20	-0.00
Product										
Spin Density						**Charge**				

	Fe	O	Por.	Sub.	SH	Fe	O	Por.	Sub.	SH
M_4	2.5	0.00	0.02	0.00	0.46	0.53	-0.60	-0.41	0.04	-0.16

3.3.2 Hydroxylation of Primaquine at para position (4PQ)

Abstraction of hydrogen atom at the para position of Primaquine is identified as 4PQ. All properties are also investigated for 4PQ by Quantum Mechanical (QM) methods.

As we discussed earlier, in this reaction, hydrogen atom at the para position of substrate (Primaquine), is abstracted by Cpd I. The energy profile for both spin surfaces LS as well as HS is studied as shown in Figure 8.

A reactant complex of doublet and quartet spin state has the same configuration as reactant complex of 2PQ. Before forming the product, both spin surfaces, high as well as low give two intermediate states IM1, IM2 with same electronic configuration as IM1, IM2 of 2PQ.

Here one can clearly notice that the LS surfaces offered formation of suicidal complexes, Also, product 4-hydroxylated Primaquine (4-OH PQ) was found to offer more energy than intermediate 2 (IM2) which further justified the formation of dead product. The optimized structure of reactant complex (RC), transition state (TS), the intermediate state (IM), and product complex (PC) for doublet or quartet spin state is shown in Figure 3.6 as well as in Figure 3.8 respectively.

The reaction followed patterns of two state reactivity (TSR) mechanism and energy landscape for doublet and the quartet was close and parallel with each other, but this pattern bifurcates at IM1. TSR behavior is transformed to single state reactivity (SSR) and shows that the reaction is possible only for high spin surface (HS). Also, electronic

configuration of first transition states (TS1) of HS as well as LS is same as electronic configuration of TS1 of 2PQ. The electronic configuration of third transition state (TS3) of high spin surface is $\delta_{x2-y2}^{*2}\ \pi_{xz}^{*1}\ \pi_{yz}^{*2}\ \sigma_{z^2}^{*1}\ \sigma_{xy}^{*0}\ a_{1u}^{2}\ a_{2u}^{2}\ \varphi_{c}^{0}$ and the product is $\delta_{x2-y2}^{*2}\ \pi_{xz}^{*1}\ \pi_{yz}^{*1}\ \sigma_{z^2}^{*1}\ \sigma_{xy}^{*0}\ a_{1u}^{2}\ a_{2u}^{2}$.

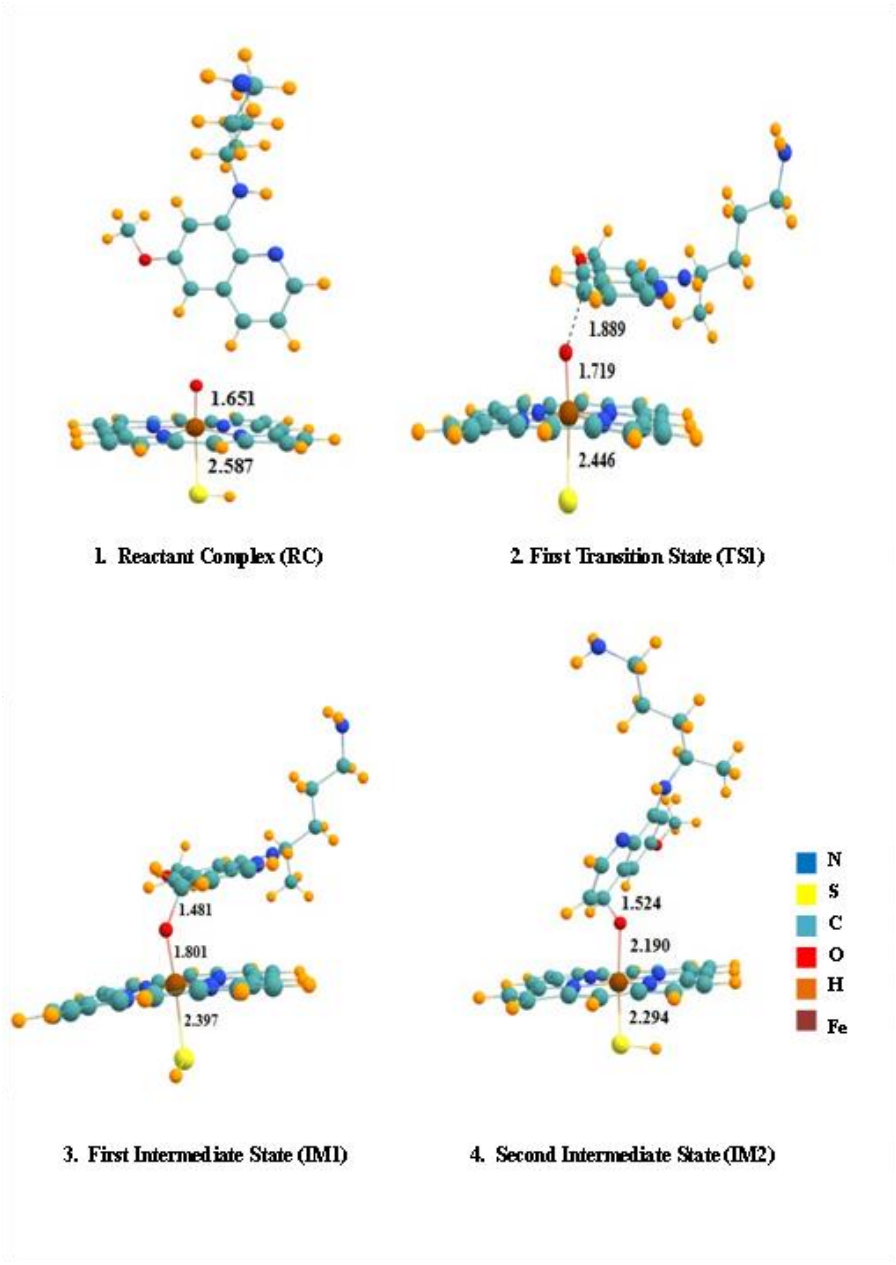

Figure 3.6: Optimized geometries of Reactant complex (RC), Transition state (TS), Intermediate complex (IM), and Product complex (PC) for doublet state (LS) of 4PQ.

The energy of reactant complex (RC) of the doublet is -3.97 kcal/mol which is very close to quartet having the energy -2.64 kcal/mol. The energy of first intermediate (IM1) of doublet and quartet is 6.47 kcal/mol as well as 3.92 kcal/mol respectively. The energy profile of para position of aromatic hydroxylation is shown in Figure 3.7. Both spin states continuously maintains 1 kcal/mol difference between them.

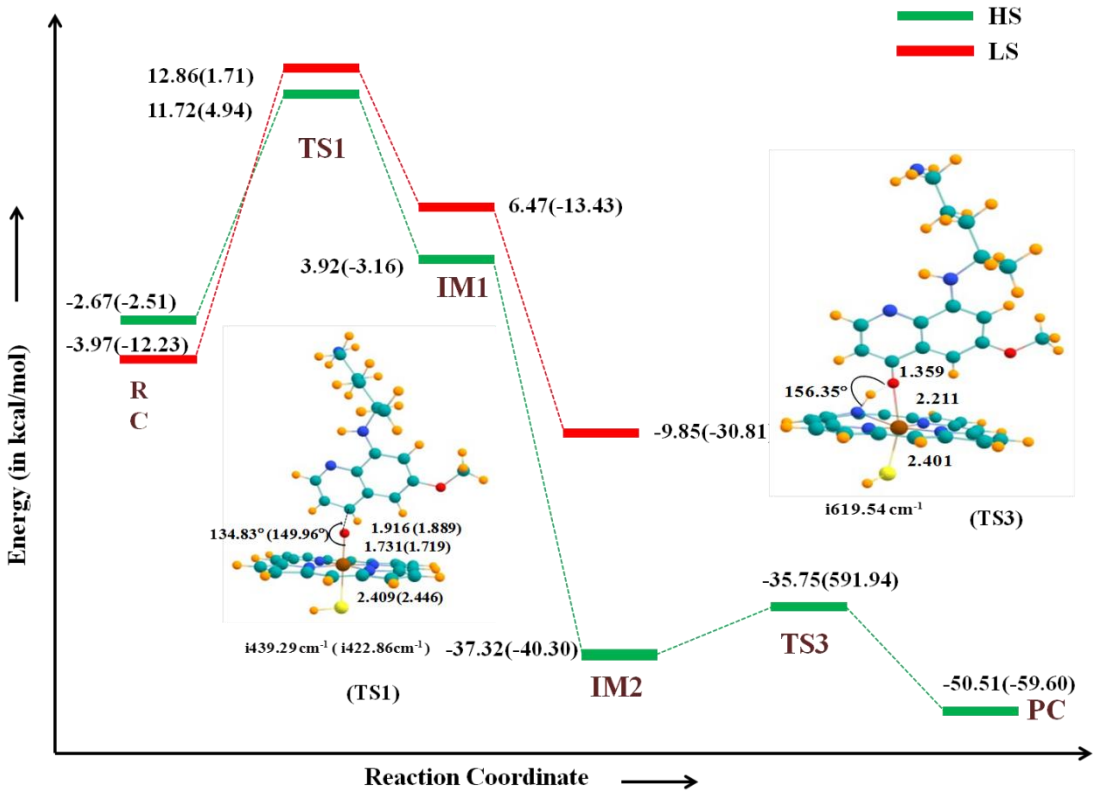

Figure 3.7: Potential energy surface of hydroxylation of Primaquine (4PQ) by Cytochrome P450 4 with energies in kcal/mol. Bond length, bond angle and imaginary frequencies (in cm^{-1}) of quartet (in green color) as well as doublet (in bracket in red color) spin state is shown. All energies are calculated at B3LYP/BS1//B3LYP/BS2 level of theory.

The energy of second intermediate (IM2) of doublet is -9.85 kcal/mol and quartet is -37.32 kcal/mol. The energy of third transition state of quartet (TS3) is -35.57 kcal/mol. Also, the energy of product of quartet spin state is -50.51 kcal/mol. The imaginary

frequency of TS1 of doublet is -422.86 cm^{-1} and quartet is -439.29 cm^{-1}. And imaginary frequency of TS3 of quartet is -619.54 cm^{-1}. Imaginary frequencies of quartet and doublet

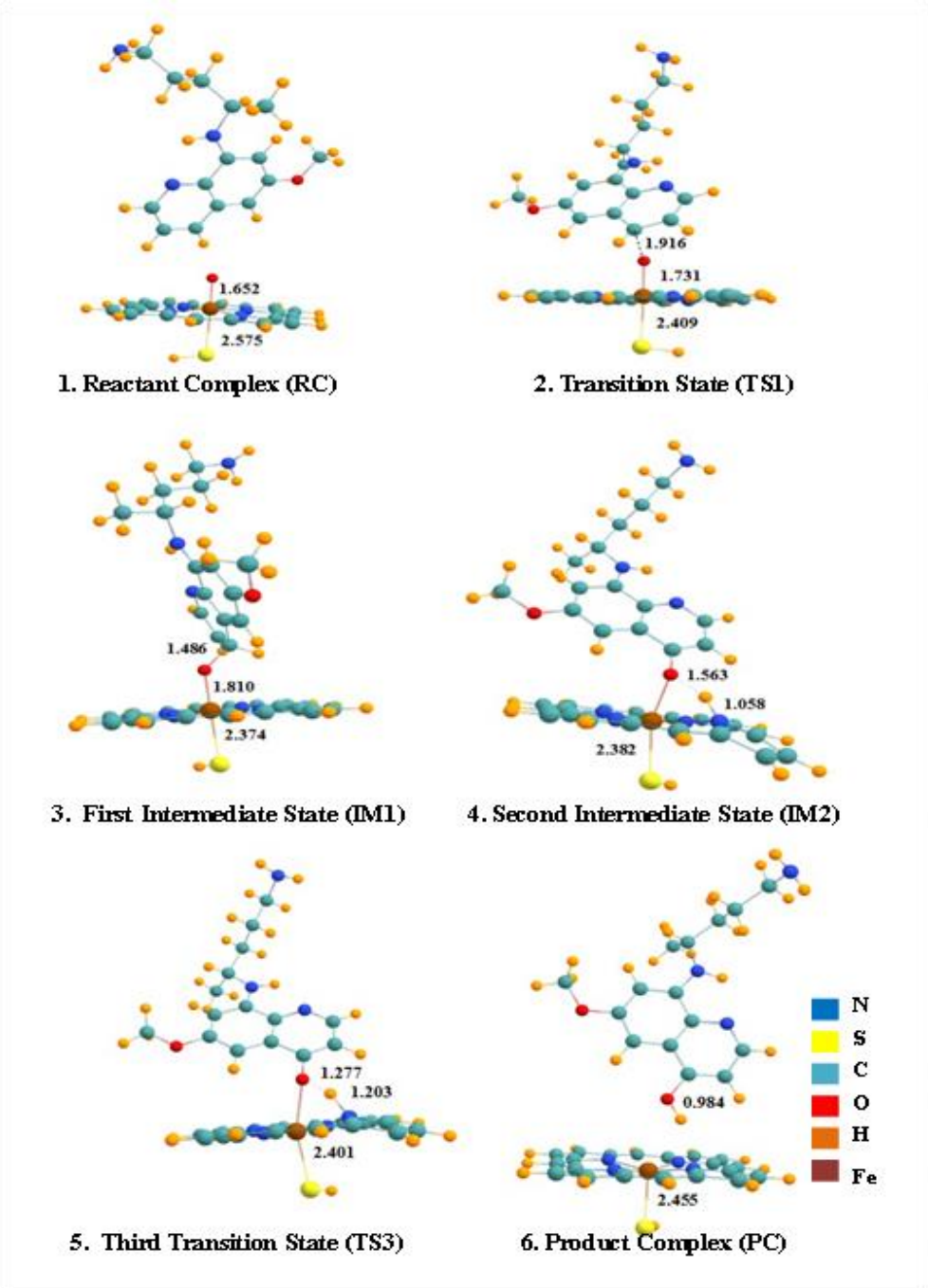

Figure 3.8: Optimized geometries of Reactant complex (RC), Transition state (TS), Intermediate complex (IM), and Product complex (PC) for quartet state (HS) of 4PQ.

spin state of transition states are shown in Figure 3.8. Optimized structures with corresponding bond length of all state of metabolic reaction for both surfaces are shown in Figure 3.6 & 3.8, respectively. These two step reactions are exothermic as expected. The overall rate of a chemical reaction is often determined by the slowest step of reaction, known as rate limiting or rate determining step. C-O bond formation step is the rate limiting step.

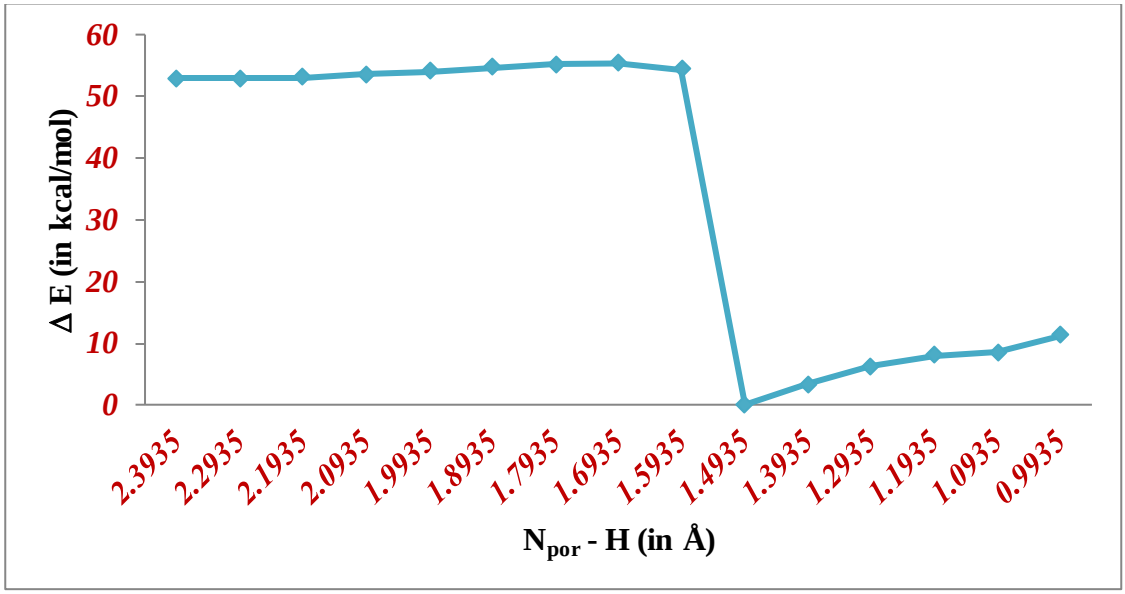

Figure 3.9: Scan results of 2PQ at low spin surface

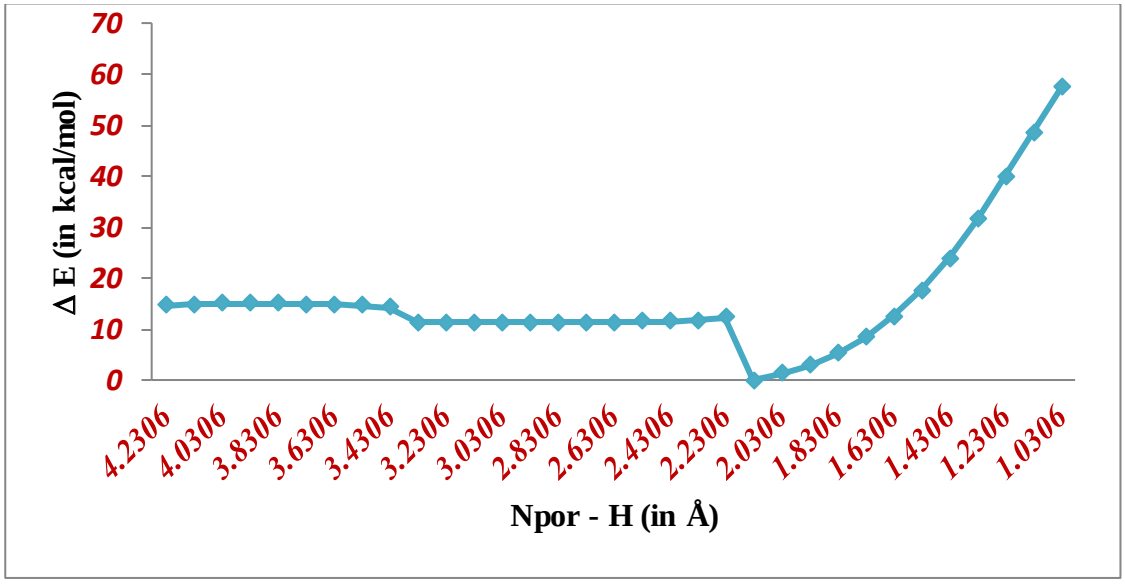

Figure 3.10: Scan results of 4PQ at low spin surface.

Rate limiting step has activation energy 10.59 and 11.23 kcal/mol, for both LS as well as HS state, respectively. Further, the transfer of electron and spins of electron is also investigated by charges and spin densities (Mulliken atomic charges) using BS1 basis set for 4PQ reported in Table 3.2. Scan graph of 2PQ and 4PQ for doublet surface is shown in Figure 3.9 and Figure 3.10 respectively.

Table 3.2: Spin densities and charges of Cpd1 & 4PQ position of substrate (Primaquine) using BS1 basis set.

Reactant Complex										
Spin Density						**Charge**				
	Fe	**O**	**Por.**	**Sub.**	**SH**	**Fe**	**O**	**Por.**	**Sub.**	**SH**
M_4	1.07	0.94	0.43	0.00	0.53	0.51	-0.34	-0.10	0.01	-0.05
M_2	1.20	0.91	-0.46	-0.05	-0.57	0.51	-0.35	-0.10	0.00	-0.05
TS1										
Spin Density						**Charge**				
	Fe	**O**	**Por.**	**Sub.**	**SH**	**Fe**	**O**	**Por.**	**Sub.**	**SH**
M_4	1.32	0.75	0.04	0.60	0.28	0.47	-0.40	-0.37	0.33	-0.02
M_2	1.62	0.40	-0.26	-0.51	-0.24	0.50	-0.45	-0.33	0.34	-0.07
Intermediate1										
Spin Density						**Charge**				

	Fe	O	Por.	Sub.	SH	Fe	O	Por.	Sub.	SH
M_4	1.84	0.37	-0.12	0.94	-0.03	0.49	-0.50	-0.34	0.32	-0.02
M_2	1.91	0.32	-0.16	-0.87	-0.19	0.55	-0.53	-0.35	0.30	0.02
Intermediate 2										
Spin Density						**Charge**				
	Fe	**O**	**Por.**	**Sub.**	**SH**	**Fe**	**O**	**Por.**	**Sub.**	**SH**
M_4	2.85	0.04	0.06	0.04	0.04	0.49	-0.72	0.07	-0.42	-0.08
M_2	1.12	-0.00	-0.09	-0.00	0.03	0.36	-0.41	-0.33	-0.27	0.02
TS 3										
Spin Density						**Charge**				
	Fe	**O**	**Por.**	**Sub.**	**SH**	**Fe**	**O**	**Por.**	**Sub.**	**SH**
M_4	2.71	0.02	0.03	-0.47	0.21	0.51	-0.71	-0.08	-0.47	-0.11
Product										
Spin Density						**Charge**				
	Fe	**O**	**Por.**	**Sub.**	**SH**	**Fe**	**O**	**Por.**	**Sub.**	**SH**
M_4	2.4	0.00	0.03	-0.00	0.46	0.53	-0.63	0.39	-0.64	-0.16

3.4 Conclusion

The present work investigate the complete reaction pathway of aromatic hydroxylation of Primaquine with Cpd I by DFT using basis set 6-31G (BS1) and the results were further cross checked using basis set 6-31+G* (BS2). Quantum mechanical calculations clearly depicted above hydroxylation reaction is rebound free process having more than one transition state with short lived intermediate state and C-O bond formation step to be rate determining step of the reaction. It can been seen from the energy profile for ortho (2PQ) and para (4PQ) position of Primaquine that quartet surface (HS) is responsible for the hydroxylated product whereas doublet spin surface profile is resulted in the formation of a *suicidal complex*.

Finally, the product at high spin state surface (HS), is formed, the reaction followed patterns of two state reactivity (TSR) mechanism and energy landscape for doublet and quartet were close and parallel with each other, but this pattern bifurcate at IM1. TSR behaviour is transformed to single state reactivity (SSR) showing that reaction is possible only for high spin surface (HS).

In the energy profile it is clearly shown that H-abstraction step is rate determining step with activation energy 11.23 kcal/mol and 10.59 kcal/mol for HS and LS respectively for hydroxylation at ortho position while for the hydroxylation at para position the activation energy is 12.86 kcal/mol and 11.72 kcal/mol for HS and LS respectively. Here it is also concluded that this process is not regioselective and the product is formed directly from intermediate. So, the present work is expanded to a great extent about to the metabolism of Primaquine via P450 by giving a reaction pathway.

Further, we calculated single point energy using basis set LACVP, solvent effect with Benzene and in presence of ammonia, and results are overlapping to each other, which

showed the reliability of results. These formed products (metabolites) are further used for treatment of malaria. These quantum mechanical calculations are considered for good accuracy results.

Present reactions mechanism is different from aliphatic hydroxylation reactions of Cytochrome P450 enzyme, due to formation of suicidal complex at the low spin surface. But further results give good accuracy as we expected and these results can be used for experimental researches and will give fruitful results. And there results have good accuracy for isolated reaction coordinates which shows the success of present work.

References

[1] S. Shaik, S. P. De Visser, "Computational Approaches to Cytochrome P450 Function. Cytochrome P450 Structure," *Mech. Biochem. Third Ed.*, 45, **2005.**

[2] S. Shaik, S. Cohen, Y. Wang, H. Chen, D. Kumar, W. Thiel, "P450 Enzymes: Their Structure, Reactivity, and Selectivity - Modeled by QM/MM Calculation", *Chem. Rev.*, 110, 949, **2010.**

[3] M. Asaka, H. Fujii, "Participation of Electron Transfer Process in Rate-Limiting Step of Aromatic Hydroxylation Reactions by Compound i Models of Heme Enzymes", *J. Am. Chem. Soc.*, 138, 8048, **2016.**

[4] N. Harris, S. Shaik, D. Schroder, H. H.Schwarz, "Single- and Two-State Reactivity in the Gas-Phase C-H Bond Activation of Norbornane by "bare" FeO+, Helv.", *Chim. Acta*, 82, 1784, **1999.**

[5] C. M. Link, A. D. Theoharides, J. C. Anders, H. Chung, C. J. Canfield, "Structure-Activity Relationships of Putative Primaquine Metabolites Causing Methemoglobin Formation in Canine Hemolysates", *Toxicol. Appl. Pharmacol.*, 192, 81, **1985.**

[6] L. Ji, A. S. Faponle, M. G. Quesne, M. A. Sainna, J. Zhang, A. Franke, D. Kumar, R. Van Eldik, W. Liu, S. P. De Visser, "Drug Metabolism by Cytochrome P450 Enzymes: What Distinguishes the Pathways Leading to Substrate Hydroxylation over Desaturation?" *Chem. - A Eur. J.*, 21, 9083–9092, **2015**.

[7] E. O'Reilly, V. Köhler, S. L. Flitsch, "Cytochromes P450 as Useful Biocatalysts: Addressing the Limitations", *Chem. Commun.*, 47, 2490–2501,

2011.

[8] F. P. Guengerich, "Cytochrome P-450 3A4: Regulation and Role in Drug Metabolism", *Annu. Rev. Pharmacol. Toxicol.*, 39, 1–17, **1999**.

[9] U. M. Zanger, M. Schwab, "Cytochrome P450 Enzymes in Drug Metabolism: Regulation of Gene Expression, Enzyme Activities, and Impact of Genetic Variation", *Pharmacol. Ther.*, 138, 103-141, **2013.**

[10] S. Shaik, W. Lai, H. Chen, Y. Wang, "The Valence Bond Way: Reactivity Patterns of Cytochrome P450 Enzymes and Synthetic Analogs", *Acc. Chem. Res.*, 43, 1154-1165, **2010.**

[11] M. S. Butler, "Natural Products to Drugs: Natural Product Derived Compounds in Clinical Trials", *Nat. Prod. Rep.*, 22, 162–195, **2005**.

[12] R. Ullrich, M. Hofrichter, "Enzymatic Hydroxylation of Aromatic Compounds", *Cell. Mol. Life Sci.*, 64, 271–293 **2007**.

[13] D. Kumar, G. N. Sastry, S. P. De Visser, "Axial Ligand Effect On The Rate Constant of Aromatic Hydroxylation", *J. Phys. Chem. B*, 116, 718–730, **2012.**

[14] C. M. Bathelt, L. Ridder, A. J. Mulholland, J. N.Harvey, "Aromatic Hydroxylation by Cytochrome P450: Model Calculations of Mechanism and Substituent Effects", *J. Am. Chem. Soc.*, 125, 15004–15005, **2003**.

[15] F. Zhang, J. L. Bolton, "Synthesis of the Equine Estrogen Metabolites 2-Hydroxyequilin and 2- Hydroxyequilenin", *Chem. Res. Toxicol.*, 12, 200–203. **1999**.

[16] Z. Huang, F. P. Guengerich, L. S. Kaminsky, "16α-Hydroxylation of Estrone by Human Cytochrome P4503A4/5", *Carcinogenesis*, 19, 867–872 **1998**.

[17] A. J. Lee, M. X. Cai, P. E.Thomas, A. H. Conney, B. T. Zhu, "Characterization of the Oxidative Metabolites of 17β-Estradiol and Estrone Formed by 15 Selectively Expressed Human Cytochrome P450 Isoforms", *Endocrinology*, 144, 3382–3398 **2003**.

[18] Guo, J.; Liu, A.; Cao, H.; Luo, Y.; Pezzuto, J. M.; Van Breemen, R. B. Biotransformation of the Chemopreventive Agent 2',4',4-Trihydroxychalcone (Isoliquiritigenin) by UDP-Glucuronosyltransferases. *Drug Metab. Dispos.*, 36, 2104–2112, **2008**.

[19] J. L. Sessler, D. Seidel, "Synthetic Expanded Porphyrin Chemistry", *Angewandte Chemie*, 56, 5134–5175. **2003.**

[20] F. Carvalho, M. E. Soares, E. Fernandes, F. Remião, M. Carvalho, J. A Duarte, R. Pires-das-Neves, M. D. L. Pereira, M. D. L. Bastos, "Repeated Administration of D-Amphetamine Results in a Time-Dependent and Dose-Independent Sustained Increase in Urinary Excretion of p-Hydroxyamphetamine in Mice", *J. Heal. Sci.*, *53*, 371–377 **2007**.

[21] S. Yoshioka, S. Takahashi, K. Ishimori, I. Morishima, "Roles of the Axial Push Effect in Cytochrome P450cam Studied with the Site-Directed Mutagenesis at the Heme Proximal Site", *J. Inorg. Biochem.*, *81*, 141–151 **2000**.

[22] S. NARIMATSU, M. TACHIBANA, Y. MASUBUCHI, S.IMAOKA, Y. FUNAE, T. SUZUKI, "Cytochrome P450 Isozymes Involved in Aromatic Hydroxylation and Side-Chain N-Desisopropylation of Alprenolol in Rat Liver Microsomes", *Biol. Pharm. Bull.*, 18, 1060–1065, **1995**.

[23] P. R. Ortiz De Montellano, J. J. De Voss, "Substrate Oxidation by Cytochrome P450 Enzymes", *Cytochrome P450 Struct. Mech. Biochem. Third Ed.*, 3, 183–

245, **2005**.

[24] T. D. Lash, "Origin of Aromatic Character in Porphyrinoid Systems", *J. Porphyr. Phthalocyanines*, 15, 1093–1115, **2011**.

[25] J. Wen, D. Chennamadhavuni, S. R. Morel, M. K. Hadden, "Truncated Itraconazole Analogues Exhibiting Potent Anti-Hedgehog Activity and Improved Drug-like Properties", *ACS Med. Chem. Lett.*, 10, 1290–1295, **2019**.

[26] S. Cohen, S. Kozuch, C. Hazan, S. Shaik, "Does Substrate Oxidation Determine the Regioselectivity of Cyclohexene and Propene Oxidation by Cytochrome P450?", *J. Am. Chem. Soc.*, 128, 11028–11029, **2006**.

[27] P. R. Ortiz de Montellano, J. J. De Voss, "Oxidizing Species in the Mechanism of Cytochrome P450", *Nat. Prod. Rep.*, 19, 477–493, **2002**.

[28] P. R. Ortiz De Montellano, J. J. De Voss, "Substrate Oxidation by Cytochrome P450 Enzymes. In *Cytochrome P450: Structure, Mechanism, and Biochemistry"*, 3, 183–245, **2005.**

[29] M. Torrent, D. G. Musaev, H. Basch, K. Morokuma, "Computational Studies of Reaction Mechanisms of Methane Monooxygenase and Ribonucleotide Reductase", *J. Comput. Chem.*, 23, 59–76, **2002**.

[30] J. C. Schöneboom, H. Lin, N. Reuter, W.Thiel, S. Cohen, F.Ogliaro, S. Shaik, "The Elusive Oxidant Species of Cytochrome P450 Enzymes: Characterization by Combined Quantum Mechanical/Molecular Mechanical (QM/MM) Calculations", *J. Am. Chem. Soc.*, *124*, 8142–8151, **2002.**

[31] S. Shaik, S. Cohen, Y. Wang, H. Chen, D. Kumar, W. Thiel, "P450 Enzymes: Their Structure, Reactivity, and Selectivity - Modeled by QM/MM Calculations", *Chemical Review*, 110, 949-1017, **2010.**

[32] D. Fishelovitch, C. Hazan, H. Hirao, H. J. Wolfson, R. Nussinov, S. Shaik, "QM/MM Study of the Active Species of the Human Cytochrome P450 3A4, and the Influence Thereof of the Multiple Substrate Binding", *J. Phys. Chem. B*, 111, 13822–13832. **2007.**

[33] Y. Wang, H. Chen, M. Makino, Y. Shiro, S. Nagano, S. Asamizu, H. Onaka, S. Shaik, "Theoretical and Experimental Studies of the Conversion of Chromopyrrolic Acid to an Antitumor Derivative by Cytochrome P450 StaP: The Catalytic Role of Water Molecules", *J. Am. Chem. Soc.*, 131, 6748–6762. **2009**.

[34] A. Altun, V. Guallar, R. A. Friesner, S. Shaik, W. Thiel, "The Effect of Heme Environment on the Hydrogen Abstraction Reaction of Camphor in P450cam Catalysis: A QM/MM Study", *J. Am. Chem. Soc.*, 128, 3924–3925, **2006**.

[35] D. Riccardi, P. Schaefer, Q. P. K. Cui, "A Calculations in Solution and Proteins with QM/MM Free Energy Perturbation Simulations: A Quantitative Test of QM/MM Protocols", *J. Phys. Chem. B*, 109, 17715–17733, **2005**.

[36] T. Benighaus, W. Thiel, "Efficiency and Accuracy of the Generalized Solvent Boundary Potential for Hybrid QM/MM Simulations: Implementation forSemiempirical Hamiltonians", *J. Chem. Theory Comput.*, 4, 1600–1609. **2008**,

[37] B. S. Pybus, J. C. Sousa, X. Jin, J. A. Ferguson, R. E. Christian, R. Barnhart, C. Vuong, R. J. Sciotti, G. A. Reichard, M. P. Kozar, "CYP450 Phenotyping and Accurate Mass Identification of Metabolites of the 8-Aminoquinoline , Anti-Malarial Drug Primaquine", *Malaria Journal*, 259, 1–9, **2012.**

[38] D. R. Hill, J. K. Baird, M. E. Parise, L. S. Lewis, E. T. Ryan, A. J. Magill,

"Primaquine: Report from CDC Expert Meeting on Malaria Chemoprophylaxis", I. *Am. J. Trop. Med. Hyg.*, 75, 402–415, **2006**.

[39] K. A. Lee, W. Nam, "Determination of Reactive Intermediates in Iron Porphyrin Complex-Catalyzed Oxygenations of Hydrocarbons Using Isotopically Labeled Water: Mechanistic Insights", *J. Am. Chem. Soc.*, 119, 1916–1922, **1997**.

[40] G. Camarda, P. Jirawatcharadech, R. S. Priestley, A. Saif, S. March, M. H. L.Wong, S. Leung, A. B. Miller, D. A. Baker, P. Alano, "Antimalarial Activity of Primaquine Operates via a Two-Step Biochemical Relay", *Nat. Commun.*, *10*, **2019**.

[41] S. Shaik, H. Hirao, D. Kumar, "Reactivity Patterns of Cytochrome P450 Enzymes: Multifunctionality of the Active Species, and the Two States-Two Oxidants Conundrum", *Nat. Prod. Rep.*, *24*, 533–552, **2007**.

[42] H. Hirao, D. Kumar, L. Que, S. Shaik, "Two-State Reactivity in Alkane Hydroxylation by Non-Heme Iron-Oxo Comolexes", *J. Am. Chem. Soc.*, 128, 8590–8606, **2006.**

[43] M. J. Frisch, G. W. Trucks, H. B. Schlegel, G. E. Scuseria, M. A. Robb, J. R. Cheeseman, G. Scalmani, V. Barone, B. Mennucci, G. A. Petersson, "Gaussian 09, Revision B.01", *Gaussian 09, Revis. B.01, Gaussian, Inc., Wallingford CT*, 1–20, **2009.**

[44] W. R.Wadt, P. J. Hay, "Ab Initio Effective Core Potentials for Molecular Calculations. Potentials for Main Group Elements Na to Bi.", *J. Chem. Phys.*, 82, 284–298, **1985**.

[45] S. Shaik, S. Cohen, S. P. De Visser, P. K. Sharma, D. Kumar, S. Kozuch, F. Ogliaro, D. Danovich, "The "Rebound Controversy": An Overview and

Theoretical Modeling of the Rebound Step in C-H Hydroxylation by Cytochrome P450", *Eur. J. Inorg. Chem.*, 2, 207–226, **2004**.

[46] R. Hussain, I. Kumari, S. Sharma, M. Ahmed, T. A. Khan, Y Akhter, "Catalytic Diversity and Homotropic Allostery of Two Cytochrome P450 Monooxygenase like Proteins from Trichoderma Brevicompactum", *J. Biol. Inorg. Chem.*, *22*, 1197–1209, **2017**.

[47] S. P. De Visser, S Shaik, "A Proton-Shuttle Mechanism Mediated by the Porphyrin in Benzene Hydroxylation by Cytochrome P450 Enzymes", *J. Am. Chem. Soc.*, *125*, 7413–7424, **2003**.

[48] M. Albeck, S. Shaik, "Publications of Sason Shaik", *J. Phys. Chem. A*, *112*, 12741–12753, **2008**.

[49] X. Y Wang, H. M.Yan, Y. L Han, Z. X Zhang, X. Y. Zhang, W. J. Yang, Z Guo,Y. R. Li, "Do Two Oxidants (Ferric-Peroxo and Ferryl-Oxo Species) Act in the Biosynthesis of Estrogens? A DFT Calculation", *RSC Adv.*, *8*, 15196–15201, **2018**.

[50] S. Shang, Z. Lin, A.Yin, S.Yang, Y Chi, Y. Wang, J. Dong, B. Liu, N. Zhen, C. L. Hill, "Self-Assembly of Ln(III)-Containing Tungstotellurates(VI): Correlation of Structure and Photoluminescence", *Inorg. Chem.*, 57, 8831–8840, **2018**.

Chapter-4

Interplay between two degenerate spin state determines the hydroxylation of 4-nitrophenol catalyzed via Cytochrome P450

Chapter-4

Interplay between two degenerate spin state determines the hydroxylation of 4-nitrophenol catalyzed via Cytochrome P450

4.1 Introduction

The Cytochrome P450 is an essential enzyme found in nature [1]. It consists of number of enzymes with varying substrate selectivity, such as CYP1A2, 2A6, 2B6, 2C9, 2C19, 2D6, 2E1 and 3A etc. These enzymes are responsible for the metabolism of about 70% of therapeutic drugs [2]. In human, P450 is found in liver [3]. It contribute in the catalysis of variety of stereo and regio-selective mono-oxygenation reaction processes and also in detoxification processes [4]. Due to their wide range versatility in activation of several substrate, CYP is very important enzyme, in biology, biotechnological and pharmaceutical applications for investigations of new drugs [5]. Moreover, its involvement in drug metabolism make this enzyme a target for research in drug industry and biomedical field [6-9]. Despite of various member of P450 enzyme, CYP2E1 has been paid a considerable attention, because of its toxicological behavior. It is contributed in the metabolism of various organic solvents and environmental pollutants like, acetone, aniline, ethanol, or nitrosamines etc [10-11]. Metabolism by CYP2E1 might result in the formation of more reactive products, such

as the toxic metabolite of acetaminophen (paracetamol) [11,12]. Formation of toxic product of acetaminophen (paracetamol) via CYP2E1, is its crucial behaviour. 4-nitrophenol hydroxylation may responsible for inhibition of toxic product of acetaminophen (paracetamol) via CYP2E1 enzyme.

4-nitrophenol is formed during the synthesis of paracetamol. Initially, it reduced to 4-aminophenol, after that acetylated via acetic anhydride [14]. It is also product of essential enzymatic reactions of several substrate like- 4-nitrophenyl phosphate, 4-nitrophenyl acetate, 4-nitrophenyl-β-D-glucopyranoside and more other derivatives. It plays a crucial role in xenobiotic metabolism process in both, human and mouse. In field of medicinal chemistry, it is used in manufacturing of drugs, insecticides, fungicides. Its structure has phenolic compound, in which nitro group is attached at the opposite of the hydroxyl group on benzene ring. It is also known as *p*-nitrophenol or 4-hydroxynitrobenzene due to presence phenol group. It is mostly used in detection of the presence of alkaline phosphatase activity [15].

The P450 enzyme metabolizes various compounds using high-valent iron (IV) oxo species complex, generally known as Cpd I. This complex is formed during the catalytic cycle of Cytochrome P450. Initially, in catalytic cycle, P450 is in the resting state and a water molecule is ligated with it. Whenever, substrate enters, it tightly binds with porphyrin by expelling the water molecule. After the oxidation step a ferric peroxide species is formed, known as compound 0 (Cpd 0), and then Cpd 0 converts into iron (IV)-oxo porphyrin cation radical oxidants, known as compound I (Cpd I) through a protonation step. It is the primary oxidant that involved in the oxidation reaction of all member of P450. Here we used a truncated model of Cpd I to explore the overall reaction. As we discussed earlier 4-nitrophenol is responsible for various Xenobiotic reactions and these reactions are mediated via CYP2E1 enzyme [16]. So,

present study addresses the aromatic hydroxylation of 4-nitrophenol via Cpd I of P450 and form a product (metabolite) known as 2-hydroxy 4-nitrophenol. CYP2E1 is a member of the P450 enzyme, so their active site is similar for both enzymes. That's why P450 enzyme is used here for hydroxylation.

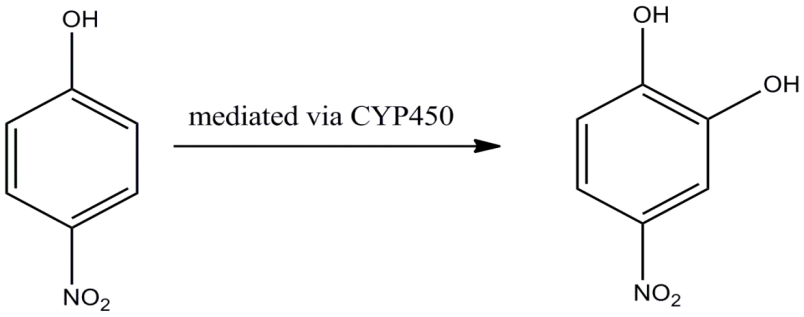

Figure 4.1: Aromatic hydroxylation of 4-nitrophenol via Cytochrome P450.

Now days, Density Functional Theory is most reliable and accurate for theoretical study of the reactivity pattern of Cpd I with hybrid function B3LYP [17]. The C-H hydroxylation of the substrate with Cpd I is followed by two different spin surfaces, one is, high spin state (HS) and the other is, low spin state (LS). These two different spin state energy barriers lead to two-state reactivity (TSR) pattern [18-20]. In the present work, we have studied aromatic hydroxylation of 4-nitrophenol (Figure 4.1). The reaction pathway for reaction complex (RC), transition state (TS), intermediate state (IM) and product complex (PC) for both spin state, doublet (LS) as well as quartet (HS), are shown in energy profiles as will discuss later. Further, we cross checked the results using basis set "LACVP" and solvent effect for benzene. We got the results overlapping to each other, which show the reliability of the results.

4.2. Methodological Overview

Present study comprises an investigation of reaction energy profile by Quantum Mechanical (QM) method. All calculations have been performed by Gaussian 09

package [21-22]. Density functional theory (DFT) with hybrid functional B3LYP [3,17,23-28] using LAN2DZ basis set on iron atom and 6-31G basis set on rest of the atom (BS1). Here, all calculations were performed for porphyrin cation radical iron (IV) oxo species i.e $Por^{+\cdot}FeIV=O$, (Cpd I), in two different spin states, doublet and quartet. Optimized geometries of reactant, intermediate, product are performed. A clear pathway for the reaction mechanism is found on potential energy surface (PES) with subsequent transition states. Analytic frequency calculations confirmed the local minima of reactant, intermediate, product by showing the real frequencies with first-order saddle point means, transition state having single imaginary frequency. Spin densities and Mulliken charges are also investigated (Table 4.1).

4.3. Key Orbital of Cpd I with substrate

Occupancy of the orbitals is the key to understanding the electronic configuration of Cpd I with substrate. $3d_{z^2}$ orbital of iron (Fe) and $2p_z$ orbital of oxygen (O38) of Cpd I together formed $\sigma^*_{z^2}$ anti-bonding orbital, whereas interaction of $3d_{xy}$ orbital of iron (Fe) and $2p_{xy}$ orbital of nitrogen atoms (N) of porphyrin together form anti-bonding orbital σ^*_{xy} . These orbitals are initially unfilled due to their high energy state and filled in later part of reaction process. Further, $\delta_{x^2-y^2}$ is orbital of porphyrin ring. The low-lying bonding orbital π_{xz}/π_{yz} and antibonding orbital π^*_{xz} / π^*_{yz} is formed by the interaction between $3d_{xz}$ /$3d_{yz}$ orbital of iron and $2p_x$ /$2p_y$ orbital of oxygen. These bonding π_{xz}/π_{yz} orbitals are always filled. Optimized orbital are shown in figure 4.2. Other than these metal orbitals, two high lying orbitals of heterocyclic ring also formed orbitals a_{1u} and a_{2u}. But, in enzymatic systems a_{2u} orbital is slightly high in energy due to mixing from sigma orbital of axial ligand thiolate. So, two spin states result with ferromagnetic and anti-ferromagnetic coupling between π^{*1}_{xz} π^{*1}_{yz} and a_{2u},

respectively, whereas a_{2u} remains fully occupied. These all three electrons of orbital π^*_{xz}, π^*_{yz} and a_{2u} combine ferromagnetically or anti-ferromagnetically to form quartet (HS) or doublet (LS) spin state respectively. These type of reaction mechanism leads to the two state reactivity (TSR) pattern [18,29-31].

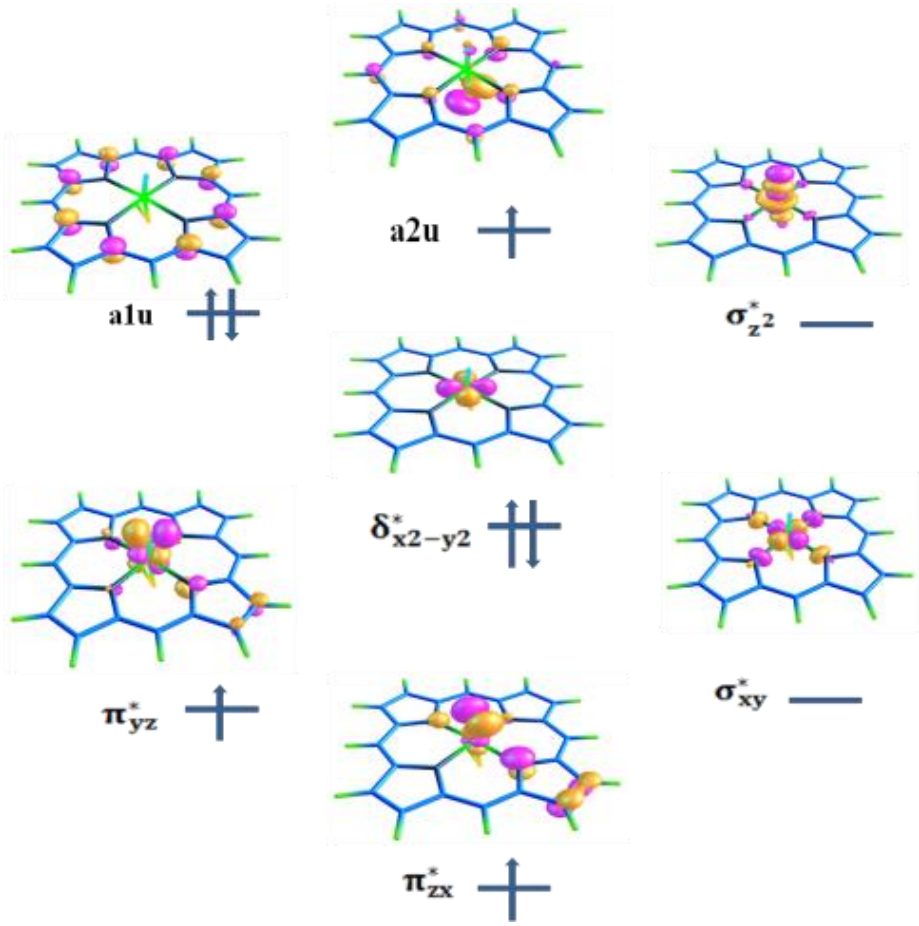

Figure 4.2: Key orbital of Cpd I in order of their energy.

4.4. Results and discussion

The proposed work to large extent explain the aromatic hydroxylation of 4-nitrophenol at ortho position of the aromatic ring (C49) via Cpd I. Initially, substrate bind with oxygen atom (O38) of Cpd I at interacting distance of 3 Å to form a stable reactant complex (RC) with energies -10.28 eV & -18.30 eV at high as well as low spin surfaces respectively. After this, charge of O38 of Cpd I is transfer to the carbon atom

(C49) of substrate, gives first transition state (TS1) with comparatively less energy 10.66 eV & 10.25 eV at high as well as low spin surfaces respectively. This step is the slowest step of reaction and commonly known as ***rate determining step***, from this we can predict the rate of reaction. We also reported the barrier energy of both surfaces is close to 10 kcal/mol, indicating requirement of less energy for crossing the both surfaces of reactant complex. Further, first intermediate complex (IM1) with energy 4.66 kcal/mol is formed only at the high spin surface. In the next step, hydrogen atom (H53) get attached with nitrogen atom (N2) of porphyrin ring forming a second intermediate state (IM2) with -46.47 kcal/mol & -48.76 kcal/mol energy at high as well as low spin surfaces respectively. Further, this hydrogen atom (H53) attached to the abstracted oxygen atom (O38) of Cpd I, and form the most stable product complex (PC) having energy -56.62 kcal/mol with third transition state (TS3) having energy -44.08 kcal/mol at high spin surface.

Negative value of third transition state shows less energy required to form product complex from second intermediate step. DFT calculations revealed nearly ~ 1kcal/mol energy gap between quartet and doublet spin state as shown in Figure 4.3.

As we already mentioned, the electronic configuration of Cpd I must be clearly identified, for better understanding of reaction pathway. The electronic configuration of reactant complex (RC) is observed for two spin states to be $\delta_{x2-y2}^{*2}\ \pi_{xz}^{*1}\ \pi_{yz}^{*1}\ \sigma_{z^2}^{*0}\ \sigma_{xy}^{*0}\ a_{1u}^{2}\ a_{2u}^{1}$. The first transition state (TS1) has electronic configuration $\delta_{x2-y2}^{*2}\ \pi_{xz}^{*1}\ \pi_{yz}^{*1}\ \sigma_{z^2}^{*0}\ \sigma_{xy}^{*0}\ a_{1u}^{2}\ a_{2u}^{2}\ \varphi_{c}^{1}$, nature of electron in substrate φ_{c}^{1} (up and down) determines the spin state and also conserves the overall quartet and doublet spins (Figure 4.3). The electronic configuration of first intermediate (IM1) is same as configuration of first transition state (TS1) at high spin surface.

After formation of first intermediate state (IM1), it leads to second intermediate (IM2) by transfer of charge from carbon (C49) to the nitrogen atom (N53) of Porphyrin ring (=N-H) following the electronic configuration $\delta^{*2}_{x2-y2}\ \pi^{*1}_{xz}\ \pi^{*1}_{yz}\ \sigma^{*0}_{z^2}\ \sigma^{*1}_{xy}\ a^{2}_{1u}\ a^{2}_{2u}\ \varphi^{2}_{c}$ at both spin surface.

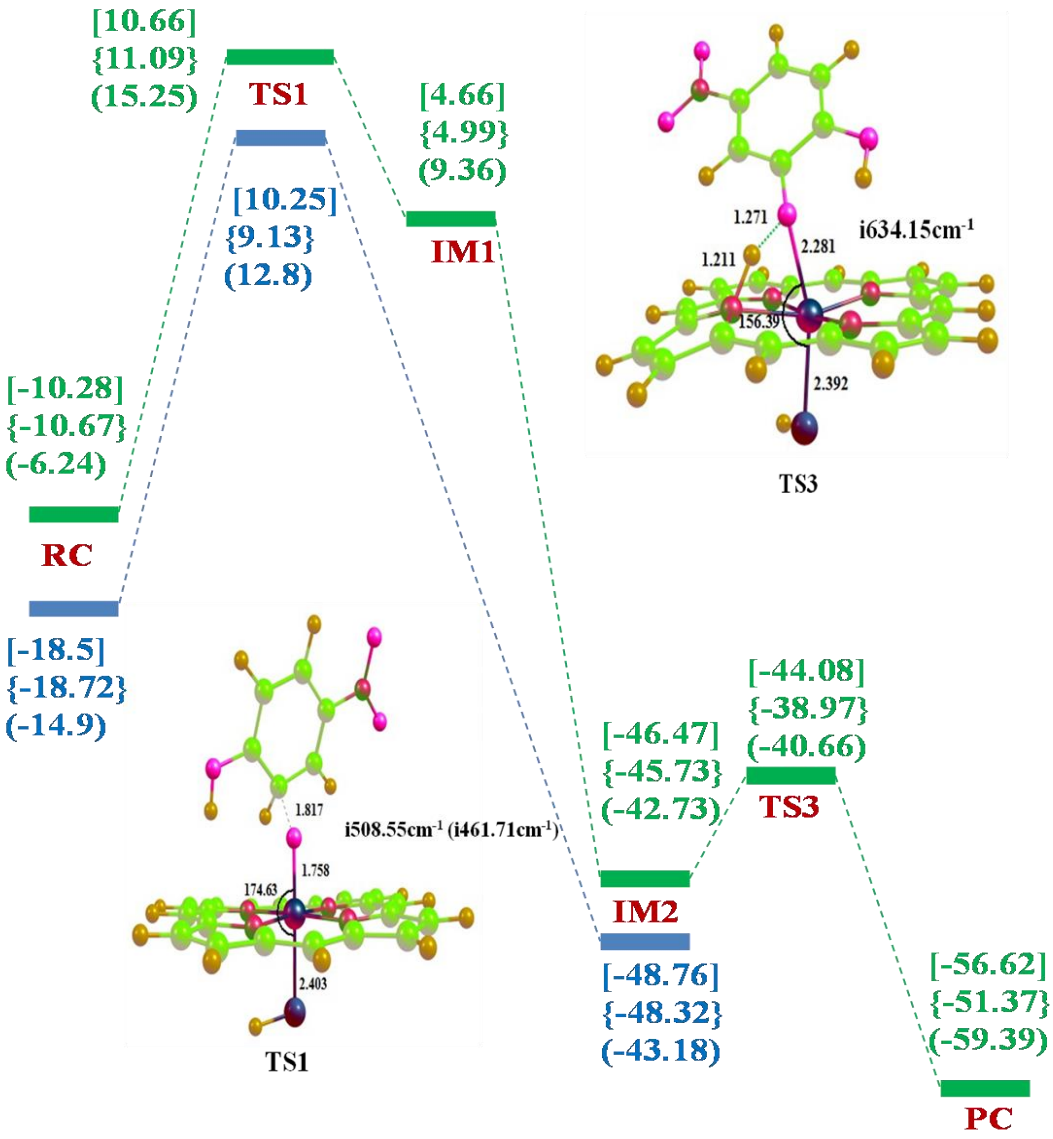

Figure 4.3: Potential energy surface of hydroxylation of 4-nitrophenol by Cytochrome P450 with energies in kcal/mol, Bond length (in Å), bond angle (in °) and imaginary frequencies (in cm^{-1}) of quartet (in green color) as well as doublet (in blue color) spin state is shown. Energies are calculated by 6-31G basis set reported in large bracket, by "LACVP" basis set reported in curly bracket and by solvent effect is in small bracket.

Third transition state (TS3) of high spin state has configuration as $\delta_{x2-y2}^{*2}\ \pi_{xz}^{*1}\ \pi_{yz}^{*1}\ \sigma_{z^2}^{*1}\ \sigma_{xy}^{*0}\ a_{1u}^{2}\ a_{2u}^{2}\ \varphi_{c}^{2}$. Further, product complex (PC) is formed by transfer of the hydrogen atom (H53) from nitrogen atom (N2) of substrate, and bind to the oxygen (O38) which has already been transferred at ortho position in second intermediate at high spin surface.

The overall configuration of product for high spin state is $\delta_{x2-y2}^{*2}\ \pi_{xz}^{*1}\ \pi_{yz}^{*1}\ \sigma_{z^2}^{*1}\ \sigma_{xy}^{*0}\ a_{1u}^{2}\ a_{2u}^{2}$. In case of doublet state, product is not formed due to formation of ***suicidal complex.*** Scan results at low spin surface is shown in Figure 4.7. Further, for more convenience for knowing the number of corresponding atoms that are responsible for hydroxylation are shown in Figure 4.6 within optimized structure of reactant complex of 4-nitrophenol with Cpd I.

Optimized structure of reactant complex (RC), transition state (TS), intermediate state (IM), and product complex (PC) for quartet as well as doublet spin state is shown in Figure 4.4 and Figure 4.5 respectively. Transfer of electron is changed occupancies of orbitals, and hence charges as well as spin densities of atoms are changed. Further, the spin densities and mulliken charges are also investigated that confirm the transfer of charges in various orbitals with suitable configuration.

Their spin densities with mulliken charges are compiled in Table 4.1. With the DFT calculations, the reported imaginary frequencies of TS1 and TS3 of quartet spin state are 508.55i cm^{-1} and 634.15i cm^{-1} respectively. And imaginary frequency of TS1 of low spin state is 461.71i cm^{-1}. As we know that, on the potential energy surface (PES), there may be a number of local maxima or minima between RC and PC. Here, only one local maxima (TS1) is present at low spin surface, while at high spin surface there are two local maxima are observed (TS1 & TS3).

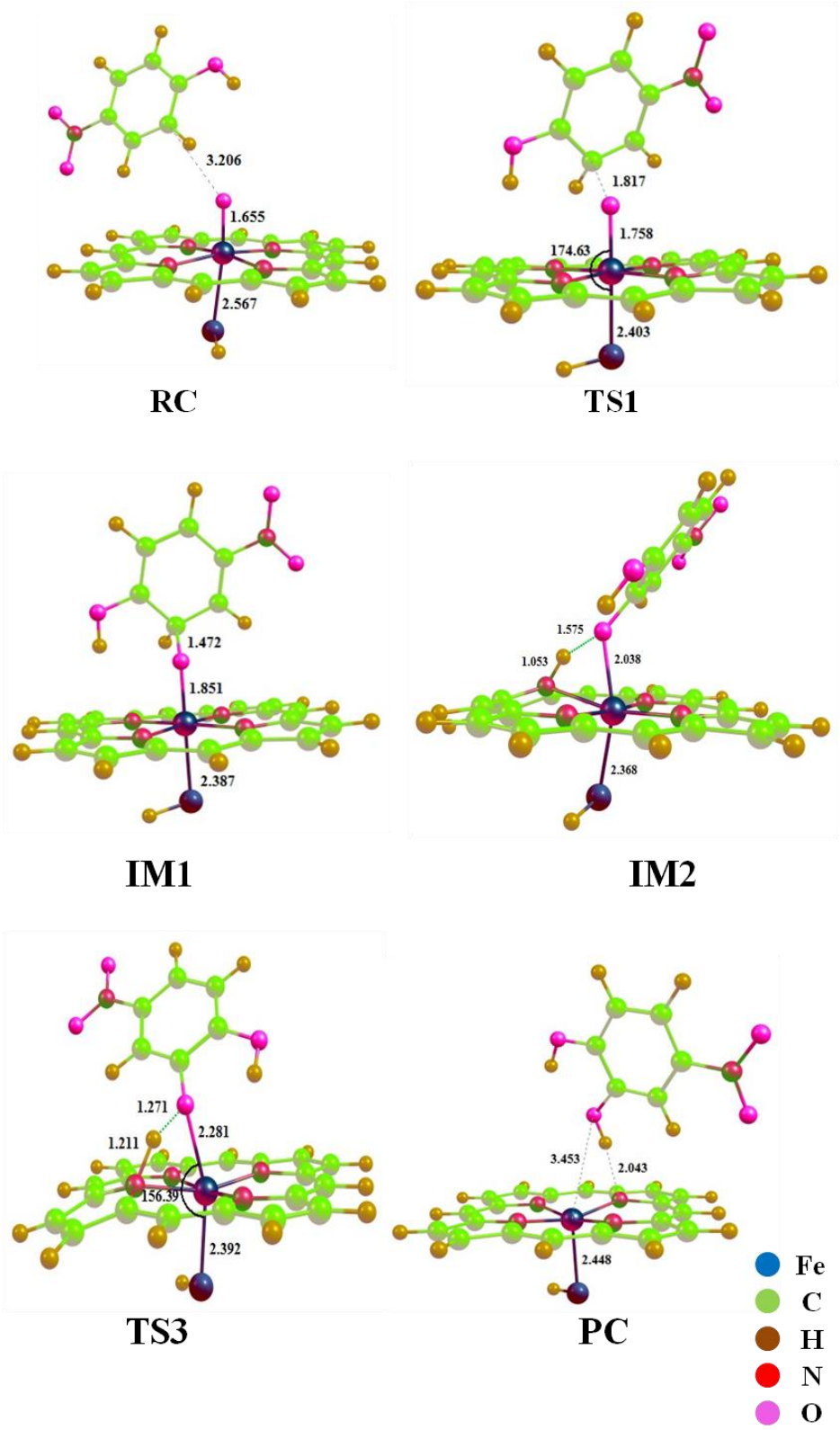

Figure 4.4: Optimized geometries of Reactant complex (RC), Transition state (TS), Intermediate complex (IM), and Product complex (PC) with differences in the bond lengths for respective atoms for HS of 4-nitrophenol.

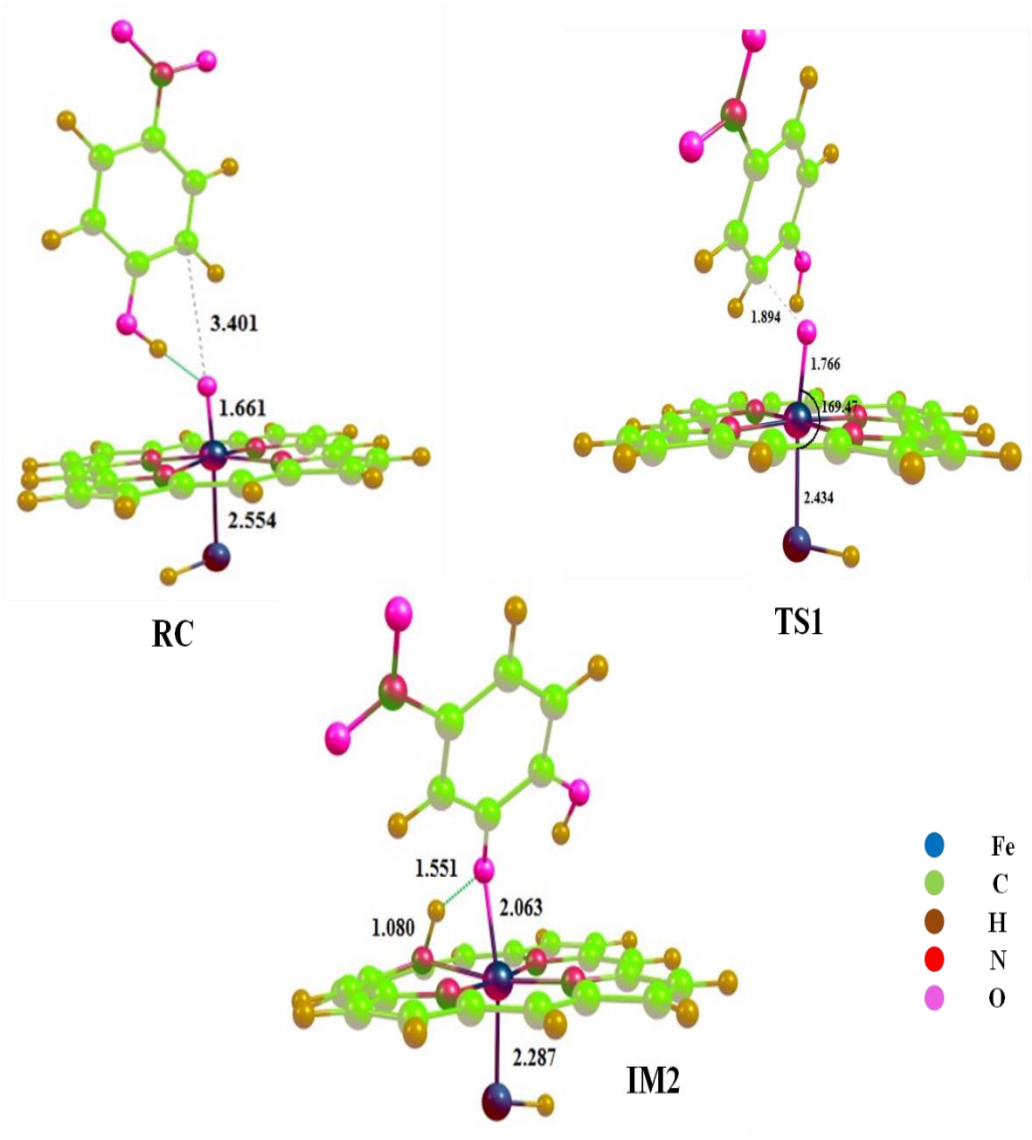

Figure 4.5: Optimized geometries of Reactant complex (RC), Transition state (TS), Intermediate complex (IM), and Product complex (PC) with differences in the bond lengths for respective atoms for LS of 4-nitrophenol.

High values of imaginary frequencies confirm several local maxima on potential energy surface. There are also local minima is observed in the formation of the IM1, IM2 on potential energy surface. Further, we cross checked the results using basis set "LACVP" and solvent effect using benzene. And we got the results overlapping to each other, as shown in energy profile Figure 4.3.

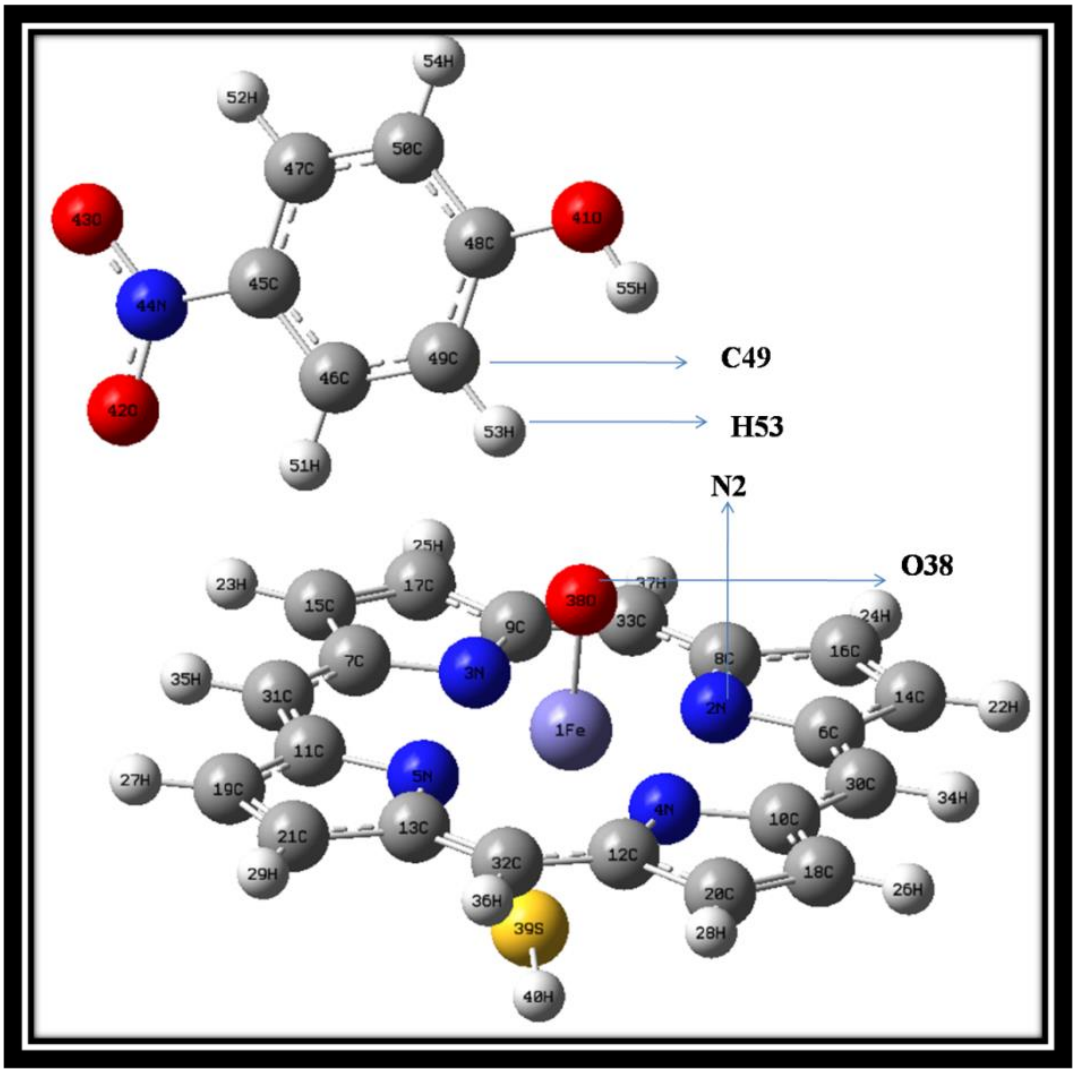

Figure 4.6: Optimized geometries of Reactant complex (RC) of 4-nitrophenol in original Gaussian view image. Arrow denotes the number of the corresponding atom.

Table 4.1: Spin densities and charges of Cpd I & substrate (4-nitrophenol) using DFT at the B3LYP/6-31G level of theory.

Reactant Complex										
Spin Density						**Charge**				
	Fe	**O**	**Por.**	**Sub.**	**SH**	**Fe**	**O**	**Por.**	**Sub.**	**SH**

M_4	1.10	0.91	0.44	0.00	0.53	0.50	-0.37	0.44	0.00	0.53
M_2	1.36	0.75	-0.58	0.00	-0.53	0.53	-0.45	-0.01	-0.05	-0.03
TS1										
Spin Density						**Charge**				
	Fe	**O**	**Por.**	**Sub.**	**SH**	**Fe**	**O**	**Por.**	**Sub.**	**SH**
M_4	1.41	0.64	0.06	0.51	0.36	0.46	-0.42	-0.28	0.21	0.03
M_2	1.15	0.46	-0.41	0.12	-0.32	0.41	-0.40	-0.22	0.23	-0.02
Intermediate1										
Spin Density						**Charge**				
	Fe	**O**	**Por.**	**Sub.**	**SH**	**Fe**	**O**	**Por.**	**Sub.**	**SH**
M_4	2.06	0.25	-0.13	0.85	-0.03	0.49	-0.53	-0.29	0.29	0.04
Intermediate 2										
Spin Density						**Charge**				
	Fe	**O**	**Por.**	**Sub.**	**SH**	**Fe**	**O**	**Por.**	**Sub.**	**SH**
M_4	2.84	0.04	0.07	0.04	0.05	0.45	-0.74	0.12	0.51	-0.05
M_2	1.05	-0.01	-0.07	-0.02	0.04	0.30	-0.72	-0.19	-0.51	0.01
Transition State 3										
Spin Density						**Charge**				

	Fe	O	Por.	Sub.	SH	Fe	O	Por.	Sub.	SH
M4	2.66	0.03	0.04	0.03	0.26	0.48	-0.74	0.13	-0.51	-0.1
Product										
Spin Density						**Charge**				
	Fe	**O**	**Por.**	**Sub.**	**SH**	**Fe**	**O**	**Por.**	**Sub.**	**SH**
M_4	2.50	0.00	0.04	-0.00	0.47	0.52	-0.68	-0.36	-0.00	-0.15

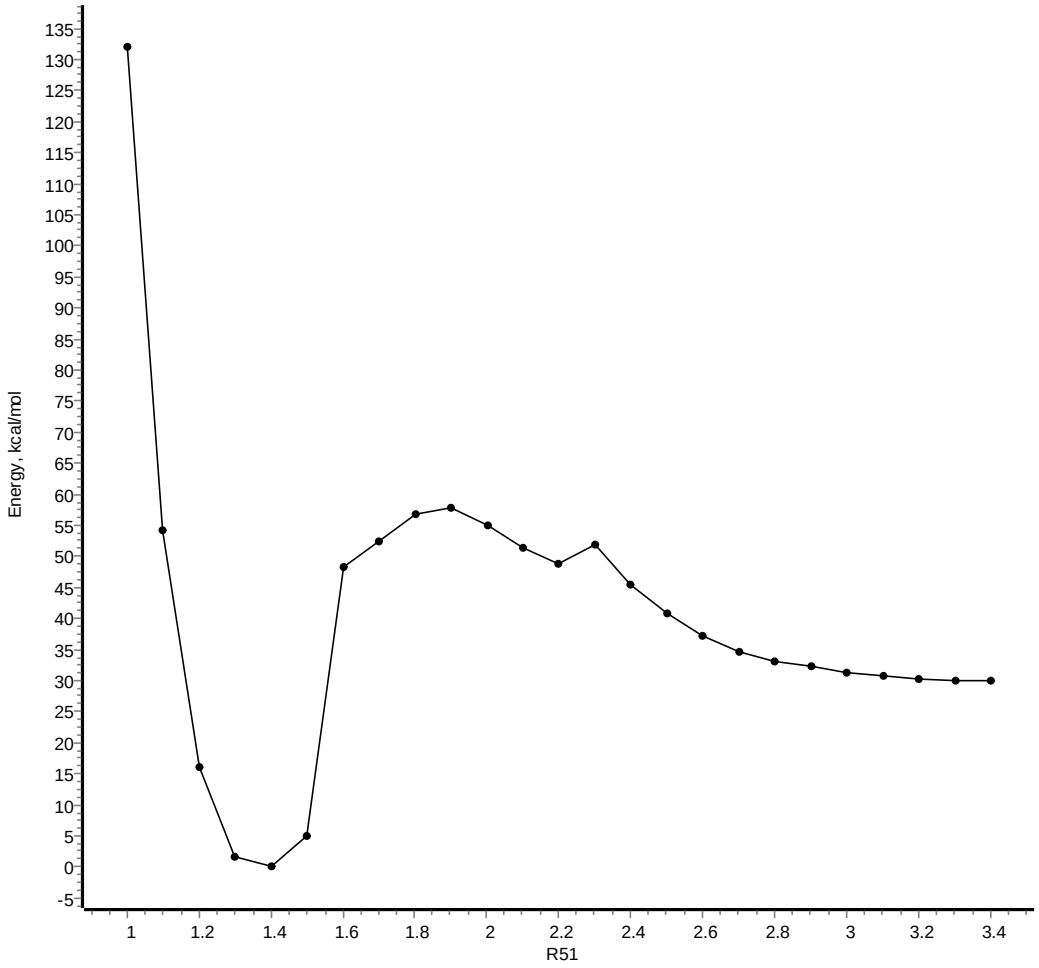

Figure 4.7: Scan results at low spin surface.

So, present study gives an internal image of aromatic hydroxylations of 4-nitrophenol via Cpd I with good accuracy, that was still blur for scientists. And hence it is also cleared that how 4-nitrophenol metabolized via Cpd I through the hydroxylation step. Present work may be helpful for further investigations of drugs metabolism and drugs discovery.

4.5 Conclusion

The present work offered a complete reaction pathway of aromatic hydroxylation of 4-nitrophenol with Cpd I by DFT at B3LYP level of theory. Quantum mechanical calculations above clearly depicted the hydroxylation reaction has more than one transition state with short lived intermediate state and C-O bond formation step to be the rate determining step of the reaction. This step clearly shows that it requires less energy in initiating the reaction at both spin surfaces. It can be seen from the energy profile of 4-nitrophenol that quartet surface (HS) is responsible for the hydroxylated product whereas doublet spin surface profile resulted in the formation of *suicidal complex*.

Finally, the product at high spin state surface (HS), is formed, the reaction followed patterns of two state reactivity (TSR) mechanism and energy landscape for doublet and quartet were close and parallel with each other, but this pattern bifurcated at IM1. TSR behavior is transformed to single state reactivity (SSR) showing that reaction is possible only for high spin surface (HS). This process is not regioselective, so the product is formed directly from intermediate. Reaction mechanism of 4-nitrophenol with Cpd I is one of the crucial process, but its reaction pathway was still hidden. Our work gives energy pathway of reaction mechanism with very good accuracy.

Present reactions mechanism is different from aliphatic hydroxylation reactions of Cytochrome P450 enzyme, due to formation of suicidal complex at the low spin surface. Hence it cleared that how 4-nitrophenol is metabolized via Cpd I through the hydroxylation step. All results are further cross checked by using LACVP basis set and solvent effect for benzene, and greatly we got the results which are overlapping to each other. Hence the results hold good accuracy and are hence reliable. So, present study gives an internal image of aromatic hydroxylation of 4-nitrophenol via Cpd I with good accuracy as we expected, that was still blur for scientists. These results can be used for experimental researches for the investigations of drugs metabolism and drugs discovery and will give fruitful results.

References

[1] H. M. Guardiola-Diaz, L. A. Foster, D. Mushrush, A. D. Vaz, "Optimization of Azole- Antifungal Drugs : An Attempt for Search of Better Drug for Treatment of TB with CYP450 From", *Tuberculosis*, 6, 53–55, **2020**.

[2] G. Smith, M. J. Stubbins, L. W. Harries, C. R. W.Olf, "Molecular Genetics of the Hum an Cytochrome P450 monooxygenase Superfam Ily", *Biomed. Res.*, 1129–1165, **1998**.

[3] S. Shaik, S. P. De Visser, "Computational Approaches to Cytochrome P450 Function", *Cytochrome P450 Struct. Mech. Biochem. Third Ed.*, 45–85, **2005**.

[4] S. Shaik, S. Cohen, Y. Wang, H. Chen, D. Kumar, W. Thiel, "P450 Enzymes: Their Structure, Reactivity, and Selectivity-Modeled by QM/MM Calculations", *Chem. Rev.*, 110, 949–1017, **2010**.

[5] E. O'Reilly, V. Köhler, S. L. Flitsch, "Cytochromes P450 as Useful Biocatalysts: Addressing the Limitations", *Chem. Commun.*, 47, 2490–2501, **2011.**

[6] F. P. Guengerich, "Cytochrome P-450 3A4: Regulation and Role in Drug Metabolism", *Annu. Rev. Pharmacol. Toxicol.*, 39, 1–17, **1999**.

[7] U. M. Zanger, M. Schwab, "Cytochrome P450 Enzymes in Drug Metabolism: Regulation of Gene Expression, Enzyme Activities, and Impact of Genetic Variation", *Pharmacol. Ther.*, 138, 103–141, **2013**.

[8] S. Shaik, W. Lai, H. Chen, Y. Wang, "The Valence Bond Way: Reactivity Patterns of Cytochrome P450 Enzymes and Synthetic Analogs", *Acc. Chem.*

Res., 43, 1154–1165, **2010**.

[9] M. S. Butler, "Natural Products to Drugs: Natural Product Derived Compounds in Clinical Trials", *Nat. Prod. Rep.*, 22, 162–195, **2005**.

[10] R. Ullrich, M. Hofrichter, "Enzymatic Hydroxylation of Aromatic Compounds", *Cell. Mol. Life Sci.*, 64, 271–293, **2007**.

[11] D. R. Koop, "Oxidative and Reductive Metabolism by Cytochrome P450 2E1", *FASEB J.*, 6, 724–730, **1992**.

[12] W. Chen, L. L. Koenigs, S. J. Thompson, R. M. Peter, A. E. Rettie, W. F. Trager, S. D. Nelson, "Oxidation of Acetaminophen to Its Toxic Quinone Imine and Nontoxic Catechol Metabolites by Baculovirus-Expressed and Purified Human Cytochromes P450 2E1 and 2A6", *Chem. Res. Toxicol.*, 11, 295–301, **1998.**

[13] J. G. M. Bessems, N. P. E. Vermeulen, "Paracetamol (Acetaminophen)-Induced Toxicity: Molecular and Biochemical Mechanisms, Analogues and Protective Approaches", *Crit. Rev. Toxicol.*, 31, 55–138, **2001**.

[14] Frank Ellis. Paracetamol - a Curriculum Resource. *R. Soc. Chem.*, **2002**.

[15] A. Ninfa, D. Ballou, M. Benore, "Approaches for Biochemistry and Biotechnology", 45, 164–179, **2010**.

[16] Monostory, K.; Hazai, E.; Vereczkey, L. Inhibition of Cytochrome P450 Enzymes Participating in P-Nitrophenol Hydroxylation by Drugs Known as CYP2E1 Inhibitors. *Chem. Biol. Interact.*, **2004**, *147* (3), 331–340.

[17] S. Shaik, H. Hirao, D. Kumar, "Reactivity Patterns of Cytochrome P450

Enzymes: Multifunctionality of the Active Species, and the Two States-Two Oxidants Conundrum", *Nat. Prod. Rep.*, 24, 533–552, **2007.**

[18] S. Shaik, S. Cohen, S. P. De Visser, P. K. Sharma, D. Kumar, S. Kozuch, F. Ogliaro, D. Danovich, "The "Rebound Controversy": An Overview and Theoretical Modeling of the Rebound Step in C-H Hydroxylation by Cytochrome P450." *Eur. J. Inorg. Chem.*, 2, 207–226, **2004**.

[19] H. Hirao, D. Kumar, L. Que, S. Shaik, "Two-State Reactivity in Alkane Hydroxylation by Non-Heme Iron-Oxo Comolexes", *J. Am. Chem. Soc.*, 128, 8590–8606. **2006.**

[20] M. Torrent, D. G. Musaev, H. Basch, K. Morokuma, "Computational Studies of Reaction Mechanisms of Methane Monooxygenase and Ribonucleotide Reductase", *J. Comput. Chem.*, 23, 59–76, **2002**.

[21] M. J .Frisch, G. W. Trucks, H. B. Schlegel, G. E. Scuseria, M. A. Robb, J. R. Cheeseman, G. V. Scalmani Barone, B. Mennucci, G. A. Petersson, "Gaussian 09, Revision B.01", *Gaussian 09, Revis. B.01, Gaussian, Inc., Wallingford CT*, 1–20, **2009.**

[22] W. R. Wadt, P. J. Hay, "Ab Initio Effective Core Potentials for Molecular Calculations. Potentials for Main Group Elements Na to Bi.", *J. Chem. Phys.*, , 82, 284–298, **1985**.

[23] C. M. Bathelt, L. Ridder, A. J. Mulholland, J. N. Harvey, "Aromatic Hydroxylation by Cytochrome P450: Model Calculations of Mechanism and Substituent Effects", *J. Am. Chem. Soc.*, 125, 15004–15005, **2003**.

[24] Y. Shiota, K. Yoshizawa, "Methane-to-Methanol Conversion by First-Row

Transition-Metal Oxide Ions: ScO+, TiO+, VO+, CrO+, MnO+, FeO+, CoO+, NiO+, and CuO+.", *J. Am. Chem. Soc.*, 122, 12317–12326, **2000**.

[25] F. Ogliaro, N. Harris, S. Cohen, M. Filatov, S. P. De Visser, S. Shaik, "A Model "rebound" Mechanism of Hydroxylation by Cytochrome P450: Stepwise and Effectively Concerted Pathways, and Their Reactivity Patterns", *J. Am. Chem. Soc.*, 122, 8977–8989, **2000**.

[26] Ai, C. Z.; Liu, Y.; Chen, D. C.; Saeed, Y.; Jiang, Y. Z. Conformational Turn Triggers Regio-Selectivity in the Bioactivation of Thiophene-Contained Compounds Mediated by Cytochrome P450. *J. Biol. Inorg. Chem.*, **2019**, *24* (7), 1023–1033.

[27] X. Y. Wang, H. M.Yan, Y. L. Han, Z. X. Zhang, X. Y. Zhang, W. J. Yang, Z. Guo, Y. R. Li, "Do Two Oxidants (Ferric-Peroxo and Ferryl-Oxo Species) Act in the Biosynthesis of Estrogens? A DFT Calculation", *RSC Adv.*, 8, 15196–15201, **2018**.

[28] D. Fishelovitch, C. Hazan, H. Hirao, H. J. Wolfson, R. Nussinov, S. Shaik, "QM/MM Study of the Active Species of the Human Cytochrome P450 3A4, and the Influence Thereof of the Multiple Substrate Binding", *J. Phys. Chem. B*, 111, 13822–13832, **2007**.

[29] R. Hussain, I. Kumari, S. Sharma, M. Ahmed, T. A. Khan, Y. Akhter, "Catalytic Diversity and Homotropic Allostery of Two Cytochrome P450 Monooxygenase like Proteins from Trichoderma Brevicompactum", *J. Biol. Inorg. Chem.*, *22*, 1197–1209, **2017**.

[30] S. P. De Visser, S. Shaik, "A Proton-Shuttle Mechanism Mediated by the

Porphyrin in Benzene Hydroxylation by Cytochrome P450 Enzymes", *J. Am. Chem. Soc.*, 125, 7413–7424, **2003**.

[31] M. Albeck, S. Shaik, "Publications of Sason Shaik", *J. Phys. Chem. A*, , 112, 12741–12753, **2008**.

Chapter-5

Computational Study of Electrical Properties of Various Drugs that Metabolized via Cytochrome P450

Chapter-5

Computational Study of Electrical Properties of Various Drugs that Metabolized via Cytochrome P450

5.1 Introduction

Cytochrome P450 is an important enzyme of biosystems. In humans, it is found in the liver [1]. But it is also highly expressed in area of the central nervous system. These enzymes undergo reaction of catalyzation of a variety of stereo-specific and Regio-selective mono-oxygenation. It is also used in detoxification process and it is a key of the drug-metabolizing enzyme which is involved in the metabolism of the drugs [2]. It reacts as mono-oxygenase that transfers an oxygen atom to the substrate. Due to its large versatility in the activation of the substrate, Cytochrome P450 is an essential enzyme, which is not only used in biology but also, in the Biotechnological and Pharmaceutical applications for the investigations of the drugs [3]. Moreover, its drug metabolism makes this enzyme a target for the drug industry and biomedical research [4-7]. Several drugs are metabolized through the Cytochrome P450. Here, we computationally investigated the physical properties of some drugs that are metabolized through the P450 enzyme.

Diacetylmorphine is also known as heroin or diamorphine, which is used as a drug due to its euphoric effect [8]. In several countries, it is used as a pain relief like, during

childbirth, heart attack, or opioid replacement therapy [9-11]. It is taken in the form of injection and can also be smoked or inhaled. It is also found in the tablet form [12-15].

Losartan is a drug which is used in the treatment of high blood pressure, a diabetic patient with kidney failure, and heart failure patients [16].

It may take six months for the complete treatment of the disease [16]. There are also some side effects of Losartan medication like cramps, cough, anemia, stuffy nose, low blood pressure, and angiotensin [16]. The above drug is not recommended during breastfeeding and pregnancy, because the blockage of the angiotensin II [17]. It is an essential drug that is listed in World Health Organization (WHO) and approved by the United States in 1995 [18, 19]. It is also highlighted as a generic medication [20]. In the United States, it is top ninth most prescribed drugs in 2017 [21, 22]. It is also combined with hydrochlorothiazide and form a new version of it [16].

This new version is 67th most prescribed drug in the United States, in 2017 [23]. Primaquine (PQ) is a prime anti-malarial drug, which is used in the treatment of malaria due to Plasmodium vivax and Plasmodiumovale [24]. It is also used in the treatment of Pneumocystispneumonia together with clindamycin, as an alternate treatments. The First Primaquine drug is made in1946 [25]. There are some anti-fungal drugs commonly known as azoles, which are metabolized through the cyp450. Some of them can also be used in the treatment of tuberculosis. Tuberculosis are rapidly spreading all over the world. According to World Health Organization (WHO), every year, approximately 2 million people are died due to tuberculosis [33]. There are many reasons for the resurgence of the Mycobacterium tuberculosis (Mtb) infection rate around the whole world. But the major factors are synergy with the Human Immunodeficiency Virus (HIV), and the development of the drug-resistant (DR) and multi-drug-resistant (MDR) strains of the pathogen [34, 35].

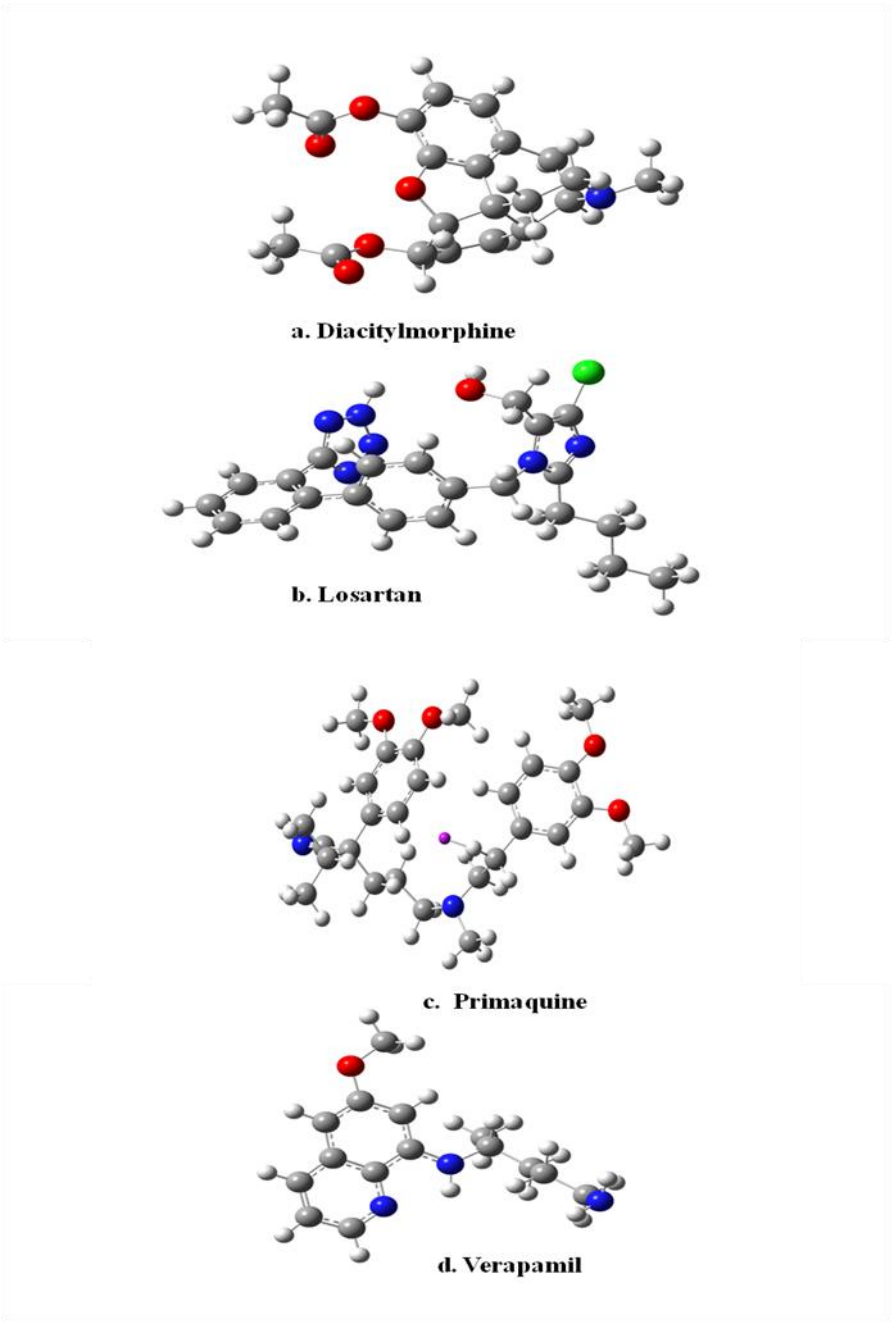

Figure 5.1: Optimized molecular structures of , **a.** Diaacetylmorphine, **b.** Losartan, **c.** Primaquine, **d.** Verapamil.

In all HIV-infected people, 15% of people ultimately die due to tuberculosis. So, the treatment of tuberculosis has become so important for the whole world. The complete treatment duration of Tuberculosis (TB), is 6-12 months, which is a long period. So, search for new drugs for the treatment of TB as well as decreasing the time duration is imperative to work of research. Therefore, it is urgent to identify a biochemical

pathway for tuberculosis treatment [36]. There are many compounds which are treated as the anti-TB drug also used in metabolism.

As discussed earlier, azoles are an antifungal drug, and it is treated as a substrate and reacts with MT CYP450 [37,38], gives a biochemical pathway for understanding the metabolism process, and also shows good results against the anti- Mycobacterium tuberculosis [39]. There are many azole compounds, but out of them, which prove to be the best for both, anti TB, as well as metabolism, is still a tough task. The stability of their configuration is not the same concerning CYP450. So, it is imperative to find out the most stable configuration against the Mtb.

In this study, by the optimization of -Azole- antifungal drugs, an attempt for the search of the better drug is carried out so, as to get a potential candidate amongst all these antifungal drugs. In this study, by the optimization and HOMO-LUMO band-gap of antifungal drugs, an attempt for the search for a better drug is carried out so, as to get a potential candidate amongst all these antifungal drugs. Azole-antifungal, containing an Azole ring, is the group of medicine used for the inhabitation of a wide range of fungal infections. They are classified into two groups: (a) Azole ring with two nitrogen called Imidazole, [i.e., Miconazole, Clotrimazole, Econazole, etc.], (b) Azole ring with three nitrogens called Triazoles, [i.e., Fluconazole, Itraconazole, Posaconazoleetc.]. Azole antifungal inhibiting the Lanosterol 14-alpha-demethylase enzyme, which is a member of the cytochrome P450 enzyme family, converts lanosterol to erosterol, which damages the cell membrane resulting in the death There are some common side effects of Primaquine like nausea, vomiting, and stomach cramps [26].It is not recommended during pregnancy due to the deficiency ofglucose-6-phosphate dehydrogenize [27,28].

Verapamil is also used for the medication for high blood pressure, angina [29]. Sometimes it is used for the prevention of migraines as well as headache [30, 31].

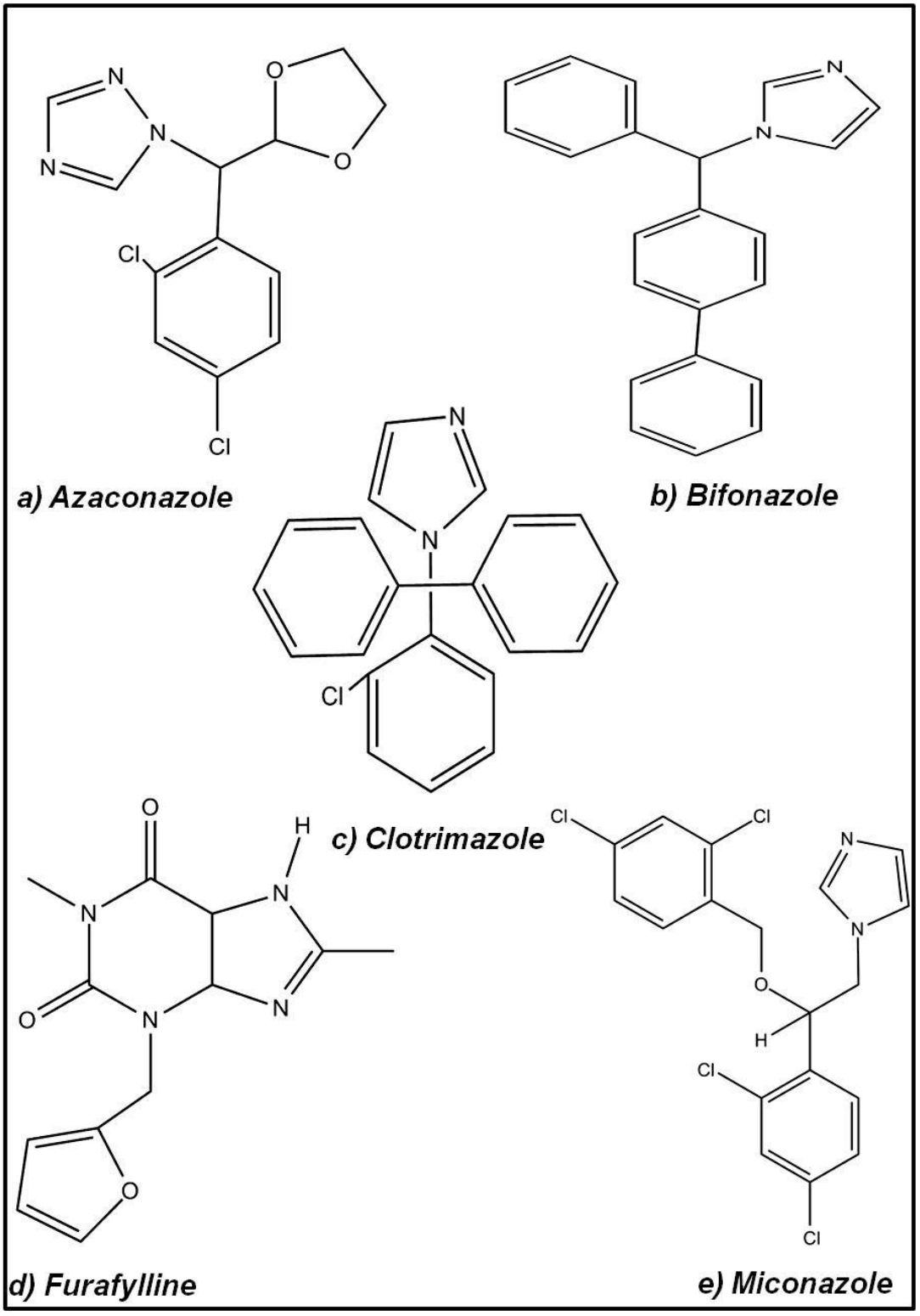

Figure 5.2: Geometrical structure of a) Azaconazole, b) Bifonazole, c) Clotrimazole, d) Furafylline, e) Miconazole.

It has some common side effects like headache, nausea, low blood pressure, allergic reactions, and muscle pain, etc. [32]. These all four drugs interact with the active site of Cytochrome P450 and form a product. This product is then further deal with a particular disease. So, we here studied some physical properties of these drugs by Quantum Mechanical (QM) method, Density Functional Theory (DFT). The optimized geometry of discussed drugs is shown in Figure 5.1.

of the cell [41]. But the configurations of azole-antifungal drugs are not equally stable. So, finding the most stable configuration amongst all azole-antifungal drugs is nthe primary requirement for understanding the metabolism. The geometrical structures of azoles are shown in Figure 5.2

Here, we optimized some other anti-fungal drugs, Econazole, Terconazole, Ketoconazole, and found the most stable configuration amongst these drugs. We also investigated the HOMO-LUMO (highest occupied molecular orbital and lowest unoccupied molecular orbital) bandgap for finding the behavior of drugs towards the external energy. All these calculations are done by using Density Functional Theory (DFT) with the 6-31G basis set.

5.2 Computational Details

For studying the most stable configuration of the molecules, the widely used method is Quantum Mechanical (QM) method. Basically, in this, various quantum mechanical theories [39] are compiled to finding the ground state energy or can say the stable structure of the molecule. In this method, the Schrodinger wave equation for multi-electron system is solved and their energies are analyzed [40]. The solution of the modified Schrodinger wave equation is based on Density Functional Theory (DFT).

All calculations are done by Gaussian 09 & Gauss view 5.0 software using density functional theory with the 6-31* basis set [41].

5.3 Results and discussion

As mentioned in Table 5.1, the highest occupied molecular orbital (HOMO) and the lowest unoccupied molecular orbital (LUMO), energy bandgap of Primaquine is 3.79 eV, which has the least energy bandgap. Diacitylmorphine and Verampil both have the largest energy bandgap i.e., 5.36 eV. Losartan has an energy bandgapof 4.70 eV, which is less than the bandgap of Diacitylmorphine as well as Verapamil. Amongst of all these four drugs as mention in Table 5.1, the HOMO-LUMO bandgap of Diacitylmorphine and Verampil is the largest, which means they need more energy for exciting the electron. Hence, these two drugs are more stable amongst all four drugs.

Table 5.1: Optimization energy and HOMO-LUMO bandgap of Diacetylmorphine, Losartan, Primaquine, Verapamil drugs

S. No.	**Name of drug**	**Optimization Energy (in eV)**	**HOMO-LUMO bandgap (in eV)**
1.	Diacitylmorphine	-33,865.29	5.36
2.	Losartan	-46,684.46	4.70
3.	Primaquine	-22,407.43	3.79
4.	Verapamil	-39,772.58	5.36

The minimum energy of all four drugs is also reported in Table 5.1. Primaquine has an energy of -22,407.43eV, which is the largest energy. Diacitylmorphine has an energy of -33,865.29 eV optimization energy, which is morethan the energy of Primaquine. -39.772.58 eV is the minimum optimization energy of Verapamil. Its energy is more than the energy of the Losartan drug. Losartan has minimum optimization energyof-46,684.46 eV. This means, amongst all four drugs Losartan has the most stable structure or can say to be a more stable configuration.

Now we are discussing the results obtained by optimization energy and HOMO-LUMO bandgap of some (Azaconazole, Bifonazole, Clotimazole, Miconazole, Furafylline) anti-fungal (azoles) drugs are shown in Table–5.2. The HOMO-LUMO bandgap of the Azaconazole is highest, indicating that its configuration is less stable. Bifonalzole's HOMO-LUMO bandgap is much smaller, so its configuration is more stable than other optimized azoles. But it is less stable than Miconazole, because the HOMO - LUMO gap is the smallest (Table 5. 2).

Table 5.2: Optimization energy and HOMO-LUMO bandgap of Azoles

S. No.	**Name of drug**	**Optimization Energy (in eV)**	**HOMO-LUMO bandgap (in eV)**
1.	Azaconazole	-46,230.40	6.0168
2.	Bifonazole	-26,070.31	3.6079
3.	Clotimazole	-38,592.54	5.0266
4.	**Miconazole**	**-74,008.74**	**3.5855**
5.	Furafylline	-24,741.05	5.0392

The optimization energy of Furafylline is the highest amongst the useless, due to this; it has a less stable configuration. But Miconazole has the lowest energy (Table 5.2), that's why may be said to have the most stable configuration amongst all azoles.

At the End of the work, we discussed the electrical properties of the rest of the azoles (Econazole, Ketoconazole, Terconazole) which we take for the investigations. After the optimization of these drugs using density functional theory, we obtained appropriate results which are shown in Table 5.3. Optimized structure (Optimized energy) gives the most stable configuration of the compound. From the result it is clear that Ketoconazole has -66569.37 eV energy, lesser than Econazole (-61470.66 eV) and Terconazole (66060.86 eV).

Table 5.3: Optimization energy and HOMO-LUMO bandgap of anti-fungal drugs

S. No.	**Name of drug**	**Optimization Energy (in eV)**	**HOMO-LUMO bandgap (in eV)**
1.	Econazole	-61470.66	5.05
2.	Ketoconazole	-66569.37	3.86
3.	Terconazole	-66060.86	4.47

It has the most stable configuration. Terconazole has optimization energy -66060.86 eV while econazole has optimization energy -61470.66 eV, which means terconazole is much more stable than econazole. The HOMO - LUMO bandgap of these drugs are reported in Table 5.3. The optimized structures are shown in Figure 5.3.

HOMO-LUMO bandgap shows the behavior of chemical reactivity of compounds. Here Econazole has the largest bandgap (5.05 eV), which means it is less chemically

reactive or more stable than the other two drugs. Terconazole has a bandgap of 4.47 eV, while Ketoconazole has a bandgap of 3.86 eV, indicating less chemical reactivity or more stability than Ketoconazole. Amongst all drugs, Ketoconazole is more chemical reactive while Econazole is less chemical reactive. So, after the investigation of the above drugs, it may be inferred that Miconazole **(-74,008.74)** has the most stable structure in all given azoles. The most stable configuration means, when it acts as a

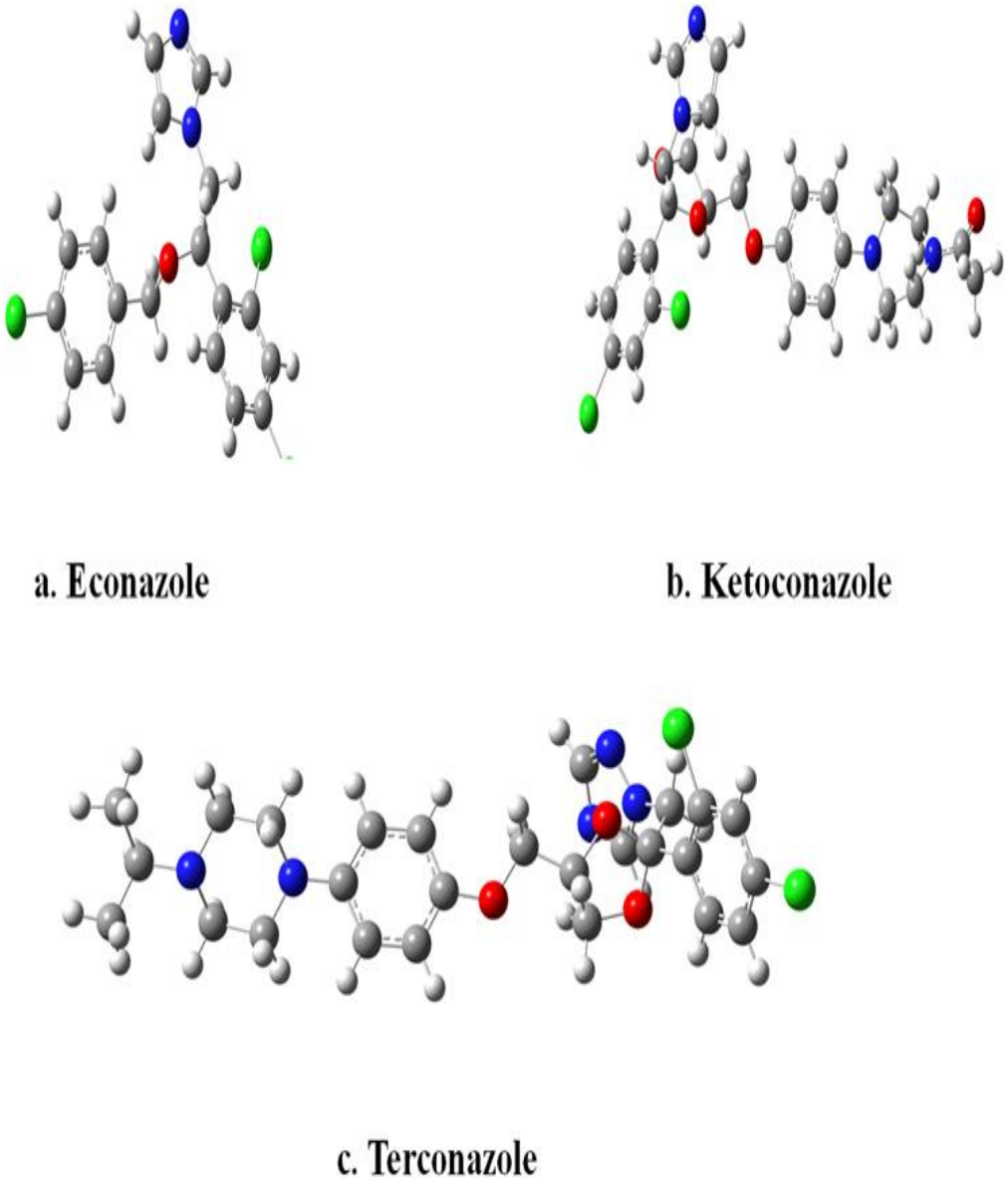

Figure 5.3: Optimized structures of a. Econazole, b. Ketoconazole, c. Terconazole.

substrate, in any biochemical reaction, it has the maximum probability to bind tightly with the enzymes.

Further Miconazole has the highest HOMO-LUMO bandgap indicating the more chemical reactivity towards a reaction. These properties of the drugs (substrate) help in understanding the reaction mechanism of many biochemical reactions, in understanding the metabolism process of various drugs (substrate) mediated by cpd1, and further use for the scientist to design a drugand do drug investigations.

5.4 Conclusion

As we discussed above, the HOMO-LUMO bandgap of Diacitylmorphine and Verapamil drug is the largest. So, for further treatment of respective diseases, these drugs would give better results. The optimization energy of the Losartan drug is minimum, which means that it has the most stable configuration. So, it will give better results for further treatment of the respective disease.

Optimization results of Azoles-antifungal drugs shows that all azoles have good stability; Miconazole has the most stable structural configuration which means that it can bind tightly with the enzymes. This result acts as an aid in understanding the reaction mechanism of many biochemical reactions. So, it is concluded that Miconazole is a good anti-fungal drug as well as a good substrate to react with enzymes. Further research work in such a field may reveal a wide range of mysteries in the understanding of metabolism, detoxification, and many other biochemical reactions as well as help in search of good anti-fungal drugs also.

Optimized results of antifungal drugs show good stability. Ketoconazole has the most stable structural configuration, which means that it can bind tightly with the enzyme. Here Econazole has the largest HOMO-LUMO bandgap among all drugs showing less

chemical reactivity. So, it is concluded that Ketoconazole has good stability to react with the P450 enzyme. Econazole has the largest HOMO-LUMO bandgap shows less chemical reactivity or more stability, so it may have good reactivity with P450.

This result acts as an aid in understanding the reaction mechanism of many biochemical reactions. Further research work in such a field may reveal a wide range of mysteries in the understanding of the metabolism, detoxification, and many other biochemical reactions as well as help in the search of good anti-fungal drugs.

References

[1] S. Shaik, S. P. De Visser, "Computational Approaches to Cytochrome P450 Function", *Cytochrome P450 Struct. Mech. Biochem. Third Ed*., 45–85, **2005**.

[2] S. Shaik, S. Cohen, Y. Wang, H. Chen, D. Kumar, W. Thiel, "P450 Enzymes: Their Structure, Reactivity, and Selectivity Modeled by QM/MM Calculations", *Chem. Rev.*, 110, 949–1017, **2010**.

[3] E. O'Reilly, V. Köhler, S. L. Flitsch, "Cytochromes P450 as Useful Biocatalysts: Addressing the Limitations", *Chem. Commun*., 47 (9), 2490–2501, **2011**.

[4] F. P. Guengerich, "Cytochrome P-450 3A4: Regulation and Role in Drug Metabolism", *Annu. Rev. Pharmacol. Toxicol*., 39, 1–17, **1999**.

[5] U. M. Zanger, Schwab, "M. Cytochrome P450 Enzymes in Drug Metabolism: Regulation of Gene Expression", *Enzyme Activities, and Impact of Genetic Variation. Pharmacol. Ther.,* 138, 103–141, **2013**.

[6] Shaik, S.; Lai, W.; Chen, H.; Wang, Y. The Valence Bond Way: Reactivity Patterns of Cytochrome P450 Enzymes and Synthetic Analogs. Acc. Chem. Res., 43 (8), 1154–1165, **2010**.

[7] M. S. Butler, "Natural Products to Drugs: Natural Product Derived Compounds in Clinical Trials.", *Nat. Prod. Rep.*, 22, 162–195, **2005**.

[8] H. P. Rang, J. M. Ritter, R. J. Flower, G. Henderson, *Rang & Dale's Pharmacology Elsevier Health Sciences,51, E-Book*, **2017**.

[9] S.J. Friedrichsdorf, A. Postier, "Management of breakthrough pain in children withcancer", *Journal of Pain Research*, 7,117–23. **2017.**

[10] National Collaborating Centre for Cancer, "Opioids in Palliative Care: Safe and

Effective Prescribing of Strong Opioids for Pain in Palliative Care of Adults", **2012**.

[11] A. A. Uchtenhagen, "Heroin maintenance treatment: from idea to research topractice" (PDF), *Drug and Alcohol Review*, 30, **2011.**

[12] Diamorphine". SPS - Specialist Pharmacy Service, **2020.**

[13] Heroin. Drugs.com. 18 May **2014**.

[14] Drug Facts-Heroin, National Institute on Drug Abuse, **2014**.

[15] National Institutes on Drug Abuse (2014), Research Report Series: Heroin (PDF), *NationalInstitutes on Drug Abuse*, **2016**.

[16] Losartan Potassium, The American Society of Health-System Pharmacists, **2017**.

[17] Losartan (Cozaar) Use During Pregnancy. Drugs.com, **2017**.

[18] Fischer, Jnos, Ganellin, C. Robin, Analogue-based Drug Discovery, *John Wiley &Sons*, 470, **2016**.

[19] World Health Organization (2019). World Health Organization model list of essential medicines: 21st list 2019, *Geneva: World Health Organization*, **2019**.

[20] British national formulary , British Medical Association, 127, **2015**

[21] The Top 300 of 2020, *Clin Calc*, **2020**.

[22] Losartan Potassium - Drug Usage Statistics, *Clin Calc*., **2020.**

[23] Hydrochlorothiazide, Losartan Potassium - Drug Usage Statistics. Clin Calc., **2020.**

[24] Vale Nuno, Moreira Rui, Gomes Paula, "Primaquine revisited six decades after

its discovery", *European Journal of Medicinal Chemistry*, 44, 937–953, **2009**.

[25] Arguin, Paul M.; Tan, Kathrine R., "Malaria - Chapter 3". In Brunette, Gary W. (ed.). *CDC Health Information for International Travel*, **2016**.

[26] Hamilton, Richart, Tarascon Pocket Pharmacopoeia, Deluxe Lab-Coat Edition, *Jones & Bartlett Learning*, 57, **2015**.

[27] D. R. Hill, J. K. Baird, M. E. Parise, L. S. Lewis, E. T. Ryan, A. J. Magill, "Primaquine: Report from CDC expert meeting on malaria chemoprophylaxis I". *The American Journal of Tropical Medicine and Hygiene*, 75, 402, **2006**.

[28] World Health Organization (2019), World Health Organization model list of essential medicines: 21st list, Geneva: World Health Organization **2019**.

[29] Verapamil Hydrochloride, *The American Society of Health-System Pharmacist*s, **2016**.

[30] T. felt-Hansen P. C., Jensen R. H., "Management of cluster headache", *C. N. S. Drugs*, 26, 571–80, **2012.**

[31] K. Merison, H. Jacobs, "Diagnosis and Treatment of Childhood Migraine". *Current Treatment Options in Neurology*. 18, 48, **2016.**

[32] World Health Organization, Stuart M. C., M. Kouimtzi, S. R. Hill. WHO Model Formulary, **2009**.

[33] P. Zumla, S. B. Mwaba, J. Squire, M. Grange, "The tuberculosis pandemic-which way now", *J. Infect*, 38, 74 –9**, 1999.**

[34] W. J. Philipp, S. Poulet, K. Eiglmeier, L. Pascopella, V. Balasubramanian, B. Heym, S. Bergh, B. R. Bloom, W. R. Jacobs Jr, S. T. Cole, "An integrated map of the genome of the tubercle bacillus, Mycobacterium tuberculosis H37Rv, and

comparison with Mycobacterium leprae", *Proceeding of National Academy of Science*, 93, 3132-3137, **1996.**

[35] J. Kirsty, Mc Lean, J. Adrian Dunford, Rajasekhar Neeli, Max D. Driscoll, Andrew W. Munro, K. J. Mc Lean, EpoK, "A Cytochrome P450 Involved in Biosynthesis of the Anticancer Agents Epothilones A and B. Substrate-Mediated Rescue of a P450 Enzyme", *Archives of Biochemistry and Biophysics*, 464, 228–240, **2007**.

[36] C. M., Sassetti, E. J. Rubin, "Genetic requirements for mycobacterial survival during infection", *Proc Natl Acad Sci U S A*, 100, 12989–12994, **2003**.

[37] C. M. Sassetti, D. H. Boyd, E. J. Rubin, "Genes required for mycobacterial growth de fined by high density mutagenesis", *Mol Microbiol* 48, 77–84, **2003**.

[38] D. C. Lamb, D. E. Kelly, S. L. Kelly, "Molecular diversity of sterol 14ademethylase substrates in plants, fungi and humans", *FEBS Letter*, 425, 263–265, **1998**.

[39] Hebe M. Guardiola-Diaza, b, Lisa-Anne Fostera, Darren Mushrusha, Alfin D. N. Vazc, H. M. Guardiola- Diaz, *Biochemical Pharmacology*, 61, 1463–1470, **2001**.

[40] L. I. Shiff, "Electron Spin and Proton Spin in the Hydrogen and Hydrogen-Like Atomic Systems", *Quantum Mechanics*, 3, 2, **1968**.

[41] Dritte Mitteilung, Stijrungatheorie Mit Anwendung den Starkeffekt der Balmerlinien, "E. Schroedinger", *Ann. Physik*, 79, 361, **1926**.

[42] T. Ziegler, "Approximate Density Functional Theory as a Practical Tool in Molecular Energetics and Dynamics", *Chemical. Review*, 91, 651, **1991**.

[43] M. J. Frisch, G. W. Trucks, H. B. Schlegel, G. E. Scuseria, M. A. Robb, J. R. Cheeseman, G. Scalmani, V. Barone, B. Mennucci, G. A. Petersson, "*Gaussian 09, Revision B.01", Gaussian, Inc., Wallingford C. T.*, 1–20, **2009.**

Chapter-6

Conclusion and Future Scope

Conclusion and Future Scope

Conclusion and Future Scope:

The present thesis highlights the following conclusions:

1. Nowadays computational Quantum Mechanical methods are highly accurate and reliable in enzymatic catalysis. Heme and non-Heme enzymes react fast with substrates, so that computational method can assist experimental studies with good accuracy and give a piece of proper information about the properties of enzymes that leads to the reaction mechanism and also provides the nature of the enzyme.
2. The present work presents the reaction mechanism of oxygen atom transfer from Cpd I to substrate through aromatic hydroxylation. The present thesis is also defined the barrier energies of various complexes and the rate-determining step in each mechanism.
3. Moreover, barrier height can be used to predict the rate of reaction or rate constant of the reaction. It also identifies the origin of the rate constant by transfer of an electron or proton.
4. The present work established the reactivity pattern of hydroxylation of the substrate via Cpd I for various drugs.
5. Moreover, study of metabolism process of various drugs via P450 is large to an extent scene for compatible collaboration of computational modeling with

experimental results for biomimetic, enzymatic work and defining the optoelectronic properties.

6. The present thesis well explained the metabolism process through the hydroxylation of various drugs (substrate) mediated by Cpd I.
7. These reaction mechanisms will be useful to scientists for investigations of various drugs or drug designing.
8. Further research work in such a field may reveal a wide range of mysteries in understanding the metabolism, detoxification, and many other biochemical reactions as well as help in the search for good anti-fungal drugs also.
9. The present study gives an internal image of aromatic hydroxylation of various drugs via Cpd I with good accuracy as we expected.
10. These results can be used for experimental researchers for the investigations of drug metabolism and drug discovery and will give fruitful results.
11. In the future, DFT studies will perform the complete metabolism process and will find as well as optimize many more drugs which can interact with CYP450.
12. Results obtained by the metabolism process investigate the reaction mechanism of all possible drugs that may be further useful for the scientists to design the drug, do the investigation, and understand the metabolism of various compounds or drug.

Contents lists available at ScienceDirect

Inorganic Chemistry Communications

journal homepage: www.elsevier.com/locate/inoche

Interplay between two degenerate spin state determines the hydroxylation of 4-nitrophenol catalyzed via Cytochrome P450

Nidhi Awasthi, Rolly Yadav, Anamika Shukla, Devesh Kumar *

Department of Physics, School of Physical and Decision Sciences, Babasaheb Bhimrao Ambedkar University, Vidya Vihar, Raebareli Road, Lucknow, Uttar Pradesh 226025, India

ARTICLE INFO

Keywords:
Cytochrome P450
Density Functional Theory
Metalloenzyme
Basis set

ABSTRACT

4-Nitrophenol is formed during the synthesis of paracetamol. It is used in various xenobiotic metabolism processes and other essential biochemical processes. It is metabolized via cytochrome P450 enzyme. The present work reported the hydroxylations of 4-nitrophenol at the ortho position by Cytochrome P450 metalloenzyme. Truncated model of putative active oxidant i.e. ferryl oxo porphyrin cation radical [Fe^{IV}(O)(heme$^{+\bullet}$)], referred as Cpd I in cytochrome P450 enzymes has been used to mimic the behavior of enzyme. In the current investigations, 4-nitrophenol (Substrate) is modeled with Cpd I and reaction mechanism for two degenerate spin states named as doublet (LS) and quartet (HS) is performed to dwell the overall potential energy landscape, along with electronic structures and properties of reactant complex (RC), transition states (TS), intermediates (IM) and product complex (PC). The reaction is stepwise with electrophillic addition as the rate determining step, spin selectivity product formation is observed only at high spin (HS) surface. So, the present reaction pathway is single state reactivity (SSR) by forming the suicidal complex at low spin state (LS).

1. Introduction

The Cytochrome P450 is an essential enzyme found in nature [1]. It consists of number of enzymes with varying substrate selectivity, such as CYP1A2, 2A6, 2B6, 2C9, 2C19, 2D6, 2E1 and 3A etc. These enzymes are responsible for the metabolism of about 70% of therapeutic drugs [2]. In human, P450 is found in liver [3]. It contribute in the catalysis of variety of stereo and regio-selective mono-oxygenation reaction processes and also in detoxification processes [4]. Due to their wide range versatility in activation of several substrate, CYP is very important enzyme, in biology, biotechnological and pharmaceutical applications for investigations of new drugs [5]. Moreover, its involvement in drug metabolism make this enzyme a target for research in drug industry and biomedical field [6–9]. Despite of various member of P450 enzyme, CYP2E1 has been paid a considerable attention, because of its toxicological behavior. It is contributed in the metabolism of various organic solvents and environmental pollutants like, acetone, aniline, ethanol, or nitrosamines etc [10,11]. Metabolism by CYP2E1 might result in the formation of more reactive products, such as the toxic metabolite of acetaminophen (paracetamol) [11–13]. Formation of toxic product of acetaminophen (paracetamol) via CYP2E1, is its crucial behaviour. 4-nitrophenol hydroxylation may responsible for inhibition of toxic product of acetaminophen (paracetamol) via CYP2E1 enzyme.

4-nitrophenol is formed during the synthesis of paracetamol. Initially, it reduced to 4-aminophenol, after that acetylated via acetic anhydride [14]. It is also product of essential enzymatic reactions of several substrate like- 4-nitrophenyl phosphate, 4-nitrophenyl acetate, 4-nitrophenyl-β-D-glucopyranoside and more other derivatives. It plays a crucial role in xenobiotic metabolism process in both, human and mouse. In field of medicinal chemistry, it is used in manufacturing of drugs, insecticides, fungicides. Its structure has phenolic compound, in which nitro group is attached at the opposite of the hydroxyl group on benzene ring. It is also known as *p*-nitrophenol or 4-hydroxynitrobenzene due to presence phenol group. It is mostly used in detection of the presence of alkaline phosphatase activity [15].

The P450 enzyme metabolizes various compound using high-valent iron (IV) oxo species complex, generally known as Cpd I. This complex is formed during the catalytic cycle of Cytochrome P450. Initially, in catalytic cycle, P450 is in the resting state and a water molecule is ligated with it. Whenever, substrate enters, it tightly binds with porphyrin by expelling the water molecule. After the oxidation step a ferric peroxide species is formed, known as compound 0 (Cpd 0), and

* Corresponding author.
E-mail addresses: nidhimsc51@gmail.com (N. Awasthi), dkclcre@yahoo.com (D. Kumar).

https://doi.org/10.1016/j.inoche.2021.108857
Received 2 May 2021; Received in revised form 10 August 2021; Accepted 13 August 2021

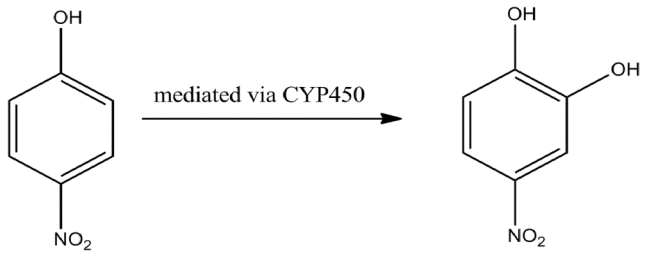

Fig. 1. Aromatic hydroxylation of 4-nitrophenol via CytochromeP450.

then Cpd 0 converts into iron (IV)-oxo porphyrin cation radical oxidants, known as compound I (Cpd I) through a protonation step. It is the primary oxidant that involved in the oxidation reaction of all member of P450. Here we used a truncated model of Cpd I to explore the overall reaction. As we discussed earlier 4-nitrophenol is responsible for various Xenobiotic reactions and these reactions are mediated via CYP2E1 enzyme [16]. So, present study addresses the aromatic hydroxylation of 4-nitrophenol via Cpd I of P450 and form a product (metabolite) known as 2-hydroxy 4-nitrophenol. CYP2E1 is a member of the P450 enzyme, so their active site is similar for both enzymes. That's why P450 enzyme is used here for hydroxylation.

Now days, density functional theory is most reliable and accurate for theoretical study of the reactivity pattern of Cpd I with hybrid function B3LYP [17]. The C-H hydroxylation of the substrate with Cpd I is followed by two different spin surfaces, one is, high spin state (HS) and the other is, low spin state (LS). These two different spin state energy barriers lead to two-state reactivity (TSR) pattern [18–20]. In the present work, we have studied aromatic hydroxylation of 4-nitrophenol (Fig. 1). The reaction pathway for reaction complex (RC), transition state (TS), intermediate state (IM) and product complex (PC) for both spin state, doublet (LS) as well as quartet (HS), are shown in energy profiles as will discuss later. Further, we cross checked the results using larger basis set "LACVP" and solvent effect for benzene. And we got the results overlapping to each other, which show the reliability of the results.

2. Methodological overview

Present study comprises an investigation of reaction energy profile by Quantum Mechanical (QM) method. All calculations have been performed by using Gaussian 09 package [21,22]. Density functional theory (DFT) with hybrid functional B3LYP [3,17,23–28] using "LAN2DZ" basis set on iron atom and 6-31G basis set on rest of the atom (BS1). Here, all calculations were performed for porphyrin cation radical iron (IV) oxo species i.e $Por^{+\cdot}FeIV = O$, (Cpd I), in two different spin states, doublet and quartet. Optimized geometries of reactant, intermediate, product is performed. A clear pathway for the reaction mechanism is found on potential energy surface (PES) with subsequent transition states. Analytic frequency calculations confirmed the local minima of reactant, intermediate, product by showing the real frequencies with first-order saddle point means, transition state having single imaginary frequency. Further, results are cross-checked by calculating single point energies using basis set "LACVP" as well as solvent correction for bezene. Spin densities and Mulliken charges are also investigated (Table 1).

Table 1
Spin densities and charges of Cpd1 & substrate (4-nitrophenol) using DFT at the B3LYP/6-31G level of theory.

Reactant Complex										
Spin Density						Charge				
	Fe	O	Por.	Sub.	SH	Fe	O	Por.	Sub.	SH
M_4	1.10	0.91	0.44	0.00	0.53	0.50	−0.37	-0.07	-0.02	-0.03
M_2	1.36	0.75	−0.58	0.00	−0.53	0.53	−0.45	0.01	−0.05	−0.03
TS1										
Spin Density						Charge				
	Fe	O	Por.	Sub.	SH	Fe	O	Por.	Sub.	SH
M_4	1.41	0.64	0.06	0.51	0.36	0.46	−0.42	−0.28	0.21	0.03
M_2	1.15	0.46	−0.41	0.12	−0.32	0.41	−0.40	−0.22	0.23	−0.02
Intermediate1										
Spin Density						Charge				
	Fe	O	Por.	Sub.	SH	Fe	O	Por.	Sub.	SH
M_4	2.06	0.25	−0.13	0.85	−0.03	0.49	−0.53	−0.29	0.29	0.04
Intermediate 2										
Spin Density						Charge				
	Fe	O	Por.	Sub.	SH	Fe	O	Por.	Sub.	SH
M_4	2.84	0.04	0.07	0.04	0.05	0.45	−0.74	0.12	0.51	−0.05
M_2	1.05	−0.01	−0.07	−0.02	0.04	0.30	−0.72	−0.19	−0.51	0.01
Transition State 3										
Spin Density					Charge					
	Fe	O	Por.	Sub.	SH	Fe	O	Por.	Sub.	SH
M4	2.66	0.03	0.04	0.03	0.26	0.48	−0.74	0.13	−0.51	−0.01
Product										
Spin Density						Charge				
	Fe	O	Por.	Sub.	SH	Fe	O	Por.	Sub.	SH
M_4	2.50	0.00	0.04	−0.00	0.47	0.52	−0.68	−0.36	−0.00	−0.15

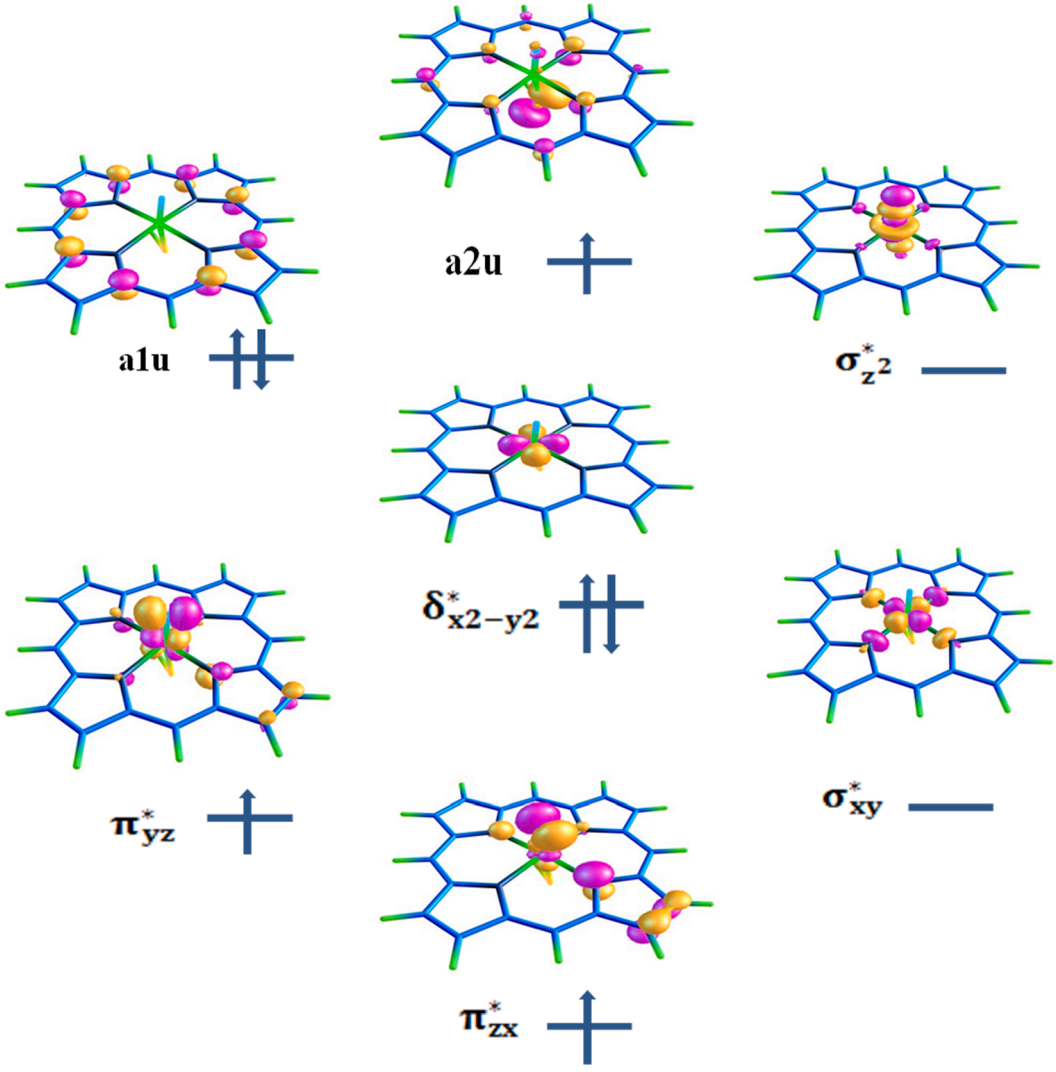

Fig. 2. Key orbital of Cpd I in order of their energy.

3. Key orbital of Cpd1 with substrate

Occupancy of the orbitals is the key to understanding the electronic configuration of Cpd I with substrate. $3d_z^2$ orbital of iron (Fe) and $2p_z$ orbital of oxygen (O38) of Cpd I together formed $\sigma^*_{z^2}$ anti-bonding orbital, whereas interaction of $3d_{xy}$ orbital of iron (Fe) and $2p_{xy}$ orbital of nitrogen atoms (N) of porphyrin together form anti-bonding orbital σ^*_{xy}. These orbitals are initially unfilled due to their high energy state and filled in later part of reaction process. Further, $\delta_{x^2-y^2}$ is orbital of porphyrin ring. The low-lying bonding orbital π_{xz}/π_{yz} and antibonding orbital π^*_{xz}/π^*_{yz} is formed by the interaction between $3d_{xz}/3d_{yz}$ orbital of iron and $2p_x/2p_y$ orbital of oxygen. These bonding π_{xz}/π_{yz} orbitals are always filled. Optimized orbital are shown in Fig. 2. Other than these metal orbitals, two high lying orbitals of heterocyclic ring also formed orbitals a_{1u} and a_{2u}. But, in enzymatic systems a_{2u} orbital is slightly high in energy due to mixing from sigma orbital of axial ligand thiolate. So, two spin states result with ferromagnetic and anti-ferromagnetic coupling between π^{*1}_{xz}, π^{*1}_{yz} and $a_{2u,}$ respectively, whereas a_{2u} remains fully occupied. These all three electrons of orbital π^*_{xz}, π^*_{yz} and a_{2u}combine ferromagnetically or anti-ferromagnetically to form quartet (HS) or doublet (LS) spin state respectively. These type of reaction mechanism leads to the two state reactivity (TSR) pattern [18,29–31].

4. Results and discussion

The proposed work is to large extent to explain the aromatic hydroxylation of 4-nitrophenol at ortho position of the aromatic ring (C49) via Cpd1. Initially, substrate bind with oxygen atom (O38) of Cpd1 at the interacting distance 3 Å to form a stable reactant complex (RC) with energies −10.28 eV & −18.30 eV at high as well as low spin surfaces respectively. After this, charge of O38 of cpd1 is transfer to the carbon atom (C49) of substrate, gives first transition state (TS1) with comparatively less energy 10.66 eV & 10.25 eV at high as well as low spin surfaces respectively. This step is the slowest step of reaction and commonly known as *rate determining step*, from that we can predict the rate of reaction. We also reported the barrier energy of both surfaces is close to 10 eV, indicating requirement of less energy for crossing the both surfaces of reactant complex. Further, first intermediate complex (IM1) with energy 4.66 eV is formed only at the high spin surface. In the next step, hydrogen atom (H53) get attached with nitrogen atom (N2) of porphyrin ring forming a second intermediate state (IM2) with −46.47 eV & −48.76 eV energy at high as well as low spin surfaces respectively. Further, this hydrogen atom (H53) attached to the abstracted oxygen atom (O38) of Cpd I, and form the most stable product complex (PC) having energy −56.62 eV with third transition state (TS3) having energy −44.08 eV at high spin surface. Negative value of third transition state shows less energy required to form product complex from second

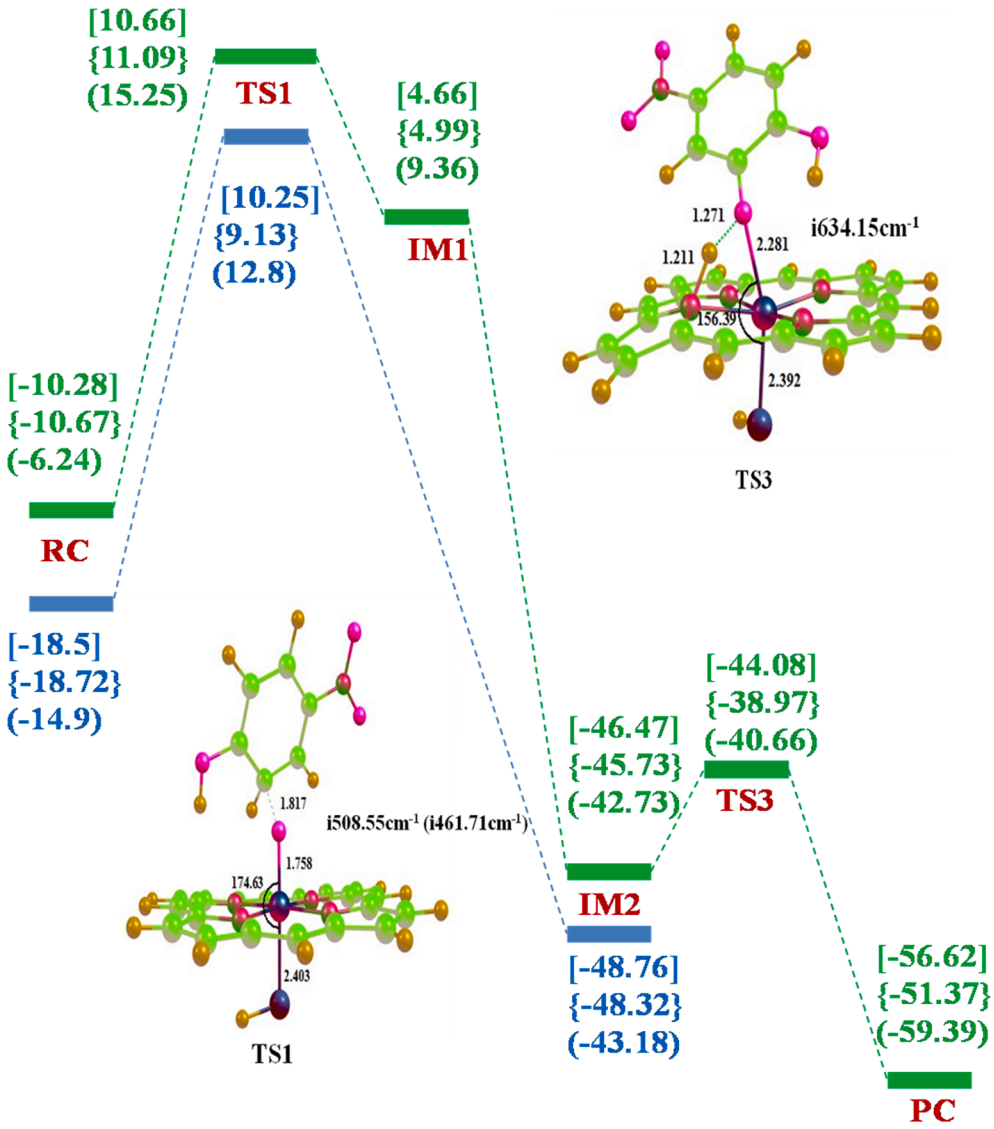

Fig. 3. Potential energy surface of hydroxylation of 4-nitrophenol by Cytochrome P450 with energies in kcal/mol, Bond length (in Å), bond angle (in °) and imaginary frequencies (in cm^{-1}) of quartet (in green color) as well as doublet (in blue color) spin state is shown. Energies are calculated by 6-31G basis set reported in large bracket, by "LACVP" basis set reported in curly bracket and by solvent effect is in small bracket.

intermediate step. Density Functional theory calculations revealed nearly ~1 kcal/mol energy gap between quartet and doublet spin state as shown in Fig. 3.

As we already mentioned, the electronic configuration of Cpd I must be clearly identified, for better understanding of reaction pathway. The electronic configuration of reactant complex (RC) is observed for two spin states to be $\delta^{*2}_{x2-y2}\ \pi^{*1}_{xz}\ \pi^{*1}_{yz}\ \sigma^{*0}_{z^2}\ \sigma^{*0}_{xy}\ a^2_{1u}\ a^1_{2u}$. The first transition state (TS1) has electronic configuration $\delta^{*2}_{x2-y2}\ \pi^{*1}_{xz}\ \pi^{*1}_{yz}\ \sigma^{*0}_{z^2}\ \sigma^{*0}_{xy}\ a^2_{1u}\ a^2_{2u}\ \varphi^1_c$, nature of electron in substrate φ^1_c (up and down) determines the spin state and also conserves the overall quartet and doublet spins (Fig. 3). The electronic configuration of first intermediate (IM1) is same as configuration of first transition state (TS1) at high spin surface.

After formation of first intermediate state (IM1), it leads to second intermediate (IM2) by transfer of charge from carbon (C49) to the nitrogen atom (N53) of porphyrin ring (=N—H) following the electronic configuration $\delta^{*2}_{x2-y2}\ \pi^{*1}_{xz}\ \pi^{*1}_{yz}\ \sigma^{*0}_{z^2}\ \sigma^{*1}_{xy}\ a^2_{1u}\ a^2_{2u}\ \varphi^2_c$ at both spin surface. Third transition state (TS3) of high spin state has configuration as $\delta^{*2}_{x2-y2}\ \pi^{*1}_{xz}\ \pi^{*1}_{yz}\ \sigma^{*1}_{z^2}\ \sigma^{*0}_{xy}\ a^2_{1u}\ a^2_{2u}\ \varphi^2_c$. Further, product complex (PC) is formed by transfer of the hydrogen atom (H53) from nitrogen atom (N2) of substrate, and bind to the oxygen (O38) which has already been transferred at ortho position in second intermediate at high spin surface. The overall configuration of product for high spin state is $\delta^{*2}_{x2-y2}\ \pi^{*1}_{xz}\ \pi^{*1}_{yz}\ \sigma^{*1}_{z^2}\ \sigma^{*0}_{xy}\ a^2_{1u}\ a^2_{2u}$. In case of doublet state, product is not formed due to formation of *suicidal complex*. Scan results at low spin surface are reported in supporting information (SI1). Further, for more convenience for knowing the number of corresponding atoms that are responsible for hydroxylation are shown in Fig. 6 within optimized structure of reactant complex of 4-nitrophenol with Cpd I.

Optimized structure of reactant complex (RC), transition state (TS), intermediate state (IM), and product complex (PC) for quartet as well as doublet spin state is shown in Figs. 4 and 5 respectively.

Transfer of electron is changed occupancies of orbitals, and hence charges as well as spin densities of atoms are changed. Further, the spin densities and mulliken charges are also investigated that confirm the transfer of charges in various orbitals with suitable configuration. Their spin densities with mulliken charges are compiled in Table 1.

With the DFT calculations, the reported imaginary frequencies of TS1 and TS3 of quartet spin state are 508.55i cm^{-1} and 634.15i cm^{-1} respectively. And imaginary frequency of TS1 of low spin state is 461.71i

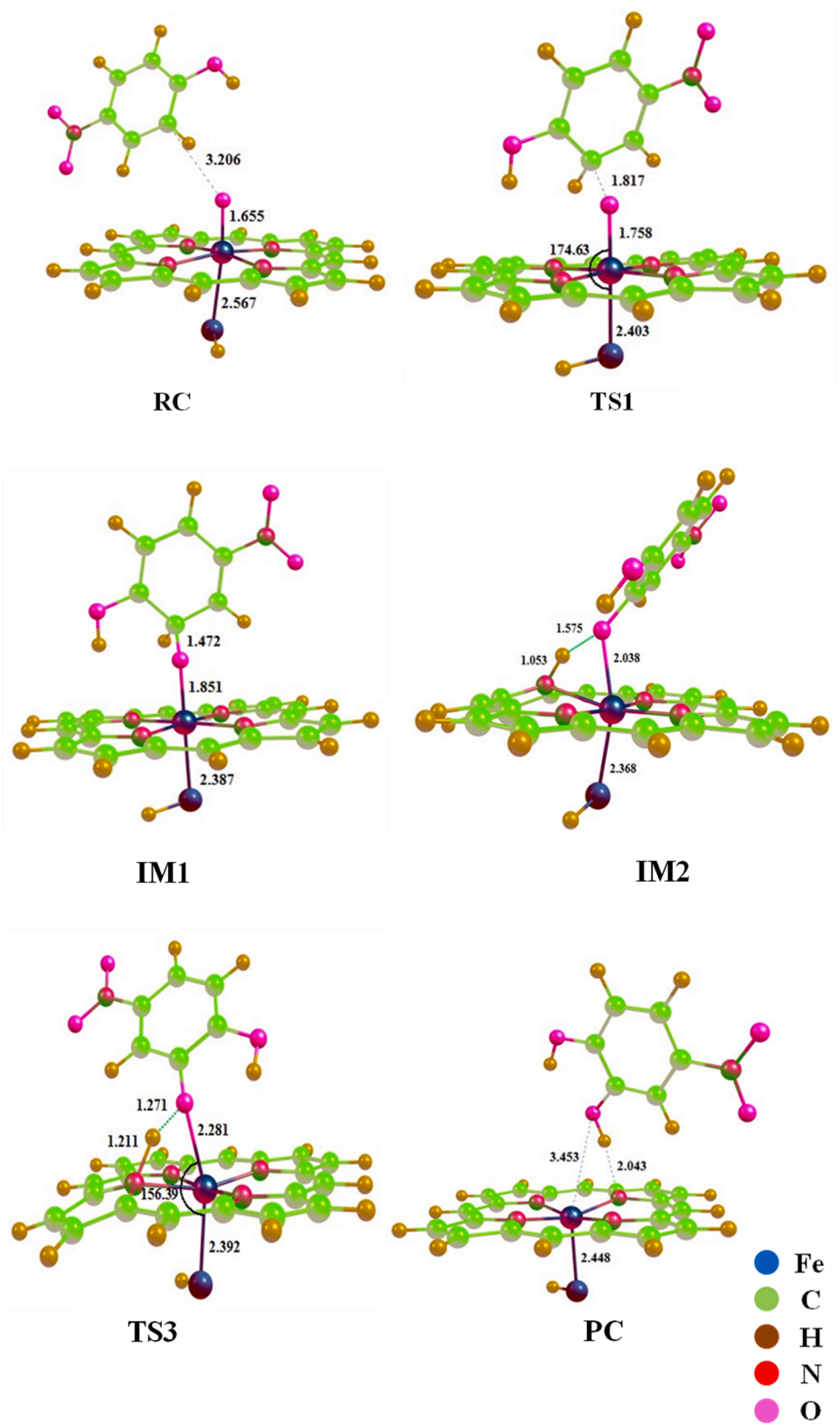

Fig. 4. Optimized geometries of Reactant complex (RC), Transition state (TS), Intermediate complex (IM), and Product complex (PC) with differences in the bond lengths for respective atoms for HS of 4-nitrophenol.

cm^{-1}. As we know that, on the potential energy surface (PES), there may be a number of local maxima or minima between RC and PC. Here, only one local maxima (TS1) is present at low spin surface, while at high spin surface there are two local maxima are observed (TS1 & TS3). High values of imaginary frequencies confirm several local maxima on potential energy surface. There are also local minima is observed by forming the IM1, IM2 on potential energy surface. Further, we cross checked the results using basis set "LACVP" and solvent effect using benzene solvent. And we got the results overlapping to each other, as shown in energy profile Fig. 3.

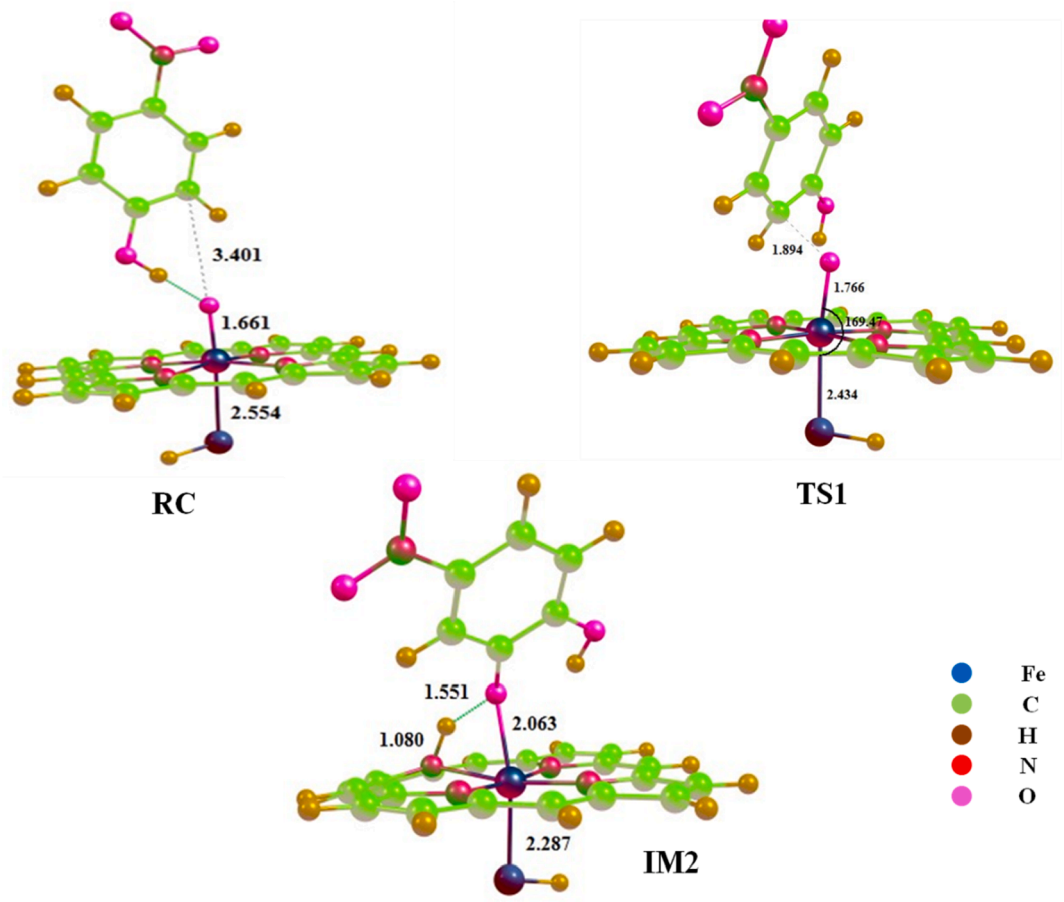

Fig. 5. Optimized geometries of Reactant complex (RC), Transition state (TS), Intermediate complex (IM), and Product complex (PC) with differences in the bond lengths for respective atoms for LS of 4-nitrophenol.

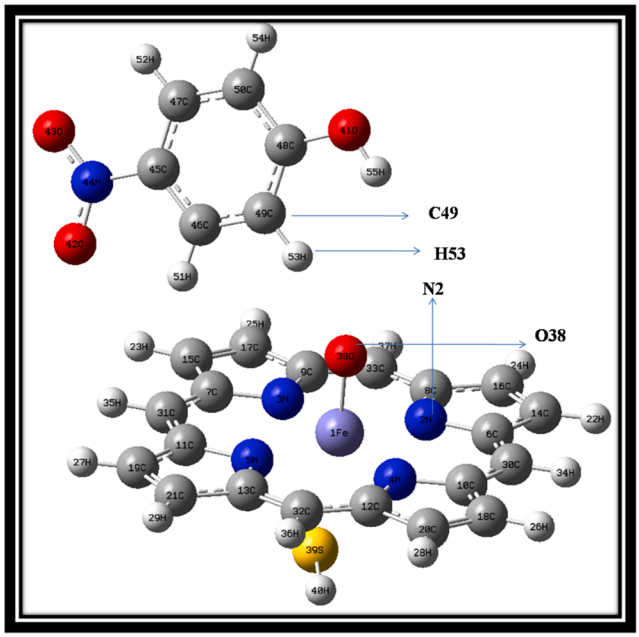

Fig. 6. Optimized geometries of Reactant complex (RC) of 4-nitrophenol in original Gaussian view image. Arrow denoted the number of the corresponding atom.

So, present study is gives an internal image of aromatic hydroxylations of 4-nitrophenol via Cpd1 with too good accuracy, that was still blur for scientists. And hence it also cleared that how 4-nitrophenol metabolized via Cpd1 through the hydroxylation step. Present work may be helpful for further investigations of drugs metabolism and new drugs designing and discovery.

5. Conclusion

The present work offered a complete reaction pathway of aromatic hydroxylation of 4-nitrophenol with Cpd I by DFT at B3LYP level of theory. Quantum mechanical calculations clearly depicted above hydroxylation reaction has more than one transition state with short lived intermediate state and C-O bond formation step to be rate determining step of the reaction. This step clearly shows that it requires less energy to initiating the reaction at both spin surfaces. It can be seen from the energy profile of 4-nitrophenol that quartet surface (HS) is responsible for the hydroxylated product whereas doublet spin surface profile is resulted in the formation of *suicidal complex*. Finally, the product at high spin state surface (HS), is formed, the reaction followed patterns of two state reactivity (TSR) mechanism and energy landscape for doublet and quartet were close and parallel with each other, but this pattern bifurcate at IM1. TSR behavior is transformed to single state reactivity (SSR) showing that reaction is possible only for high spin surface (HS). This process is not regioselective, so the product is formed directly from intermediate. Reaction mechanism of 4-nitrophenol with cpd1 is one of the crucial process, but its reaction pathway was still hidden. Our work gives energy pathway of reaction mechanism with very good accuracy. Present reactions mechanism is different from aliphatic hydroxylation reactions of Cytochrome P450 enzyme, due to formation of suicidal

complex at the low spin surface. Hence it cleared that how 4-nitrophenol metabolized via Cpd1 through the hydroxylation step. All results are further cross checked by using basis set and solvent effect for benzene, and greatly we got the results which are overlapping to each other. Hence the results have too good accuracy "LACVP" and reliable. So, present study gives an internal image of aromatic hydroxylation of 4-nitrophenol via Cpd1 with good accuracy as we expected, that was still blur for scientists. These results can be used for experimental researches for the investigations of drugs metabolism and drugs discovery and will give fruitful results.

6. Author's statement

The corresponding author (Devesh Kumar) is responsible for ensuring that the results are accurate and agreed by all authors.

Computational work and preparation of the manuscript including figures, tables and data compilation has been done by Nidhi Awasthi.

Computational work has been suggested and review of manuscript has been done by Rolly Yadav and Anamika Shukla.

Declaration of Competing Interest

The authors declare that they have no known competing financial interests or personal relationships that could have appeared to influence the work reported in this paper.

Acknowledgement

NA is thankful to University Grant Commission (UGC) for national fellowship for higher education. RY and AS acknowledge to Department of Science and Technology for DST-inspire fellowship (DST/INSPIRE/IF170546). We would also like to thank Prof. C.V. Shastri IIT Guwahati for providing computational facilities.

Appendix A. Supplementary material

Supplementary data to this article can be found online at https://doi.org/10.1016/j.inoche.2021.108857.

References

[1] M. Tuberculosis, Optimization of Azole-Antifungal Drugs: An Attempt for Search of Better Drug for Treatment of TB with CYP450 From, 6(2) (2020) 53–55.
[2] G. Smith, M.J. Stubbins, L.W. Harries, C.R. Wolf, M Olecular Genetics of the Hum an Cytochrom e P450 m Onooxygenase Superfam Ily, Biomed. Res. 28 (12) (1998) 1129–1165.
[3] S. Shaik, S.P. De Visser, Computational Approaches to Cytochrome P450 Function, in: Cytochrome P450, Springer US, Boston, MA, 2005, pp. 45–85, https://doi.org/10.1007/0-387-27447-2_2.
[4] S. Shaik, S. Cohen, Y. Wang, H. Chen, D. Kumar, W. Thiel, P450 Enzymes: Their Structure, Reactivity, and Selectivity-Modeled by QM/MM Calculations, Chem. Rev. 110 (2) (2010) 949–1017, https://doi.org/10.1021/cr900121s.
[5] E. O'Reilly, V. Köhler, S.L. Flitsch, N.J. Turner, Cytochromes P450 as Useful Biocatalysts: Addressing the Limitations, Chem. Commun. 47 (9) (2011) 2490, https://doi.org/10.1039/c0cc03165h.
[6] F.P. Guengerich, Cytochrome P-450 3A4: Regulation and Role in Drug Metabolism, Annu. Rev. Pharmacol. Toxicol. 39 (1) (1999) 1–17, https://doi.org/10.1146/annurev.pharmtox.39.1.1.
[7] U.M. Zanger, M. Schwab, Cytochrome P450 Enzymes in Drug Metabolism: Regulation of Gene Expression, Enzyme Activities, and Impact of Genetic Variation, Pharmacol. Ther. 138 (1) (2013) 103–141, https://doi.org/10.1016/j.pharmthera.2012.12.007.
[8] S. Shaik, W. Lai, H. Chen, Y. Wang, The Valence Bond Way: Reactivity Patterns of Cytochrome P450 Enzymes and Synthetic Analogs, Acc. Chem. Res. 43 (8) (2010) 1154–1165, https://doi.org/10.1021/ar100038u.
[9] M.S. Butler, Natural Products to Drugs: Natural Product Derived Compounds in Clinical Trials, Nat. Prod. Rep. 22 (2) (2005) 162–195, https://doi.org/10.1039/b402985m.
[10] R. Ullrich, M. Hofrichter, Enzymatic Hydroxylation of Aromatic Compounds, Cell. Mol. Life Sci. 64 (3) (2007) 271–293, https://doi.org/10.1007/s00018-007-6362-1.
[11] D.R. Koop, Oxidative and Reductive Metabolism by Cytochrome P450 2E1, FASEB J. 6 (2) (1992) 724–730, https://doi.org/10.1096/fsb2.v6.210.1096/fasebj.6.2.1537462.
[12] W. Chen, L.L. Koenigs, S.J. Thompson, R.M. Peter, A.E. Rettie, W.F. Trager, S. D. Nelson, Oxidation of Acetaminophen to Its Toxic Quinone Imine and Nontoxic Catechol Metabolites by Baculovirus-Expressed and Purified Human Cytochromes P450 2E1 and 2A6, Chem. Res. Toxicol. 11 (4) (1998) 295–301, https://doi.org/10.1021/tx9701687.
[13] J.G.M. Bessems, N.P.E. Vermeulen, Paracetamol (Acetaminophen)-Induced Toxicity: Molecular and Biochemical Mechanisms, Analogues and Protective Approaches, Crit. Rev. Toxicol. 31 (1) (2001) 55–138, https://doi.org/10.1080/20014091111677.
[14] F. Ellis, Paracetamol - a Curriculum Resource, R. Soc. Chem. (2002).
[15] A. Ninfa, D. Ballou, M. Benore, Approaches Biochem. Biotechnol. (2010) 164–179.
[16] K. Monostory, E. Hazai, L. Vereczkey, Inhibition of Cytochrome P450 Enzymes Participating in P-Nitrophenol Hydroxylation by Drugs Known as CYP2E1 Inhibitors, Chem. Biol. Interact. 147 (3) (2004) 331–340, https://doi.org/10.1016/j.cbi.2004.03.003.
[17] S. Shaik, H. Hirao, D. Kumar, Reactivity Patterns of Cytochrome P450 Enzymes: Multifunctionality of the Active Species, and the Two States-Two Oxidants Conundrum, Nat. Prod. Rep. 24 (3) (2007) 533–552, https://doi.org/10.1039/b604192m.
[18] S. Shaik, S. Cohen, S.P. De Visser, P.K. Sharma, D. Kumar, S. Kozuch, F. Ogliaro, D. Danovich, The "Rebound Controversy": An Overview and Theoretical Modeling of the Rebound Step in C-H Hydroxylation by Cytochrome P450, Eur. J. Inorg. Chem. No. 2 (2004) 207–226, https://doi.org/10.1002/ejic.200300448.
[19] H. Hirao, D. Kumar, L. Que, S. Shaik, Two-State Reactivity in Alkane Hydroxylation by Non-Heme Iron-Oxo Comolexes, J. Am. Chem. Soc. 128 (26) (2006) 8590–8606, https://doi.org/10.1021/ja061609o.
[20] M. Torrent, D.G. Musaev, H. Basch, K. Morokuma, Computational Studies of Reaction Mechanisms of Methane Monooxygenase and Ribonucleotide Reductase, J. Comput. Chem. 23 (1) (2002) 59–76, https://doi.org/10.1002/(ISSN)1096-987X10.1002/jcc.v23:110.1002/jcc.1157.
[21] M.J. Frisch, G.W. Trucks, H.B. Schlegel, G.E. Scuseria, M.A. Robb, J.R. Cheeseman, G. Scalmani, V. Barone, B. Mennucci, G.A. Petersson, et al., Gaussian 09, Revision B.01, Gaussian, Inc., Wallingford CT, 2009, pp. 1–20.
[22] W.R. Wadt, P.J. Hay, Ab Initio Effective Core Potentials for Molecular Calculations. Potentials for Main Group Elements Na to Bi, J. Chem. Phys. 82 (1) (1985) 284–298, https://doi.org/10.1063/1.448800.
[23] C.M. Bathelt, L. Ridder, A.J. Mulholland, J.N. Harvey, Aromatic Hydroxylation by Cytochrome P450: Model Calculations of Mechanism and Substituent Effects, J. Am. Chem. Soc. 125 (49) (2003) 15004–15005, https://doi.org/10.1021/ja035590q.
[24] Y. Shiota, K. Yoshizawa, Methane-to-Methanol Conversion by First-Row Transition-Metal Oxide Ions: ScO+, TiO+, VO+, CrO+, MnO+, FeO+, CoO+, NiO+, and CuO+, J. Am. Chem. Soc. 122 (49) (2000) 12317–12326, https://doi.org/10.1021/ja0017965.
[25] F. Ogliaro, N. Harris, S. Cohen, M. Filatov, S.P. De Visser, S. Shaik, A Model, "rebound" Mechanism of Hydroxylation by Cytochrome P450: Stepwise and Effectively Concerted Pathways, and Their Reactivity Patterns, J. Am. Chem. Soc. 122 (37) (2000) 8977–8989, https://doi.org/10.1021/ja991878x.
[26] C.Z. Ai, Y. Liu, D.C. Chen, Y. Saeed, Y.Z. Jiang, Conformational Turn Triggers Regio-Selectivity in the Bioactivation of Thiophene-Contained Compounds Mediated by Cytochrome P450, J. Biol. Inorg. Chem. 24 (7) (2019) 1023–1033, https://doi.org/10.1007/s00775-019-01699-6.
[27] X.Y. Wang, H.M. Yan, Y.L. Han, Z.X. Zhang, X.Y. Zhang, W.J. Yang, Z. Guo, Y.R. Li, Do Two Oxidants (Ferric-Peroxo and Ferryl-Oxo Species) Act in the Biosynthesis of Estrogens? A DFT Calculation, RSC Adv. 8 (27) (2018) 15196–15201, https://doi.org/10.1039/c8ra01252k.
[28] D. Fishelovitch, C. Hazan, H. Hirao, H.J. Wolfson, R. Nussinov, S. Shaik, QM/MM Study of the Active Species of the Human Cytochrome P450 3A4, and the Influence Thereof of the Multiple Substrate Binding, J. Phys. Chem. B 111 (49) (2007) 13822–13832, https://doi.org/10.1021/jp076401j.s001.
[29] R. Hussain, I. Kumari, S. Sharma, M. Ahmed, T.A. Khan, Y. Akhter, Catalytic Diversity and Homotropic Allostery of Two Cytochrome P450 Monooxygenase like Proteins from Trichoderma Brevicompactum, J. Biol. Inorg. Chem. 22 (8) (2017) 1197–1209, https://doi.org/10.1007/s00775-017-1496-6.
[30] S.P. De Visser, S. Shaik, A Proton-Shuttle Mechanism Mediated by the Porphyrin in Benzene Hydroxylation by Cytochrome P450 Enzymes, J. Am. Chem. Soc. 125 (24) (2003) 7413–7424, https://doi.org/10.1021/ja034142f.
[31] M. Albeck, S. Shaik, Publications of Sason Shaik, J. Phys. Chem. A 112 (50) (2008) 12741–12753, https://doi.org/10.1021/jp806628j.

Journal of Organometallic Chemistry

Metabolism of 8-aminoquinoline (8AQ) Primaquine via aromatic hydroxylation step mediated by Cytochrome P450 enzyme using Density Functional Theory

--Manuscript Draft--

Manuscript Number:	
Article Type:	Regular Paper
Keywords:	Cytochrome P450; Basis Set; Density Functional Theory; Primaquine; Metabolism
Corresponding Author:	DEVESH KUMAR, Ph.D. Lucknow, UP India
First Author:	Nidhi Awasthi
Order of Authors:	Nidhi Awasthi
	DEVESH KUMAR, Ph.D.
	Rolly Yadav
	Anamika Shukla
Abstract:	The 8-aminoquinoline (8AQ) drug primaquine (PQ) is a prime anti-malarial drug, used in the treatment of malaria due to plasmodium vivax and plasmodium ovale. The hydroxylated metabolite of Primaquine is also responsible for many essential sexual transmission stages of Plasmodium falciparum. Present work reported the hydroxylation of Primaquine at ortho (2PQ) and para (4PQ) position by Cytochrome P450 enzyme. Density functional theory (DFT) is used to investigate the underlying pathway for aromatic hydroxylation at ortho (2PQ) and para (4PQ) position to produce 2-hydroxylated and 4-hydroxylated Primaquine respectively. Truncated model of putative active oxidant i.e. ferryl oxo porphyrin cation radical [FeIV(O)(heme+•)], which is referred as Cpd I in Cytochrome P450 enzymes has been used to mimic the behaviour of enzyme. Substrate was modelled and reaction mechanism for two degenerate spin states namely doublet and quartet were performed to dwell the overall potential energy landscape, along with electronic structure and properties of reactant complex (RC), transition states (TS), intermediates (IM) and product complex (PC). The reaction was stepwise with electrophillic addition as the rate determining step, spin selectivity product formation was observed for hydroxylated product formation on high spin (HS) surface. All calculations are done for isolated reaction coordinate.
Suggested Reviewers:	Dr. Garikapati Narahari Sastry gnsastry@gmail.com
	Prof. Prasad V. Bharatam pvbharatam@niper.ac.in
	Dr. Samuel De Visser sam.devisser@manchester.ac.uk
Opposed Reviewers:	

Metabolism of 8-aminoquinoline (8AQ) Primaquine via aromatic hydroxylation step mediated by Cytochrome P450 enzyme using Density Functional Theory

Nidhi Awasthi[1], Rolly Yadav[1], Anamika Shukla[1], Devesh Kumar[1]*

[1]Department of Physics,
School of Physical and Decision Sciences,
Babasaheb Bhimrao Ambedkar University,
Vidya Vihar, Raebareli Road, Lucknow, Uttar Pradesh
226025, India.

*Email Id: *dkclcre@yahoo.com*

Abstract

The 8-aminoquinoline (8AQ) drug primaquine (PQ) is a prime anti-malarial drug, used in the treatment of malaria due to plasmodium vivax and plasmodium ovale. The hydroxylated metabolite of Primaquine is also responsible for many essential sexual transmission stages of Plasmodium falciparum. Present work reported the hydroxylation of Primaquine at ortho (2PQ) and para (4PQ) position by Cytochrome P450 enzyme. Density functional theory (DFT) is used to investigate the underlying pathway for aromatic hydroxylation at ortho (2PQ) and para (4PQ) position to produce 2-hydroxylated and 4-hydroxylated Primaquine respectively. Truncated model of putative active oxidant i.e. ferryl oxo porphyrin cation radical [Fe^{IV}(O)(heme$^{+\bullet}$)], which is referred as Cpd I in Cytochrome P450 enzymes has been used to mimic the behaviour of enzyme. Substrate was modelled and reaction mechanism for two degenerate spin states namely doublet and quartet were performed to dwell the overall potential energy landscape, along with electronic structure and properties of reactant complex (RC), transition states (TS), intermediates (IM) and product complex (PC). The reaction was stepwise with electrophillic addition as the rate determining step, spin selectivity product formation was observed for hydroxylated product formation on high spin (HS) surface. All calculations are done for isolated reaction coordinate.

Keywords: Cytochrome P450, Basis Set, Density Functional Theory, Primaquine, Metabolism.

1. Introduction

Cytochrome P450 is an important enzyme of nature, basically in biosystems. In humans, it is found in the liver [1]. But it is also highly expressed in areas of the central nervous system. These enzymes catalyze a variety of stereo-specific and regio-selective mono-oxygenation reaction processes. It is also used in detoxification processes and is a key drug-metabolizing enzyme involved in the metabolism of drugs [2]. It reacts as mono-oxygenase that transfer oxygen atom to the substrate. This oxygen can be transferred either by hydroxylation, epoxidation or sulfoxidation [3–6]. Due to its large versatility in the activation of the substrate, Cytochrome P450 is an essential enzyme, not only in biology but also, in biotechnological and pharmaceutical applications for investigations of drugs [7]. Moreover, its drug metabolism and involvement in brain chemistry make this enzyme a target for the drug industry and biomedical research [8–11].

Fundamentally, hydroxylation is of two types – one is (a) aliphatic, another is (b) aromatic. Both hydroxylations are important and their reaction pattern is different. Present research is focused on study of aromatic hydroxylation. In the modern synthesis chemistry, direct insertion of hydroxyl group into the aromatic compound is one of the most challenging fields, because of the strong bond of hydrogen and carbon (C-H) atom of the benzene ring. But, despite this ambivalence, Cytochrome P450 catalyzes aromatic compound in relatively easy way. Hydroxylations of aromatic rings are important chemical reactions and are catalyzed by several metalloenzymes [8-9]. In biosystems, there are various essential processes of chemical reactions which lead to aromatic hydroxylation with Cytochrome P450 and convert several non-degradable compounds into biodegradable compounds [10-11]. Aromatic hydroxylation step via P450s is responsible for the breakdown of xenobiotics into water-soluble enzymes [3] . P450 catalyse estrogen hormone into 16-hydroxy-estrogen via aromatic hydroxylation step, which basically triggers breast cancer [15–17]. Moreover, plant P450 enzyme catalyze the isoliquiritigenin into the product, which has antitumor, antioxidant and phytoestrogenic activity [18]. Aromatic hydroxylation via P450 is also the centre of research for drug metabolism including para-hydroxylation of Amphetamine and Tamoxifen [19–21] and several other substrates, like, β-blocker alprenolol [22] and the neurotoxin 1-methyl-4-phenyl-1,2,3,6-tetrahydropyridine which is a chemical inducer of Parkinson's disease [23]. So, in the field of bio-chemistry, aromatic hydroxylation via P450 is a crucial activity, but researchers are always fascinated by aromatic hydroxylation due to its unknown reaction mechanism with Cytochrome P450 [21-22]. The Cytochrome P450 is metabolize various compound using high-valent iron (iv) oxo species complex, generally known as Cpd1. This complex is formed during the catalytic cycle of Cytochrome P450 [26–29]. Initially, in

catalytic cycle, Cytochrome P450 is at the resting state and the water molecule is ligated. The entry of the substrate expels the water molecule and tightly binds with the enzyme. Further, the oxidation step forms ferric peroxide species known as compound 0 (Cpd 0), and then after the protonation step Cpd 0 converts into active species of enzyme, iron (IV)-oxo complex, known as compound I (Cpd I). It is the primary oxidant involved in the oxidation reaction of all superfamily of P450s and here truncated model of Cpd I is used to explore the overall reaction.

For large number of atoms a more suitable method is used generally known as QM/MM (quantum mechanical/ molecular mechanical) method. The utility of this method is revealed by the first QM/MM study [30] of the active species. It was done by increasing molecules in all the species in the catalytic cycle of P450cam, [31] the active species of human isoforms, [26-32] and some of organic molecules [33-34] .

Moreover the QM/MM approach, is used for two- layer to three-layer of system, one can easily understand it by continuum solvation model which is used for third layer [35] or by ONIOM-type method in which system is divided in two layers two different layers one is inner QM layers and another is outer MM layer [36]. Such more involved QM/MM treatments have not yet been applied to P450 enzymes.

Present study addresses the aromatic hydroxylation of 8-aminoquinoline (8AQ), an anti-malarial drug primaquine via Cpd I of P450. Primaquine is metabolized by CYP 2D6 enzyme [37]. CYP 2D6 is a member of the P450 enzyme, so their active site is similar for both enzymes. That's why P450 enzyme is used here for hydroxylation.

The 8-aminoquinoline (8AQ) drug primaquine (PQ) is a prime anti-malarial drug, used in the treatment of malaria due to plasmodium vivax and plasmodium ovale [38]. It is also used in the treatment of pneumocystis pneumonia together with clindamycin, as an alternate treatment. It is one of the safest and most effective drugs and is placed in the list of essential drugs of World Health Organization (WHO) [39]. It was developed over 70 years ago. But, unfortunately, the reaction pathway was still blurred.

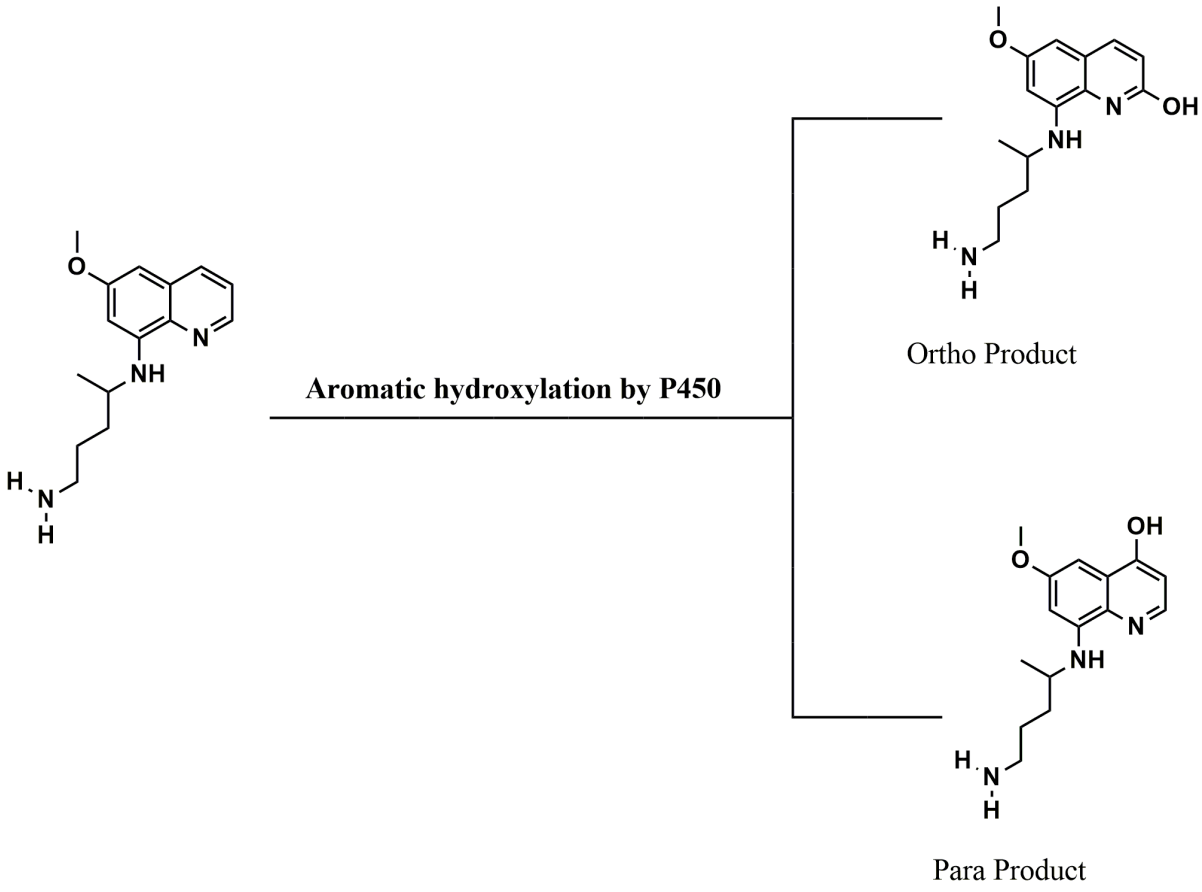

Figure 1: Aromatic hydroxylation of Primaquine at ortho (2PQ) and para (4PQ) position by Cytochrome P450.

The hydroxylated metabolite of Primaquine is also responsible for many essential sexual transmission stages of Plasmodium falciparum [40]. There are six metabolites of 8AQ identified [37]. These metabolites are formed by the hydroxylation step, at each position of the benzene ring. Current study is investigating the hydroxylation step at ortho (2PQ) as well as para (4PQ) position of the benzene ring of Primaquine. DFT method is the most accurate and reliable for studying the reactivity pattern of Cpd I and also of several other essential metalloenzyme with hybrid function B3LYP of DFT [41]. The C-H hydroxylation of the substrate with Cpd I is followed by two different spin surfaces, one is, high spin state (HS) and the other is, low spin state (LS). These two different spin state energy barriers lead to two-state reactivity (TSR) pattern [25-26]. In the present work, we have studied aromatic hydroxylation at the ortho position (2PQ) as well as at the para position of Primaquine (4PQ) (Figure 1). The reaction patterns for reaction complex (RC), transition state (TS), intermediate state (IM) and product complex (PC) for both spin state, doublet (LS) as well as quartet (HS), are shown in energy profiles as will discuss later. All calculations are done for isolated reaction coordinate. Further, we cross checked the results calculating single point energy using basis set LACVP, solvent effect with benzene, and in presence of two

ammonium molecule, and results are overlapping to each other, which showed the reliability of results.

2.Methodology

Present study comprises an investigation of reaction energy profile by Quantum Mechanical (QM) method. Density functional theory (DFT) was involved using Gaussian 09 software [43]. In this work, all calculations were performed for porphyrin cation radical iron (IV) oxo species i.e $Por^{+\cdot}Fe^{iv}=O$, which is commonly referred as (Cpd I), in two different spin states, doublet as well as quartet with primaquine as a substrate. Optimization geometries of reactant, intermediate, product is performed and a genuine pathway for the reaction mechanism is found on potential energy surface (PES) with subsequent transition states. Initially, optimization of geometry was calculated by hybrid density functional B3LYP using LANL2DZ basis set on iron atom and 6-31G basis set on the rest of the atom (BS1) abbreviated as B3LYP/BS1 [44]. Analytic frequency calculations performed after optimization confirmed the local minima of reactant, intermediate, product by showing the real frequencies and first-order saddle point i.e., transition state with single imaginary frequency. Moreover, results are crosschecked at B3LYP/BS2 theory by performing single-point calculations. This basis set involves triple zeta effective core potential on iron and 6-31+G* basis rest on remaining atoms. Further, we calculated single point energy using basis set LACVP, solvent effect with Benzene and in presence of ammonia and results are overlapping to each other, which showed the reliability of results.

Barrier heights are calculated by isolated reactant geometries using 6-31G, 6-31+G*, LACVP, solvent effect with benzene, and in presence of ammonia are shown in Figures 2 and 7.

3. Results and Discussion

3.1. Hydroxylation of Primaquine at ortho position (2PQ)

The proposed work tried to explain aromatic hydroxylation of Primaquine at ortho position of the aromatic ring (C-2), to a complex intermediate (IM1) by attaching at the ortho position of carbon (C-2) with oxygen atom of Cpd I. In the next step, hydrogen atom (H-2) at ortho position gets attached with one of nitrogen atom of porphyrin ring forming a second intermediate state (IM2). Further, this hydrogen atom attaches to the abstracted oxygen atom of Cpd I, and form a product complex (PC).

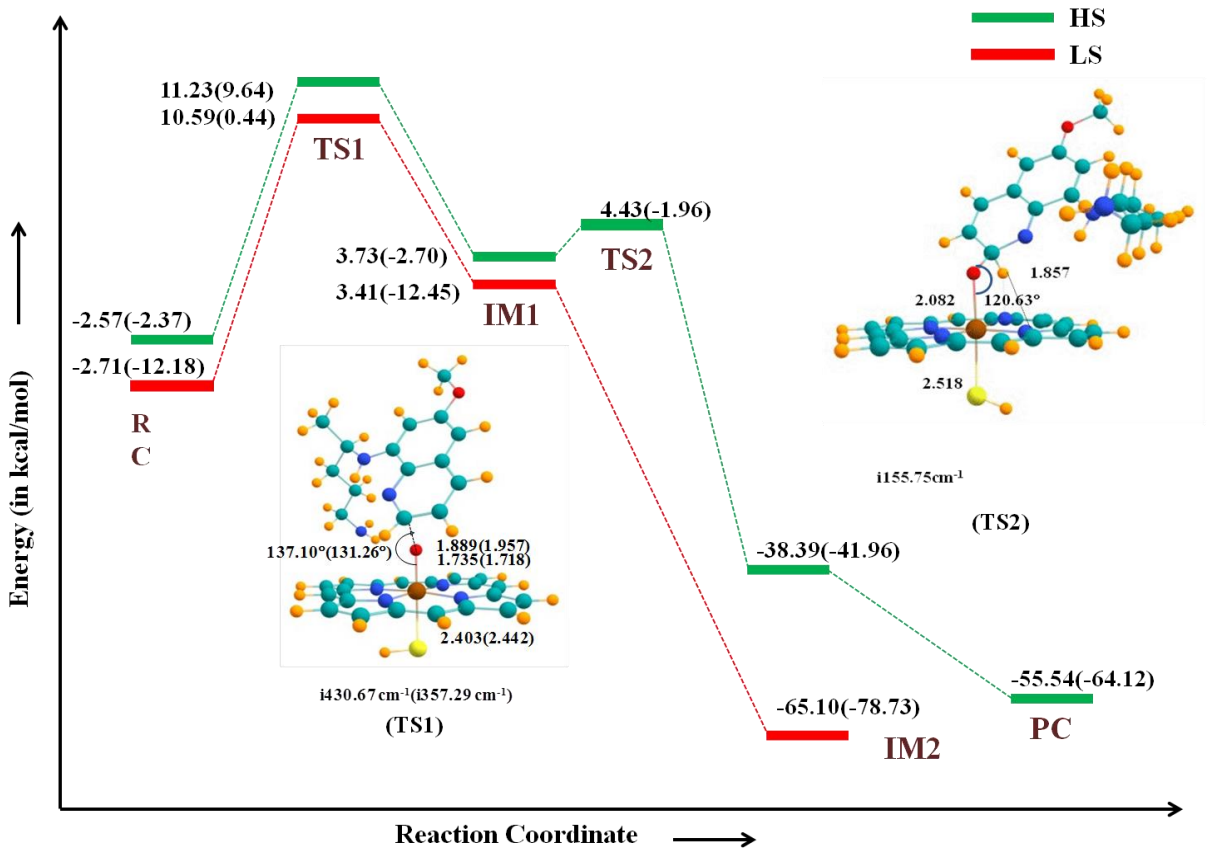

Figure 2: Potential energy surface of hydroxylation of Primaquine (2PQ) by Cytochrome P450 with energies in kcal/mol. Bond length, bond angle and imaginary frequencies (in cm^{-1}) of quartet as well as doublet (in bracket) spin state is shown. All energies are calculated at B3LYP/BS1//B3LYP/BS2 level of theory.

The electronic configuration of CpdI must be clearly identified, for better understanding of its reaction pathway $3d_z^2$ orbital of iron and $2p_z$ orbital of oxygen of Cpd I together formed $\sigma_{z^2}^*$ anti-bonding orbital, whereas interaction of $3d_{xy}$ orbital of iron and $2p_{xy}$ orbital of nitrogen atoms of porphyrin together form anti-bonding orbital σ_{xy}^*. These orbitals are found to be unfilled initially due to their high energy state and filled in later part of reaction process. Further, $\delta_{x^2-y^2}$ is orbital of lone pair electron of porphyrin ring. The low-lying bonding orbital π_{xz} /π_{yz} as well as antibonding orbital π_{xz}^* / π_{yz}^* is formed by the interaction between $3d_{xz}$ /$3d_{yz}$ orbital of iron and $2p_x$ /$2p_y$ orbital of oxygen. These low-lying bonding π_{xz} /π_{yz} orbitals are always filled. Optimized orbitals are shown in Figure 3.

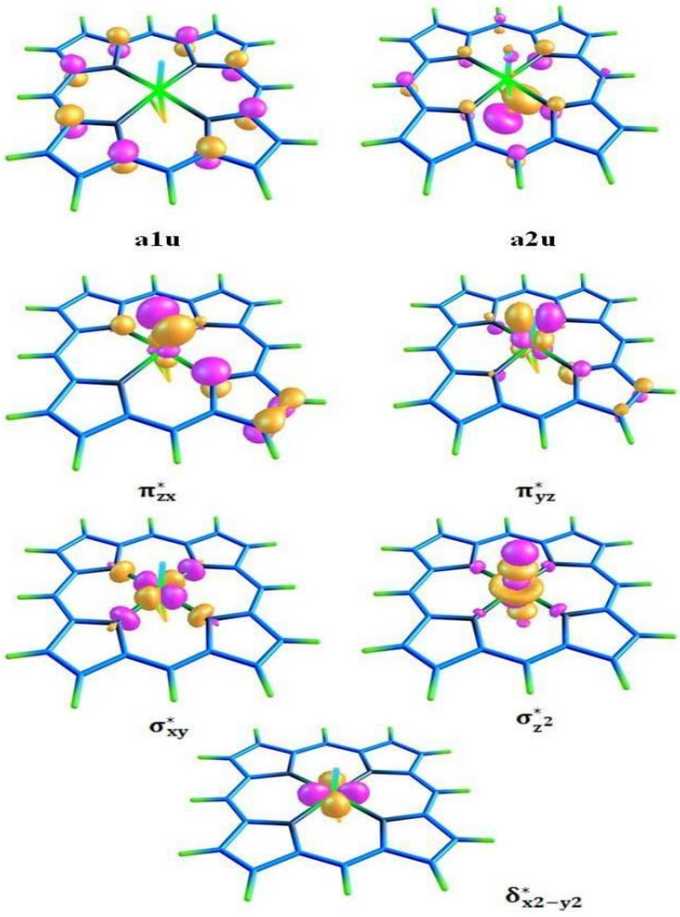

Figure 3: Key orbitals of Cpd I in order of their energy.

Other than these five metal orbitals, two highlying orbitals of heterocyclic ring (a_{1u} and a_{2u}) are also involved. But, in enzymatic systems a_{2u} orbital is slightly high in energy due to mixing from sigma orbital of axial ligand thiolate. So, two spin states result with ferromagnetic and anti-ferromagnetic coupling between π^{*1}_{xz} π^{*1}_{yz} and a^2_{1u} respectively, whereas a_{1u} remains fully occupied. DFT calculations revealed nearly ~ 1kcal/mol energy gap between quartet and doublet spin state as shown in Figure 3.

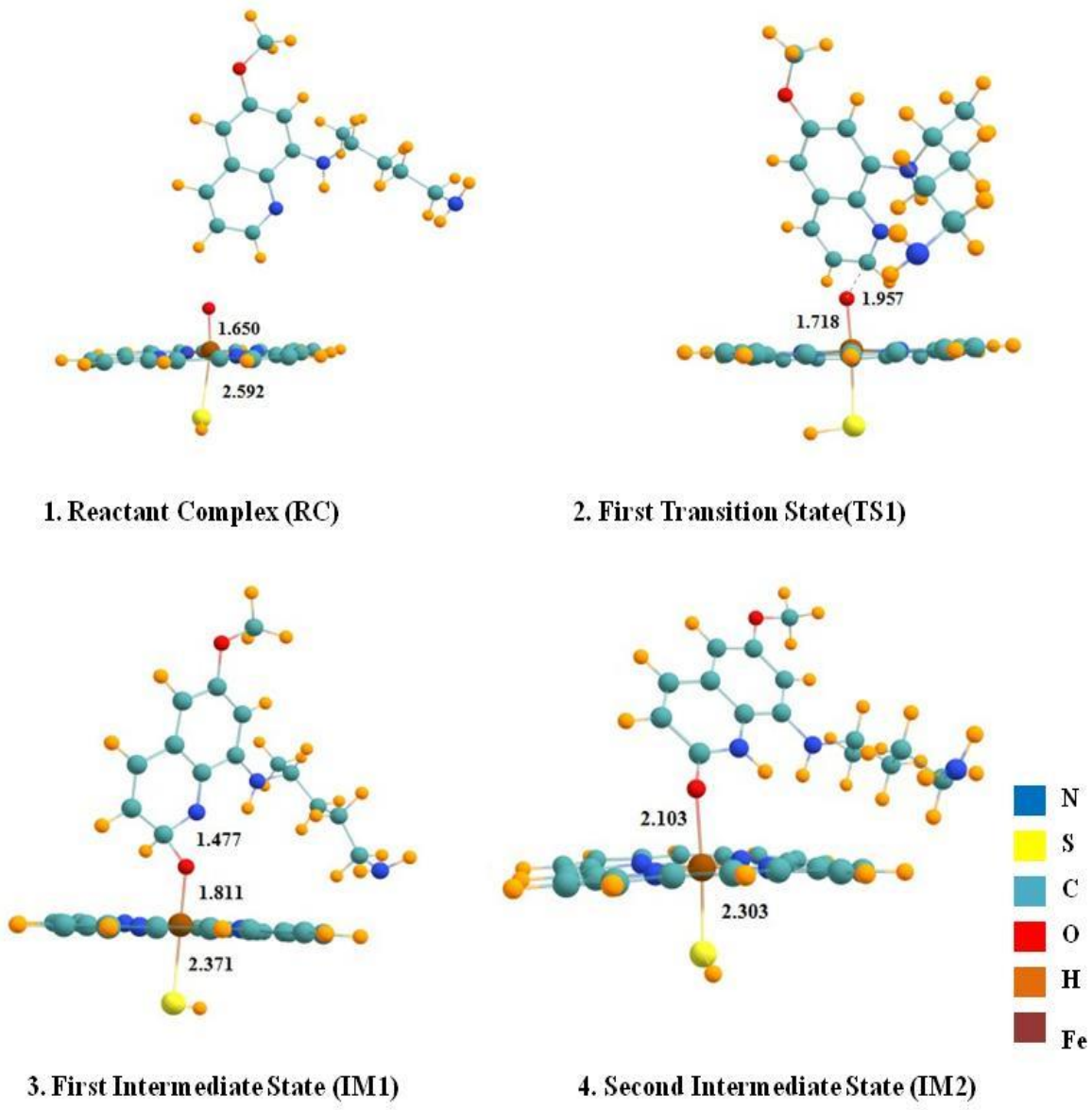

Figure 4: Optimized geometries of Reactant complex (RC), Transition state (TS), Intermediate complex (IM), and Product complex (PC) with differences in the bond lengths for respective atoms for LS of 2PQ.

Substrate (Primaquine) and Cpd I together form reactant complex (RC) when put at interacting distance with each other. The electronic configuration of reactant complex (RC) for two spin states found to be $\delta_{x2-y2}^{*2}\ \pi_{xz}^{*1}\ \pi_{yz}^{*1}\ \sigma_{z^2}^{*0}\ \sigma_{xy}^{*0}\ a_{1u}^{2}\ a_{2u}^{1}$. The transfer of electron from ortho position of carbon (C-2) to oxygen atom of Cpd I, leads to the formation of first intermediate complex (IM1) with electronic configuration $\delta_{x2-y2}^{*2}\ \pi_{xz}^{*1}\ \pi_{yz}^{*1}\ \sigma_{z^2}^{*0}\ \sigma_{xy}^{*0}\ a_{1u}^{2}\ a_{2u}^{2}\ \varphi_{c}^{1}$, nature of electron in substrate φ_{c}^{1} (up and down) determines the spin state and also conserves the overall quartet and doublet spins (Figure 2). The electronic configuration of first transition state (TS1) is same as configuration of first intermediate (IM1).

After this, in the high spin (HS) state, first intermediate leads to second intermediate (IM2) by transfer of charge from ortho carbon (C-2) to one of the nitrogen atom of porphyrin ring (=N-H) following the electronic configuration $\delta_{x2-y2}^{*2}\ \pi_{xz}^{*1}\ \pi_{yz}^{*1}\ \sigma_{z^2}^{*1}\ \sigma_{xy}^{*0}\ a_{1u}^{2}\ a_{2u}^{2}\ \varphi_{c}^{0}$, and the configuration of low spin state of second intermediate (IM2) state is $\delta_{x2-y2}^{*2}\ \pi_{xz}^{*1}\ \pi_{yz}^{*2}\ \sigma_{z^2}^{*1}\ \sigma_{xy}^{*0}\ a_{1u}^{2}\ a_{2u}^{2}\ \varphi_{c}^{0}$. Second transition state (TS2) of high spin state is observed as $\delta_{x2-y2}^{*2}\ \pi_{xz}^{*1}\ \pi_{yz}^{*1}\ \sigma_{z^2}^{*1}\ \sigma_{xy}^{*0}\ a_{1u}^{2}\ a_{2u}^{2}\ \varphi_{c}^{1}$. Further, product complex (PC) is formed by transfer of the hydrogen atom from nitrogen, and bind to the oxygen which has already been transferred at ortho position in second intermediate. The overall configuration of product is $\delta_{x2-y2}^{*2}\ \pi_{xz}^{*1}\ \pi_{yz}^{*1}\ \sigma_{z^2}^{*1}\ \sigma_{xy}^{*0}\ a_{1u}^{2}\ a_{2u}^{2}\ \varphi_{c}^{2}$, product formation is not observed in case of doublet spin state, due to formation of suicidal complex.

The electronic configurations must change due to transfer of charge, so that occupancy of orbital a_{2u} ,π^{*}, σ^{*} and φ_{c} is also changed. As we discussed earlier, all three electrons of orbital π_{xz}^{*}, π_{yz}^{*} and a_{2u} combine ferromagnetically or anti-ferromagnetically to form quartet or doublet spin state respectively. These type of reaction mechanism leads to the two state reactivity (TSR) pattern [45–48].

These calculations are done by quantum mechanical (QM) method using B3LYP basis set. There is a minor energy difference between doublet -2.71 kcal/mol and quartet spin state with energy -2.57 kcal/mol, of optimized reactant complex (RC) as shown in Figure 3. The energy gap between these two states is very close, i.e., these are degenerate energy state as we have discussed above. Optimized structure of reactant complex (RC), transition state (TS), intermediate state (IM), and product complex (PC) for doublet and quartet spin state is shown in Figure 4 and Figure 5 respectively. And their spin densities with mulliken charges are compiled in Table 1. Further, cross checked charge and spin densities using BS2 basis set for 2PQ are reported in Table S1 in supplementary information.

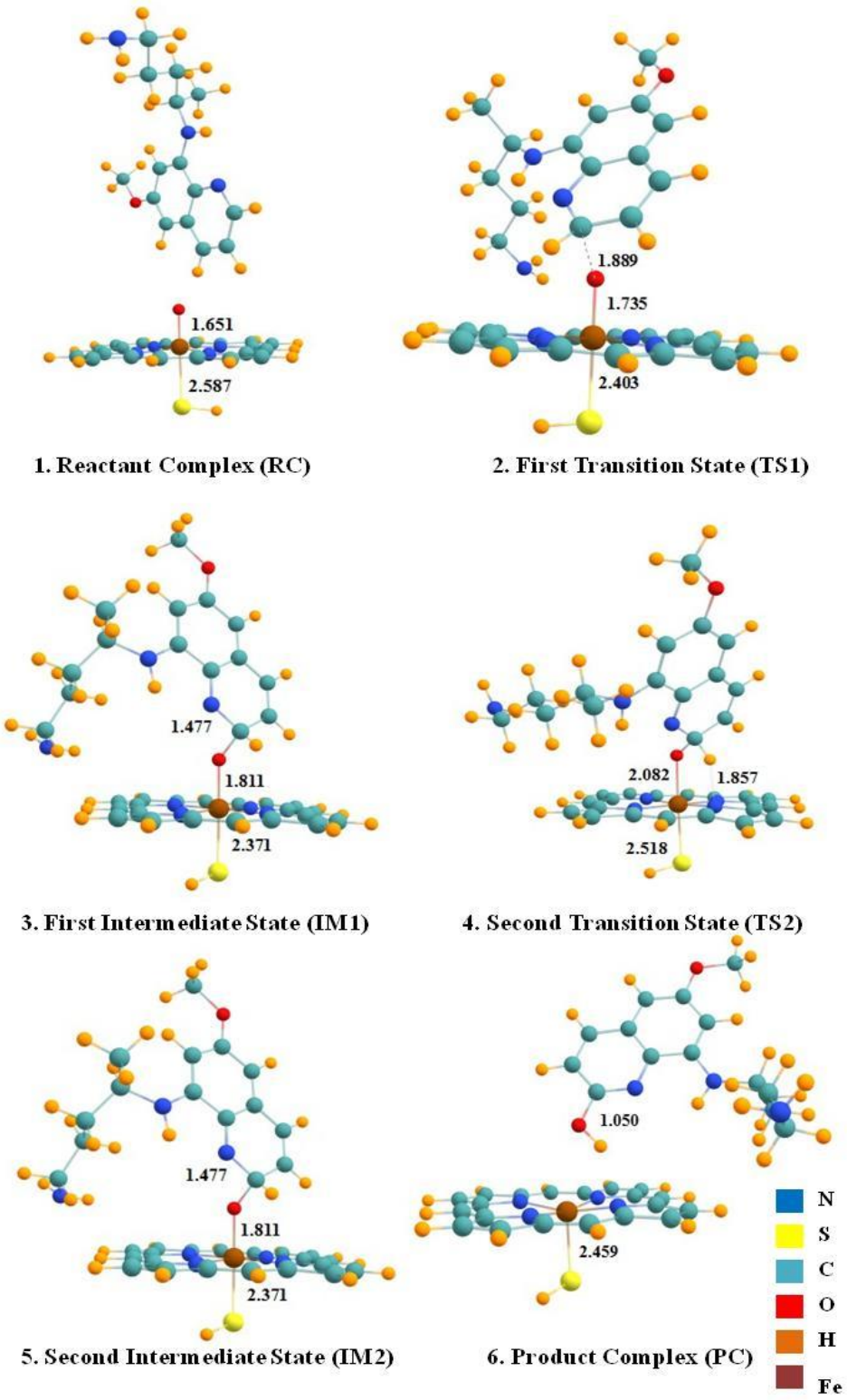

Figure 5: Optimized geometries of Reactant complex (RC), Transition state (TS), Intermediate complex (IM), and Product complex (PC) of quartet spin state (HS) of 2PQ.

The energy of first transition state (TS1) of doublet spin state is 10.59 kcal/mol, it forms more stable state than quartet spin state having energy 11.23 kcal/mol. The energy of first intermediate (IM1) of doublet spin state is 3.41 kcal/mol, and it is comparable to quartet spin state 3.73 kcal/mol. Further, the energy of second transition state (TS2) of quartet spin state is

4.40 kcal/mol. These two degenerate states continuously maintain energy gap of (<1kcal/mol) between them. The energy of second intermediate (IM2) of doublet spin state is -65.10 kcal/mol, and the energy of quartet spin state is -38.39 kcal/mol, this means it is more stable than quartet. LS surfaces offered formation of suicidal complexes, confirmed by reverse scan curves (shown in supporting information in S1). At the end, it forms product complex (PC) with energy -55.54 kcal/mol at high spin state. And the formed product is chemically named as 2-hydroxylated Primaquine (2-OH PQ).

With the frequency calculations, the reported imaginary frequencies of TS1 and TS2 of quartet spin state are 430.67i cm^{-1} and 155.75i cm^{-1} respectively. And imaginary frequency of TS1 of low spin state is 357.29i cm^{-1}. As shown in the energy profile Figure 2, intercrossing of the energy states indicates the spin cross over during the catalytic cycle [33- 34].

Moreover, the transfer of electron and spins of electron is also investigated by charges and spin densities (Mulliken and NBO atomic charges) using BS1 basis set and is reported in Table 1.

Table 1: Spin densities and charges of Cpd1 & 2PQ position of substrate (Primaquine) using BS1 basis set.

Reactant Complex										
Spin Density						**Charge**				
	Fe	**O**	**Por.**	**Sub.**	**SH**	**Fe**	**O**	**Por.**	**Sub.**	**SH**
M_4	**1.07**	**0.94**	**0.43**	**-0.00**	**0.54**	**0.50**	**-0.34**	**0.10**	**0.00**	**-0.04**
M_2	**1.20**	**0.89**	**-0.50**	**-0.00**	**-0.58**	**0.51**	**-0.34**	**-0.11**	**0.00**	**-0.05**
TS1										
Spin Density						**Charge**				
	Fe	**O**	**Por.**	**Sub.**	**SH**	**Fe**	**O**	**Por.**	**Sub.**	**SH**
M_4	**1.35**	**0.74**	**0.02**	**0.60**	**0.27**	**0.45**	**-0.41**	**-0.37**	**0.35**	**-0.02**
M_2	**1.59**	**0.33**	**-0.22**	**-0.49**	**0.21**	**0.45**	**-0.42**	**-0.34**	**0.37**	**-0.07**
Intermediate1										
Spin Density						**Charge**				
	Fe	**O**	**Por.**	**Sub.**	**SH**	**Fe**	**O**	**Por.**	**Sub.**	**SH**
M_4	**1.89**	**0.35**	**-0.13**	**0.91**	**-0.03**	**0.49**	**-0.50**	**-0.35**	**0.35**	**0.01**

M_2	1.77	0.28	-0.13	-0.85	-0.08	0.47	-0.50	-0.35	0.35	0.02
TS 2										
Spin Density						**Charge**				
	Fe	**O**	**Por.**	**Sub.**	**SH**	**Fe**	**O**	**Por.**	**Sub.**	**SH**
M_4	2.62	0.09	-0.10	0.22	0.26	0.53	-0.54	-0.44	0.15	-0.23
Intermediate 2										
Spin Density						**Charge**				
	Fe	**O**	**Por.**	**Sub.**	**SH**	**Fe**	**O**	**Por.**	**Sub.**	**SH**
M_4	2.83	0.09	0.04	-0.11	0.00	0.51	-0.62	0.02	-0.41	-0.12
M_2	1.10	0.00	-0.08	0.00	-0.28	0.35	-0.51	-0.56	0.20	-0.00
Product										
Spin Density						**Charge**				
	Fe	**O**	**Por.**	**Sub.**	**SH**	**Fe**	**O**	**Por.**	**Sub.**	**SH**
M_4	2.5	0.00	0.02	0.00	0.46	0.53	-0.60	-0.41	0.04	-0.16

3.2. Hydroxylation of Primaquine at para position (4PQ)

Abstraction of hydrogen atom at para position of primaquine is identified as 4PQ. All properties are also investigated for 4PQ by quantum mechanical (QM) methods. As we discussed earlier, in this reaction, hydrogen atom at the para position of substrate (Primaquine), is abstracted by Cpd I. The energy profile for both spin surfaces LS as well as HS is studied as shown in Figure 8. Reactant complex of doublet and quartet spin state has same configuration as reactant complex of 2PQ. Before forming the product, both spin surfaces, high as well as low spin surfaces give two intermediate states IM1, IM2 with same electronic configuration as IM1, IM2 of 2PQ. Here one can clearly notice that the LS surfaces offered formation of suicidal complexes, which was further confirmed by running reverse scan curves (shown in supporting information in S2). Also, product 4-hydroxylated Primaquine (4-OH PQ) was found to offer more energy than intermediate 2 (IM2) which further justified the formation of dead product. Optimized structure of reactant complex (RC), transition state (TS), intermediate state (IM), and product complex (PC) for doublet or quartet spin state is shown in Figure 6 as well as in Figure 8 respectively.

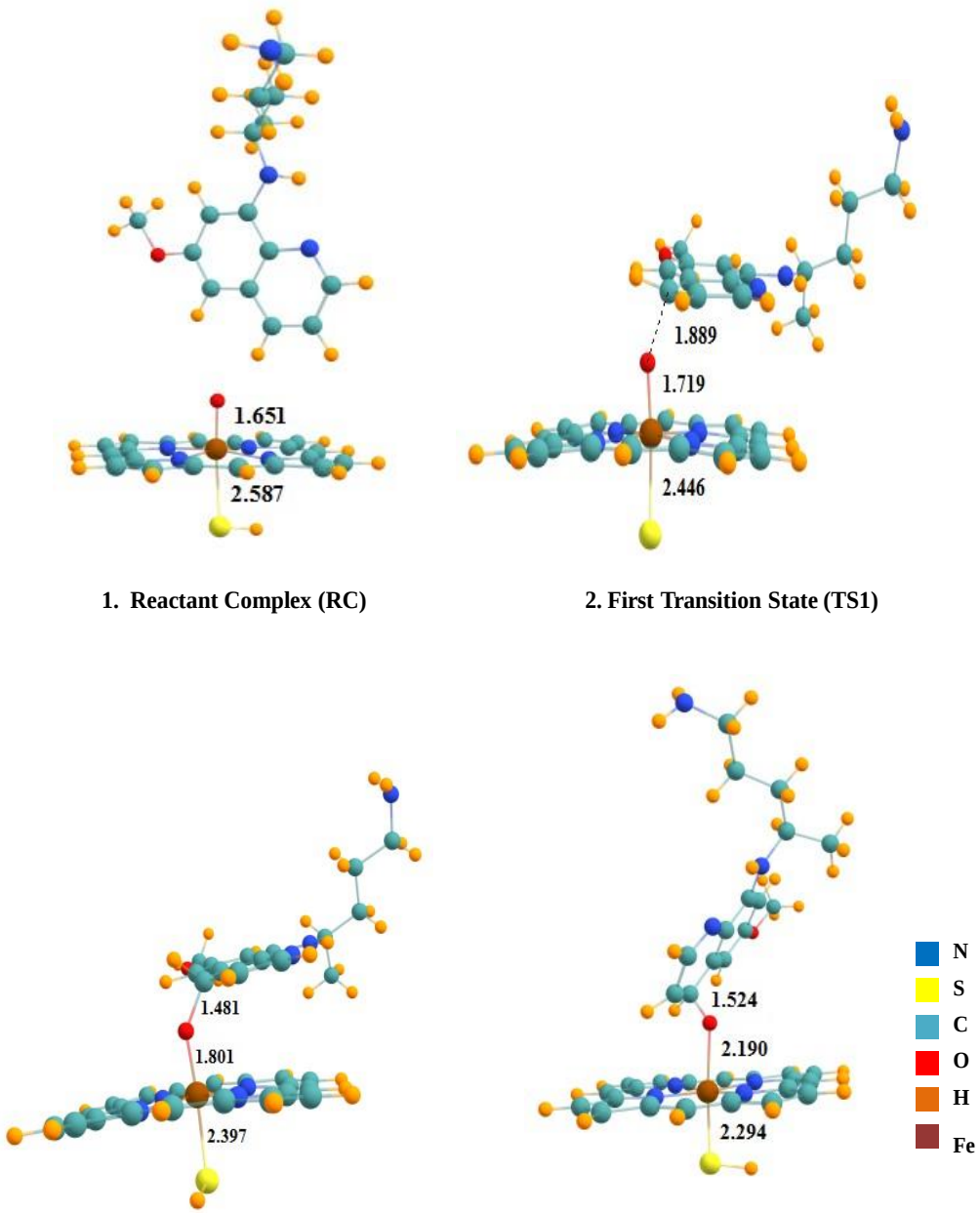

1. Reactant Complex (RC) **2. First Transition State (TS1)**

3. First Intermediate State (IM1) **4. Second Intermediate State (IM2)**

Figure 6: Optimized geometries of Reactant complex (RC), Transition state (TS), Intermediate complex (IM), and Product complex (PC) for doublet state (LS) of 4PQ.

The reaction followed patterns of two state reactivity (TSR) mechanism and energy landscape for doublet and quartet was close and parallel with each other, but this pattern bifurcate at IM1. TSR behaviour is transform to single state reactivity (SSR) and shows that the reaction is possible only for high spin surface (HS).

Also, electronic configuration of first transition states (TS1) of HS as well as LS is same as electronic configuration of TS1 of 2PQ. The electronic configuration of third transition state (TS3) of high spin surface is $\delta_{x2-y2}^{*2}\ \pi_{xz}^{*1}\ \pi_{yz}^{*2}\ \sigma_{z^2}^{*1}\ \sigma_{xy}^{*0}\ a_{1u}^{2}\ a_{2u}^{2}\ \varphi_{c}^{0}$ and product is $\delta_{x2-y2}^{*2}\ \pi_{xz}^{*1}\ \pi_{yz}^{*1}\ \sigma_{z^2}^{*1}\ \sigma_{xy}^{*0}\ a_{1u}^{2}\ a_{2u}^{2}$. The energy of reactant complex (RC) of doublet is -3.97 kcal/mol which is very close to quartet having the energy -2.64 kcal/mol. The first transition state (TS1) of doublet gives energy 12.86 kcal/mol and quartet gives the energy 11.72 kcal/mol. The energy of first intermediate (IM1) of doublet and quartet is 6.47 kcal/mol as well as 3.92 kcal/mol respectively. The energy profile of para position of aromatic hydroxylation is shown in Figure 7. Both spin state continuously maintains 1 kcal/mol difference between them.

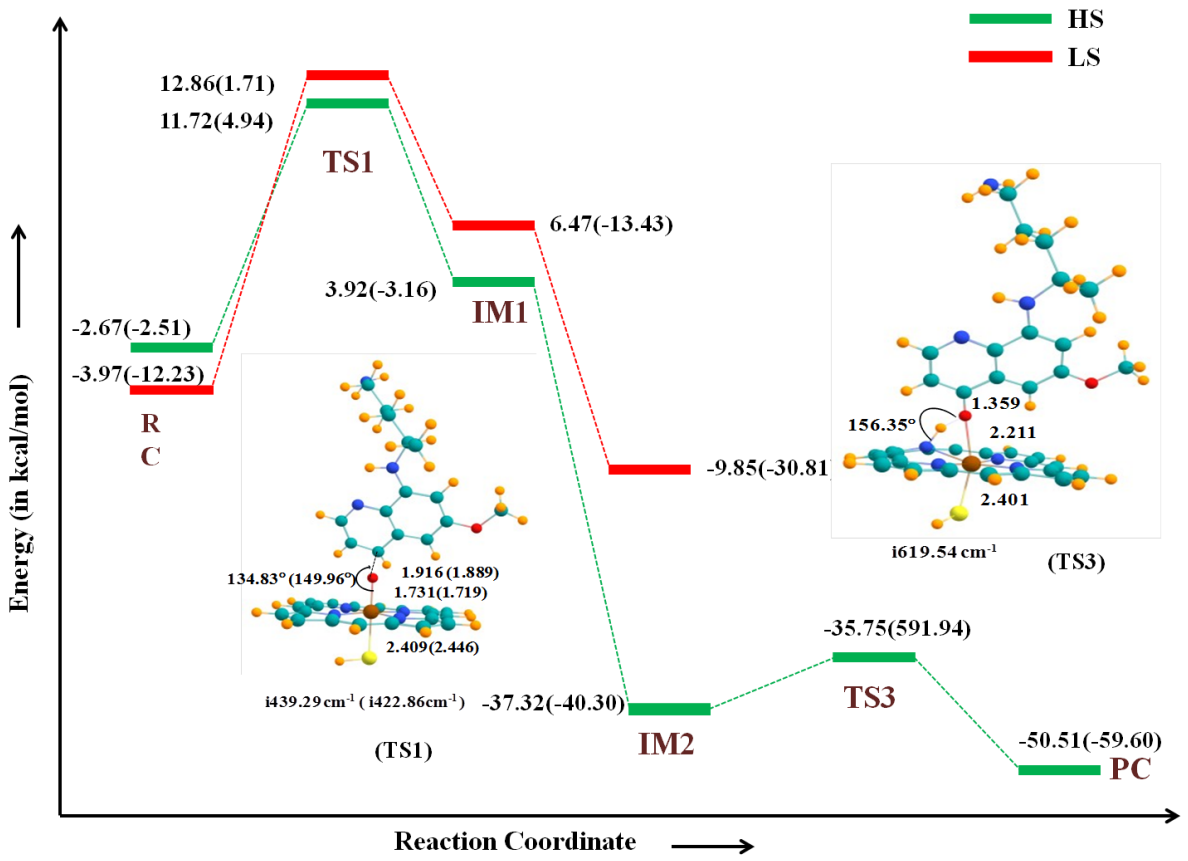

Figure 7: Potential energy surface of hydroxylation of Primaquine (4PQ) by Cytochrome P450 4 with energies in kcal/mol. Bond length, bond angle and imaginary frequencies (in cm^{-1}) of quartet (in green color) as well as doublet (in bracket in red color) spin state is shown. All energies are calculated at B3LYP/BS1//B3LYP/BS2 level of theory. **Coordinate of third transition state (TS3) are not properly conversed for BS2.*

The energy of second intermediate (IM2) of doublet is -9.85 kcal/mol and quartet is -37.32 kcal/mol. The energy of third transition state of quartet (TS3) is -35.57 kcal/mol. Also, the energy of product of quartet spin state is -50.51 kcal/mol. The imaginary frequency of TS1 of doublet is -422.86 cm^{-1} and quartet is -439.29 cm^{-1}. And imaginary frequency of TS3 of

quartet is -619.54 cm^{-1}. Imaginary frequencies of quartet and doublet spin state of transition states are shown in Figure 8. Optimized structure with corresponding bond length of all state of metabolic reaction for both surfaces is shown in Figure 6 & 8, respectively.

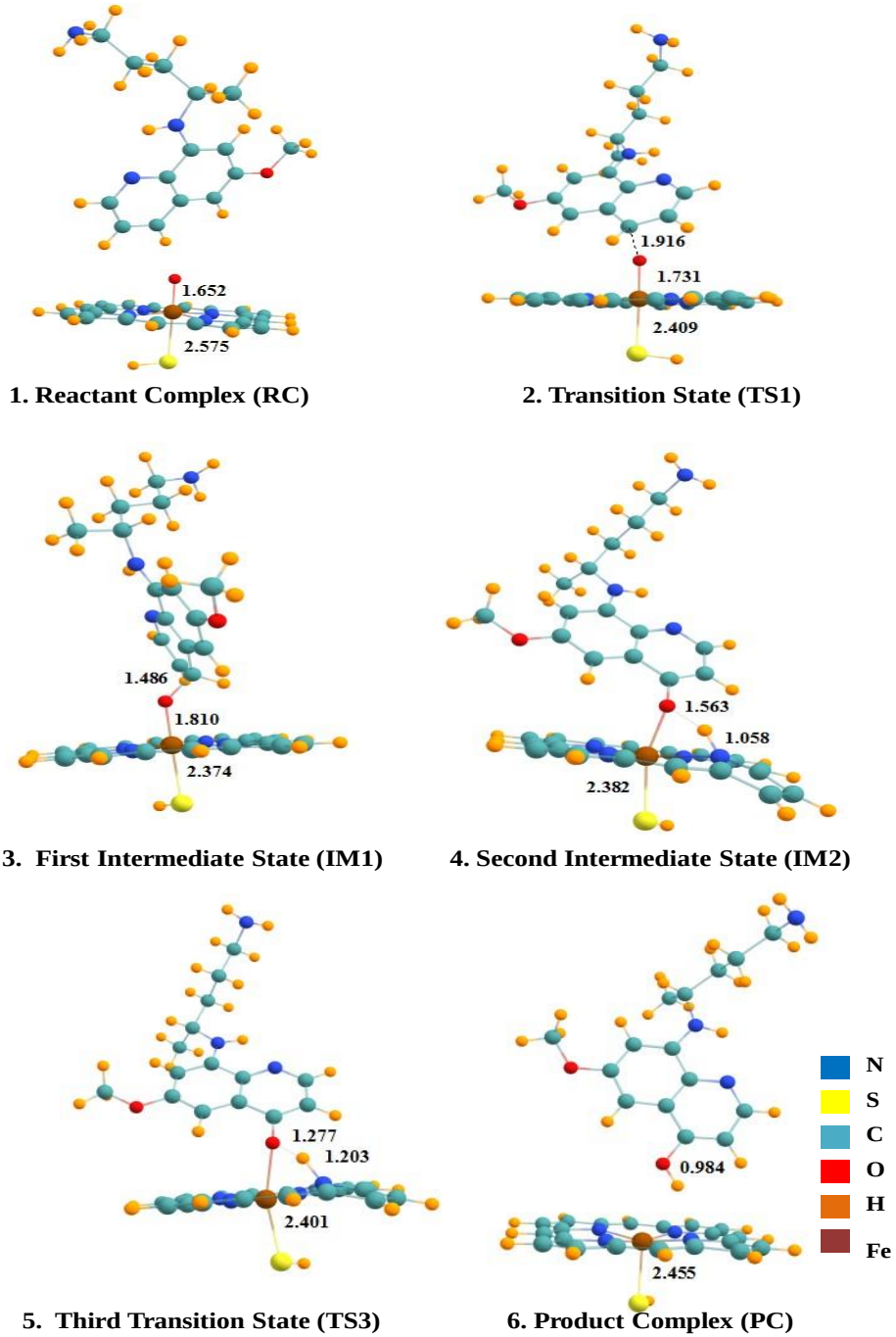

Figure 8: Optimized geometries of Reactant complex (RC), Transition state (TS), Intermediate complex (IM), and Product complex (PC) for quartet state (HS) of 4PQ.

These two step reactions are exothermic as expected. The overall rate of a chemical reaction is often determined by the slowest step of reaction, known as rate limiting or rate determining step. C-O bond formation step is the rate limiting step.

Rate limiting step has activation energy 10.59 and 11.23 kcal/mol, for both LS as well as HS state, respectively. Further, the transfer of electron and spins of electron is also investigated by charges and spin densities (Mulliken atomic charges) using BS1 basis set for 4PQ reported in Table 2. Crosschecked charge and spin densities using BS2 basis set are reported as Table S2 in supplementary information.

Table 2: Spin densities and charges of Cpd1 & 4PQ position of substrate (Primaquine) using BS1 basis set.

Reactant Complex										
Spin Density						**Charge**				
	Fe	**O**	**Por.**	**Sub.**	**SH**	**Fe**	**O**	**Por.**	**Sub.**	**SH**
M_4	**1.07**	**0.94**	**0.43**	**0.00**	**0.53**	**0.51**	**-0.34**	**-0.10**	**0.01**	**-0.05**
M_2	**1.20**	**0.91**	**-0.46**	**-0.05**	**-0.57**	**0.51**	**-0.35**	**-0.10**	**0.00**	**-0.05**
TS1										
Spin Density						**Charge**				
	Fe	**O**	**Por.**	**Sub.**	**SH**	**Fe**	**O**	**Por.**	**Sub.**	**SH**
M_4	**1.32**	**0.75**	**0.04**	**0.60**	**0.28**	**0.47**	**-0.40**	**-0.37**	**0.33**	**-0.02**
M_2	**1.62**	**0.40**	**-0.26**	**-0.51**	**-0.24**	**0.50**	**-0.45**	**-0.33**	**0.34**	**-0.07**
Intermediate1										
Spin Density						**Charge**				
	Fe	**O**	**Por.**	**Sub.**	**SH**	**Fe**	**O**	**Por.**	**Sub.**	**SH**
M_4	**1.84**	**0.37**	**-0.12**	**0.94**	**-0.03**	**0.49**	**-0.50**	**-0.34**	**0.32**	**-0.02**
M_2	**1.91**	**0.32**	**-0.16**	**-0.87**	**-0.19**	**0.55**	**-0.53**	**-0.35**	**0.30**	**0.02**
Intermediate 2										
Spin Density						**Charge**				
	Fe	**O**	**Por.**	**Sub.**	**SH**	**Fe**	**O**	**Por.**	**Sub.**	**SH**
M_4	**2.85**	**0.04**	**0.06**	**0.04**	**0.04**	**0.49**	**-0.72**	**0.07**	**-0.42**	**-0.08**
M_2	**1.12**	**-0.00**	**-0.09**	**-0.00**	**0.03**	**0.36**	**-0.41**	**-0.33**	**-0.27**	**0.02**
TS 3										

Spin Density						Charge				
	Fe	O	Por.	Sub.	SH	Fe	O	Por.	Sub.	SH
M_4	2.71	0.02	0.03	-0.47	0.21	0.51	-0.71	-0.08	-0.47	-0.11
Product										
Spin Density						Charge				
	Fe	O	Por.	Sub.	SH	Fe	O	Por.	Sub.	SH
M_4	2.4	0.00	0.03	-0.00	0.46	0.53	-0.63	0.39	-0.64	-0.16

4. Conclusion

The current work investigated the complete reaction pathway of aromatic hydroxylation of Primaquine with Cpd I by DFT using basis set 6-31G (BS1) and the results were further cross checked using basis set 6-31+G* (BS2). Quantum mechanical calculations clearly depicted above hydroxylation reaction is rebound free process having more than one transition state with short lived intermediate state and C-O bond formation step to be rate determining step of the reaction. It can been seen from the energy profile for ortho (2PQ) and para (4PQ) position of Primaquine that quartet surface (HS) is responsible for the hydroxylated product whereas doublet spin surface profile is resulted in the formation of a *suicidal complex*. Finally, the product at high spin state surface (HS), is formed, the reaction followed patterns of two state reactivity (TSR) mechanism and energy landscape for doublet and quartet were close and parallel with each other, but this pattern bifurcate at IM1. TSR behaviour is transformed to single state reactivity (SSR) showing that reaction is possible only for high spin surface (HS). In the energy profile it is clearly shown that H-abstraction step is rate determining step with activation energy 11.23 kcal/mol and 10.59 kcal/mol for HS and LS respectively for hydroxylation at ortho position while for the hydroxylation at para position the activation energy is 12.86 kcal/mol and 11.72 kcal/mol for HS and LS respectively. Here it is also concluded that this process is not regioselective and the product is formed directly from intermediate. So, the present work is expanded to a great extent about to the metabolism of Primaquine via P450 by giving a reaction pathway. Further, we calculated single point energy using basis set LACVP, solvent effect with Benzene and in presence of ammonia, and results are overlapping to each other, which showed the reliability of results. These formed products (metabolites) are further used for treatment of malaria. These quantum mechanical calculations are considered for good accuracy results. Present reactions mechanism is

different from aliphatic hydroxylation reactions of Cytochrome P450 enzyme, due to formation of suicidal complex at the low spin surface. But further results give good accuracy as we expected and these results can be used for experimental researches and will give fruitful results. And there results have good accuracy for isolated reaction coordinates which shows the success of present work.

Acknowledgement

NA is thankful to University Grant Commission (UGC) for non-net fellowship for higher education. RY and AS acknowledge to Department of Science and Technology for DST-inspire fellowship (DST/INSPIRE). We would also like to thank Prof. C.V. Sastri IIT Guwahati for providing computational facilities.

References

[1] Shaik, S.; De Visser, S. P. Computational Approaches to Cytochrome P450 Function. *Cytochrome P450 Struct. Mech. Biochem. Third Ed.*, **2005**, 45–85. https://doi.org/10.1007/0-387-27447-2_2.

[2] Shaik, S.; Cohen, S.; Wang, Y.; Chen, H.; Kumar, D.; Thiel, W. P450 Enzymes: Their Structure, Reactivity, and Selectivity - Modeled by QM/MM Calculations. *Chem. Rev.*, **2010**, *110* (2), 949–1017. https://doi.org/10.1021/cr900121s.

[3] Asaka, M.; Fujii, H. Participation of Electron Transfer Process in Rate-Limiting Step of Aromatic Hydroxylation Reactions by Compound i Models of Heme Enzymes. *J. Am. Chem. Soc.*, **2016**, *138* (26), 8048–8051. https://doi.org/10.1021/jacs.6b03223.

[4] Harris, N.; Shaik, S.; Schroder, D.; Schwarz, H. H. Single- and Two-State Reactivity in the Gas-Phase C-H Bond Activation of Norbornane by “bare” FeO+. *Helv. Chim. Acta*, **1999**, *82* (10), 1784–1797. https://doi.org/10.1002/(SICI)1522-2675(19991006)82:10<1784::AID-HLCA1784>3.0.CO;2-M.

[5] Link, C. M.; Theoharides, A. D.; Anders, J. C.; Chung, H.; Canfield, C. J. Structure-Activity Relationships of Putative Primaquine Metabolites Causing Methemoglobin Formation in Canine Hemolysates. *Toxicol. Appl. Pharmacol.*, **1985**, *81* (2), 192–202. https://doi.org/10.1016/0041-008X(85)90155-3.

[6] Ji, L.; Faponle, A. S.; Quesne, M. G.; Sainna, M. A.; Zhang, J.; Franke, A.; Kumar, D.; Van Eldik, R.; Liu, W.; De Visser, S. P. Drug Metabolism by Cytochrome P450 Enzymes: What Distinguishes the Pathways Leading to Substrate Hydroxylation over Desaturation? *Chem. - A Eur. J.*, **2015**, *21* (25), 9083–9092.

https://doi.org/10.1002/chem.201500329.

[7] O'Reilly, E.; Köhler, V.; Flitsch, S. L. Cytochromes P450 as Useful Biocatalysts: Addressing the Limitations. *Chem. Commun.*, **2011**, *47* (9), 2490–2501. https://doi.org/10.1039/c0cc03165h.

[8] Guengerich, F. P. Cytochrome P-450 3A4: Regulation and Role in Drug Metabolism. *Annu. Rev. Pharmacol. Toxicol.*, **1999**, *39*, 1–17. https://doi.org/10.1146/annurev.pharmtox.39.1.1.

[9] Zanger, U. M.; Schwab, M. Cytochrome P450 Enzymes in Drug Metabolism: Regulation of Gene Expression, Enzyme Activities, and Impact of Genetic Variation. *Pharmacol. Ther.*, **2013**, *138* (1), 103–141. https://doi.org/10.1016/j.pharmthera.2012.12.007.

[10] Shaik, S.; Lai, W.; Chen, H.; Wang, Y. The Valence Bond Way: Reactivity Patterns of Cytochrome P450 Enzymes and Synthetic Analogs. *Acc. Chem. Res.*, **2010**, *43* (8), 1154–1165. https://doi.org/10.1021/ar100038u.

[11] Butler, M. S. Natural Products to Drugs: Natural Product Derived Compounds in Clinical Trials. *Nat. Prod. Rep.*, **2005**, *22* (2), 162–195. https://doi.org/10.1039/b402985m.

[12] Ullrich, R.; Hofrichter, M. Enzymatic Hydroxylation of Aromatic Compounds. *Cell. Mol. Life Sci.*, **2007**, *64* (3), 271–293. https://doi.org/10.1007/s00018-007-6362-1.

[13] Kumar, D.; Sastry, G. N.; Visser, S. P. De. Axial Ligand Effect On The Rate Constant of Aromatic Hydroxylation. *J. Phys. Chem. B*, **2012**, *116* (Iv), 718–730.

[14] Bathelt, C. M.; Ridder, L.; Mulholland, A. J.; Harvey, J. N. Aromatic Hydroxylation by Cytochrome P450: Model Calculations of Mechanism and Substituent Effects. *J. Am. Chem. Soc.*, **2003**, *125* (49), 15004–15005. https://doi.org/10.1021/ja035590q.

[15] Zhang, F.; Bolton, J. L. Synthesis of the Equine Estrogen Metabolites 2-Hydroxyequilin and 2- Hydroxyequilenin. *Chem. Res. Toxicol.*, **1999**, *12* (2), 200–203. https://doi.org/10.1021/tx980189g.

[16] Huang, Z.; Guengerich, F. P.; Kaminsky, L. S. 16α-Hydroxylation of Estrone by Human Cytochrome P4503A4/5. *Carcinogenesis*, **1998**, *19* (5), 867–872. https://doi.org/10.1093/carcin/19.5.867.

[17] Lee, A. J.; Cai, M. X.; Thomas, P. E.; Conney, A. H.; Zhu, B. T. Characterization of

the Oxidative Metabolites of 17β-Estradiol and Estrone Formed by 15 Selectively Expressed Human Cytochrome P450 Isoforms. *Endocrinology*, **2003**, *144* (8), 3382–3398. https://doi.org/10.1210/en.2003-0192.

[18] Guo, J.; Liu, A.; Cao, H.; Luo, Y.; Pezzuto, J. M.; Van Breemen, R. B. Biotransformation of the Chemopreventive Agent 2',4',4-Trihydroxychalcone (Isoliquiritigenin) by UDP-Glucuronosyltransferases. *Drug Metab. Dispos.*, **2008**, *36* (10), 2104–2112. https://doi.org/10.1124/dmd.108.021857.

[19] Sessler, J. L.; Seidel, D. Synthetic Expanded Porphyrin Chemistry. *Angewandte Chemie - International Edition*. November 3, 2003, pp 5134–5175. https://doi.org/10.1002/anie.200200561.

[20] Carvalho, F.; Soares, M. E.; Fernandes, E.; Remião, F.; Carvalho, M.; Duarte, J. A.; Pires-das-Neves, R.; Pereira, M. D. L.; Bastos, M. D. L. Repeated Administration of D-Amphetamine Results in a Time-Dependent and Dose-Independent Sustained Increase in Urinary Excretion of p-Hydroxyamphetamine in Mice. *J. Heal. Sci.*, **2007**, *53* (4), 371–377. https://doi.org/10.1248/jhs.53.371.

[21] Yoshioka, S.; Takahashi, S.; Ishimori, K.; Morishima, I. Roles of the Axial Push Effect in Cytochrome P450cam Studied with the Site-Directed Mutagenesis at the Heme Proximal Site. *J. Inorg. Biochem.*, **2000**, *81* (3), 141–151. https://doi.org/10.1016/S0162-0134(00)00097-0.

[22] NARIMATSU, S.; TACHIBANA, M.; MASUBUCHI, Y.; IMAOKA, S.; FUNAE, Y.; SUZUKI, T. Cytochrome P450 Isozymes Involved in Aromatic Hydroxylation and Side-Chain N-Desisopropylation of Alprenolol in Rat Liver Microsomes. *Biol. Pharm. Bull.*, **1995**, *18* (8), 1060–1065. https://doi.org/10.1248/bpb.18.1060.

[23] Ortiz De Montellano, P. R.; De Voss, J. J. Substrate Oxidation by Cytochrome P450 Enzymes. *Cytochrome P450 Struct. Mech. Biochem. Third Ed.*, **2005**, 183–245. https://doi.org/10.1007/0-387-27447-2_6.

[24] Lash, T. D. Origin of Aromatic Character in Porphyrinoid Systems. *J. Porphyr. Phthalocyanines*, **2011**, *15* (11–12), 1093–1115. https://doi.org/10.1142/S1088424611004063.

[25] Wen, J.; Chennamadhavuni, D.; Morel, S. R.; Hadden, M. K. Truncated Itraconazole Analogues Exhibiting Potent Anti-Hedgehog Activity and Improved Drug-like Properties. *ACS Med. Chem. Lett.*, **2019**, *10* (9), 1290–1295.

https://doi.org/10.1021/acsmedchemlett.9b00188.

[26] Cohen, S.; Kozuch, S.; Hazan, C.; Shaik, S. Does Substrate Oxidation Determine the Regioselectivity of Cyclohexene and Propene Oxidation by Cytochrome P450? *J. Am. Chem. Soc.*, **2006**, *128* (34), 11028–11029. https://doi.org/10.1021/ja063269c.

[27] Ortiz de Montellano, P. R.; De Voss, J. J. Oxidizing Species in the Mechanism of Cytochrome P450. *Nat. Prod. Rep.*, **2002**, *19* (4), 477–493. https://doi.org/10.1039/b101297p.

[28] Ortiz De Montellano, P. R.; De Voss, J. J. Substrate Oxidation by Cytochrome P450 Enzymes. In *Cytochrome P450: Structure, Mechanism, and Biochemistry: Third edition*; Springer US, 2005; pp 183–245. https://doi.org/10.1007/0-387-27447-2_6.

[29] Torrent, M.; Musaev, D. G.; Basch, H.; Morokuma, K. Computational Studies of Reaction Mechanisms of Methane Monooxygenase and Ribonucleotide Reductase. *J. Comput. Chem.*, **2002**, *23* (1), 59–76. https://doi.org/10.1002/jcc.1157.

[30] Schöneboom, J. C.; Lin, H.; Reuter, N.; Thiel, W.; Cohen, S.; Ogliaro, F.; Shaik, S. The Elusive Oxidant Species of Cytochrome P450 Enzymes: Characterization by Combined Quantum Mechanical/Molecular Mechanical (QM/MM) Calculations. *J. Am. Chem. Soc.*, **2002**, *124* (27), 8142–8151. https://doi.org/10.1021/ja026279w.

[31] Shaik, S.; Cohen, S.; Wang, Y.; Chen, H.; Kumar, D.; Thiel, W. *P450 Enzymes: Their Structure, Reactivity, and Selectivity - Modeled by QM/MM Calculations*; 2010; Vol. 110. https://doi.org/10.1021/cr900121s.

[32] Fishelovitch, D.; Hazan, C.; Hirao, H.; Wolfson, H. J.; Nussinov, R.; Shaik, S. QM/MM Study of the Active Species of the Human Cytochrome P450 3A4, and the Influence Thereof of the Multiple Substrate Binding. *J. Phys. Chem. B*, **2007**, *111* (49), 13822–13832. https://doi.org/10.1021/jp076401j.

[33] Wang, Y.; Chen, H.; Makino, M.; Shiro, Y.; Nagano, S.; Asamizu, S.; Onaka, H.; Shaik, S. Theoretical and Experimental Studies of the Conversion of Chromopyrrolic Acid to an Antitumor Derivative by Cytochrome P450 StaP: The Catalytic Role of Water Molecules. *J. Am. Chem. Soc.*, **2009**, *131* (19), 6748–6762. https://doi.org/10.1021/ja9003365.

[34] Altun, A.; Guallar, V.; Friesner, R. A.; Shaik, S.; Thiel, W. The Effect of Heme Environment on the Hydrogen Abstraction Reaction of Camphor in P450cam Catalysis: A QM/MM Study. *J. Am. Chem. Soc.*, **2006**, *128* (12), 3924–3925.

https://doi.org/10.1021/ja058196w.

[35] Riccardi, D.; Schaefer, P.; Cui, Q. PK a Calculations in Solution and Proteins with QM/MM Free Energy Perturbation Simulations: A Quantitative Test of QM/MM Protocols. *J. Phys. Chem. B*, **2005**, *109* (37), 17715–17733. https://doi.org/10.1021/jp0517192.

[36] Benighaus, T.; Thiel, W. Efficiency and Accuracy of the Generalized Solvent Boundary Potential for Hybrid QM/MM Simulations: Implementation for Semiempirical Hamiltonians. *J. Chem. Theory Comput.*, **2008**, *4* (10), 1600–1609. https://doi.org/10.1021/ct800193a.

[37] Pybus, B. S.; Sousa, J. C.; Jin, X.; Ferguson, J. A.; Christian, R. E.; Barnhart, R.; Vuong, C.; Sciotti, R. J.; Reichard, G. A.; Kozar, M. P.; et al. CYP450 Phenotyping and Accurate Mass Identification of Metabolites of the 8-Aminoquinoline , Anti-Malarial Drug Primaquine. **2012**, 1–9.

[38] Hill, D. R.; Baird, J. K.; Parise, M. E.; Lewis, L. S.; Ryan, E. T.; Magill, A. J. Primaquine: Report from CDC Expert Meeting on Malaria Chemoprophylaxis I. *Am. J. Trop. Med. Hyg.*, **2006**, *75* (3), 402–415. https://doi.org/10.4269/ajtmh.2006.75.402.

[39] Lee, K. A.; Nam, W. Determination of Reactive Intermediates in Iron Porphyrin Complex-Catalyzed Oxygenations of Hydrocarbons Using Isotopically Labeled Water: Mechanistic Insights. *J. Am. Chem. Soc.*, **1997**, *119* (8), 1916–1922. https://doi.org/10.1021/ja9629118.

[40] Camarda, G.; Jirawatcharadech, P.; Priestley, R. S.; Saif, A.; March, S.; Wong, M. H. L.; Leung, S.; Miller, A. B.; Baker, D. A.; Alano, P.; et al. Antimalarial Activity of Primaquine Operates via a Two-Step Biochemical Relay. *Nat. Commun.*, **2019**, *10* (1). https://doi.org/10.1038/s41467-019-11239-0.

[41] Shaik, S.; Hirao, H.; Kumar, D. Reactivity Patterns of Cytochrome P450 Enzymes: Multifunctionality of the Active Species, and the Two States-Two Oxidants Conundrum. *Nat. Prod. Rep.*, **2007**, *24* (3), 533–552. https://doi.org/10.1039/b604192m.

[42] Hirao, H.; Kumar, D.; Que, L.; Shaik, S. Two-State Reactivity in Alkane Hydroxylation by Non-Heme Iron-Oxo Comolexes. *J. Am. Chem. Soc.*, **2006**, *128* (26), 8590–8606. https://doi.org/10.1021/ja061609o.

[43] Frisch, M. J.; Trucks, G. W.; Schlegel, H. B.; Scuseria, G. E.; Robb, M. A.;

Cheeseman, J. R.; Scalmani, G.; Barone, V.; Mennucci, B.; Petersson, G. A.; et al. Gaussian 09, Revision B.01. *Gaussian 09, Revis. B.01, Gaussian, Inc., Wallingford CT*, **2009**, 1–20.

[44] Wadt, W. R.; Hay, P. J. Ab Initio Effective Core Potentials for Molecular Calculations. Potentials for Main Group Elements Na to Bi. *J. Chem. Phys.*, **1985**, *82* (1), 284–298. https://doi.org/10.1063/1.448800.

[45] Shaik, S.; Cohen, S.; De Visser, S. P.; Sharma, P. K.; Kumar, D.; Kozuch, S.; Ogliaro, F.; Danovich, D. The "Rebound Controversy": An Overview and Theoretical Modeling of the Rebound Step in C-H Hydroxylation by Cytochrome P450. *Eur. J. Inorg. Chem.*, **2004**, No. 2, 207–226. https://doi.org/10.1002/ejic.200300448.

[46] Hussain, R.; Kumari, I.; Sharma, S.; Ahmed, M.; Khan, T. A.; Akhter, Y. Catalytic Diversity and Homotropic Allostery of Two Cytochrome P450 Monooxygenase like Proteins from Trichoderma Brevicompactum. *J. Biol. Inorg. Chem.*, **2017**, *22* (8), 1197–1209. https://doi.org/10.1007/s00775-017-1496-6.

[47] De Visser, S. P.; Shaik, S. A Proton-Shuttle Mechanism Mediated by the Porphyrin in Benzene Hydroxylation by Cytochrome P450 Enzymes. *J. Am. Chem. Soc.*, **2003**, *125* (24), 7413–7424. https://doi.org/10.1021/ja034142f.

[48] Albeck, M.; Shaik, S. Publications of Sason Shaik. *J. Phys. Chem. A*, **2008**, *112* (50), 12741–12753. https://doi.org/10.1021/jp806628j.

[49] Wang, X. Y.; Yan, H. M.; Han, Y. L.; Zhang, Z. X.; Zhang, X. Y.; Yang, W. J.; Guo, Z.; Li, Y. R. Do Two Oxidants (Ferric-Peroxo and Ferryl-Oxo Species) Act in the Biosynthesis of Estrogens? A DFT Calculation. *RSC Adv.*, **2018**, *8* (27), 15196–15201. https://doi.org/10.1039/c8ra01252k.

[50] Shang, S.; Lin, Z.; Yin, A.; Yang, S.; Chi, Y.; Wang, Y.; Dong, J.; Liu, B.; Zhen, N.; Hill, C. L.; et al. Self-Assembly of Ln(III)-Containing Tungstotellurates(VI): Correlation of Structure and Photoluminescence. *Inorg. Chem.*, **2018**, *57* (15), 8831–8840. https://doi.org/10.1021/acs.inorgchem.8b00693.

Article

Advanced Science, Engineering and Medicine
Vol. 11, 1–5, 2019
www.aspbs.com/asem

Molecular Docking Studies of Enzyme Binding Drugs on Family of Cytochrome P450 Enzymes

Rolly Yadav, Anwesh Pandey, Nidhi Awasthi, and Anamika Shukla*

Department of Physics, School of Physical and Decision Sciences, Babasaheb Bhimrao Ambedkar University, Lucknow, UP, India

The combination of experimental and computational strategies has been of great value in the identification and development of metabolism of drugs. Nowadays modern drug design, molecular docking methods are helpful in exploring the ligand conformations adopted within the binding sites of macromolecular targets such as DNA, proteins, and enzymes, there by reducing cost, time and wayward efforts of chemist. Since the development of the algorithms in the 1980s, molecular docking became an important tool in drug discovery like investigation of crucial molecular events, including ligand binding modes and the corresponding intermolecular interactions that stabilize the ligand-receptor complex, can be conveniently performed. In present study we have tried to investigate the drug binding pocket of various cytochrome (CYP) enzymes found in humans. All structures of drugs are optimized at B3LYP/6-31** level of theory using Gaussian program suite. Docking of substrate-enzyme duo was done using AUTODOCK 4.0. Computational docking revealed that almost all drugs have same binding pocket with varied binding affinities due to change in interactions and interacting distance from heme prosthetic moiety with transition metal iron as chelating ion.

Keywords: CYP1A2, CYP2C9, CYP2D6, Docking, Enzyme.

1. INTRODUCTION

Enzymes are protein macromolecules which are present in cells of all living organisms ranging from simple micro-organisms to largest mammals. These protein structures act as a catalyst in various biological processes thereby making required product at faster rate without changing their original form after completion of reaction. Drug metabolism [1] is an extremely important area of research, as side effects of a particular drug can be known and resolved, designing of new and advanced drugs can be done etc. Cytochrome P450 (CYP450) is one of the most versatile enzymes in nature [2] usually found in abundance in liver cells of mammals and is involved in detoxification of xenobiotics [3, 4]. Primarily three families of P450s i.e., CYP1, CYP2, and CYP3 [1] are involved in human drug metabolism amongst them CYP1A2, CYP2A6, CYP2B6, CYP2C9, CYP2C19, CYP2D6, CYP2E1, and CYP3A4 appear to be the major contributors. In the present work CYP1A2, CYP2C9 and CYP2D6 are used. The CYP1A subfamily contains two members, CYP1A1 and CYP1A2 [5] which are involved in drug metabolism and have sparked considerable interest because they also seem to be associated with the metabolic activation of procarcinogens to mutagenic species, of the two members CYP1A2 is the major player. It is found in human liver and is responsible for metabolism of heterocyclic groups and aromatic rings. The enzyme CYP2C9 is another P450 monoxygenase enzyme which plays role in drug metabolism. It provides instructions for making enzymes found in liver microsomes. It is also responsible for the synthesis of steroids, cholesterol and other lipids. Among CYP enzymes CYP2D6 is known for its inability to be induced by xenobiotics [3, 4]. It can metabolize nearly 20% of drugs such as antidepressant, antiarrhythmics, beta blockers and opioid analgesics.

In the present study docking of drugs with enzyme is been analyzed the parameters that are put under consideration are binding free energies, the distance between the heme iron [6–8] and substrate reacting groups, interaction between the substrate and residue lining the active site [9]. The different values of binding free energies are a direct result of various interactions that takes place at microscopic level such as

*Author to whom correspondence should be addressed.

Table I. Binding energies of enzymes docked with drugs.

CYP450 family	PDB ID	Drug	Binding energy (Kcal/mol)
1A2	2HI4	Amitriptyline	−7.36
		Clozapine	−8.93
2C9	1OG2	Diclophenac	−7.09
		Ibuprofen	−6.19
		Phenytoin	−7.32
2D6	5TFT	Amitriptyline	−8.98
		Metoprolol	−5.96
		Nortriptyline	−9.25

hydrogen bonding interactions, hydrophobic interactions, hydrophilic interactions, and electrostatic interactions [9]. These values are also consequence of drug heme distance. This study will through light upon the binding pockets (i.e., residues) of enzymes which are prime targets of drug substrates.

2. METHODOLOGY

The crystal structures of the selected cytochromes CYP1A2, CYP2C9 and CYP2D6 were downloaded from Protein Data Bank (PDB) [10] and are listed above in Table I. The generalised structure of drugs that were docked to the selected CYP gene was obtained from literature and is shown in Figure 1.

The drugs amitriptyline, clozapine, diclofinac, ibuprofen, phenytoin were modelled using Gauss View 5.0 and they were then optimized for energy minimisation using Gaussian 09 [11] software package using B3LYP

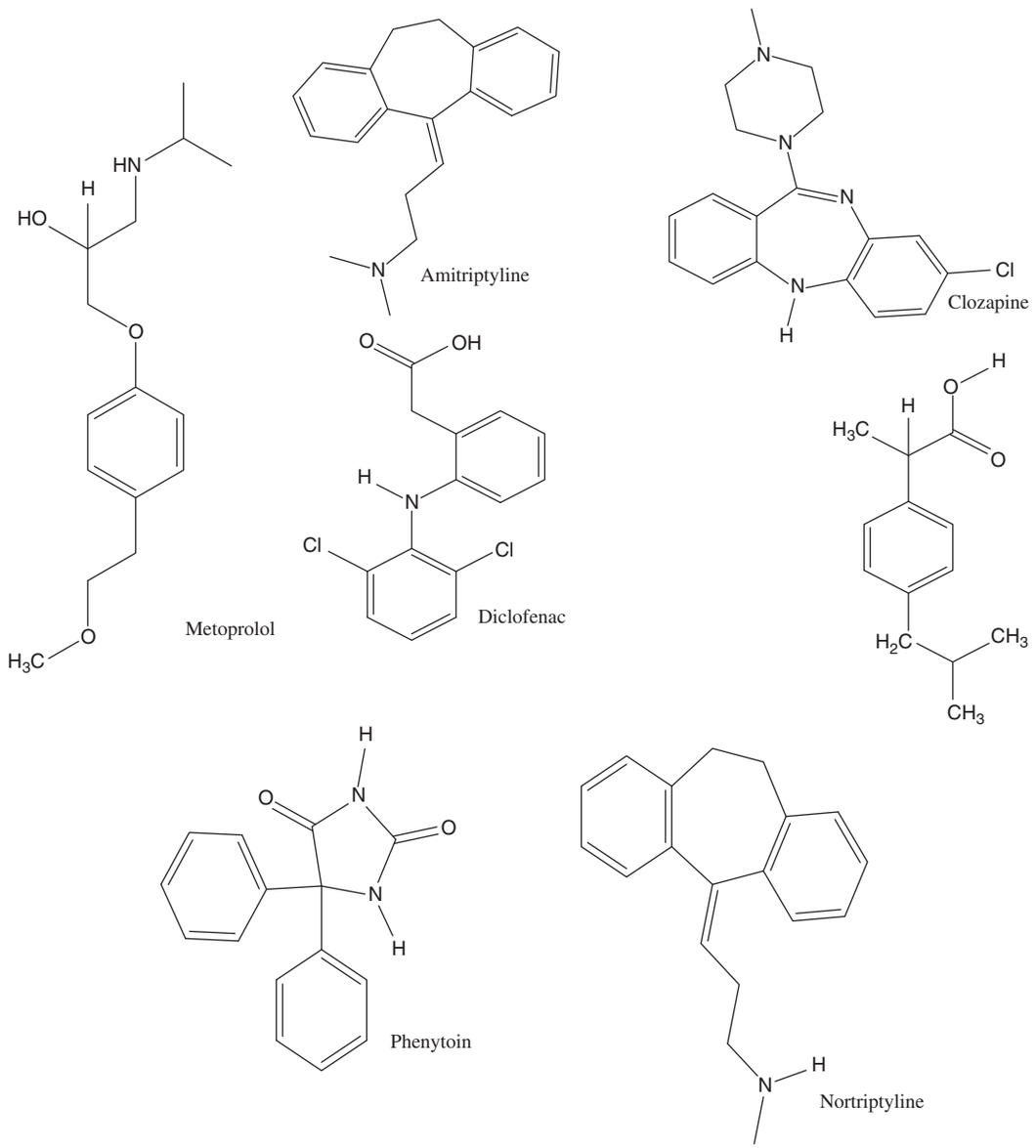

Figure 1. Structure of drugs used for docking in enzymes as substrates.

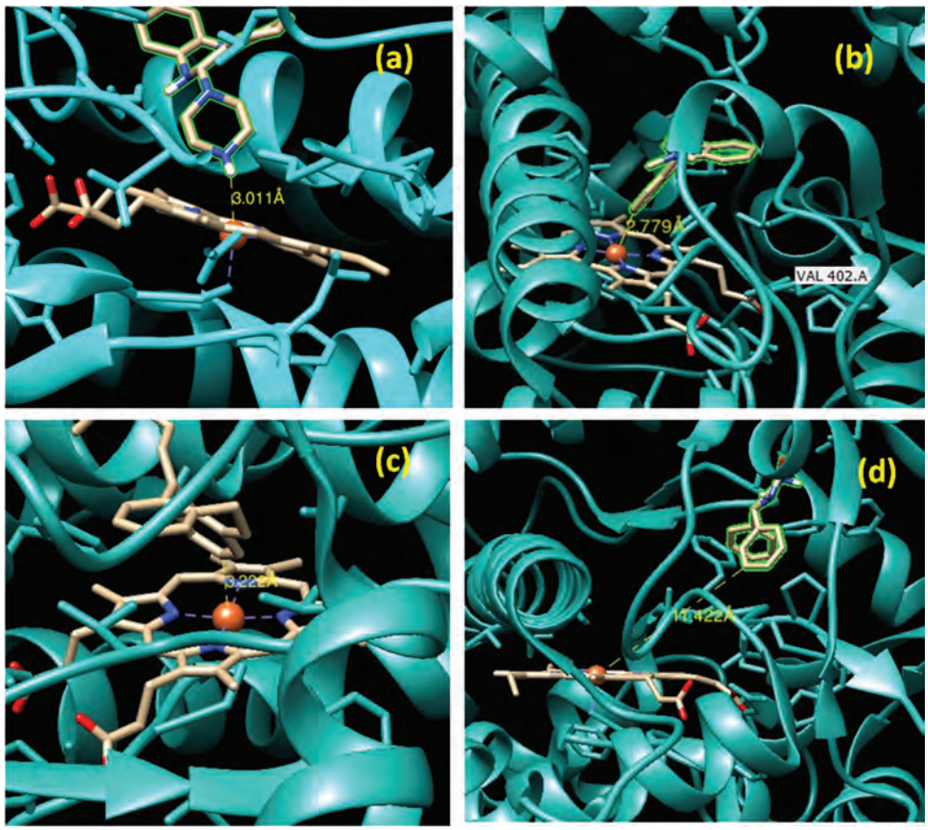

Figure 2. Distances of various drugs from heme prosthetic group (a) CYP1A2 with clozapine (b) CYP2D6 with amitriptyline (c) with nortriptyline (d) CYP2C9 with phenyltoin.

functional and 6-31G** basis set. The crystal structures of the cytochromes so obtained from protein data bank (PDB) were then visualized using Chimera [12] before docking them with substrates, enzymes were prepared. From cytochrome having PDB ID 2HI4 inhibitor alpha-napthoflavone was removed along with the water molecules. Similarly from CYP2D6 BACE 1 inhibitor complex was removed from crystal structure 5TFT along with removal of water molecules. The crystal structure 1OG2 of CYP2C9 which is a structure of human cytochrome was taken as such, only water molecules were removed before docking. Molecular Docking was performed using Autodock4 software package [13]. The Gasteiger charges were added to the drug-enzyme complex using Autodock Tools (ADT) before starting the docking calculations. A grid box, of different dimensions, was prepared for each drug-enzyme complex that enclosed the macromolecule. This helped the drug in finding the most preferential binding pocket in the vicinity of heme prosthetic group while the docking calculations were performed [14]. Docking calculations were set up using the classical Lamarckian Genetic Algorithm (LGA). A 20 LGA run with a maximum cycle of 2500000 energy evaluations was performed for each of the drug-DNA complex.

3. RESULTS AND DISCUSSION

All the binding energies obtained by computational docking method are listed below in Table I. Further interactions between drugs and cytochrome sites having the maximum binding affinity are shown in Figure 2, this reveals the active binding site of the drug to cytochrome's heme region. Out of three drugs which are docked with CYP1A2, clozapine was in closest proximity with heme iron showing distance of 3.01 Å as can be seen in Figure 2. The present study shows that for CYP1A2 the amitriptyline drug is not in close proximity of metal centre compared to CYP2D6 for which the drug to metal centre distance is approximately 2.77 Å. This is also confirmed from binding energy which is −7.36 kcal/mol for CYP1A2 and for CYP2D6 it is approximately 9 kcal/mol. The interacting distance of drugs phenytoin and ibuprofen is coming nearly 11.4 Å and 14.5 Å respectively for CYP2C9 and can be seen in Figure 2, which is not close to active site of enzyme but they do form hydrogen bonds with residues and their binding energies reflect the same, Figure 3. The main aim of this study was to validate the effective binging site/pocket where the drug metabolism chemical reactions; such as, functionalization reactions; i.e., oxidation,

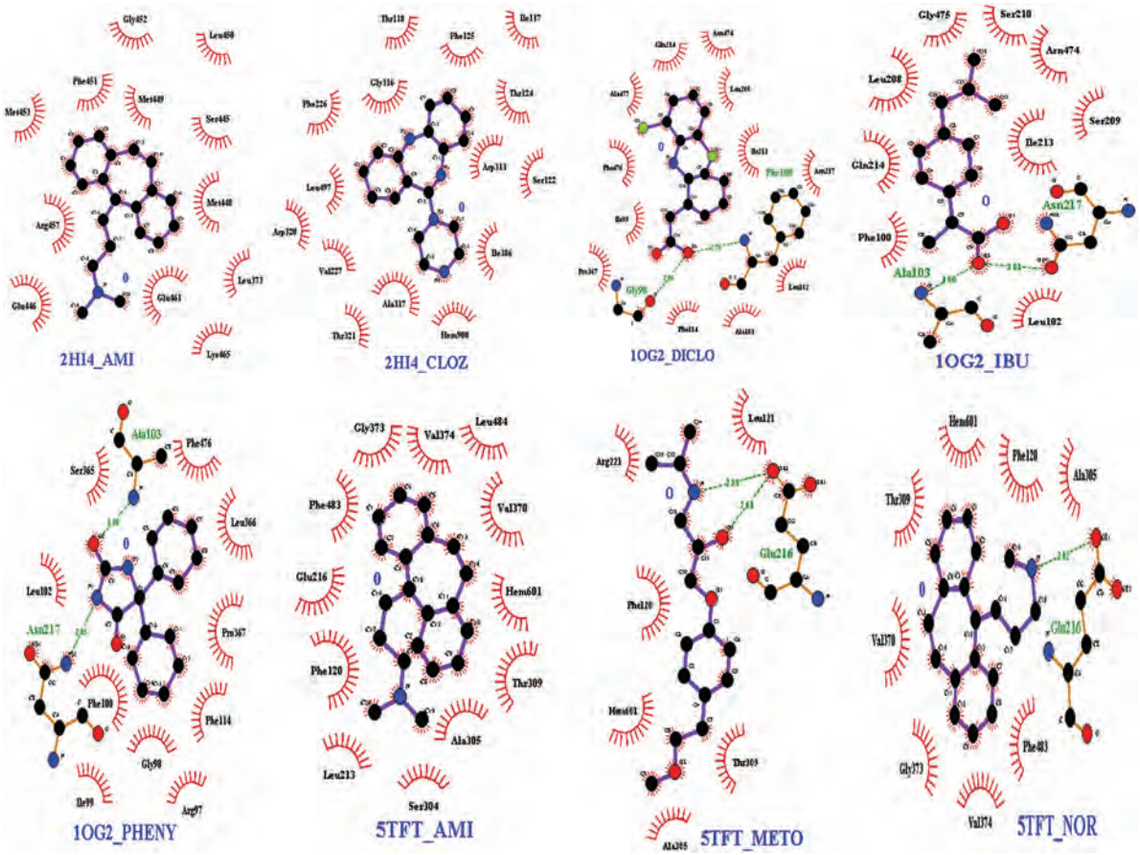

Figure 3. Hydrogen bonding interaction of all enzyme-drug complexes.

hydrolysis; and conjugation reactions i.e., glucuronidation, sulphate conjugation takes place.

4. CONCLUSIONS

Chemical reactions involved in drug metabolism are not only a fascinating field of study but also a useful link between chemistry and biology. Most of the metabolic reactions are carried out by a large family of heme-containing CYP 450 enzymes. Such computational Molecular Docking, Molecular Dynamics and QM, QM/MM studies are vastly used now days to model these drug metabolism reactions. Hence, extensive studies on drug metabolism to elucidate the scientific principles are in progress, and this docking study adds to one of them.

Acknowledgments: Rolly Yadav and Anamika Shukla would like to acknowledge DST for their financial support through INSPIRE fellowship. Anwesh Pandey and Nidhi Awasthi would like to acknowledge UGG fellowship for their financial support trough UGC Central University fellowship. Authors would also like to acknowledge Professor Devesh Kumar for providing computational facilities.

References and Notes

1. Taxak, N. and Bharatam, V., **2014**. Drug metabolism a fascinating link between chemistry and biology. *Resonance, 19*, pp.259–282.
2. (a) Ortiz de Montellano, P.R., ed., **1995**. *Cytochrome P450: Structure, Mechanism and Biochemistry*, 2nd edn., New York, Plenum Press; (b) Ortiz de Montellano, P.R., ed., **2004**. *Cytochrome P450: Structure, Mechanism and, Biochemistry*, 3rd edn., New York, Kluwer Academic/Plenum Publishers.
3. Coleman, M., **2010**. *Human Drug Metabolism: An Introduction*, 1st edn., UK, John Wiley & Sons.
4. Tirona, R.G., Richard, B. and Kim, **2017**. *Clinical and Translational Science*, 2nd edn., Amsterdam, Elsevier/Academic Press.
5. Uetrecth, J.P. and Trager, W., **2007**. *Drug Metabolism: Chemical and Enzymetic Aspects*. New York, London.
6. Liston, H., Markowitz, J. and Devane, C., **2001**. Drug glucuronidation in clinical psychopharmacology. *Journel of Clinical Sychopharmacology, 21*, pp.500–515.
7. Hrycay, E.G. and Bandiera, S.M., **2008**. *Preclinical Development Handbook*. edited by S. Cox, UK, John Wiley & Sons.
8. Taxak, N. and Bharatam, P.V., **2010**. An insight into the concept and details of mechanism-based inhibition of CYP450. *Current Research and Information in Pharmaceutical Sciences, 11*, pp.62–67.
9. Sridhar, J., Goyal, N., Liu, J. and Foroozesh, M., **2017**. Review of ligand specificity factors for CYP1A subfamily enzymes from molecular modeling studies reported to-date. *Molecules, 22*(7), p.1143.
10. Berman, H.M., Westbrook, J., Feng, Z., Gilliland, G., Bhat, T.N., Weissig, H., Shindyalov, I.N. and Bourne, P.E., **2000**. The protein data bank. *Nucleic Acids Research, 28*, pp.235–242.

11. Frisch, M.J., Trucks, G.W., Schlegel, H.B., Scuseria, G.E., Robb, M.A., Cheeseman, J.R., Scalmani, G., Barone, V., Mennucci, B., Petersson, G.A., Nakatsuji, H., Caricato, M., Li, X., Hratchian, H.P., Izmaylov, A.F., Bloino, J., Zheng, G., Sonnenberg, J.L., Hada, M., Ehara, M., Toyota, K., Fukuda, Hasegawa, J., Ishida, M., Nakajima, T., Honda, Y., Kitao, O., Nakai, H., Vreven, T., Montgomery, Jr., J.A., Peralta, J.E., Ogliaro, F., Bearpark, M., Heyd, J.J., Brothers, E., Kudin, K.N., Staroverov, K.N., Keith, T., Kobayashi, R., Normand, J., Raghavachari, K., Rendell, A., Burant, J.C., Iyengar, S.S., Tomasi, J., Cossi, M., Rega, N., Millam, J.M., Klene, M., Knox, J.E., Cross, J.B., Bakken, V., Adamo, C., Jaramillo, J., Gomperts, J., Stratmann, R.E., Yazyev, O., Austin, A.J., Cammi, R., Pomelli, C., Ochterski, J.W., Martin, R.L., Morokuma, K., Zakrzewski, V.G., Voth, G.A., Salvador, P., Dannenberg, J.J., Dapprich, S., Daniels, A.D., Farkas, O., Foresman, J.B., Ortiz, J.V., Cioslowski, J. and Fox, D.J., **2013**. Gaussian 09, Revision D.01, Gaussian, Inc., Wallingford C.T.

12. Pettersen, E.F., Goddard, T.D., Huang, C.C., Couch, G.S., Greenblatt, D.M., Meng, E.C. and Ferrin, T.E., **2004**. UCSF Chimera—A visualization system for exploratory research and analysis. *Journal of Computational Chemistry, 25*, pp.1605–1612.

13. Morris, G.M., Huey, R., Lindstrom, W., Sanner, M.F., Belew, R.K., Goodsell, D.S. and Olson, A.J., **2009**. AutoDock4 and AutoDockTools4: Automated docking with selective receptor flexibility. *Journal Computational Chemistry, 16*, pp.2785–2791.

14. Huang, S.Y. and Zou, X., **2010**. Advances and challenges in protein-ligand docking. *International Journel of Molecular Science, 11*(8), pp.3016–3034.

Received: 23 July 2019. Accepted: xx Xxxx xxxx.

Journal of Molecular Modeling (2021) 27: 199
https://doi.org/10.1007/s00894-021-04815-z

ORIGINAL PAPER

Modeling the hydroxylation of estragole via human liver cytochrome P450

Rolly Yadav[1] · Nidhi Awasthi[1] · Anamika Shukla[1] · Devesh Kumar[1]

Received: 5 April 2021 / Accepted: 2 June 2021 / Published online: 11 June 2021

Abstract

Natural compounds derived from plants are generally regarded safe and devoid of adverse effects. However, there are individual ingredients that possess toxic, genotoxic, and carcinogenic activities. These compounds when exposed at specific level become hazardous to health. Estragole (1-allyl-4-methoxybenzene) is a common component of spice plants. Its toxicity gets activated with the hydroxylation at benzylic carbon (C1') position by P450 enzymes present in the human liver. The present study grounds to explore the reaction mechanism of conversion of estragole to hydroxylated metabolite using computational methodology. Density functional theory (DFT)-based calculations were employed to explore the cytochrome P450–catalyzed mechanism at C1 position aliphatic hydroxylation of estragole. Overall reaction energy profile, electronic configuration, and 3D structure of all intermediates, transition states, and product complexes formed during the reaction along with their free energies were tried to be investigated.

Keywords Estragole · DFT · P450 · Hydroxylation · Genotoxic

Introduction

Estragole (1-allyl-4-methoxybenzene) is a common component of spice plants like star anise, fennel, and basil oil. Additionally, estragole is used in flavorings, as essential oils that are added in many food, detergents, and cosmetic products. It is regarded as a genotoxic hepatocarcinogen in rats, and its potential toxicity in humans is still under prime debate. *Foeniculum vulgare* Mill. (fennel) is a major source responsible for the human exposure to this phytochemical [1]. Its toxicity gets activated with the hydroxylation at benzylic (C1') position [2] by the following P450 enzymes present in the human liver: 1A2, 2A6, 2CI9, 2D6, and 2E1. The major P450 enzymes that are involved in the catalysis of estragole are 1A2 and 2A6. Other enzymes play their role in the catalysis of estragole at relatively higher concentration. The metabolite obtained upon hydroxylation at C1 position is not toxic within itself; however, its conjugation with sulfate by a sulfotransferase to produce 3′-sulfoxyestragole is genotoxic [2]. Figure 1 marks the general reaction scheme that was studied computationally.

Cytochrome P450 enzymes are versatile biological catalyst found in nature in all living forms such as bacteria, mammals, fungi, and plants [3, 4]. P450 enzymes are key players responsible for metabolic conversion of chemical compounds to reactive metabolites which later binds macromolecules.

They activate and oxidize a fairly large variety of substrates [5, 6]. Due to their broad chemical functions, they are well studied with potential application in the field of biotechnology and medicine. P450 enzymes are a monooxygenase class of heme enzymes. Their common reaction mechanism with substrates occurs through single-oxygen-atom transfer [7–9]. Initially, in resting state, the heme iron(III) is hexacoordinated. At the distal side, it is connected to water molecule and is axially ligated to the thiolate of cysteinate residue which eventually connects it to the rest of the protein. The catalytic cycle of P450 gets initiated with the entry of substrate inside the binding pocket. As the substrate approaches the heme, it transpires the release of water molecule ligated to iron and changes the spin state, which triggers electron transfer from the reduction partner of P450. Later, the molecular oxygen binds itself to the iron and gets reduced and protonated to form ferric hydroperoxo species also known as compound (Cpd) 0.

✉ Devesh Kumar
dkclcre@yahoo.com

[1] Molecular Modeling Lab, Department of Physics, School of Physical and Decision Sciences, Babasaheb Bhimrao Ambedkar University, Lucknow, UP 226025, India

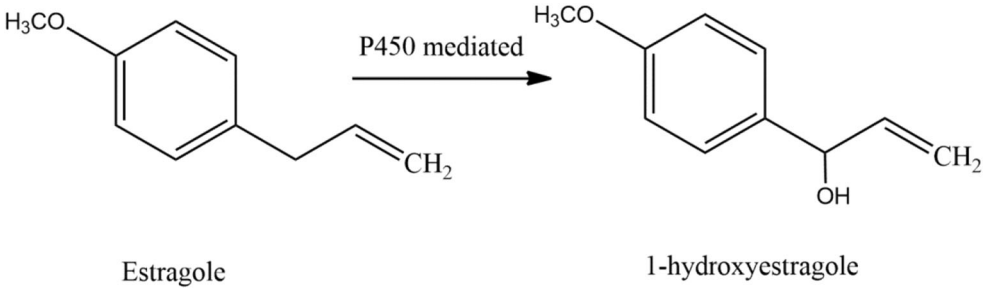

Fig. 1 Activation reaction of estragole to produce 1-hydroxyestragole by Cpd I of P450 enzymes, a precursor for the formation of genotoxic 3′-sulfoxyestragole

Subsequent protonation leads to the formation of ultimate oxidant iron(IV) oxo porphyrin cation radical species compound I (Cpd I). The structure of Cpd I is depicted in Scheme 1a, along with short representation used to show porphyrin ring. Cpd I reacts with the substrate to form oxidized product through various reactions like desaturation/ring closure and oxygen atom transfer reactions like aliphatic and aromatic hydroxylation, sulfoxidation, epoxidation etc. It is well studied through many experimental and theoretical [10–13] studies that alkane (C–H) hydroxylation is stepwise and proceeds through rebound mechanism [14], and this is shown in Scheme 1b. The first step is associated with the removal of hydrogen atom from the carbon to be hydroxylated to form ferric hydroperoxo intermediate via hydrogen abstraction transition state (TS_H), while the later step involves the rebound of radical carbon to produce hydroxylated product complex via rebound transition state (TS_{reb}).

Quantum mechanical (QM) calculations are valuable methods that provide us a tool to deeply penetrate and understand the formation of toxic metabolites from drugs and chemical compounds followed by analysis of their reaction energy profiles. In the present work, density functional theory (DFT)-based QM calculations were employed to explore the cytochrome P450–catalyzed reaction mechanism for aliphatic hydroxylation of estragole at benzylic carbon C1 position to explore the overall reaction energy profile and to understand the formation of involved intermediates and transition states. The mechanism was modeled on two spin surfaces for Cpd I-estragole complex, viz. quartet (high spin (HS)) and doublet (low spin (LS)). Furthermore, this study was helpful in gaining substantial insights into the electronic arrangement and 3D structural features of intermediates, transition states, and product complexes formed during the progress of the reaction along with their free energies.

Methodology

The calculations provided in this study were computed using Gaussian 09 [15] software and implemented DFT method. To support our results from previous studies [11, 16–18], B3LYP hybrid density functional method has been chosen, using LACVP (Los Almos)-type basis set on iron that uses double ζ-core potential along with 6–31 G basis set on the rest of the atoms (basis set (BS1) [19]. Optimization of geometry and scans were performed at the B3LYP/BS1 level of the theory. Geometry scan maxima are used for the transition state searches along with frequency calculations that confirm

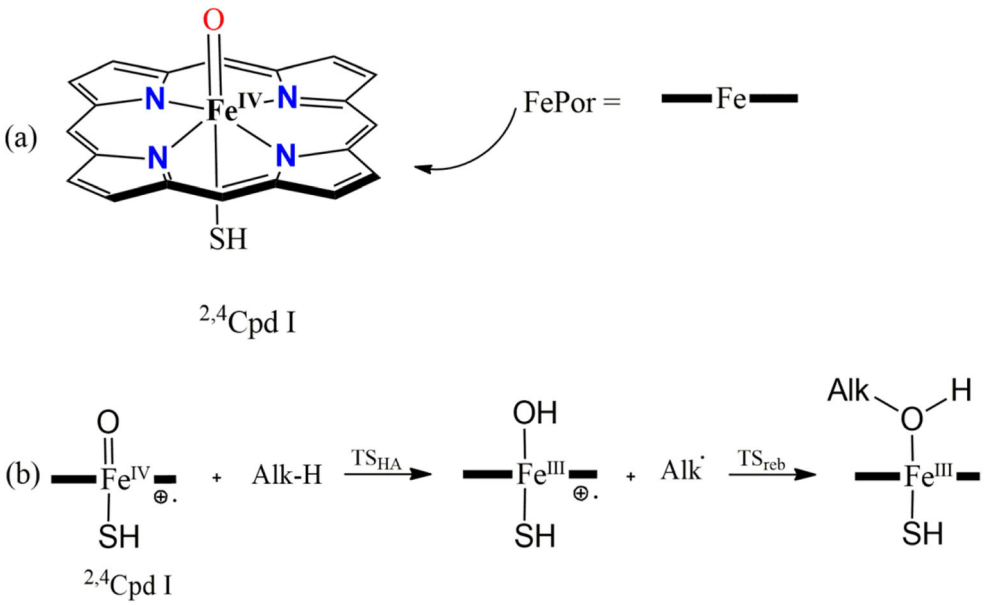

Scheme 1 **a** Structure of compound 1 (Cpd I) along with porphyrin ring representation in the right. **b** Two-state rebound mechanism used by P450 for aliphatic hydroxylation

structures to be a first-order saddle point depicting single imaginary frequency for the correct mode. Full geometry optimization at the same level of the theory has been performed, followed with frequency calculations that confirmed structures to be local minima and transition states to be the first-order saddle point. Cpd I used in present investigation was modeled as iron embedded in protoporphyrin IX, side chains were removed to make calculations less extensive, and also replacement of side chain will not greatly affect the energies of high-lying occupied and low-lying virtual orbitals of a chemical system. Similarly for simplification of the substrate, the structure 3-4-methoxyestragole is replaced by the 4-methoxy substituent to reduce computation cost.

Results and discussion

Electronic structure of Cpd I

Cpd I possess a dense manifold of orbitals [20–22], and therefore, it has multiple closely lying spin states and electromeric states. An understanding of its orbital picture is necessary to understand the trends and pattern during the course of the reaction. Figure 2 shows all the high-lying occupied and low-lying virtual orbitals of a heme system that are key orbitals involved in the catalyst mechanism. In the extreme left of the figure, we have porphyrin ring orbitals which are π-type high-lying non-bonding orbitals and, under D_{4th} symmetry, their labels are assigned as a_{1u} and a_{2u}. The a_{2u} orbital is bit higher in energy than a_{1u} due to its mixing with the axial thiolate ligand. Other than these porphyrin ring orbitals, there are five metal 3*d* orbitals that mix with axial ligand oxygen. The uppermost orbital in the figure is $\sigma^*_{z^2}$ anti-bonding orbital, and this arises due to the mixing of $3d_{z^2}$ orbital on iron and $2p_z$ orbital of oxygen along the S–Fe–O bond axis. Right below in the figure lies σ^*_{xy} which is a planar orbital formed due to the mixing of $3d_{xy}$ orbital of iron and $2p_{xy}$ orbital of porphyrin nitrogen along the Fe–N bond axis. With the combination of $3d_{xz}/3d_{yz}$ metal orbital and oxygen $2p_x/2p_y$ orbital arising the formation of low-lying π_{xz}/π_{yz} orbital, these are found to be always filled and their anti-bonding pairs of π^*_{xz}/π^*_{yz} orbital are along the Fe–O axis. The $\delta_{x^2-y^2}$ is a non-bonding doubly occupied orbital that resides into the heme plane.

Aliphatic hydroxylation

In accordance with previously calculated and benchmarked studies, we investigated our reaction mechanism with a modeled active site complex of cytochrome P450, i.e., Cpd I with substrate [16, 20, 23]. We are focused at the C1 position aliphatic hydroxylation of estragole, and it starts with hydrogen abstraction step via the transition state TS_H to generate a radical intermediate INT. This radical intermediate rebounds

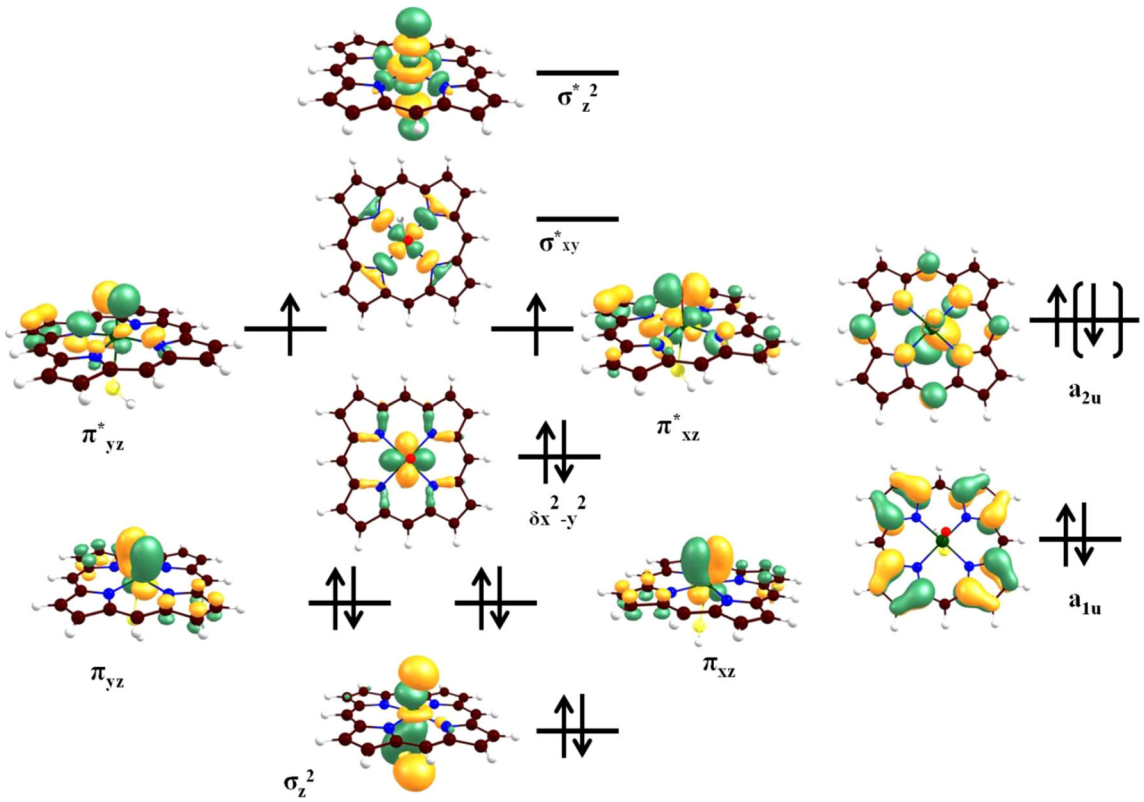

Fig. 2 Molecular orbitals of Cpd I involved in the reaction [5]

to generate product complex (PC) crossing a rebound transition state (TS_{reb}). The potential energy surface of the reaction mechanism is shown in Fig. 3. The reaction analogous to previously reported studies is stepwise and is highly exothermic after radical intermediate to product formation. The reaction follows a two-state reaction (TSR) mechanism, and results are in good agreement with previous studied reactions following TSR mechanism. Hydrogen atom abstraction is the rate-determining step of the reaction, and barrier heights for doublet and quartet are observed to be 10.43 kcal/mol and 9.85 kcal/mol, respectively. Frequency calculations showed single-large imaginary frequencies for both spin states: i1508.20 cm^{-1} (doublet) and i1455.38 cm^{-1} (quartet) [24–26], and these results are reminiscent of typical H-abstraction barrier which simply means that large kinetic isotope effect (KIE) will be observed after replacement of deuterium with hydrogen [27].

Optimized three-dimensional structures of the transition state $^{2,4}TS_H$ showed the transferring hydrogen atom is close to the carbon atom, and this kind of transition state shows less barrier height in comparison to the late transition state. Subsequent formation of radical intermediate occurs, and their formation is exothermic with energy values − 12.85 kcal/mol and − 12.57 kcal/mol for doublet and quartet, respectively. Typical TSR mechanism reactant complex for both spin surfaces is close in energy and virtually degenerates till the H-abstraction barrier [5, 10–13, 28]. With the formation of the radical intermediate ^{2,4}INT, both spin surfaces bifurcate, and rebound transition state is observed for HS state with the barrier height of − 8.56 kcal/mol to form product complex whereas the reaction was barrier-less on LS surface and concerted product formation is observed. The last reaction step for product formation was highly exothermic for both spin surfaces showing an energy value below − 40.00 kcal/mol.

The reaction between Cpd I and substrate is modeled. The reactant complex electronic configuration was investigated and found to be $\delta^{*2}_{x2-y2}\ \pi^{*1}_{xz}\ \pi^{*1}_{yz}\ a^{1}_{2u}$. The reactant complex (RC) was followed with the formation of the transition state $^{2,4}TS_H$ having the electronic configuration $\delta^{*2}_{x2-y2}\ \pi^{*1}_{xz}\ \pi^{*1}_{yz}\ a^{2}_{2u}\ \varphi^{1}_{c}$ to form the intermediate complex ^{2,4}INT. Validity of spin and electron densities was further confirmed by Mulliken analysis and charge analysis Table 1. The spin density showed transition states to be radical in nature. The intermediate spin densities along with electronic configuration depicted one electron transfer from the substrate to the porphyrin a_{2u} orbital. The nature of both the intermediates was found to be radical, and electron density accumulates at the C1 position of the substrate with spin density (ρ_{sub} − 0.98 and 0.99) doublet and quartet, respectively. Intercrossing of spin is also observed in energy profile Fig. 2, and this is indicative of spin crossover in the catalytic cycle. Throughout the reaction process, the orbital occupancy changes for a_{2u}, $\pi^{*}_{xz}/\pi^{*}_{yz}$, $\sigma^{*}_{z}{}^{2}$, and substrate orbital φ_c to conserve the overall spin during the entire reaction and also for electron sharing in the making and breaking of bonds. First electron transfer for the formation of the bond between oxo group and H atom is achieved by electron transfer from the substrate to the Cpd I, and one of the electrons is transferred to the heme a_{2u} orbital, making it fully occupied leaving substrate to be singly occupied φ^1. Last step of the reaction is radical rebound which occurs to generate a PC with the electronic configuration $\delta^{*2}_{x2-y2}\ \pi^{*1}_{xz}\ \pi^{*1}_{yz}\ \sigma^{*1}_{z^2}\ \sigma^{*0}_{xy}\ a^{2}_{2u}\ \varphi^{0}_{c}$ for quartet spin state and $\delta^{*2}_{x2-y2}\ \pi^{*2}_{xz}\ \pi^{*1}_{yz}\ \sigma^{*0}_{z^2}\ \sigma^{*0}_{xy}$

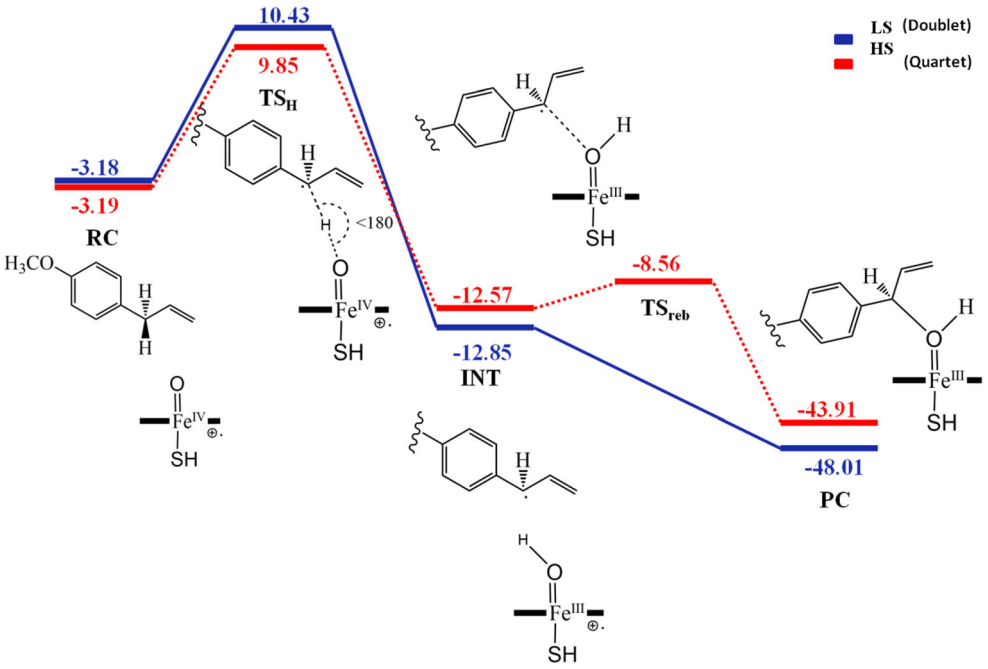

Fig. 3 Potential energy profile for aliphatic hydroxylation at the benzylic position of estragole calculated using DFT methodology at the B3LYP/BS1 level of the theory. All energies here are reported in kcal/mol, the bond lengths in angstrom (Å), the bond angles in degree (°), and the frequencies in wavenumber (cm^{-1})

Table 1 Spin densities and Mulliken atomic charges

	Spin densities					Charges				
	ρ_{Fe}	ρ_{O}	ρ_{Por}	ρ_{SH}	ρ_{Sub}	Q_{Fe}	Q_{O}	Q_{Por}	Q_{SH}	Q_{Sub}
Reactant complex (RC)										
LS	1.20	0.89	−0.51	−0.58	0.00	0.51	−0.35	−0.10	−0.04	−0.01
HS	1.07	0.94	0.44	0.53	0.00	0.50	−0.34	−0.09	−0.04	−0.01
Transition state (TS_H)										
LS	1.62	0.39	−0.32	−0.32	−0.37	0.49	−0.49	−0.21	−0.06	0.28
HS	1.20	0.77	0.19	0.40	0.43	0.46	−0.47	−0.26	0.00	0.27
Intermediate complex (INT)										
LS	1.81	0.25	−0.12	0.28	−0.98	0.44	−0.59	−0.28	0.03	0.38
HS	1.81	0.28	−0.12	0.03	0.99	0.44	−0.59	−0.30	0.03	0.42
Rebound transition state (TS_{reb})										
HS	2.27	0.04	−0.12	0.10	0.70	0.52	−0.61	−0.40	−0.09	0.58
Product complex (PC)										
LS	1.09	−0.00	−0.08	−0.00	0.00	0.33	−0.59	−0.54	0.02	0.76
HS	2.53	0.01	−0.00	0.46	−0.00	0.52	−0.58	−0.45	−0.16	0.68

SH thiolate group, *Sub* substrate (estragole), *Por* porphyrin

$a_{2u}^2\ \varphi_c^0$ for doublet spin state. The rebound transition state $^4TS_{reb}$ is observed only on HS with the electronic configuration $\delta_{x2-y2}^{*2}\ \pi_{xz}^{*1}\ \pi_{yz}^{*1}\ \sigma_{z^2}^{*1}\ \sigma_{xy}^{*0}\ a_{2u}^2\ \varphi_c^0$. In case of LS, the rebound barrier required is usually ~ 1 kcal/mol and hence the potential energy surface is flat. The value for rebound transition state (TS_{reb}) was observed to be − 8.56 kcal/mol, and its adequacy is confirmed by a single imaginary frequency of i231.43 cm^{-1} for the correct mode of vibrations. The discrepancies in the potential surface in rebound step for both spins can be understood from the transfer of electron to the respective orbitals. In LS, the second electron from φ_c gets transferred to the low-lying π_{xz}^* orbital to generate ^{2}P(III) whereas more energy is required to transfer an electron to the high-lying virtual orbital $\sigma_{z^2}^*$ to form ^{4}P(III).

There must be some changes in three-dimensional geometries in structure from RC to PC (Fig. 4) which helped in the easy transfer of electron in the making and breaking of bonds.

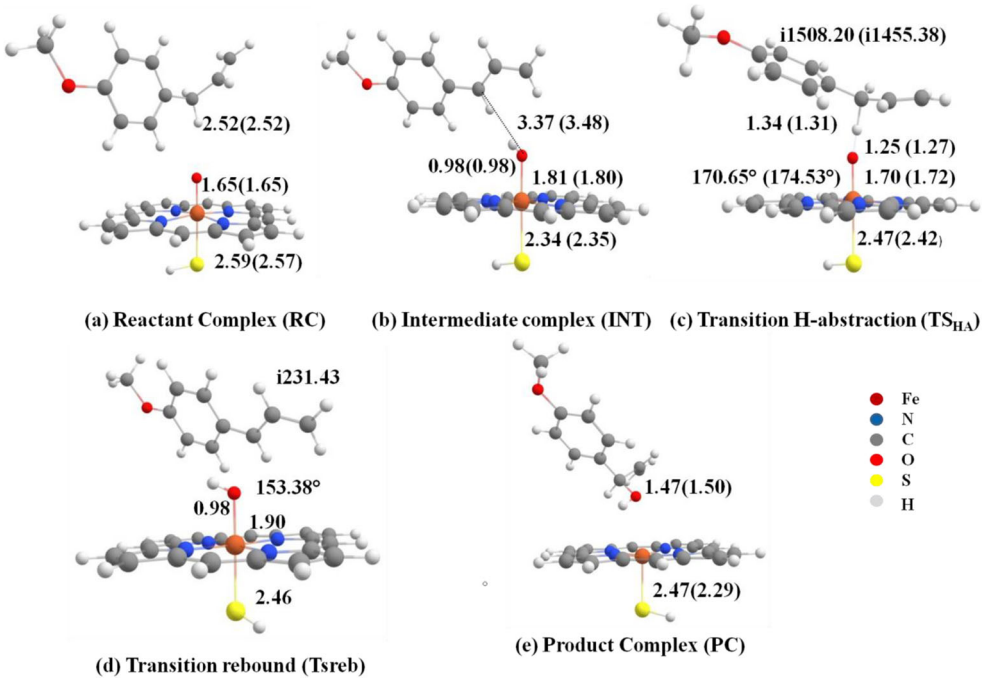

Fig. 4 Optimized 3-D geometries of **a** reactant complex (RC), **b** intermediate complex (INT), **c** H-abstraction transition state (TS_H), **d** rebound transition state (TS_{reb}), and **e** product complex (PC) for doublet (quartet) spin states, along with the necessary bond lengths in Å and the imaginary frequency of TS in cm^{-1}. In the figure, without and within parentheses are indicative of LS (HS) doublet and quartet. All geometries were optimized at the B3LYP/BS1 level of theory

The geometric features of the H-atom abstraction are similar to those of direct H-atom abstraction from methane via bare FeO^+ [29] and diiron model complexes [30]. The transition state TS_H for H abstraction at C1 position is shown in Fig. 4, with the O–H bond and C–H bond of 1.25 Å (1.27 Å) and 1.34 Å (1.31 Å), respectively, for doublet (quartet). The bond angle for C–H–O is linear with the value 170.65° (174.53°) which is a genuine pattern for the H-abstraction process by various FeO species. As previously discussed, smaller distances of the C–H bond compared with those of the O–H bond are regarded as earlier transition state and barrier heights associated with such geometrical features are lower than those of late TS. Intermediate cluster formation occurs after crossing the transition state (TS_H), and the C1 radical center is oriented towards the hydroxyl group, which can be seen from Fig. 4. The second half of the reaction is the oxygen rebound mechanism where carbon radical and iron-hydroxo species combine to form product complex, and the essential part of this process is the formation of the C–O bond. For the formation of the C–O bond, carbon radical needs to rotate to attack on iron-hydroxo species, and this step requires an energy barrier to cross. On the quartet spin surface where the rebound transition state TS_{reb} is observed during geometric scan, we see sharp changes in bond lengths, the C–O bond decreases, and the Fe–O bond increases, coupled with a decrease in the Fe–S bond length at the same time. This effect is known as "push-effect" [5], which is shown in Fig. 4, and is observed in the hydroxylation reaction catalyzed by P450 enzymes, whereas on the doublet spin surface, our calculations predicted no direct transition state and it could be regarded as virtually barrier-less to produce product. This step is highly exothermic in nature and proceeds at a very low cost of energy. The driving force is a direct consequence of large product stability.

Conclusions

Present studies on cytochrome P450 monooxygenases found in the human liver by utilizing DFT-based QM calculations completely elucidate the reaction energy profile of C–H hydroxylation of estragole. The hydroxylated product is a precursor in the activation of toxic metabolite by sulfotransferase to produce 3′-sulfoxyestragole. The theoretical investigation revealed that a two-state reactivity (TSR) mechanism is followed for both HS and LS. The reaction is exothermic throughout, and the LS surface offers an easier pathway for the product formation once the hydrogen abstraction barrier is overcomed. The rate-limiting step was found to be H-abstraction step with 9.85 kcal/mol and 10.43 kcal/mol for quartet and doublet spin states, respectively. It can be asserted from above-discussed results that the C1 position hydroxylation of estragole with Cpd I of P450 is a rebound mechanism for the HS surface and concerted for the LS surface. The intermediates are highly short-lived, and the product formation directly occurs from an intermediate on the LS surface, although the possibility of stereochemical scrambling is present on HS.

Acknowledgements RY is thankful to the Department of Science and Technology (DST), Government of India, for the INSPIRE fellowship (DST/INSPIRE FELLOWSHIP IF-170546). AS is also thankful for DST-INSPIRE fellowship. NA would like to acknowledge the UGC Non-NET fellowship.

Code availability Software programs used are already cited at appropriate places. No codes are used to perform the study.

Author contribution Rolly Yadav and Prof. (Dr.) Devesh Kumar conceived the presented idea. Rolly Yadav performed the computation and prepared the manuscript. Nidhi Awasthi and Anamika Shukla contributed in the analysis of the results. Dr. Devesh Kumar supervised the findings of the work. All authors approved the final draft of the manuscript.

Data availability Data can be made available upon request to corresponding author.

Declarations

Conflict of interest The authors declare no competing interests.

References

1. Levorato S et al (2018) In vitro toxicity evaluation of estragole-containing preparations derived from Foeniculum vulgare Mill. (fennel) on HepG2 cells. Food Chem Toxicol 111:616–622
2. Monien BH, Sachse B, Niederwieser B, Abraham K (2019) Detection of N-acetyl-S-[3′-(4-methoxyphenyl)allyl]-l-Cys (AMPAC) in human urine samples after controlled exposure to fennel tea: a new metabolite of estragole and *trans*-anethole. Chem Res Toxicol 32(11):2260–2267
3. Shaik S, Cohen S, Wang Y, Chen H, Kumar D, Thiel W (2010) P450 enzymes: their structure, reactivity, and selectivity—modeled by QM/MM calculations. Chem Rev 110(2):949–1017
4. Shaik S, De Visser SP (2005) Computational approaches to cytochrome P450 function3rd edn, edited by P. R. O. de Montellano. Kluwer Academic/Plenum, New York
5. De Visser P, Altun A, Thiel W (2005) Theoretical perspective on the structure and mechanism of cytochrome P450. Chem Rev 105: 2279–2328
6. Blomberg MRA, Borowski T, Himo F, Liao R, Siegbahn PEM (2014) Quantum chemical studies of mechanisms for metalloenzymes. Chem Rev 114:3601–3658
7. Meunier B, de Visser SP, Shaik S (2004) Mechanism of oxidation reactions catalyzed by cytochrome P450 enzymes. Chem Rev 104(9):3947–3980
8. Groves JT (2003) The bioinorganic chemistry of iron in oxygenases and supramolecular assemblies. Proc Natl Acad Sci 100(7):3569 LP–3563574
9. Watanabe Y, Nakajima H, Ueno T (2007) Reactivities of oxo and peroxo intermediates studied by hemoprotein mutants. Acc Chem Res 40(7):554–562
10. Ogliaro F, Harris N, Cohen S et al (2000) A model "rebound" mechanism of hydroxylation by cytochrome P450: stepwise and

effectively concerted pathways, and their reactivity patterns. J Am Chem Soc 122:8977–8989
11. Kamachi T, Yoshizawa K (2003) A theoretical study on the mechanism of camphor hydroxylation by compound I of cytochrome P450. J Am Chem Soc 125:4652–4661
12. De Visser SP, Kumar D, Cohen S, Shacham R, Shaik S (2004) A predictive pattern of computed barriers for C-H hydroxylation by compound I of cytochrome P450. J Am Chem Soc 126:8362–8363
13. De Visser AS et al (2017) Reactivity patterns of protonated compound II and compound I of cytochrome P450: what is the better oxidant? Chem Eur J 13:6406–6418
14. Shaik S, Cohen S, Danovich D (2004) The "rebound controversy": an overview and theoretical modeling of the rebound step in C–H hydroxylation by cytochrome P450. Eur J Inorg Chem:207–226
15. D. J. Frisch, M. J. Trucks, G. W. Schlegel, H. B. Scuseria, G. E. Robb, M. A. Cheeseman, J. R. Scalmani, G Barone, V. Mennucci, B. Petersson, G. A. Nakatsuji, H. Caricato, M. Li, X. Hratchian, H. P. Izmaylov, A. F. Bloino, J. Zheng, G. Sonnenb, Official Gaussian 09 Literature Citation. 2009
16. Reinhard FGC, De Visser SP (2017) Oxygen atom transfer using an iron(IV)-oxo embedded in a tetracyclic N-heterocyclic carbene system: how does the reactivity compare to cytochrome P450 compound I? Chem Eur J 23:2935–2944
17. Kumar D, De Visser P, Shaik S (2003) How does product isotope effect prove the operation of a two-state "rebound" mechanism in C–H hydroxylation by cytochrome P450? J Am Chem Soc 125: 13024–13025
18. Hussain YAR, Yadav R, Ahmed M, Khan TA, Kumar D (2020) Interplay between two spin states determines the hydroxylation catalyzed by P_{450} monooxygenase from *Trichoderma brevicompactum*. J Comput Chem:1–7
19. Hay PJ, Wadt WR, Hay PJ, Wadt WR (1985) Ab initio effective core potentials for molecular calculations. Potentials for K to Au including the outermost core orbitals. J Chem Phys 82:299
20. Perman B et al (2001) The experimentally elusive oxidant of cytochrome P450: a theoretical "trapping" defining more closely the "real" species. ChemBioChem 11:848–851
21. M. E. C. and S. P. de V. Mala A. Sainna, Suresh Kumar, Devesh Kumar, Simonetta Fornarini, A comprehensive test set of epoxidation rate constants for iron(IV) – oxo porphyrin cation radical. Chem Sci, vol. 6, pp. 1516–1529, 2015
22. de Visser SP, Ogliaro F, Sharma PK, Shaik S (2002) What factors affect the regioselectivity of oxidation by cytochrome P450? A DFT study of allylic hydroxylation and double bond epoxidation in a model reaction. J Am Chem Soc 124(39):11809–11826
23. De Visser SP, Shaik S, Sharma PK, Kumar D (2003) Active species of horseradish peroxidase (HRP) and cytochrome P450: two electronic chameleons. J Am Chem Soc 4:15779–15788
24. Barman P et al (2016) Communication: Deformylation reaction by a nonheme manganese(III)–peroxo complex via initial hydrogen-atom abstraction. Angew Chem Int Ed 55:11091–11095
25. Timmins A, Saint-André M, de Visser SP (2017) Understanding how prolyl-4-hydroxylase structure steers a ferryl oxidant toward scission of a strong C–H bond. J Am Chem Soc 139(29):9855–9866
26. de Visser SP (2006) What external perturbations influence the electronic properties of catalase compound I? Inorg Chem 45(23): 9551–9557
27. De Visser SP (2006) Substitution of hydrogen by deuterium changes the regioselectivity of ethylbenzene hydroxylation by an oxo–iron–porphyrin catalyst. Chem Eur J 12:8168–8177
28. Sharma PK, de Visser SP, Ogliaro F, Shaik S (2003) Is the ruthenium analogue of compound I of cytochrome P450 an efficient oxidant? A theoretical investigation of the methane hydroxylation reaction. J Am Chem Soc 125(8):2291–2300
29. Yoshizawa K, Shiota Y, Yamabe T (1998) Abstraction of the hydrogen atom of methane by iron-oxo species: the concerted reaction path is energetically more favorable. Organometallics 17:2825–2831
30. Basch H, Mogi K, Musaev DG, Morokuma K (1999) Mechanism of the methane → methanol conversion reaction catalyzed by methane monooxygenase: a density functional study. J Am Chem Soc 121(31):7249–7256

"A Theoretical Perspective of controversy in rebound mechanism of hydroxylatiom by Cytochrome P450: A Microreview"

Arvind Kumar[1], Rajesh Kumar Singh[2] , Janardan Prasad Pandey[1] , Alok Shukla*[1] , Nidhi Awasthi [3], Rolly Yadav [*3]

[1]Department of Physics, M L K P G College, Balrampur, U.P., 271201

[2]Department of Chemistry, M L K P G College, Balrampur, U.P., 271201

[3]Department of Physics, Babasaheb Bhimrao Ambedkar University,Vidya Vihar, Raebareile Road, Lucknow, U.P., 226025

Corresponding Author

Email Id: dr.alokmlk@gmail.com, rydapbbau@gmail.com

Abstract

Hydroxylation process occurs in many bio-reactions which are often ubiquitous. Hydroxylation by Cytochrome P450 enzyme is very important and useful natural process. It is a multistep process that was believed to occur by initial hydrogen atom abstraction from the alkane, by the iron(iv)-oxo species followed by the rebound of the alkyl radical to form the iron(III) alcohol complexes. Later, radical-clock experiments deduced that the lifetime of radical is ultrashort, then how can the radicals be established to exist? This question arose a controversy. This microreview throws some light on the tale of controversy. Its resolution proposed by various theories over the years. Theoretical studies of reactivity pattern of cytochrome P450 enzyme gives two-state reactivity (TSR), in which radicals are formed in two different spin state, so they react differently. On the low-spin surface, there is no rebound barrier and radical's lifetime is ultrashort, while on the high-spin surface the rebound barrier is high and radical's lifetime is sufficiently high. Radicals intermediates of low spin state either undergo rebound to form unrearranged (U) alcohol complex, keeping the original stereochemical information, or it can

Study of Physical Properties of Several Cyp450 Inhibiting Drugs, Using DFT Methodology

Janardan Prasad Pandey[1], Arvind Kumar Dwivedi[1*], Rajesh Kumar Singh[2], Alok Shukla[1], Anamika Shukla[3], Nidhi Awasthi[3*]

1. *Department of Physics, M L K P G College, Balrampur, 271201, U.P.*
2. *Department of Chemistry, M L K P G College, Balrampr, 271201, U.P.*
3. *Department of Physics, B.B.A.U., Lucknow, 226020, U.P.*

Corresponding Author: dr.arvindmlk@gmail.com, nidhimsc51@gmail.com

Abstract

There many drugs that are interacting and inhibiting the processes of Cytochrome P450 enzyme present in human. The drugs studied in present work in morphine whch is know to be the most powerful pankiller.So, the study the properties of these molecules are essential for understanding their mechanism. Here, some physical properties of these drugs like- HOMO-LUMO bandgap as well as optimization energy are studies using quantum mechanical (QM) tools, generally known as Density Functional Theory (DFT).

Keywords: CYP450, HOMO-LUMO bandgap, DFT etc.

Introduction:

Diacetylmorphine is also known as heroin or diamorphine, used as drug due to its euphoric effect [1]. In several countries it is used as pain relief like- during childbirth, heart attack or in opioid replacement therapy [2,3,4]. Basically, it is taken in form of injection and can also smoked or inhaled. It also found in tablet form [5,6,7,8].

Losartan is a drug that is used in treatment of high blood pressure, infected kidney of diabetic patient, heart failure [9]. It may takes six months for complete treatment of decease [9]. There are also some side effects of losartan medication like-cramps, cough, anemia, stuffy nose, low blood pressure and angiotensin [9]. It is not recommended during breasfeeding and pregnancy, because blocks the angiotensin II [10]. It is essential drug listed in World Health Organization

Intl. J. Engg. Sci. Adv. Research 2020 June; 6(2): 53-55 ISSN NO: 2395-0730

Optimization of Azole- Antifungal Drugs: An Attempt for Search of Better Drug for Treatment of TB with CYP450 from Mycobacterium Tuberculosis.

Nidhi Awasthi[1*], Rolly Yadav, Anamika Shukla, Devesh Kumar
Department of Physics, Babasaheb Bheemrao Ambedkar Central University, Vidya Vihar, Raebareli Road, Lucknow, U.P., Pin Code 226025.
*Registered email id: nidhimsc51@gmail.com

Abstract- **CYP450 from Mycobacterium tuberculosis is an important enzyme responsible for many biochemical reactions like metabolism, detoxification etc. These enzymes react with Azole - antifungal drug and give fruitful results helpful in treatment of tuberculosis. But the search of better drugs is still a tough task which can be achieved by study of catalytic reactions and associated reaction barriers in reaction mechanism. The drug molecules attach to enzymes in various configurations. In this study, by the optimization of "Azole- antifungal drugs", an attempt for search of better drug is carried out so as to get a potential candidate amongst all these antifungal drugs.**

Keywords: CYP450, Optimization, Mycobacterium Tuberculosis

1. INTRODUCTION

Tuberculosis is rapidly spreading all over the world. World Health Organization (WHO) data indicate that every year, approximately 2 million people are dead due to tuberculosis [1]. There are many reasons for resurgence of the Mycobacterium tuberculosis (Mtb) infection rate around the whole world. But the major factors are synergy with the Human Immunodeficiency Virus (HIV), and development of drug-resistant (DR) and multi drug resistant (MDR) strains of the pathogen [2,3]. In all HIV infected people, 15% people ultimately die due to tuberculosis. So, treatment of tuberculosis has become so important for whole world. The complete treatment duration of Tuberculosis (TB), is 6-12 month, which is a long time period. So, the search of new drugs for treatment of TB as well as decreasing the time duration, is imperative work of research. Therefore, it is urgent to identify biochemical pathway in M. tuberculosis treatment that for new anti-mycobacterial drugs [4]. There are many compounds which are treated as anti-TB drug also used in metabolism.

Azole is antifungal drug, which is treated as a substrate and reacts with MT CYP450 [5,6], gives a biochemical pathway for understanding the metabolism process and also shows good results against the anti- mycobacterium tuberculosis [7]. There are many azole compounds, but which proves to be the best for both, anti TB as well as metabolism is still a tough task. The stability of their configuration is not same with respect to CYP450. So, it is imperative to find out the most stable configuration against the Mtb. In this study, by the optimization of "Azole- antifungal drugs", an attempt for search of better drug is carried out so, as to get a potential candidate amongst all these antifungal drugs.

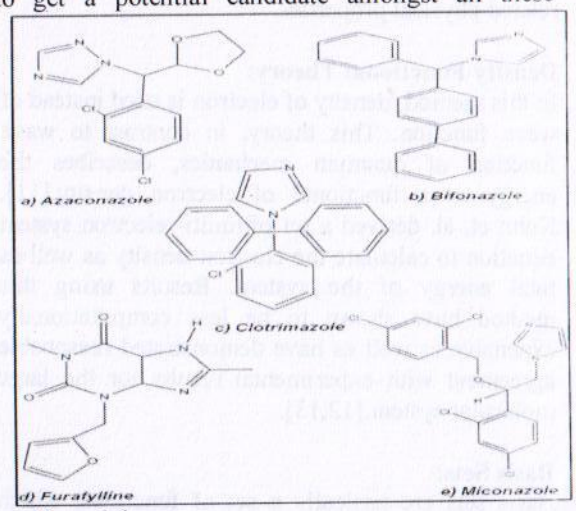

Figure 1: Structures of Azoles.

1.2. AZOLE-ANTIFUNGAL DRUGS

Azole-antifungals, containing an Azole ring, are

Computational study of electrical properties of various anti fungal drugs that metabolised via Cytochrome P450

Abhishek Tiwari[1], Nidhi [*2]

[1]*Department of Applied Science Physics*

SR Institute of Management and Technology/ Dr A P J Abdul Kalam Technical University, Lucknow (UP)-226201, India

[2]*Department of Physics, Babasaheb Bheemrao Ambedkar Central University, Vidya Vihar, Raebareli Road, Lucknow, U.P., Pin Code 226025.*

**Registered email id: nidhimsc51@gmail.com*

Abstract

Cytochrome P450 is an important enzyme of nature. In humans, it is found in the liver [4]. It is responsible for various metabolism, detoxification reactions etc. P450 is also metabolize the antifungal drugs and their metabolites are further responsible for treatment of fungal infection. But finding the most stable form of anti-fungal drugs that tightly bind with P450 is essential for study of further treatment. Present work is investigated the finding of better anti-fungal drug amongst the econazole, ketoconazole, terconazole which may tightly bind with P450 enzyme. These all calculations are computationally done using DFT method using Gaussian software.

Keyword: CYP450, Optimization, Metabolism, HOMO-LUMO bandgap.

Introduction

Azole is antifungal drug, which is treated as a substrate and reacts with CYP450 [1,2], gives a reaction pathway for understanding the metabolism process , and these results are also useful in treatment of Tuberculosis [3]. There are many anti-fungal drugs but the stability of their configuration is not same with respect to CYP450. So, it is very important to find out the most stable configuration against P450. In this study, by the optimization and HOMO-LUMO bandgap of antifungal drugs, an attempt for search of better drug is carried out so, as to get a potential candidate amongst all these antifungal drugs.

Azole-antifungals, containing an Azole ring, are the group of medicine used for the inhabitation of wide range of fungal infection. They are classified into two groups: (a) Azole ring with two nitrogen called imidazole, [i.e. miconazole, clotrimazole, econazole, etc], (b) Azole ring with

Spectroscopic Analysis of Porphyrin ($C_{20}H_{12}N_4$) ring studied by DFT Methodology

A. K. Dwivedi[1], Nidhi Awasthi[2], Rolly Yadav[2], Shivani Chaudhary, Anamika Shukla, Narinder Kumar*[2]

[1]Department of Physics,
M. L. K. P. G College, Balrampur (U.P) 271201 INDIA
[2]Department of Physics, School of Physical & Decision Sciences,
Babasaheb Bhimrao Ambedkar University,
VidyaVihar, Raebareli Road, Lucknow (U.P.) 226025 INDIA
*Email: knarinder7@gmail.com

Abstract

In this work, we have performed specrtroscopic analysis of the porphyrin. It has been observed that Hydrogen (H) atom wagging is responsible for the strong IR absorbance, Raman spectrum, Dipole strength and Rotational strength of porphyrin ring. The C-C and C-H stretching of nearly same frequencies were observed in both IR and raman spectrum. In Porphyrin ring every four atom (Nitrogen, Hydrogen and Carbon) have same charges.

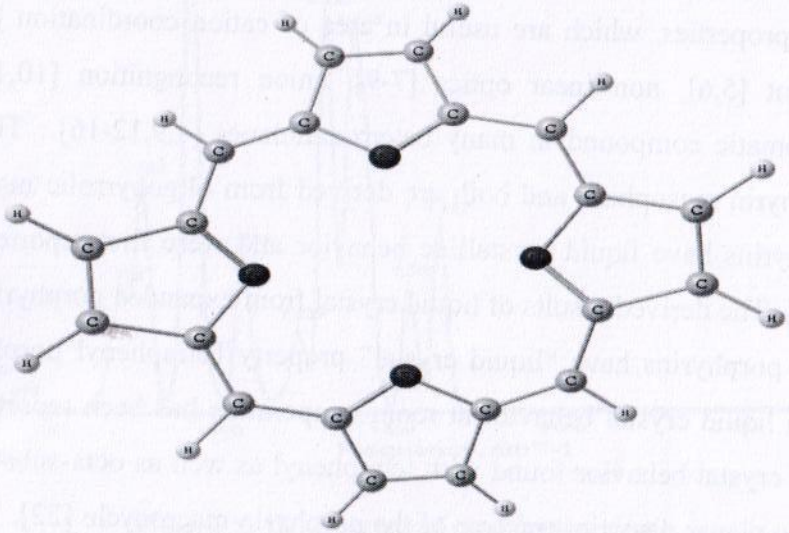

Figure 1. Molecular Structure of Porphyrin ring

Keywords

Porphyrin ring, Molecular Spectroscopy, Molecular Stretching, DFT(B3LYP)

INVERTIS UNIVERSITY BAREILLY
Established by Govt. of U.P. u/s 2(f) of UGC Act, 1956 vide U.P. Act 22 of 2010.

5th International Conference

On

RECENT ADVANCES IN SCIENCE

(ICRAS-2021)

Organised by

FACULTY OF SCIENCE, INVERTIS UNIVERSITY, BAREILLY

on

30-April and 01-May – 2021

Certificate of Merit

This is to certify that Prof./Dr./Mr./Ms./... ***NIDHI AWASTHI*** …from… ***BBAU, Lucknow***... has been given the ***Best Paper Award*** in the category of… ***Physics***....for the oral presentation of his/ her paper entitled… ***Revealing activation energy and rate-determining step of chlorzoxazone drug metabolism through Cytochrome P450***...during 5th International Conference on Recent Advances in Science (ICRAS-2021) held at Invertis University, Bareilly in online mode on 30-April and 01-May, 2021.

(Prof. P. P. Singh)
Dean, Faculty of Science

Date: 5th May 2021

(Dr.Satendra Singh)
Convenor

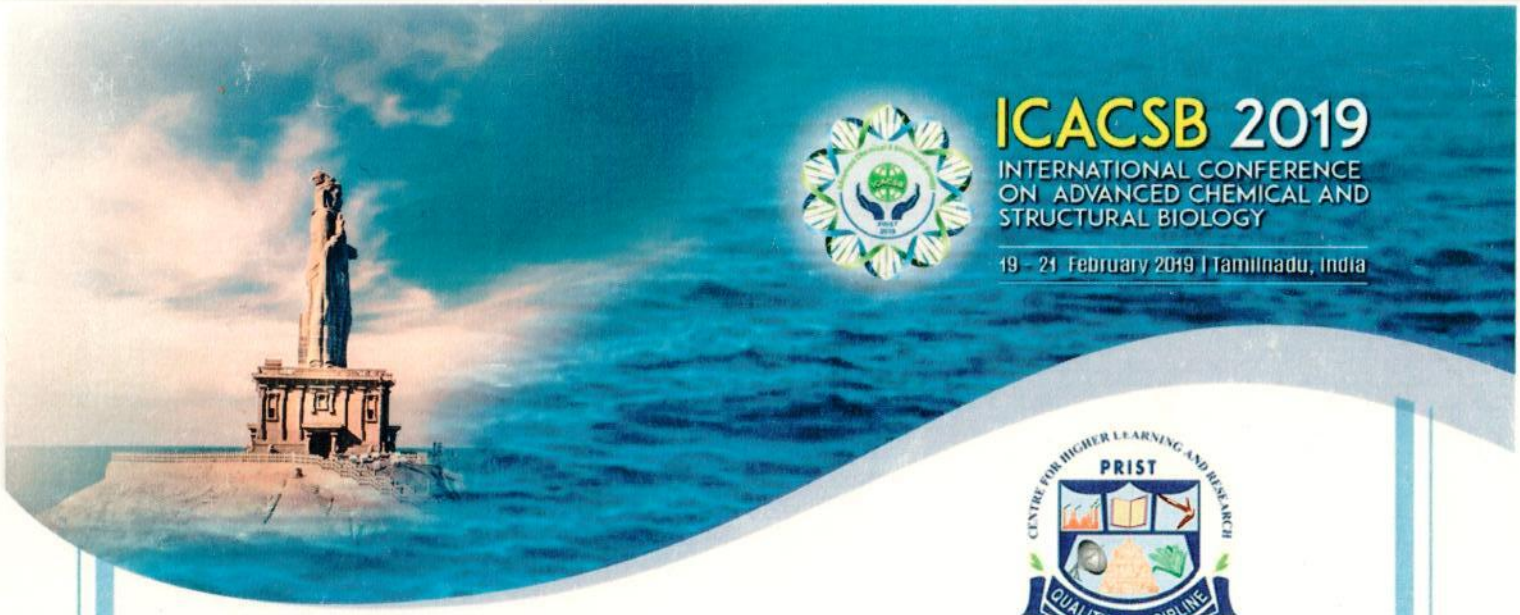

ICACSB 2019

INTERNATIONAL CONFERENCE ON ADVANCED CHEMICAL AND STRUCTURAL BIOLOGY

19 - 21 February 2019 | Tamilnadu, India

PRIST

CENTRE FOR HIGHER LEARNING AND RESEARCH

QUALITY & DISCIPLINE

Certificate

This is to certify that Dr/Mr/Ms **NIDHI AWASTHI** *of*

Babasaheb Bheemrao Ambedkar University, Lucknow

has participated as a poster presenter in the International Conference on Advanced Chemical and Structural Biology from February 19 -21, 2019 Organized by PRIST Deemed to be University, Thanjavur.

Presented Poster Title:

QM calculations on a P450 mediated hydroxylation from Trichoderma brevicompactum

PONNAIYAH RAMAJAYAM INSTITUTE OF SCIENCE & TECHNOLOGY, PRIST

THANJAVUR
613 403

Convener, ICACSB

Vice Chancellor

TEQIP

ULTRASONICS SOCIETY OF INDIA • Founded 1974 •

International Conference on
Ultrasonics and Materials Science for Advanced Technology 2019 (ICUMSAT-2019)
Theme: Ultrasonics in Materials Science
November 16-18, 2019

CERTIFICATE

Certified that Prof. / Dr. / Mr. / Ms. Nidhi Awasthi

from Department of Physics, BBAU, Lucknow.

participated as Chairperson of a Session / Plenary Speaker / Invited Speaker / Contributor of a Research Paper for Oral / Poster Presentation.

Title of the Talk / Paper Optimization - - - - - - - - - - Tuberculosis.

(Dr. Punit K. Dhawan)
Organizing Secretary

(Dr. Giridhar Mishra)
Convener

In collaboration with :
Ultrasonics Society of India
National Physical Laboratory
New Delhi – 110012, India

Organized by :
Department of Physics
Prof. Rajendra Singh (Rajju Bhaiya) Institute of Physical Sciences for Study and Research
VBS Purvanchal University, Jaunpur-222003 (U.P.) India

THE INDIAN SCIENCE CONGRESS ASSOCIATION

(Professional Body under Department of Science & Technology,
Ministry of Science & Technology, Government of India)

14, Dr. Biresh Guha Street, Kolkata – 700 017

Participation Certificate

This is to certify that Prof./Dr./Shri/Smt. Nidhi Awasthi

of Babasaheb Bheemrao Bheemrao Ambedkar University, Lucknow

has participated in the 107th Indian Science Congress held at University of Agricultural Sciences, Bangalore from January 3 to 7, 2020.

His/Her Membership Number is. SLM877

Date. 7/1/2020

Dr. S. Ramakrishna
General Secretary
(Membership Affairs)

Office Seal

Dr. Anoop Kumar Jain
General Secretary
(Scientific Activities)

National Symposium

on

Advanced Materials Science

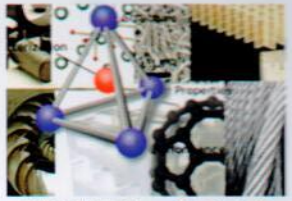

NSAMS - 2018

Department of Physics

Deen Dayal Upadhyaya Gorakhpur University, Gorakhpur

7 & 8 December 2018

Certificate

This is to certify that Prof./Dr./Mr./Ms. Nidhi Awasthi

Dept. of Physics, B.B.A.U. Lucknow attended the symposium

and Chaired a session/delivered Invited Talk/presented paper in Oral/Poster session. The title of his/her talk/paper is

Theoratical - - - . - - - - . - - - - - Cytochrome P450

(Sugriva Nath Tiwari)
Convener & HoD

(Umesh Yadava)
Organising Secretary

BABASAHEB BHIMRAO AMBEDKAR UNIVERSITY
LUCKNOW
प्रज्ञा शील करुणा
ESTABLISHED 1996

National Science Day Celebration and Seminar

on the theme

"Fostering Scientific Temper for Welfare of Society and Surroundings"

27th – 28th February, 2018

भारतीय प्राणी विज्ञान मंडल
1938
ZOOLOGICAL SOCIETY OF INDIA

Certificate

This is to certify that Dr./Mr./Ms. Nidhi Awasthi has participated & presented model/poster/oral paper entitled _____ and was awarded _____ on the occasion of "National Science Day" and Seminar organized by Babasaheb Bhimrao Ambedkar University, Lucknow, Uttar Pradesh in association with the Zoological Society of India, Bodhgaya.

President
Zoological Society of India

Vice Chancellor
Babasaheb Bhimrao Ambedkar University